



UNIVERSITÀ DEGLI STUDI DI MILANO

DEPARTMENT OF PHYSICS

PHD SCHOOL IN

PHYSICS, ASTROPHYSICS AND APPLIED PHYSICS

CYCLE XXXVI

Dualities and exact results in supersymmetric QFTs

Disciplinary Scientific Sector FIS/02

Supervisor of the Thesis: Professor Antonio Amariti

PhD Thesis of:

Simone Rota

A.Y. 2022-2023

Referees of the Thesis:

External Referee:
Sergio Benvenuti

External Referee:
Sara Pasquetti

Commission of the final examination:

External Member and President:
Massimo Bianchi

External Member:
Sergio Benvenuti

External Member:
Marco Fazzi

Final examination:

Friday, February 02, 2024

Università degli Studi di Milano, Dipartimento di Fisica, Milano, Italy

To my aunt Silvia

Cover illustration:

Eye of the universe, Outer Wilds

MIUR subjects:

FIS/02 - FISICA TEORICA, MODELLI E METODI MATEMATICI

PACS:

11.30.Pb Supersymmetry

11.30.-j Symmetry and conservation laws

11.10.Kk Field theories in dimensions other than four

Contents

List of Figures	ix
List of Tables	xv
Introduction	xvi
Motivation	xvii
1 Seiberg duality	1
1.1 $N_f = N_c$: quantum deformed moduli space	4
1.2 $N_f = N_c + 1$: s-confinement	5
1.3 $N_f = 2N_c$: conformal manifold	6
1.4 Seiberg duality for $SO(N_c)$ groups: 1-form symmetries	8
Part I : IR Dualities and Confinement in 3d SQFTs	13
2 Aharony duality and the S^3 partition function	13
2.1 Introduction	13
2.2 Three-sphere partition function	16
3 Webs of 3d $\mathcal{N} = 2$ dualities with D-type superpotentials	19
3.1 Known dualities with D-type superpotential	20
3.2 4d/3d reduction of $USp(2n)$ SQCD with two rank-two anti-symmetric tensors	28
3.3 Reconsidering the 4d/3d reduction of $U(n)$ SQCD with two adjoints	37
3.4 Discussion and future developments	41
4 S-confinement in 3d $\mathcal{N} = 2$ SO/USp adjoint SQCD	43
4.1 3d confining models with real gauge groups and adjoint matter	44
4.2 Proving known results	47
4.3 New results	50
4.4 Discussion	68

Part II : Exploring Conformal Manifolds of 4d SCFTs	73
5 Conformal S-dualities from O-planes	73
5.1 Conformal dualities from Type IIA elliptic models with orientifolds	73
6 $\mathcal{N} = 1$ conformal dualities from unoriented chiral quivers	79
6.1 Orientifolds and conformal duality	81
6.2 Glide orientifold and $L^{a,b,a}/\mathbb{Z}_2$ models	91
6.3 Family \mathcal{A}	96
6.4 Family \mathcal{B}	106
6.5 Discussion and conclusions	111
7 Multi-planarizable quivers, orientifolds, and conformal dualities	115
7.1 Toy models for conformal dualities	116
7.2 Gauging the flavor: PdP _{3b} vs. PdP _{3c} and their orientifolds	125
7.3 Embedding in string theory	131
7.4 Case study	136
7.5 Discussion and conclusions	143
Part III : Generalized Symmetries, S-folds and $\mathcal{N} = 2$ SCFTs	149
8 $\mathcal{N} = 3$ S-folds	149
8.1 S-fold SCFTs	151
8.2 Exceptional S-folds	153
9 A recipe for genuine lines: 1-form symmetries in S-fold SCFTs	155
9.1 Generalities	156
9.2 Lines in S-folds with $\mathcal{N} = 4$ enhancement	164
9.3 Lines in $\mathcal{N} = 3$ S-folds	169
9.4 Non-invertible symmetries	178
9.5 Conclusions	179
10 Exceptional S-folds and discrete gauging	181
10.1 Another look at S-folds SCFTs	183
10.2 Exceptional S-folds	192
11 Charge lattices in $\mathcal{N} = 2$ SCFTs with $\varkappa \neq \{1, 2\}$	207
11.1 1-form symmetries of rank-2 $\mathcal{N} = 2$ SCFTs with $\varkappa \neq \{1, 2\}$	208
11.2 A constraint for the stratification of $\mathcal{N} = 2$ SCFTs	210
11.3 Discussion and conclusions	212
Future directions	215
Appendices	216
A Dualities with adjoint and without W_{monopole} on Z_{S^3}	219
B 3d $SO(N)$ with $N + 1$ flavors and linear monopole superpotential	223

C Further examples of multiplanarizable quivers	225
D Counting phases of multiplanarizable quivers	239
List of Publications	243
Acknowledgments	245
Bibliography	247

List of Figures

1.1	On the LHS: couplings of the electric SQCD for $N_f = 2N_c$ SQCD deformed by a quartic superpotential for the quarks. On the RHS couplings of the dual magnetic SQCD for $N_f = 2N_c$ SQCD deformed by a quadratic superpotential for the meson. The red lines represent the dual marginal deformations on both sides of the duality after the addition of the respective deformations.	7
3.1	Survey of the dualities and the flows studied in this thesis. The blue boxes and arrows represents dualities and flows that have already been proposed and studied in the literature. The red boxes and arrows represent the dualities and the flows proposed and analyzed here.	21
4.1	Schematic representation of one step of the deconfinement procedure used to prove the confinement of the $USp(2n)$ model with monopole superpotential. The superpotential and three-sphere partition function of each model in Figure are:	57
4.2	Quiver description of the deconfinement of the adjoint S of the $USp(2n)$ model with superpotential (4.18). In this and in the following quivers we decided to omit to represent the various singlets.	58
4.3	Quiver representation of the $SO(2n)$ model after the adjoint field has been deconfined	61
4.4	Quiver representation of the $SO(2n + 1)$ model after the adjoint field has been deconfined	67
5.1	IIA picture of an elliptic model with O6-planes. The low-energy effective quiver theory can have orthogonal and/or symplectic gauge groups.	74
6.1	Examples of chiral orbifolds for the $L^{a,b,a}$ family.	81
6.3	The brane tiling of $\mathbb{C}^2/\mathbb{Z}_2 \times \mathbb{C}$ with the four fixed points of the orientifold projection.	83

- 6.4 The various matter fields and their representations that we will use in quiver diagrams. We draw multiple arrows for multiple fields connecting the same pair of nodes. When nodes are both SO and/or USp groups, we drop the arrow and connect them with an edge, signaling the fact that representations are real. For tensor representations, when not specified if they are symmetric or antisymmetric, we simply denote them by T_a . 83
- 6.5 The quiver diagram for $\mathbb{C}^2/\mathbb{Z}_2 \times \mathbb{C}$ with the orientifold projection Ω on the top left, while on the top right the associated (linear) ‘unoriented’ quiver after the $\mathcal{N} = 2$ choice for the orientifold and the $\mathcal{N} = 1$ choice at the bottom. 85
- 6.7 On the left, the quiver diagram for \mathcal{C} , where the red line represents the orientifold projection. On the right, the linear ‘unoriented’ quiver for the theory after the orientifold [1]. 87
- 6.8 The chain of toric diagrams connected by mass deformation for $n = 6$: $\mathbb{C}^2/\mathbb{Z}_6 \times \mathbb{C} \rightarrow L^{2,4,2} \rightarrow L^{3,3,3}$, the number of points remains $n + 2 = 8$ all along. It holds also with the orientifold projection, mutatis mutandis. 87
- 6.9 The theories $\mathbb{C}^2/\mathbb{Z}_3 \times \mathbb{C}$ and suspended pinch point (SPP) represented via IIA elliptic models. Rotating NS5 branes results in mass deforming the theory. 88
- 6.10 The chain of five-brane diagrams connected by mass deformation for $n = 6$: $\mathbb{C}^2/\mathbb{Z}_6 \times \mathbb{C} \rightarrow L^{2,4,2} \rightarrow L^{3,3,3}$, the number of vectors remains $n + 2 = 8$ all along. It holds also with the orientifold projection, provided a \mathbb{Z}_2 symmetry is preserved. 89
- 6.11 The chain of linear quiver diagrams after the orientifold connected by mass deformation for $n = 6$: $\mathbb{C}^2/\mathbb{Z}_6 \times \mathbb{C} \rightarrow L^{2,4,2} \rightarrow L^{3,3,3}$. 89
- 6.12 The two inequivalent ways of accommodating the horizontal branes for $L^{2,8,2}$ and the associated linear quivers. 90
- 6.13 The orientifold projection of $L^{2,4,2}$ with four fixed points that yields unitary groups and pairs of conjugate tensor fields and the choice $\tau_{00} = -1$, $\tau_{22} = +1$. 90
- 6.14 An example with n odd obtained from mass deformation of $\mathbb{C}^2/\mathbb{Z}_3 \times \mathbb{C}$ and the orientifold projection with fixed points. On the left, the toric diagram of $L^{1,2,1}$ or SPP, center its five-brane and on the right the quiver after the orientifold with $\tau_0 = +1$, $\tau_{00} = +1$, $\tau_{11} = -1$. 91
- 6.16 The linear quiver resulting from the glide orientifold of $\mathbb{C}^3/\mathbb{Z}_2$. 92
- 6.17 An example of a chain of toric diagrams of family \mathcal{A} connected by mass deformation for $k = 3$: $L^{0,6,0}/\mathbb{Z}_2 \rightarrow L^{2,4,2}/\mathbb{Z}_2 \rightarrow L^{3,3,3}/\mathbb{Z}_2$. It holds also with the orientifold projection, mutatis mutandis. 94
- 6.18 The chain of five-brane diagrams of family \mathcal{A} connected by mass deformation for $k = 3$: $L^{0,6,0}/\mathbb{Z}_2 \rightarrow L^{2,4,2}/\mathbb{Z}_2 \rightarrow L^{3,3,3}/\mathbb{Z}_2$. It holds also with the orientifold projection, provided a \mathbb{Z}_2 symmetry is preserved. 94
- 6.19 The quiver for the orientifold theory of $L^{0,6,0}/\mathbb{Z}_2 \rightarrow L^{2,4,2}/\mathbb{Z}_2 \rightarrow L^{3,3,3}/\mathbb{Z}_2$ in Family \mathcal{A} with choice ($\tau_{00} = +$, $\tau_{55} = -$). Colored fields represent the pairs that are mass deformed in the chain, the color match the chain of five-branes in Fig. 6.18. 95
- 6.20 The chain of five-brane diagrams of family \mathcal{B} connected by mass deformation for $k = 3$: $L^{0,6,0}/\mathbb{Z}_2 \rightarrow L^{2,4,2}/\mathbb{Z}_2 \rightarrow L^{3,3,3}/\mathbb{Z}_2$. It holds also with the orientifold projection, provided a \mathbb{Z}_2 symmetry is preserved. 95

- 6.21 The quiver for the orientifold theory of $L^{0,6,0}/\mathbb{Z}_2 \rightarrow L^{2,4,2}/\mathbb{Z}_2 \rightarrow L^{3,3,3}/\mathbb{Z}_2$ in Family \mathcal{B} with choice ($\tau_0 = \tau_1 = +$, $\tau_6 = \tau_7 = -$). Colored fields represent the pairs that are mass deformed in the chain, the color match the chain of five-branes in Fig. 6.20. 96
- 6.22 The generic quiver of family \mathcal{A} models. Colored fields are the mass deformed pairs. All gauge nodes are $SU(N)$. 96
- 6.23 The model $L^{0,2,0}/\mathbb{Z}_2$. On the left the toric diagram is drawn, at the center the five-brane and its orientifold projection with fixed points, on the right the quiver resulting from the orientifold projection. 97
- 6.24 The model $L^{1,1,1}/\mathbb{Z}_2$. On the left the toric diagram is drawn, at the center the five-brane and its glide projection, on the right the quiver resulting from the orientifold projection. 99
- 6.25 The model $L^{0,4,0}/\mathbb{Z}_2$. On the left the toric diagram is drawn, at the center the five-brane and its orientifold projection with fixed points, on the right the quiver resulting from the orientifold projection. 100
- 6.26 The model $L^{2,2,2}/\mathbb{Z}_2$. On the left the toric diagram is drawn, at the center the five-brane and its glide orientifold, on the right the quiver resulting from the projection. 101
- 6.27 The model $L^{1,3,1}/\mathbb{Z}_2$. On the left the toric diagram is drawn, at the center the five-brane and its orientifold projection with fixed points, on the right the quiver resulting from a choice of orientifold projection consistent with gauge anomalies. This does not belong to family \mathcal{A} . 103
- 6.28 A portion of generic quiver of the orientifold of $L^{0,2k,0}/\mathbb{Z}_2$ from node $2i$. 104
- 6.29 The general quiver of family \mathcal{B} models. Colored fields are the mass deformed pairs. 106
- 6.30 The model $L^{0,2,0}/\mathbb{Z}_2$. On the left the toric diagram is drawn, at the center the five-brane and its orientifold projection with fixed points, on the right the quiver resulting from the orientifold projection. 108
- 6.31 The model $L^{1,1,1}/\mathbb{Z}_2$. On the left the toric diagram is drawn, at the center the five-brane and its orientifold with fixed lines, on the right the quiver resulting from the orientifold projection. 108
- 6.32 The model $L^{0,4,0}/\mathbb{Z}_2$. On the left the toric diagram is drawn, at the center the five-brane and its orientifold projection with fixed points, on the right the quiver resulting from the orientifold projection. 109
- 6.33 The model $L^{2,2,2}/\mathbb{Z}_2$. On the left the toric diagram is drawn, at the center the five-brane and its orientifold with fixed lines, on the right the quiver resulting from the projection. 110
- 7.2 The quiver for SQCD with singlets with gauge group $SU(N)$ and non-abelian global symmetry $SU(F_1) \times SU(G_1) \times SU(F_3)^2 \times SU(G_3)^2$. 120
- 7.3 The notation we use for quivers: a blue circle for a $SU(N)$ gauge factor, a blue diamond for a $SO(N)$ or $USp(N)$ gauge factor and a red square for a flavor factor. 121
- 7.8 The dimers of Pseudo del Pezzo $3b$ and $3c$ with the fixed lines and fixed points projections, drawn in red. 127
- 7.9 Generic toric diagram labeled by (k_1, k_2, k_3) . 132
- 7.10 Fundamental cell of the (k_1, k_2, k_3) model. 132

- 7.11 In this picture we represent the flip on the dimer that preserves the quiver. We consider a pair of faces A and B obtained by cutting an hexagon with a NW-SE diagonal and we flip it into a NE-SW one. By relabeling the faces one can see that the quiver remains identical even if in general it is associated to a different toric diagram. 133
- 7.12 On the LHS we summarize the general rank assignation on the dimer that we have considered in the whole Chapter. We start by considering the same rank for each node and then we shift the ranks by $j\tau$ where $j = 0, 2, 4$ following the coloring of the arrows in the figure. On the RHS we consider the choices of the charges τ for a generic fixed line and fixed point projection. 135
- 7.13 The generic quiver associated to a toric theory with (k_1, k_2, k_3) and $k_3 = k_1 + k_2 = 2k$ and $\ell = 0, \dots, k$. 136
- 7.14 The generic quiver associated to a toric theory with (k_1, k_2, k_3) and $k_3 > k_1 + k_2 = 2k$ and $\ell = 1, \dots, (k + 1)$. 136
- 7.15 The dimers representing the orientifold projection of toric diagrams $(2, 2, 5)$, on the left, and $(0, 4, 5)$ on the right. For $(2, 2, 5)$, there are both fixed lines and fixed points projections. 137
- 7.16 The quiver for the theories $(2, 2, 5)$ and $(0, 4, 5)$, after the orientifold projection. 138
- 7.17 The dimers representing the orientifold projection of toric diagrams $(2, 2, 6)$, on the left, and $(0, 4, 6)$ on the right. For $(2, 2, 6)$, there are both fixed-line and fixed-point projections. 140
- 7.18 The quiver for the theories $(2, 2, 6)$ and $(0, 4, 6)$, after the orientifold projection. 141
- 9.1 A pictorial representation of two D3-branes probing the $O3^+$ orientifold on a generic point of the Coulomb branch. The light blue shaded area is a possible choice of fundamental domain under the spacetime identification induced by the orientifold. Black (gray) dots represent (images of) D3-branes. Black lines correspond to (p, q) -strings stretched between D3-branes. In particular, we drew (p, q) -strings generating the \mathcal{W} -bosons corresponding to simple roots $\mathcal{N} = 4 \text{usp}(4)$ SYM. 162
- 9.2 A pictorial representation of two D3-branes probing the $S_{3,1}$ -fold. The transverse directions to the S -fold are shown. The light blue dot represents the position of the $S_{3,1}$ -fold. The light blue shaded area is a possible choice of fundamental domain under the spacetime identification induced by the $S_{3,1}$ -fold. Black (gray) dots represent (images of) D3-branes. Black lines correspond to (p, q) -strings stretched between D3-branes. In particular, we drew (p, q) -strings corresponding to \mathcal{W} -bosons of $\mathcal{N} = 4 \text{su}(3)$ SYM. 165
- 10.1 Cartan matrices of the exceptional algebras $E_r, r = 6, 7, 8$. 192
- A.1 Schematic representation of one step of the deconfinement procedure of [2] for the $USp(2n)$ model with adjoint. The partition functions of the model are: 221
- C.1 Fixed-line and fixed-point projections for the $(1, 1, 3)$ and the $(0, 2, 3)$ models. 226
- C.2 Fixed lines and fixed points projections for $(1, 1, 4)$ and $(0, 2, 4)$. This is the first conformal duality obtained projecting these models. 228

C.3	Fixed-line and fixed-point projections for $(1, 1, 4)$ and $(0, 2, 4)$. This is the second conformal duality obtained projecting these models.	229
C.4	Fixed lines and fixed points projections for $(1, 1, 5)$ and $(0, 2, 5)$.	231
C.5	Fixed lines and fixed-point projections for $(2, 2, 4)$ and $(0,4,4)$.	232
C.6	Fixed-line and fixed-point projections for $(2, 2, 6)$ and $(0, 4, 6)$. This is the second conformal duality obtained projecting these models. The first one has been discussed in the body of Chapter 7 in Sec. 7.4.2.	234
C.7	Fixed-line projection of $(3, 3, 6)$ and fixed-point projections of $(2, 4, 6)$ and $(0, 6, 6)$.	236

List of Tables

5.1	Conventions for representing tensorial matter in quiver diagrams. When there are two possible representations for a tensorial field (e.g. the anti-symmetric representation for an orthogonal gauge group) we choose to represent it as an adjoint.	75
5.2	Elliptic models with O6-planes and corresponding quivers. Models connected by \leftrightarrow are S-dual. Configurations denoted by ‘flavor’ need additional flavor hypermultiplets in order to make all the β function vanish. The dashed line in the middle of the quiver corresponds to the intermediate $n_g - 1$ nodes with unitary gauge groups. In this table we have assumed that all the NS5-branes are in the (012345) directions; the generalization to non-parallel branes is straightforward. Models in the first row were considered in [3]; models in the fourth row were considered in [4].	78
7.1	The various patterns for breaking the global symmetry $SU(F) \times SU(F)$ of SQCD introducing four singlets M_{ℓ_j} and four couplings h_{ℓ_j} , $\ell, j = 1, 2$, referring to Fig. 7.1b with $F_1 + F_2 = F = G_1 + G_2$.	117
7.2	The global symmetry charges for the matter fields, both for $W_A + W_\lambda$ and for $W_B + W_\lambda$.	119
7.3	The global symmetry charges for the matter fields, both for $W_A + W_\lambda$ and for $W_B + W_\lambda$.	122
7.4	The global symmetry charges for the matter fields, at large N , both for PdP_{3b} and for PdP_{3c} .	129
9.1	Summary of the results of Chapter 9. $\mathbb{1}$ represents a trivial group.	156
9.2	Elements ρ_k of $SL(2, \mathbb{Z})$ of order k used in S -fold projections, and the corresponding fixed coupling τ .	157
9.3	Different discrete torsions on O3-planes.	159
9.4	F1-string, D1-string, and the F1-D1 bound state providing respectively the electric, magnetic, and dyonic charges of the projected $\mathcal{N} = 4$ gauge theory.	162
9.5	The charges of allowed lines in the $S_{3,1}$ -fold theories. The charges w_i, m_i, P and Q are given in (9.69), and $r, s = 0, 1, 2$. The mutual locality condition for two lines with charges $\ell_{r,s}$ and $\ell_{r',s'}$ is $rs' - sr' = 0 \pmod{3}$.	171

- 9.6 The charges of allowed lines in the $S_{4,1}$ -fold theories. The charges w_i, m_i, P and Q are given in (9.98), (9.77), and $r, s = 0, 1$. The mutual locality condition for two lines with charges $\ell_{r,s}$ and $\ell_{r',s'}$ is $rs' - sr' = 0 \pmod{2}$. 175
- 10.1 Properties of exceptional S-folds of type $\mathfrak{g} = E_n$. For each theory the Coulomb branch \mathcal{C} is reproduced from [5] and we specify whether the theory is a discrete gauging (d.g) of a free theory. Red cells are theories whose Coulomb branch do not admit any consistent charge lattice, orange cells are theories where the charge lattice is incompatible with the constraints on the central charges. For the only interacting SCFT the 1-form symmetry group $G^{(1)}$ is written and the central charge is reproduced from [5]. 183
- 10.2 Degrees and codegrees of the exceptional algebras E_r . 194
- 10.3 Elements $w \in \mathcal{W}[E_6]$ that characterize the S-fold actions for the S-fold theories of type E_6 through (10.38) and (10.39). Here c_{E_6} is the Coxeter element of E_6 , r is the rank of the S-fold theory and in the fourth and fifth columns the exceptional complex crystallographic reflection group (ECCRG) associated to the S-fold theories and its degrees Δ_i are reproduced. 194
- 10.4 Elements $w \in \mathcal{W}[E_7]$ that characterize the S-fold actions for the S-fold theories of type E_7 through (10.38) and (10.39). Here c_{E_7} and c_{E_6} are the Coxeter element of E_7 and the E_6 subalgebra, respectively, r is the rank of the S-fold theory and in the fourth and fifth columns the exceptional complex crystallographic reflection group (ECCRG) associated to the S-fold theories and its degrees Δ_i are reproduced. 202
- 10.5 Elements $w \in \mathcal{W}[E_8]$ that characterize the S-fold actions for the S-fold theories of type E_8 through (10.38) and (10.39). Here c_{E_8} is the Coxeter element of E_8 , s_i are the reflection along the i -th simple root, r is the rank of the S-fold theory and in the fourth and fifth columns the exceptional complex crystallographic reflection group (ECCRG) associated to the S-fold theories and its degrees Δ_i are reproduced. 204
- C.1 List of cases (ordered by increasing number n_G^Ω of gauge groups after the projection) analyzed in detail in the Chapter 7. 225

Motivation

The dynamics of quantum field theories (QFTs) has been a major field of research in theoretic physics for decades. The interest in the study of QFTs originates from the description of fundamental interactions provided by the Standard Model which poses interesting theoretical challenges such as the understanding of the confining behavior of QCD.

The analysis of the strongly coupled regime of QFTs is particularly challenging due to the fact that perturbative methods are no longer reliable and exact non-perturbative techniques must be employed. Some non-perturbative techniques are always available, with the most notable example being the constraints imposed by global symmetries through the associated Ward identities. A class of QFTs where we have more control over the non-perturbative regime is given by supersymmetric theories. Here many non-perturbative results have been obtained in the last decades, including non-renormalization theorems, exact computations for various partition functions and infrared dualities.

Our motivation for the study of supersymmetric QFTs relies on the expectation that they provide a good sample of field theories with respect to general behaviors and phenomena that they present. We will consider the landscape of supersymmetric QFTs as a playground which is relatively under control where we can learn “how QFTs work”. As an example where such a mindset was successful, in [6] it was shown that a supersymmetric version of QCD exhibits confinement, and furthermore it was shown that this phenomenon can be understood as a consequence of the condensation of monopoles.

Motivated by this, in this thesis we will analyze supersymmetric QFTs in three and four spacetime dimensions. Our main goals will be to study the infrared behavior of these theories, as well as to derive general constraints for the existence of the theories themselves. Our main goals include the identification and checking of infrared dualities, both in three and four spacetime dimensions, and the study of some RG flows for the associated theories. We will study exactly marginal deformations of 4d SCFTs and identify instances of conformally dual theories. In the last Part of the thesis we will focus on the topic of generalized symmetries in the context of highly supersymmetric non-lagrangian

SCFTs, and provide non-trivial consistency constraints for the existence of a certain class of maximally strongly coupled SCFTs.

Organizational note

The present Thesis consists of three Parts, for a total of eleven Chapters. Part I is composed of Chapters 2, 3 and 4 and presents various results in the context of IR dualities and s-confinement in 3d SQFTs with four supercharges. Part II spans from Chapter 5 to Chapter 7 and addresses the analysis of conformally dual 4d $\mathcal{N} = 1$ SCFTs obtained from toric theories with orientifolds. Part III spans from Chapter 8 to Chapter 11 and is devoted to the study of generalized symmetries in $\mathcal{N} = 3$ four dimensional SCFTs, including a full classification of 1-form symmetries for regular S-folds and exceptional S-folds of type E_r . Parts I, II, and a substantial fraction of Part III have appeared as refereed publications in scientific journals; co-authors of the relevant articles are mentioned below.

Chapter 1: Seiberg duality: We review Seiberg duality for $\mathcal{N} = 1$ four dimensional SQCD. We introduce concepts such as IR dualities, s-confinement, conformal dualities and 1-form symmetris.

Chapter 2: Aharony duality and the S^3 partition function: We briefly review Aharony duality and the computation of the partition function of 3d $\mathcal{N} \geq 2$ QFTs on the squashed three-sphere Z_{S^3} .

Chapter 3: Webs of 3d $\mathcal{N} = 2$ dualities with D-type superpotentials: We analyze various dualities involving 3d $\mathcal{N} = 2$ theories with two tensor or adjoint fields and D-type superpotential. New dualities are discovered and we show relations between those and other 3d and 4d dualities already studied in the literature, supporting our claims through computation of exact partition functions. This work has been completed in collaboration with A. Amariti and has been published as an article in *JHEP* ([7]), on which the Chapter is based.

Chapter 4: S-confinement in 3d $\mathcal{N} = 2$ SO/USp adjoint SQCD: We study 3d $\mathcal{N} = 2$ SQCD theories with orthogonal or symplectic gauge groups and monopole superpotential that exhibit s-confinement. The results are checked through the computation of the S^3 partition function and via confinement/deconfinement procedures. This work has been completed in collaboration with A. Amariti and has been published as an article in *Nucl.Phys.B* ([8]), on which the Chapter is based.

Chapter 5: Conformal S-dualities from O-planes: We review the construction of 4d $\mathcal{N} = 1$ theories obtained from Type IIA elliptic models with orientifolds that have a conformal manifold discussed in [9]. Different models can engineer theories living on the same conformal manifold. Part of this Chapter has already appeared in as an article in *JHEP* ([10]) written in collaboration with A. Amariti, M. Fazzi and A. Segati.

Chapter 6: $\mathcal{N} = 1$ conformal dualities from unoriented chiral quivers: We study a series of 4d $\mathcal{N} = 1$ theories engineered by a stack of D3-branes in Type IIB probing a Calabi-Yau toric singularity in the presence of an orientifold. We build infinite families of pairs of conformally dual theories. This work has been completed in collaboration with A. Amariti, M. Bianchi, M. Fazzi, S. Mancani and F. Riccioli and has been published as an article in *JHEP* ([11]), on which the Chapter is based.

Chapter 7: Multi-planarizable quivers, orientifolds, and conformal dualities: We expand upon the results of the previous chapters building other families of conformally dual theories which generalize the conformal duality between the unoriented PdP3_b and PdP3_c toric theories [12]. This work has been completed in collaboration with A. Amariti, M. Bianchi, M. Fazzi, S. Mancani and F. Riccioni and has been published as an article in *JHEP* ([13]), on which the Chapter is based.

Chapter 8: $\mathcal{N} = 3$ S-folds: We review the construction of $\mathcal{N} = 3$ S-fold SCFTs and exceptional S-fold SCFTs.

Chapter 9: A recipe for genuine lines: 1-form symmetries in S-fold SCFTs: We classify the 1-form symmetry groups of S-fold SCFTs as well as their global structures by analyzing the maximal refinements of their charge lattices. We also discuss the presence of non-invertible symmetries in some of these theories. This work has been completed in collaboration with A. Amariti, D. Morgante, A. Pasternak, and V. Tatitschieff and has been published as an article in *SciPost* ([14]), on which the Chapter is based.

Chapter 10: Exceptional S-folds and discrete gauging: We study the charge lattices of exceptional S-fold SCFTs of type E_n . We find that all but one of these theories do not admit a charge lattice consistent with the moduli space and must be discrete gaugings of free theories. We compute the 1-form symmetry group of the remaining SCFT.

Chapter 11: Charge lattices in $\mathcal{N} = 2$ SCFTs with $\varkappa \neq \{1, 2\}$: We develop constraints on the stratification of Coulomb branch and bounds for the 1-form symmetry group for $\mathcal{N} = 2$ SCFTs with $\varkappa \neq \{1, 2\}$ by combining the classification of rank-1 $\mathcal{N} = 2$ SCFTs and general notions about the Coulomb branch stratification. This Chapter is both inspired by the results of the previous Chapter and provides additional evidence for the claims of that Chapter.

In this Chapter we review Seiberg duality [15], which is an infrared duality between $\mathcal{N} = 1$ SQCD theories in four dimensions. This Chapter does not aim to provide a comprehensive analysis of SQCD, rather we will highlight some phenomena of this theory to contextualize and motivate the main body of the thesis. We review the various IR behaviors of SQCD as the number of flavors is varied and introduce the concepts of s-confinement, IR duality, *conformal duality* and higher form symmetries. For a more details on this topic we refer the reader to the original literature [15, 16, 17, 18, 19, 20] as well as to more extensive reviews [21, 22, 23].

The available supermultiplets in $\mathcal{N} = 1$ field theories are the vector multiplet and the chiral multiplet. On-shell the vector multiplet is composed by a vector field and a Weyl fermion while the chiral multiplet is composed of a Weyl fermion and a complex scalar. SQCD is a non-Abelian gauge theory whose field content is given by a vector multiplet transforming in the adjoint representation of the gauge group $SU(N_c)$, N_f chiral multiplets Q_i transforming in the fundamental representation of the gauge group, usually called quarks, and N_f antifundamentals \tilde{Q}^j , usually called antiquarks. The classical global symmetry is $SU(N_f)_L \times SU(N_f)_R \times U(1)_B \times U(1)_A \times U(1)_R$, and the charges of the fields are:

	$SU(N_f)_L$	$SU(N_f)_R$	$U(1)_B$	$U(1)_A$	$U(1)_R$
Q_i	\square	1	1	1	R_Q
\tilde{Q}^j	1	$\bar{\square}$	-1	1	R_Q
λ	1	1	0	0	1

(1.1)

where λ is the fermion in the vector multiplet and R_Q are the R-charges of the scalars in the chiral multiplets. Anomaly cancellation for $U(1)_R$ imposes:

$$\begin{aligned}
 U(1)_R SU(N_c)^2 : 2N_f(R_Q - 1)\mathbf{T}(\square_{SU(N_c)}) + \mathbf{T}(\text{Adj}_{SU(N_c)}) &= 0 \\
 \Rightarrow R_Q &= \frac{N_f - N_c}{N_f}
 \end{aligned}
 \tag{1.2}$$

and the axial $U(1)_A$ symmetry is anomalous. Therefore the non-anomalous global symmetry of the theory is $SU(N_f)_L \times SU(N_f)_R \times U(1)_B \times U(1)_R$, and the charges of the

fields are:

	$SU(N_f)_L$	$SU(N_f)_R$	$U(1)_B$	$U(1)_R$
Q_i	\square	1	1	$\frac{N_f - N_c}{N_f}$
\tilde{Q}^j	1	$\bar{\square}$	-1	$\frac{N_f - N_c}{N_f}$

(1.3)

It is known that for $1 \leq N_f < N_c$ a runaway potential is generated [19] and the theory does not have supersymmetric vacua, while for $N_f > 3N_c$ the beta function is positive and the theory is IR free. In the range $\frac{3}{2}N_c \leq N_f \leq 3N_c$ SQCD is believed to flow to a non-trivial interacting IR fixed point. At large values of N_c and N_f for N_f/N_c inside the conformal window the IR fixed point can be understood as the Banks-Zaks fixed point, which is an attractive fixed point with non-trivial gauge coupling. It is widely believed that such an IR fixed point also exists for finite values of N_f and N_c inside of the conformal window, although a definitive proof of its existence is not available. At the conformal fixed point the unitarity bound for the gauge invariant meson $Q_i \tilde{Q}^j$ implies:

$$\begin{aligned} \Delta[Q_i \tilde{Q}^j] &= \frac{3}{2}R[Q_i \tilde{Q}^j] = 3R_Q = 3\frac{N_f - N_c}{N_f} \geq 1 \\ \Rightarrow N_f &\geq \frac{3}{2}N_c \end{aligned} \quad (1.4)$$

where the relation:

$$\Delta = \frac{3}{2}R \quad (1.5)$$

holds for chiral multiplets if the R-charge $U(1)_R$ is the superconformal one, meaning that its conserved current lies in the same supermultiplet as the conserved stress tensor. For $\frac{3}{2}N_c \leq N_f$ the mesons $Q_i \tilde{Q}^j$ violate the unitarity bound. Then we expect an accidental $U(1)$ symmetries charging the mesons to appear along the RG flow. This accidental symmetry can mix with the $U(1)_R$, so that $U(1)_R$ is no longer the superconformal R-charge. The analysis of the IR dynamics is better understood in terms of a magnetic dual theory through Seiberg duality.

Seiberg duality is the statement that for $N_f > N_c + 1$ the following theories are infrared dual, meaning that they describe the same infrared fixed point [15]:

- An electric $SU(N_c)$ SQCD with N_f flavors Q, \tilde{Q} and vanishing superpotential:

$$W = 0 \quad (1.6)$$

- A magnetic $SU(N_f - N_c)$ SQCD with N_f flavors q, \tilde{q} and N_f^2 gauge singlet chiral fields M_j^i with superpotential:

$$W = h q_i \tilde{q}^j M_j^i \quad (1.7)$$

therefore M_j^i transforms in the $\bar{\square} \times \square$ representation of the non-abelian global symmetry $SU(N_f)_L \times SU(N_f)_R$.

More explicitly the statement that these theories are dual means that the spectrum and correlation functions in the IR are exactly the same. Nevertheless the mapping of operators between the two descriptions is non-trivial, the meson $Q_i \tilde{Q}^j$ of the electric theory are mapped to M_j^i in the magnetic theory. The (anti-)baryons of the electric and magnetic

theory B and b are mapped as follows:

$$\begin{aligned}
B_{j_1, \dots, j_{N_f - N_c}} &= Q^{i_1} \dots Q^{i_{N_c}} \epsilon_{j_1, \dots, j_{N_f - N_c}, i_1, \dots, i_{N_c}} \\
b_{j_1, \dots, j_{N_f - \tilde{N}_c}} &= q^{i_1} \dots q^{i_{\tilde{N}_c}} \epsilon_{j_1, \dots, j_{N_f - \tilde{N}_c}, i_1, \dots, i_{\tilde{N}_c}} \\
b^{j_1, \dots, j_{N_c}} &\leftrightarrow \epsilon^{i_1, \dots, i_{N_f - N_c}, j_1, \dots, j_{N_c}} B_{j_1, \dots, j_{N_f - N_c}}
\end{aligned} \tag{1.8}$$

where the color indices are contracted with the ϵ symbol. The charges under $U(1)_R$ and $U(1)_B$ of the (anti-)baryons of the electric and magnetic theories match.

Computing the full spectrum of the IR theories and the correlation functions is, up to now, not possible. We can nevertheless perform non-trivial checks of Seiberg duality, starting from the mapping of the global symmetries:

	$SU(N_f)_L$	$SU(N_f)_R$	$U(1)_B$	$U(1)_R$
Q_i	\square	1	1	$\frac{N_f - N_c}{N_f}$
\tilde{Q}^j	1	$\overline{\square}$	-1	$\frac{N_f - N_c}{N_f}$
q_i	$\overline{\square}$	1	$\frac{N_c}{N_f - N_c}$	$\frac{N_c}{N_f}$
\tilde{q}^j	1	\square	$-\frac{N_c}{N_f - N_c}$	$\frac{N_c}{N_f}$
M	\square	$\overline{\square}$	0	$2\frac{N_f - N_c}{N_f}$

(1.9)

A non-trivial check of the duality is given by the matching of the 't Hooft anomalies for the global symmetries. For example the cubic 't Hooft anomaly $U(1)_B^2 U(1)_R$ in the electric theory is given by:

$$\begin{aligned}
U(1)_B^2 U(1)_R : N_f N_c B[\psi_Q]^2 R[\psi_Q] + N_f N_c B[\psi_{\tilde{Q}}]^2 R[\psi_{\tilde{Q}}] \\
= N_f N_c \left(\frac{N_f - N_c}{N_f} - 1 \right) + N_f \left(\frac{N_f - N_c}{N_f} - 1 \right) = -2N_c^2
\end{aligned} \tag{1.10}$$

where ψ_q is the fermion in the chiral multiplet q . On the magnetic side we have:

$$\begin{aligned}
U(1)_B^2 U(1)_R : N_f(N_f - N_c) \left(B[\psi_q]^2 R[\psi_q] + B[\psi_{\tilde{q}}]^2 R[\psi_{\tilde{q}}] \right) \\
= 2N_f(N_f - N_c) \left(\frac{N_c}{N_f - N_c} \right)^2 \left(\frac{N_c}{N_f} - 1 \right) = -2N_c^2
\end{aligned} \tag{1.11}$$

the results on the sides match, and similarly one can check that all the other 't Hooft anomalies match in a non-trivial way. Other checks of the duality involve the matching of the moduli space of vacua, the superconformal index as well as geometric construction of SQCD in string theory.

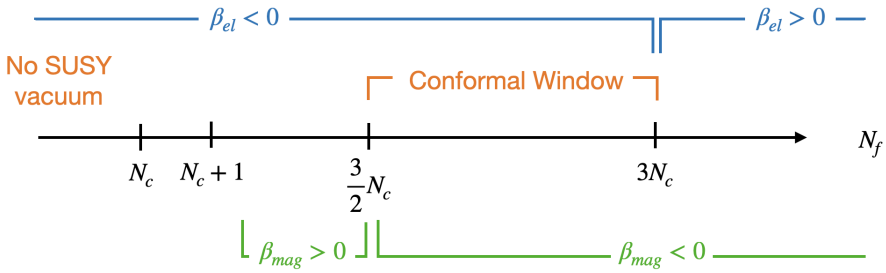
We may now go back to the case of $N_c + 1 < N_f < \frac{3}{2}N_c$. In the dual $SU(N_f - N_c)$ the beta functions for the gauge coupling and for h are positive, therefore the quarks are weakly interacting and the singlets M_j^i are free. If $U(1)_R$ was the superconformal R-charge the singlets M_j^i would violate the unitarity bound, therefore we expect that an accidental $U(1)_M$ symmetry arises along the RG flow and mixes with $U(1)_R$ to form the true superconformal R-symmetry $U(1)_{\tilde{R}}$. We can fix the mixing parameter α by requiring

that the singlets M are free in the IR:

$$\begin{aligned} \tilde{R}[M_j^i] &= R[M_j^i] + \alpha M[M_j^i] = 2 \frac{N_f - N_c}{N_f} + \alpha = 1 \\ \Rightarrow \alpha &= \frac{2N_c - N_f}{N_f} \end{aligned} \quad (1.12)$$

Then the IR dynamics of SQCD for $N_c + 1 < N_f < \frac{3}{2}N_c$ is described by a dual theory that contains weakly interacting quarks and free chirals.

So far our understanding of the dynamics of SQCD as we vary the number of flavors is summarized in the following image:



There are two more values of flavor number N_f that we still need to study, namely $N_f = N_c$ and $N_f = N_c + 1$.

1.1 $N_f = N_c$: quantum deformed moduli space

Let us look for an effective description of SQCD with $N_f = N_c$ in terms of the gauge invariant composites of the theory. For $N_f = N_c$ the (anti-)baryons are given by:

$$B = \det(Q), \quad \tilde{B} = \det(\tilde{Q}) \quad (1.13)$$

and classically satisfy:

$$\det(M) = B\tilde{B} \quad (1.14)$$

Notice that in particular the origin of moduli space where $\langle M \rangle = \langle B \rangle = \langle \tilde{B} \rangle = 0$ satisfies this constraint. At the quantum level this constraint can be modified as follows:

$$\det(M) - B\tilde{B} = \Lambda^{2N_c} \quad (1.15)$$

which is consistent with all the symmetries and includes the holomorphic scale Λ , treated as a spurion. We can enforce such a constraint by introducing an auxiliary field λ that acts as a Lagrange multiplier through an effective superpotential:

$$W = \lambda(\det(M) - B\tilde{B} - \Lambda^{2N_c}) \quad (1.16)$$

By integrating out one flavor and flowing to $N_f = N_c - 1$ the superpotential (1.16) reproduces the correct Affleck-Dine-Seiberg superpotential, therefore (1.16) is the correct effective superpotential for $N_f = N_c$.

Notice that the origin of moduli space c , which is the singular point of the classical moduli space, does not satisfy the quantum corrected constraint (1.15), therefore it is not part of the quantum moduli space. Then the classical moduli space is smoothed out by quantum corrections, and in particular there is no vacuum where the full global symmetry is preserved.

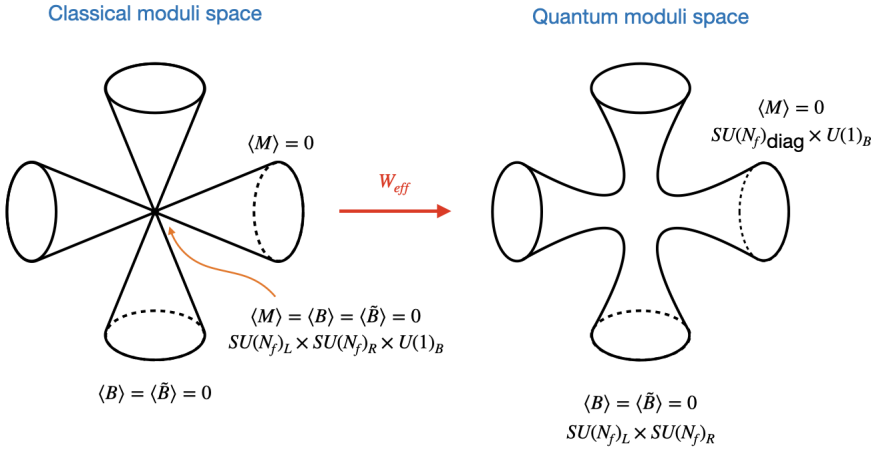
The moduli space includes a mesonic branch:

$$\begin{aligned} \langle M_j^i \rangle &= \Lambda \delta_j^i \\ \langle B \rangle = \langle \tilde{B} \rangle &= 0, \quad SU(N_f)_L \times SU(N_f)_R \rightarrow SU(N_f)_{\text{diag}} \end{aligned} \quad (1.17)$$

and a baryonic branch:

$$\begin{aligned} \langle M_j^i \rangle &= 0 \\ \langle B \rangle = -\langle \tilde{B} \rangle &= \Lambda^{N_c}, \quad U(1)_B \text{ broken} \end{aligned} \quad (1.18)$$

as well as mixed branches where both the mesons and baryons have non-zero vevs. The mesonic and baryonic branches merge smoothly, in contrast to the classical picture:



1.2 $N_f = N_c + 1$: s-confinement

Now consider SQCD with $N_f = N_c + 1$ flavors. The gauge invariant composites are the mesons M_j^i and the baryon and antibaryon which transform in the antifundamental representations of $SU(N_f)_L$ and $SU(N_f)_R$, respectively. The most general effective superpotential is:

$$W_{\text{eff}} = \Lambda^{1-2N_c} (\det(M) - B_i M_j^i \tilde{B}^j) \quad (1.19)$$

One can check that turning on a mass to one flavor and flowing to SQCD with $N_f = N_c$ reproduces the correct superpotential (1.16). The equation of motion for the mesons and baryons of the effective low energy theory impose:

$$\begin{aligned} M \tilde{B} &= B M = 0 \\ \text{minor}(M) - B \tilde{B} &= 0 \end{aligned} \quad (1.20)$$

where $\text{minor}(M)$ is matrix of minors of M_j^i .

The origin of moduli space $\langle M \rangle = \langle B \rangle = \langle \tilde{B} \rangle = 0$ satisfies both constraints and therefore is a vacuum even at the quantum level. Therefore there is a vacuum where the full symmetry group $SU(N_f)_L \times SU(N_f)_R \times U(1)_B$ is preserved.

Therefore the IR dynamics of SQCD with $N_f = N_c + 1$ is fully described by the gauge invariant operators of the theory, mesons and baryons, and preserves all the symmetries including in particular the chiral symmetry. This is an example of confinement without chiral symmetry breaking, and is usually called s(oft)-confinement.

1.3 $N_f = 2N_c$: conformal manifold

Another case worth analyzing in more detail is Seiberg duality for $SU(N_c)$ SQCD with $N_f = 2N_c$, which sits in the middle of the conformal window. For this amount of flavor we have $\tilde{N}_c = N_f - N_c = N_c$, therefore the two phases of Seiberg duality only differ by the presence of singlets and cubic superpotentials. The electric theory has $W_{\text{ele}} = 0$ while in the dual theory there is a non-vanishing superpotential $W_{\text{mag}} = h\text{Tr}(Mq\tilde{q})$, where $M = Q\tilde{Q}$ is the meson of the electric theory that corresponds to an elementary singlet in the magnetic description. This theory can be deformed on the electric side by quartic operators in the gauge invariant combinations of Q and \tilde{Q} . These deformations are exactly marginal, they do not imply any RG flow and they just explore the conformal manifold. Indeed we have:

$$R[Q] = R[\tilde{Q}] = \frac{N_f - N_c}{N_f} = \frac{1}{2} \quad (1.21)$$

therefore at least classically:

$$R[(Q\tilde{Q})^2] = 2 \quad \Rightarrow \quad \Delta[(Q\tilde{Q})^2] = 3 \quad (1.22)$$

which means that quartic deformations are classically marginal.

The quartic deformations could have a non-zero anomalous dimension, spoiling (1.22). In such cases the deformation is called marginally (ir)relevant. The quantum corrections to classically marginal deformations in $\mathcal{N} = 1$ QFTs has been analyzed in generality in [16]. The two main results are:

- In $\mathcal{N} = 1$ 4d QFTs classically marginal deformations are either exactly marginal or marginally irrelevant. In other words the anomalous dimension is non-negative.
- A marginal deformation can fail to be exactly marginal only if it recombines with a conserved current.

More precisely the quantum conformal manifold of a QFT is obtained as the Kähler quotient between the classical conformal manifold and the complexified global symmetry group $G^{\mathbb{C}}$:

$$\mathcal{M} = \frac{\mathcal{M}_{\text{class}}}{G^{\mathbb{C}}} \quad (1.23)$$

The construction of the Kähler quotient is usually involved, but we can infer that our theory has a conformal manifold by a simple counting argument. For large N_f there are $\mathcal{O}(N_f^2)$ conserved currents because the dimension of the adjoint representation of

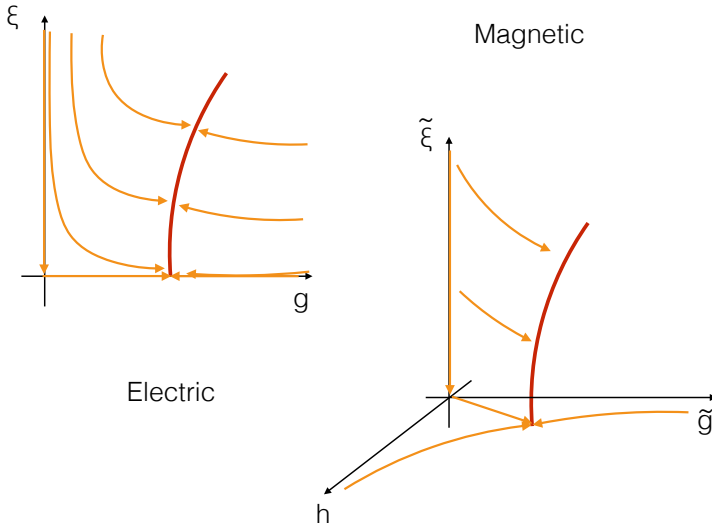


Figure 1.1 On the LHS: couplings of the electric SQCD for $N_f = 2N_c$ SQCD deformed by a quartic superpotential for the quarks. On the RHS couplings of the dual magnetic SQCD for $N_f = 2N_c$ SQCD deformed by a quadratic superpotential for the meson. The red lines represent the dual marginal deformations on both sides of the duality after the addition of the respective deformations.

$SU(N_f)$ is $\dim(\text{Adj}_{N_f}) \sim \mathcal{O}(N_f^2)$. On the other hand we have $\mathcal{O}(N_f^4)$ marginal deformations $Q_i \tilde{Q}^j Q_k \tilde{Q}^l$, therefore for large enough N_f there are not enough conserved currents that can recombine with all the marginal deformations and at least some marginal deformations must be exactly marginal.

For example if we perturb the electric superpotential by $\Delta W_{\text{ele}} = \xi \text{Tr}(Q\tilde{Q})^2$ such an exactly marginal deformation corresponds to one direction in the conformal manifold, emanating from the point $(g, \xi) = (g^*, 0)$ (see the LHS of figure 1.1). This deformation modifies the dual superpotential as $\Delta W_{\text{mag}} = \hat{\xi} \text{Tr} M^2$, which is marginal as well, because of Seiberg duality. Indeed for $N_f = 2N_c$ the singlet M has R-charge $R_M = 1$. Also in this case turning on the deformation correspond to moving on a line of conformal fixed points, emanating in this case from the point $(\tilde{g}, h, \tilde{\xi}) = (\tilde{g}^*, h^*, 0)$ (see the RHS of figure 1.1). Each point along this line is IR dual to the corresponding point in the dual magnetic theory.

We can consider a weaker notion of duality under which all the point on the line are dual, indeed along this line of the conformal manifold the two models share the same central charges, global anomalies and superconformal index. We will refer to these types of duals as *conformal duals*, borrowing the terminology of [24, 25, 26]. Two *conformally dual* theories are not IR dual, and the spectrum and correlation functions can be different, but one can smoothly interpolate between them without triggering RG flows. In this sense $SU(N_c)$ SQCD with $N_f = 2N_c$ and $W = \xi \text{Tr}(Q\tilde{Q})^2$ is *conformally dual* to $SU(N_c)$ SQCD with $N_f = 2N_c$ and $W = h \text{Tr}(Mq\tilde{q})$.

Another crucial point of having a singlet M with R-charge equal to 1 is that this field allows us to write down a (marginal) *mass* deformation in the superpotential. By *integrating out* such a mass term the theory becomes self-dual and Seiberg duality can be considered as an identification between points of the conformal manifold of the theory.

In Chapters 5 through 7 we will analyze the conformal manifolds of 4d toric theories and provide many examples of theories associated to different Type IIB setups that, upon the introduction of an orientifold, flow to different points of the same conformal manifold.

1.4 Seiberg duality for $SO(N_c)$ groups: 1-form symmetries

Several generalizations of Seiberg dualities have been discovered since the original paper [15], for example by considering SQCD with an orthogonal gauge group already discussed in [15] or with a symplectic gauge group [17]. Let us consider the case of orthogonal gauge group, where the flavor are chirals in the vector representation of the gauge group.

The following theories are claimed to be IR dual for $N_f > N_c - 2$:

- SQCD with gauge group $SO(N_c)$ and N_f flavors Q_i and vanishing superpotential.
- SQCD with gauge group $SO(N_f - N_c + 4)$ and N_f flavors q_i and $N_f(N_f + 1)/2$ gauge singlets $M^{i,j}$ with superpotential:

$$W = hQ_iQ_jM^{i,j} \quad (1.24)$$

therefore $M^{i,j}$ transforms in the rank-2 symmetric representation of the non-abelian global symmetry $SU(N_f)$.

SQCD with orthogonal gauge groups presents many phenomena which are qualitatively similar to those encountered in the $SU(N_c)$ case. Here we will focus on an aspect which is qualitatively new, which is due to the fact that $SO(N_c)$ SQCD allows for different global variants of the gauge group. Given a gauge algebra \mathfrak{g} the gauge group could be either the simply connected group G associated to the algebra or a quotient of G by a subgroup H of the center of the algebra G/H . In the case at hand the algebra is either C_n or D_n , and examples of the possible gauge groups are $Spin(N_c)$ or $Spin(N_c)/\mathbb{Z}_2^s = SO(N_c)$. Here \mathbb{Z}_2^s is the element of the center of $Spin(N_c)$ that charges the spinor representations. When the gauge algebra is A_n the possible gauge groups are $SU(n)$ or $SU(n)/\mathbb{Z}_k$, with k a divisor of n . It is important to notice that one can quotient by an element of the center of the gauge algebra only when there are no fields that are charged under that element.

Different global structures for the gauge groups are associated to the presence of non-trivial Wilson-'t Hooft lines [20, 27]. In the case of $SU(N_c)$ SQCD the presence of matter in the fundamental representation screens all the Wilson lines, and the only possible gauge group is $SU(N_c)$. Similarly, we can not quotient by any element of the center \mathbb{Z}_{N_c} of $SU(N_c)$ because the fundamentals are charged under all the elements of the center, with the exception of the identity.

On the other hand in SQCD with orthogonal gauge group there are no fields charged under \mathbb{Z}_2^s , the subgroup of the center that charges the spinorial representation S . Then there are two gauge groups compatible with the matter content, namely $Spin(N_c)$ and $Spin(N_c)/\mathbb{Z}_2^s = SO(N_c)$. Furthermore when performing the \mathbb{Z}_2^s quotient one can add a \mathbb{Z}_2 -valued torsion, which correspond to a topological term in the action called a discrete

theta angle [20]. In total are three choices for the gauge group that correspond to three choices of line operators:

$$\begin{array}{lll}
 Spin(N_c) & SO(N_c)_+ & SO(N_c)_- \\
 \text{Wilson line in } S & \text{'t Hooft line in } S & \text{dyonic line in } S
 \end{array} \tag{1.25}$$

Therefore there are three version of SQCD with gauge algebra $\mathfrak{so}(N_c)$ which have the same local dynamic but differ by the spectrum of line operators. The line operators are charged under a \mathbb{Z}_2 symmetry under which they transform by a phase shift. This symmetry, called a 1-form symmetry, only charges the lines which are extended operators and is an example of a generalized symmetry introduced in [28]. Regular symmetry, called 0-form symmetry in this language, are associated to codimension-1 topological operators that implement the action of the symmetry itself. In the case of continuous 0-form symmetry this operator is given by the integral of the conserved Nöether current over a codimension-1 surface. More generally the topological operators define the symmetry, and we can generalize the notion of symmetries to different codimensions. The 1-form symmetry in this case is generated by codimension-2 topological operators, and their action on the lines is given by the linking number of the codimension-2 surface with the line multiplied with the charge.

Seiberg duality maps these different global structures non-trivially [20]:

$$\begin{aligned}
 Spin(N_c) &\longleftrightarrow SO(N_f - N_c + 4)_- \\
 SO(N_c)_+ &\longleftrightarrow SO(N_f - N_c + 4)_+ \\
 SO(N_c)_- &\longleftrightarrow Spin(N_f - N_c + 4)
 \end{aligned} \tag{1.26}$$

Therefore there is a non-trivial map between the line operators of the electric and magnetic theories.

In Chapters 9 through 11 we will study the global structure for a class of non-lagrangian theories called S-folds. The analysis of [20] does not directly apply because we lack a lagrangian description for many of these theories, therefore we will adopt an alternative approach based on the analysis of the Coulomb branch of these theories presented in [29].

Part I

IR Dualities and Confinement in 3d SQFTs

Aharony duality and the S^3 partition function

2.1 Introduction

In this Part we mainly consider 3d gauge theories with $\mathcal{N} = 2$ supersymmetry (four preserved supercharges). We will study IR dualities between various SCQD theories involving tensorial matter (adjoints, symmetric and antisymmetric), superpotentials (including monopole superpotentials) and s-confining theories. In preparation for the main body of this Part, which consists in Chapter 3 and 4, let us briefly review the most well known IR duality in this context. Aharony duality[30], which relates:

- 3d $U(N_c)$ gauge theory with N_f chiral fields Q_i in the fundamental representation of the gauge group and N_f chiral fields \tilde{Q}_i in the antifundamental representation, with vanishing superpotential:

$$W = 0 \tag{2.1}$$

- 3d $U(N_f - N_c)$ gauge theory with N_f chiral fields q_i in the fundamental representation and N_f chiral fields \tilde{q}_i in the antifundamental representation, with superpotential:

$$W = M_i^{\tilde{j}} q^i q_{\tilde{j}} + v_+ V_- + v_- V_+ \tag{2.2}$$

Here $M_i^{\tilde{j}}$ with $i, j = 1, \dots, N_f$ are singlets under the gauge group and correspond to the mesons of the electric theory:

$$Q_i \tilde{Q}_{\tilde{j}} \rightarrow M_i^{\tilde{j}} \tag{2.3}$$

Similarly, v_{\pm} are singlets of the magnetic gauge group and correspond to the monopole and antimonopole of the electric theory. V_{\pm} are the monopole and antimonopole of the magnetic theory, respectively.

These two theories are IR dual, therefore they describe the same theory in the infrared despite being described by different UV fundamental fields. In particular the gauge groups of the electric and magnetic theories are different for generic values of N_c and N_f . This is not an obstruction for the two gauge theory to be dual because gauge symmetry is a redundancy in the description of a theory. On the other hand, gauge invariant operators must be mapped one to one between the electric and magnetic theories. The

explicit map of gauge invariant operator is:

$$\begin{array}{ccc}
 U(N_c) & & U(N_f - N_c) \\
 Q_i \tilde{Q}_{\bar{j}} & \rightarrow & M_i^{\bar{j}} \\
 \overline{V_{\pm}} & & v_{\pm}
 \end{array} \quad (2.4)$$

where $\overline{V_{\pm}}$ are the monopole and antimonopole of the electric theory. Notice that in the magnetic theory the mesons $q^i \tilde{q}_{\bar{j}}$ and the monopoles V_{\pm} are set to zero by the equation of motion of $M_i^{\bar{j}}$ and v_{\pm} , respectively, therefore they do not contribute to the chiral ring and do not need to be mapped to the electric theory. The global symmetry group must match between the electric and magnetic description. In the case of Aharony duality the full global symmetry group is “visible” in the UV, meaning that the symmetries of the Lagrangian are the same as the symmetries of the IR fixed point. The symmetry group is $SU(N_f) \times \overline{SU(N_f)} \times U(1)_A \times U(1)_T \times U(1)_R$ where $U(1)_T$ is the topological symmetry and $U(1)_R$ is the R-symmetry. The charges of the fields under the global symmetry are as follows:

	$U(1)_R$	$U(1)_A$	$SU(N_f)$	$\overline{SU(N_f)}$	$U(1)_T$
Q	1/2	1	\mathbf{N}_f	$\mathbf{1}$	0
\tilde{Q}	1/2	1	$\mathbf{1}$	\mathbf{N}_f	0
$M_i^{\bar{j}}$	1	2	\mathbf{N}_f	\mathbf{N}_f	0
v_{\pm}	$N_f - N_c + 1$	$-N_f$	$\mathbf{1}$	$\mathbf{1}$	± 1
q	1/2	1	\mathbf{N}_f	$\mathbf{1}$	0
\tilde{q}	1/2	1	$\mathbf{1}$	\mathbf{N}_f	0
$M_i^{\bar{j}}$	1	2	\mathbf{N}_f	\mathbf{N}_f	0
v_{\pm}	$N_f - N_c + 1$	$-N_f$	$\mathbf{1}$	$\mathbf{1}$	± 1
V_{\pm}	$N_c - N_f + 1$	N_f	$\mathbf{1}$	$\mathbf{1}$	± 1

(2.5)

which is compatible with the operator map (2.4) and the superpotential of the magnetic theory.

Generally it is possible that for one or both of the gauge theories the full global symmetry group of the IR fixed point is not visible in the UV and only emerges in the IR. When this is the case the two lagrangian descriptions appear to describe different IR fixed points, and more care is required. On the other hand the emergent symmetries of one of the phases often appear as symmetries of the lagrangian description of the other phase. Then the duality can be used as an indicator of the emergence of a symmetry in the IR. A notable example in this regard is the so-called E_7 surprise [31], a theory where the global symmetry enhances to E_7 in the IR. The enhancement can be inferred from a web of self-dualities of the theory.

It is interesting to consider variations of Aharony duality, for example one can modify the electric theory in the following ways:

- Introduce a Chern-Simons term for the gauge group. The resulting duality is known as Giveon-Kutasov duality [32].
- Consider a different amount of fundamental and antifundamental chiral fields, see [33].
- Consider other gauge groups, for example $SU(N_c)$, $SO(N_c)$ and $USp(2N_c)$, see for

example [34, 35, 36].

- Introducing a non-trivial superpotential to the electric theory.
- Introducing matter in tensorial representation of the gauge group [37, 38, 39].

In particular the dimensional reduction from 4d theories on $S^3 \times S^1$ to 3d theories on S^3 , naturally started from Seiberg duality for SQCD [15] with unitary gauge group, has been extended in various directions, either considering 4d dualities with real gauge groups [18, 17], or a rank-two tensor matter field with a power law superpotential [40] or both [41, 42]. It is sometimes possible to trigger an RG flow in the electric theory and follow the flow on the magnetic theory, obtaining a new pair of dual models. This opens two main possibilities in the study of dualities. The first one is to look for new dualities by deforming known dualities, often by triggering an RG flow to a new IR fixed point. The second is to relate different dualities, creating a web where some dualities can be considered as a consequence of other dualities. Notice that such a web is not necessarily unidirectional, for example Giveon-Kutasov duality can be obtained from Aharony duality with a suitable RG flow [43], but the opposite is true as well [44]. In Chapter 3 we explore the duality web involving gauge theories with two adjoint matter fields and a D-type superpotential, which generalizes a similar picture for theories with one adjoint matter field and A-type superpotential [45, 46, 37].

An interesting possibility is that the dual model is described in terms of the confined degrees of freedom of the original one. When this happens without breaking global symmetries the electric theory is said to s-confine. Such phenomena often occur as a limiting case of a duality, that is by suitably choosing N_c and N_f , see for example the case of 4d SQCD with $N_f = N_c + 1$ flavors discussed in Chapter 1. In the 4d $\mathcal{N} = 1$ case with a single gauge group with $W = 0$ a systematic classification has been proposed by [47, 48], and elaborating on that results many other examples have been found. Many examples of this phenomenon in the 3d $\mathcal{N} = 2$ case can be obtained through the circle compactification of the 4d parent cases, along the lines of [49]. In s-confining dualities fundamental degrees of freedom of the magnetic theory correspond to gauge invariant operators of the electric theory, in this regard s-confining dualities represent an explicit realization of the fact that gauge symmetries are a redundancy of a particular description of a field theory. Finding s-confining theories will be a major goal of the study of 3d field theories carried out in this Section, in particular in Chapter 4, where we will analyze gauge theories with orthogonal or symplectic gauge groups, adjoint matter and monopole superpotential.

The main results of this Part of the thesis can be classified in three categories:

- New dualities between 3d gauge theories.
- Relations between known dualities.
- Checks of dualities.

The checks of dualities consist in computing some property of the IR fixed point from the two UV descriptions and matching the results between them. We already discussed examples of such checks for Aharony duality in the form of the map of gauge invariant operators and the match of the global symmetries. Another precision check that has been extremely useful in the literature is the computation of the euclidean partition function on S^3 via localization techniques. The partition function of lagrangian $\mathcal{N} = 2$ gauge theories can be computed exactly and can be further refined by introducing fugacities

for the global symmetries. The computation and matching of the partition function represents arguably the most precise and reliable check of dualities available, and we will discuss it in the next Section.

Alongside RG flows and dimensional reduction another interesting approach to study the relations between dualities is the confinement/deconfinement procedure [50]. More generally, one can perform a local duality on certain fields of a theory. This provides an alternative UV description for the physics associated to those fields, while other fields are still described by the original lagrangian. As an example if we consider a gauge theory with two gauge groups we may apply a duality to only one of the gauge groups, provided that a dual description of the gauge group with the correct matter content and superpotential is known. An iterative application of such local dualities provides a large amount of dual phases and can be exploited to obtain a new duality from the knowledge of the local dualities. This procedure has proven to be particularly insightful when the “local” dualities are confining dualities. As an example, all the 4d s-confining theories with a single gauge groups and vanishing superpotential can be “proven” to confine from iterative application of Seiberg and Intriligator-Pouliot dualities [51]. We will exploit this procedure in Chapter 4 as a consistency check for the new confining dualities that we study there.

2.2 Three-sphere partition function

In this section we report some useful facts on the analysis of the three sphere partition function that play a central role in our analysis of 3d $\mathcal{N} = 2$ theories. The euclidean partition function on the squashed three sphere S^3 can be computed exactly for $\mathcal{N} = 2$ theories via the localization technique [52, 53, 54, 55]. The infinite dimensional path integral reduces to a finite dimensional matrix integral over a vector $\vec{\sigma}$ representing the scalar field in the Cartan of the gauge group. The functions that appear in the integrand are the one loop determinants of the chiral and vector multiplets and they can be formulated in terms of hyperbolic Gamma functions. These are defined as

$$\Gamma_h(x; \omega_1, \omega_2) \equiv \Gamma_h(x) \equiv e^{\frac{\pi i}{2\omega_1\omega_2} \left((x-\omega)^2 - \frac{\omega_1^2 + \omega_2^2}{12} \right)} \prod_{j=0}^{\infty} \frac{1 - e^{\frac{2\pi i}{\omega_1}(\omega_2 - x)} e^{\frac{2\pi i \omega_2 j}{\omega_1}}}{1 - e^{-\frac{2\pi i}{\omega_2}x} e^{-\frac{2\pi i \omega_1 j}{\omega_2}}}. \quad (2.6)$$

where $\omega_1 = ib$ and $\omega_2 = i/b$ are related to the squashing parameter of the three sphere, defined by the equation $b^2(x_1^2 + x_2^2) + b^{-2}(x_3^2 + x_4^2) = 1$. The parameter ω is defined as $2\omega = \omega_1 + \omega_2$. The other argument corresponds to the sum of the weights of the representation of each field with respect to the scalar in the gauge multiplet $\vec{\sigma}$ and the scalar obtained by weakly gauging the flavor symmetries (corresponding to the real masses in the field theory language). There are also classical contributions to the integral, arising from CS and FI terms. As an example the partition function of a $U(n)$ gauge theory with vanishing CS level, FI parameter ξ and N_f fundamental and antifundamental fields is given by:

$$\begin{aligned} Z_{U(N_c)}^{N_f}(\vec{\mu}; \vec{\nu}; \xi) &= \frac{1}{\sqrt{-\omega_1\omega_2}^{N_c} N_c!} \int \prod_{i=1}^{N_c} d\sigma_i e^{-2i\pi\xi\sigma_i} \prod_{a=1}^{N_f} \Gamma_h(\sigma_i + \mu_a) \Gamma_h(-\sigma_i + \nu_a) \\ &\times \prod_{i < j} \frac{1}{\Gamma_h(\pm(\sigma_i - \sigma_j))} \end{aligned} \quad (2.7)$$

where we use the shortcut notation:

$$\Gamma_h(a \pm b) = \Gamma_h(a + b)\Gamma_h(a - b) \quad (2.8)$$

The Gamma functions in the first row are the contributions of the 1-loop determinants of the fundamental and antifundamental fields, while the Gamma functions at the denominator of the second row are the 1-loop determinants of the vector multiplet in the adjoint representation. The fugacities $\vec{\mu}$ and $\vec{\nu}$ are associated to the $SU(f) \times SU(f) \times U(1)_A$ global symmetry under which the fundamental fields are charged, therefore they satisfy:

$$\sum_{i=1}^{N_f} \mu_i = \sum_{i=1}^{N_f} \nu_i = m_A \quad (2.9)$$

and the FI parameter ξ is the fugacity for the topological symmetry $U(1)_T$. As discussed above this theory is Aharony dual to a magnetic $U(\tilde{N}_c)$ gauge theory with N_f flavors and singlets $M_i^{\tilde{j}}$ and v_{\pm} . Aharony duality implies the identity of the partition functions of the electric and magnetic theories:

$$\begin{aligned} Z_{U(N_c)}^{N_f}(\vec{\mu}; \vec{\nu}; \xi) &= Z_{U(\tilde{N}_c)}^{N_f}(\omega - \vec{\mu}; \omega - \vec{\nu}; -\xi) e^{\frac{i\pi}{2\omega_1\omega_2}(\lambda \sum_{r=0}^{n+m-1}(\mu_r - \nu_r))} \\ &\quad \sum_{i,j=1}^{N_f} \Gamma_h(\mu_i + \nu_j) \Gamma_h \left((N_f + N_c + 1)\omega - \frac{1}{2} \sum_{r=0}^{n+m-1} (\mu_r + \nu_r) \pm \frac{\xi}{2} \right) \end{aligned} \quad (2.10)$$

with $\tilde{N}_c = N_f - N_c$. The identity (2.10) is known to hold [56], providing a precision check of Aharony duality.

Finally it is interesting to notice that the presence of a superpotential only affect the three sphere partition function through a constraint on the fugacities. This will be important when studying theories with a monopole superpotential in the next Chapters.

If an RG flow is triggered it is useful to follow it on the partition function. For example a flow triggered by a large mass can be implemented by taking a the limit where some combinations of the fugacities μ_a, ν_a are large. A useful formula in practical applications is the following:

$$\lim_{|x| \rightarrow \infty} \Gamma_h(x) = e^{-\frac{i\pi}{2} \text{sign}(x)(x-\omega)^2} \quad (2.11)$$

Large fugacity limits usually produce divergent phases from (2.11), we have to provide an Higgs flow on the dual side such that these divergent phases cancel between the electric and magnetic theories. This reflects in a large mass limit for the parameters associated to the gauge algebra $\vec{\sigma}$, corresponding to the real scalar in the vector multiplet. This is a delicate step, because it requires to commute limits and integral and some care is necessary. The new gauge sector created by such a dual Higgsing are then usually associated to confining gauge theories. Locally dualizing these sectors corresponds to computing the associated integrals.

Another useful formula is the inversion formula for the hyperbolic Gamma functions $\Gamma_h(2\omega - x)\Gamma_h(x) = 1$. This formula corresponds in field theory to integrate fields appearing in the superpotential through a holomorphic mass term. Notice that no diver-

gent phase is generated when a holomorphic mass term is introduced.

Webs of 3d $\mathcal{N} = 2$ dualities with D-type superpotentials

In this Chapter we study 3d $\mathcal{N} = 2$ $U(n)$ SQCD with two adjoints and $USp(2n)$ SQCD with two rank-two antisymmetric tensors, recovering some of the results already found in the literature and finding new dualities. We exploit the construction of 3d $\mathcal{N} = 2$ dualities from the dimensional reduction of 4d $\mathcal{N} = 1$ parents on S^1 which been a fertile field of research recently (see [57, 58, 49, 59, 60, 38, 61, 62, 63, 64, 65, 66, 67, 68, 69, 37, 70, 71] for a partial list of references). Furthermore the possibility of engineering real mass flows in 3d has been crucial for constructing large webs of dualities without a 4d counterpart.

Cases with two rank-two tensors are less studied [45, 46], and only quite recently the case of $U(n)$ SQCD has been investigated [37]. The 4d duality shows indeed some differences with respect to the cases with a single or without any adjoint. For example the chiral ring is conjectured to be truncated at quantum level in some cases and this duality does not have a brane engineering in the Hanany-Witten setup [72] so far.

The analysis of [37] was based on the general 4d/3d prescription of [49]: the authors obtained first an effective duality on S^1 and then they arrived to the pure 3d limit by a real mass flow. Similarly to the analysis performed in the case with a single adjoint in [38] the construction was pursued by breaking the $U(n)$ gauge group in a product of $U(n_i)$ SQCD sectors and then using known results from the reduction of 4d Seiberg duality to 3d $U(n)$ Aharony duality [30]. Eventually the unbroken gauge theory was reconstructed and the 3d duality was proposed. Then in a more recent paper [39] a generalization of this duality, adding linear superpotentials for the monopole and the anti-monopole with topological charge one, has been claimed, generalizing the ordinary SQCD construction of [67] and the case with an adjoint of [70]. In the case with two adjoints it was observed that there is a second type of superpotential, for the monopole and the anti-monopole with topological charge two. Non trivial checks have been done by comparing the expansion of the 3d superconformal index of [73] up to very high orders in the fugacities. This is the state of the art in the analysis of 3d $\mathcal{N} = 2$ SQCD with two adjoints. The large web of dualities obtained for other families of SQCD-like models has not been studied yet and further generalizations in this direction are desirable.

We start our analysis with the case of 4d $USp(2n)$ SQCD with $2N_f$ fundamentals and two rank-two antisymmetric tensors A and B and superpotential $W = AB^2 + A^{k+1}$. This model was studied in [46] and it was shown to be dual to $USp(2(3kN_f - n - 4k - 2))$ SQCD, with a similar matter content and a non trivial superpotential involving the dressed symmetric and anti-symmetric mesons of the electric model. This model is the

starting point of our analysis because it leads to the 3d dualities discussed in [37] and [39], through dimensional reduction and real mass flows. By circle reduction we first obtain an effective duality, with a KK monopole superpotential turned on. Then through a real mass and a Higgs flow on both the electric and the magnetic side we arrive at the 3d $U(n)$ duality recently discovered in [39] with two linear superpotential deformations, for the bare monopole V_+ and anti-monopole V_- respectively.

The next step consists of eliminating the monopole deformations. This is the more delicate and intricate step of our construction, because it requires a dual Higgsing of the gauge group. This dual Higgsing produces extra gauge sectors that are expected to be dual to singlets. We conjecture the existence of such confining dualities, involving $U(k-1)$ SQCD with one flavor, two adjoints X and Y and superpotential $W = XY^2 + Y^{k+1} + V_{\pm}$. By the help of this confining duality we remove either the linear monopole (or anti-monopole) superpotential or both from the $U(n)$ model. In the first case we obtain a new duality, that reduces in the limiting case to the conjectured confining duality discussed above. In the second case we find the pure 3d duality obtained in [37] by reducing the 4d Brodie duality with $U(n)$ gauge group.

Eventually we can also remove the KK monopole superpotential from the $Usp(2n)$ duality, finding another new duality for pure 3d $Usp(2n)$ with two rank-two antisymmetric tensors. Also in this last case we observe that the confining sector, obtained after the dual Higgsing, corresponds to the limiting case of the 3d $U(n)$ duality with a linear monopole superpotential turned on.

For ease of reading we have summarized the various flows and dualities illustrated in this introduction in figure 3.1. We stress that this figure can be compared with the ones appearing in [70] for the cases of $U(n)$ SQCD and $Usp(2n)$ SQCD with an adjoint. The search for such a homogenous picture for the web generated by the reduction of 4d Brodie and Brodie-Strassler duality was one of the main motivations of our work.

A central role in our analysis is played by the study of the 4d superconformal index and by the 3d three sphere partition function [52, 53, 54, 55]. Indeed we will show that each step taken on the field theory side can be reproduced by localization. Nevertheless, as already stressed in the case with a single adjoint, the 4d identities relating the superconformal indices of Brodie and Brodie-Strassler dualities are conjectural. At large n the 4d superconformal index of [74] has been matched in [75], while a complete proof of such relation still lacks for finite n .

Anyway, starting from such conjectural identities we can obtain the 3d identities for the $U(n)$ and the $Usp(2n)$ cases with a KK monopole turned on, using the procedure of [49]. All the other steps, corresponding to real mass flow and Higgs flow on the field theory side, can be studied on the partition function by considering large limits for some of the parameters. If the divergent terms cancel in the identities we remain with a finite result that can be interpreted as the new duality obtained after the flow.

In all of the derivation we have conjectured an identity, relating $U(k-1)$ with two adjoints and a linear monopole superpotential and a set of (interacting) singlets. As a consistency check we have obtained this identity as a limiting case of a more general duality and we have recovered the integral identities for the partition functions for dualities already checked in terms of the superconformal index in the literature.

3.1 Known dualities with D-type superpotential

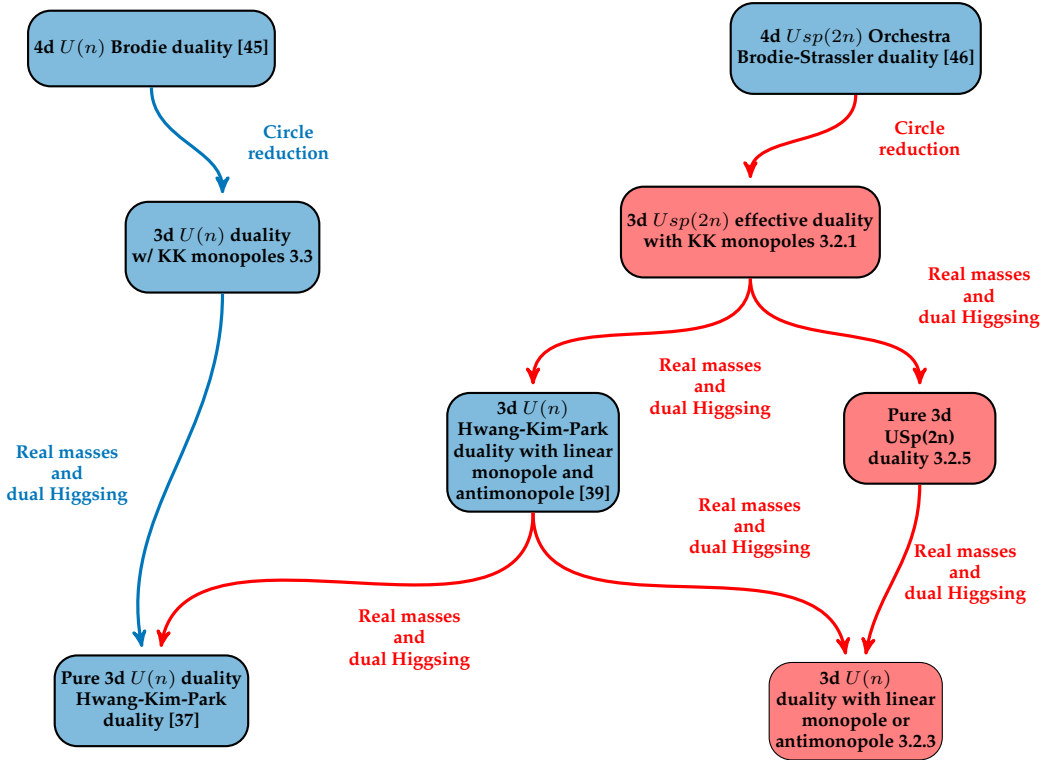


Figure 3.1 Survey of the dualities and the flows studied in this thesis. The blue boxes and arrows represents dualities and flows that have already been proposed and studied in the literature. The red boxes and arrows represent the dualities and the flows proposed and analyzed here.

3.1.1 The 4d dualities

The original duality of [45] relates

- 4d $SU(n)$ SQCD with F flavors Q and \tilde{Q} with two adjoints X and Y interacting through the superpotential

$$W = \text{Tr} XY^2 + \text{Tr} X^{k+1} \quad (3.1)$$

with k odd.

- 4d $SU(\tilde{n} = 3kF - n)$ SQCD with F dual flavors q and \tilde{q} with two adjoints x and y interacting through the superpotential

$$W = \text{Tr} xy^2 + \text{Tr} x^{k+1} + \sum_{j=0}^{k-1} \sum_{\ell=0}^2 \text{Tr} \mathcal{M}_{j,\ell} q x^{k-1-j} y^\ell \tilde{q} \quad (3.2)$$

where the singlets $\mathcal{M}_{j,\ell}$ correspond under the duality map to the dressed mesons $QX^jY^\ell\tilde{Q}$ for $j = 0, \dots, k-1$ and $\ell = 0, 1, 2$ of the electric phase.

The non anomalous global symmetry is $SU(f)_L \times SU(f)_R \times U(1)_B \times U(1)_R$. The fields transform under the gauge and global symmetries as follows:

Field	$SU(n)$	$SU(\tilde{n})$	$SU(f)_L$	$SU(f)_R$	$U(1)_B$	$U(1)_R$
Q	n	1	f	1	1	$1 - \frac{n}{f(k+1)}$
\tilde{Q}	\tilde{n}	1	1	\tilde{f}	-1	$1 - \frac{n}{\tilde{f}(k+1)}$
X	$n^2 - 1$	1	1	1	0	$\frac{2}{k+1}$
Y	$n^2 - 1$	1	1	1	0	$\frac{k}{k+1}$
q	.1	\tilde{n}	\tilde{f}	1	$\frac{n}{\tilde{n}}$	$1 - \frac{\tilde{n}}{\tilde{f}(k+1)}$
\tilde{q}	1	\tilde{n}	1	f	$-\frac{n}{\tilde{n}}$	$1 - \frac{\tilde{n}}{f(k+1)}$
x	1	$\tilde{n}^2 - 1$	1	1	0	$\frac{2}{k+1}$
y	1	$\tilde{n}^2 - 1$	1	1	0	$\frac{k}{k+1}$
$\mathcal{M}_{j\ell}$	1	1	f	\tilde{f}	0	$2 - \frac{2}{k+1} + \frac{2(\ell-1)+k(j-1)}{k+1}$

(3.3)

Here we are actually interested in the $U(n)$ version of this duality, which is obtained by the standard procedure of gauging the baryonic symmetry, normalized opportunely, in both the electric and in the magnetic phase.

The other 4d dualities necessary for our analysis was found in [46] and it relates

- $Usp(2n)$ SQCD with $2f$ fundamentals Q and two rank-two antisymmetric tensors A and B interacting through a superpotential

$$W = \text{Tr} A^{k+1} + \text{Tr} AB^2 \quad (3.4)$$

- $USp(2\tilde{n} = 2(3kf - n - 4k - 2))$ SQCD with $2f$ fundamentals q , two rank-two antisymmetric¹ tensors a and b and the dressed mesons $M_{rs}^{(j,\ell)} = Q_r A^j B^\ell Q_s$ sym-

¹Here we refer to the reducible antisymmetric representation, made out of an irreducible traceless tensor

metric (antisymmetric) for $j\ell$ odd (even) with $j = 0, \dots, k-1$ and $\ell = 0, 1, 2$. The superpotential of the dual phase is

$$W = \text{Tr} a^{k+1} + \text{Tr} ab^2 + \sum_{j=0}^{k-1} \sum_{\ell=0}^2 M_{j\ell} qa^{k-j-1} b^{2-\ell} q \quad (3.5)$$

where the singlets $\mathcal{M}_{j,\ell}$ correspond under the duality map to the dressed mesons $QX^jY^\ell Q$ for $j = 0, \dots, k-1$ and $\ell = 0, 1, 2$ of the electric phase. Furthermore k here is required to be odd, otherwise the global anomalies do not match.

The non anomalous global symmetry is $SU(2f) \times U(1)_B \times U(1)_R$. The fields transform under the gauge and global symmetries as follows:

Field	$Usp(2n)$	$USp(2\tilde{n})$	$SU(2f)$	$U(1)_R$
Q	n	1	$2f$	$1 - \frac{n+2k+1}{f(k+1)}$
A	$n(2n-1)$	1	1	$\frac{2}{k+1}$
B	$n(2n-1)$	1	1	$\frac{k}{k+1}$
q	1	\tilde{n}	$\overline{2f}$	$1 - \frac{n+2k+1}{f(k+1)}$
a	1	$\tilde{n}(2\tilde{n}-1)$	1	$\frac{2}{k+1}$
b	1	$\tilde{n}(2\tilde{n}-1)$	1	$\frac{k}{k+1}$
$\mathcal{M}_{j0} (j = 0, \dots, k-1)$	1	1	$f(2f-1)$	$2 - \frac{2(n+2k+1)}{f(k+1)} + \frac{2j}{k+1}$
$\mathcal{M}_{2j1} (j = 0, \dots, \frac{k-1}{2})$	1	1	$f(2f-1)$	$2 - \frac{2(n+2k+1)}{f(k+1)} + \frac{4j+k}{k+1}$
$\mathcal{M}_{2j+11} (j = 0, \dots, \frac{k-3}{2})$	1	1	$f(2f+1)$	$2 - \frac{2(n+2k+1)}{f(k+1)} + \frac{4j+k+2}{k+1}$
$\mathcal{M}_{j2} (j = 0, \dots, k-1)$	1	1	$f(2f-1)$	$2 - \frac{2(n+2k+1)}{f(k+1)} + \frac{2j+2k}{k+1}$

(3.6)

The 4d dualities discussed here can be translated in integral identities between the superconformal index of the electric and of the magnetic phase. These identities have been conjectured in [77] for the $SU(n)$ and the $Usp(2n)$ dualities. The identity for the $SU(n)$ duality corresponds to the equivalence between the integral

$$I_{SU(n)} = \frac{(p,p)^{n-1}(q,q)^{n-1}}{n!} \Gamma_e^{n-1}(u) \Gamma_e^{n-1}(u^{\frac{k}{2}}) \quad (3.7)$$

$$\times \int \prod_{\alpha=1}^n \frac{dz_\alpha}{2\pi i z_\alpha} \prod_{a=1}^f \Gamma_e(s_a z_\alpha) \Gamma_e(t_a^{-1} z_\alpha^{-1}) \prod_{1 \leq \alpha < \beta \leq n} \frac{\Gamma_e(u(z_\alpha/z_\beta)^{\pm 1}) \Gamma_e(u^{\frac{k}{2}}(z_\alpha/z_\beta)^{\pm 1})}{\Gamma_e((z_\alpha/z_\beta)^{\pm 1})}$$

with $\prod_{\alpha=1}^n z_\alpha = 1$, $u = (pq)^{\frac{1}{k+1}}$ and the integral

$$I_{SU(\tilde{n})} = \frac{(p,p)^{\tilde{n}-1}(q,q)^{\tilde{n}-1}}{\tilde{n}!} \Gamma_e^{\tilde{n}-1}(u) \Gamma_e^{\tilde{n}-1}(u^{\frac{k}{2}}) \prod_{j=0}^{k-1} \prod_{\ell=0}^2 \prod_{a,b=1}^f \Gamma_e(u^{\frac{2j+\ell k}{2}} s_a/t_b) \quad (3.8)$$

$$\times \int \prod_{\alpha=1}^{\tilde{n}} \frac{dz_\alpha}{2\pi i z_\alpha} \prod_{a=1}^f \Gamma_e(\tilde{s}_a z_\alpha^{-1}) \Gamma_e(\tilde{t}_a^{-1} z_\alpha) \prod_{1 \leq \alpha < \beta \leq \tilde{n}} \frac{\Gamma_e(u(z_\alpha/z_\beta)^{\pm 1}) \Gamma_e(u^{\frac{k}{2}}(z_\alpha/z_\beta)^{\pm 1})}{\Gamma_e((z_\alpha/z_\beta)^{\pm 1})}$$

and a singlet. See [76] for a more complete discussion on this subtlety.

with $\prod_{\alpha=1}^{\tilde{n}} z_{\alpha} = 1$, $\tilde{s}_{\alpha} = u^{\frac{2-k}{2}} \prod_{a=1}^f (s_a t_a)^{\frac{3k}{2n}} s_a^{-1}$ and $\tilde{t}_{\alpha}^{-1} = u^{\frac{2-k}{2}} \prod_{a=1}^f (s_a t_a)^{-\frac{3k}{2n}} t_a$.

In this thesis we skip most of the details of the index, referring the reader to [78] for conventions. For completeness we just report the definitions of the q-Pochhammer symbols and of the elliptic Gamma functions

$$(x; p) \equiv \prod_{j=0}^{\infty} (1 - xp^j), \quad \Gamma_e(z) \equiv \prod_{j,k=0}^{\infty} \frac{1 - p^{j+1} q^{k+1} / z}{1 - zp^j q^k} \quad (3.9)$$

The arguments appearing in these functions are fugacities associated to the symmetries. For example p and q are associated to the isometries of S^3 , z_{α} are associated to the gauge symmetry and the other fugacities refer to the matter fields. The fugacities are constrained by the anomaly cancellation as

$$u^n \prod_{a=1}^f s_a t_a^{-1} = (pq)^f \quad (3.10)$$

This relation, commonly referred as balancing condition, is required for the validity of the integral identity. Observe that here we will be interested in the $U(n)$ version of the duality. As explained in [49] the $U(n)$ identity can be obtained by gauging the baryonic symmetry, i.e. by integrating over the corresponding fugacity and by turning on the contribution of the FI term.

Similarly the $U_{Sp}(2n)$ duality corresponds to the equivalence between the integral

$$\begin{aligned} I_{U_{Sp}(2n)} &= \frac{(p, p)^n (q, q)^n}{2^n n!} \Gamma_e^n(u) \Gamma_e^n(u^{\frac{k}{2}}) \\ &\times \int \prod_{\alpha=1}^n \frac{dz_{\alpha}}{2\pi i z_{\alpha}} \frac{\prod_{a=1}^{2f} \Gamma_e(s_a z_{\alpha}^{\pm 1})}{\Gamma_e(z_{\alpha}^{\pm 2})} \prod_{1 \leq \alpha < \beta \leq n} \frac{\Gamma_e(u z_{\alpha}^{\pm 1} z_{\beta}^{\pm 1}) \Gamma_e(u^{\frac{k}{2}} z_{\alpha}^{\pm 1} z_{\beta}^{\pm 1})}{\Gamma_e(z_{\alpha}^{\pm 1} z_{\beta}^{\pm 1})} \end{aligned} \quad (3.11)$$

with the balancing condition

$$u^{n+2k+1} \prod_{a=1}^{2f} s_a = (pq)^f \quad (3.12)$$

and the integral

$$\begin{aligned} I_{U_{Sp}(2\tilde{n})} &= \frac{(p, p)^{\tilde{n}} (q, q)^{\tilde{n}}}{2^{\tilde{n}} \tilde{n}!} \Gamma_e^{\tilde{n}}(u) \Gamma_e^{\tilde{n}}(u^{\frac{k}{2}}) \prod_{j=0}^{k-1} \prod_{\ell=0}^2 \prod_{a < b} \Gamma_e(u^{\frac{2j+k\ell}{2}} s_a s_b) \prod_{q=0}^{\frac{k-3}{2}} \prod_{a=1}^{2f} \Gamma_e(u^{2q+1+\frac{k}{2}} s_a^2) \\ &\times \int \prod_{\alpha=1}^{\tilde{n}} \frac{dz_{\alpha}}{2\pi i z_{\alpha}} \frac{\prod_{a=1}^{2f} \Gamma_e(u^{1-\frac{k}{2}} / s_a z_{\alpha}^{\pm 1})}{\Gamma_e(z_{\alpha}^{\pm 2})} \prod_{1 \leq \alpha < \beta \leq \tilde{n}} \frac{\Gamma_e(u z_{\alpha}^{\pm 1} z_{\beta}^{\pm 1}) \Gamma_e(u^{\frac{k}{2}} z_{\alpha}^{\pm 1} z_{\beta}^{\pm 1})}{\Gamma_e(z_{\alpha}^{\pm 1} z_{\beta}^{\pm 1})} \end{aligned} \quad (3.13)$$

3.1.2 The 3d dualities

The 3d duality obtained in [37] from the dimensional reduction of Brodie duality relates

- 3d $U(n)$ SQCD with f flavors Q and \tilde{Q} with two adjoints X and Y interacting through the superpotential

$$W = \text{Tr} XY^2 + \text{Tr} X^{k+1} \quad (3.14)$$

with k odd.

- 3d $U(\tilde{n} = 3kf - n)$ SQCD with f dual flavors q and \tilde{q} with two adjoints x and y interacting through the superpotential

$$\begin{aligned} W = & \text{Tr} xy^2 + \text{Tr} x^{k+1} + \sum_{j=0}^{k-1} \sum_{\ell=0}^2 \text{Tr} \mathcal{M}^{j,\ell} q x^{k-1-j} y^{2-\ell} \tilde{q} \\ & + \sum_{j=1}^{k-1} V_{j,0}^{\pm} \tilde{V}_{k-j,0}^{\pm} + \sum_{\ell=0}^2 V_{0,\ell}^{\pm} \tilde{V}_{0,2-\ell}^{\pm} + \sum_{q=0}^{\kappa=\frac{k-3}{2}} W_q^{\pm} \tilde{W}_{\kappa-q}^{\pm} \end{aligned} \quad (3.15)$$

where the mesons correspond to the one discussed on the 4d side. There are also dressed monopoles operators of the electric theory, carrying topological charge 1 and 2, denoted as $V_{j,\ell}^{\pm}$ and W_q^{\pm} respectively, acting as singlets in the dual phase, interacting through (3.15) with the dual dressed monopoles, carrying topological charge 1 and 2, denoted as $\tilde{V}_{j,\ell}^{\pm}$ and \tilde{W}_q^{\pm} respectively. These monopole operators are defined by radial quantization from states on S^2 carrying a non trivial magnetic flux background. The dressed monopole are then mapped to the following states

$$\begin{aligned} V_{j,\ell}^{\pm} & \leftrightarrow \text{Tr} X^j Y^{\ell} | \pm 1, 0, \dots, 0 \rangle \\ W_q^{\pm} & \leftrightarrow \text{Tr} X^{2q} | \pm 1, \pm 1, 0, \dots, 0 \rangle \end{aligned} \quad (3.16)$$

and an analogous definition is given for the monopoles appearing in the dual phase. As stressed in [37] the appearance of the W_q^{\pm} and \tilde{W}_q^{\pm} monopoles is one of the most interesting novelties of models with two adjoints that does not have a counterpart in any supersymmetric duality worked out so far.

The global symmetry is $SU(f)_L \times SU(f)_R \times U(1)_A \times U(1)_T \times U(1)_R$. The fields and the

monopoles transform under the gauge and global symmetries as follows:

Field	$U(n)$	$U(\tilde{n})$	$SU(f)_L$	$SU(f)_R$	$U(1)_A$	$U(1)_T$	$U(1)_R$
Q	n	1	f	1	1	0	r
\tilde{Q}	\bar{n}	1	1	\bar{f}	1	0	r
X	n^2	1	1	1	0	0	$\frac{2}{k+1}$
Y	n^2	1	1	1	0	0	$\frac{k}{k+1}$
$V_{j\ell}^\pm$	1	1	1	1	$-f$	± 1	$(1-r)f + \frac{2j+k\ell-(n-1)}{k+1}$
W_q^\pm	1	1	1	1	$-2f$	± 2	$2(1-r)f + \frac{2+4q-2(n-1)}{k+1}$
q	1	$\bar{\tilde{n}}$	\bar{f}	1	-1	0	$\frac{2-k}{k+1} - r$
\tilde{q}	1	\tilde{n}	1	f	-1	0	$\frac{2-k}{k+1} - r$
x	1	\tilde{n}^2	1	1	0	0	$\frac{2}{k+1}$
y	1	\tilde{n}^2	1	1	0	0	$\frac{k}{k+1}$
$\mathcal{M}_{j\ell}$	1	1	f	\bar{f}	2	0	$2r + \frac{2j+k\ell}{k+1}$
$\tilde{V}_{j\ell}^\pm$	1	1	1	1	f	∓ 1	$(r-1)f + \frac{2j+k\ell+(n+1)}{k+1}$
\tilde{W}_q^\pm	1	1	1	1	$2f$	∓ 2	$2(r-1)f + \frac{2+4q+2(n+1)}{k+1}$

(3.17)

Another useful duality was obtained in the more recent paper [39]. It relates

- 3d $U(n)$ SQCD with F flavors Q and \tilde{Q} with two adjoints X and Y interacting through the superpotential

$$W = \text{Tr} XY^2 + \text{Tr} X^{k+1} + V_{0,0}^+ + V_{0,0}^- \quad (3.18)$$

with k odd.

- 3d $U(\tilde{n} = 3kf - n - 4k - 2)$ SQCD with F dual flavors q and \tilde{q} with two adjoints x and y interacting through the superpotential

$$W = \text{Tr} xy^2 + \text{Tr} x^{k+1} + \sum_{j=0}^{k-1} \sum_{\ell=0}^2 \text{Tr} \mathcal{M}^{j,\ell} q x^{k-1-j} y^{2-\ell} \tilde{q} + \tilde{V}_{0,0}^+ + \tilde{V}_{0,0}^- \quad (3.19)$$

where the mesons are defined as above

In this case the monopole superpotentials (3.18) and (3.19) break the axial and the topological symmetry. Furthermore they fix the R -charge r in (3.17) to $r = 1 - \frac{n+2k+1}{k+1}$, that can be computed from $R[V_{0,0}] = R[\tilde{V}_{0,0}] = 2$.

Another duality studied in [39], involves $U(n)$ with the linear monopole and anti-monopole superpotential for $W_{0,0}^\pm$ and $\tilde{W}_{0,0}^\pm$

$$W = \text{Tr} XY^2 + \text{Tr} X^{k+1} + W_{0,0}^+ + W_{0,0}^- \quad (3.20)$$

and a dual $U(3kF - n - 2k - 2)$ gauge theory with superpotential

$$W = \text{Tr}xy^2 + \text{Tr}x^{k+1} + \sum_{j=0}^{k-1} \sum_{\ell=0}^2 \text{Tr} \mathcal{M}^{j,\ell} q x^{k-1-j} y^{2-\ell} \tilde{q} + \widetilde{W}_{0,0}^+ + \widetilde{W}_{0,0}^- \quad (3.21)$$

Here we will not consider this case, even it may be interesting to derive this duality flowing from some of the other cases studied here.

3.1.3 3d partition function

Focusing on the models of interest here, the partition function for $Usp(2n)$ SQCD with $2f$ fundamentals and two antisymmetric A and B is given by

$$\begin{aligned} Z_{Usp(2n)}^{2f}(\vec{\mu}; \tau_A, \tau_B) &= \frac{\Gamma_h(\tau_A)^n \Gamma_h(\tau_B)^n}{\sqrt{-\omega_1 \omega_2}^{-n} 2^n n!} \int \prod_{i=1}^n d\sigma_i \frac{\prod_{a=1}^{2f} \Gamma_h(\pm\sigma_i + \mu_a)}{\Gamma_h(\pm 2\sigma_i)} \\ &\times \prod_{i < j} \frac{\Gamma_h(\pm\sigma_i + \pm\sigma_j + \tau_A) \Gamma_h(\pm\sigma_i + \pm\sigma_j + \tau_B)}{\Gamma_h(\pm\sigma_i \pm \sigma_j)} \end{aligned} \quad (3.22)$$

The superpotential $W = A^{k+1} + AB^2$ fixes as $\tau_A = \frac{2}{k+1}\omega$ and $\tau_B = \frac{k}{k+1}\omega$. Furthermore in presence of a KK monopole superpotential we must impose the further constraints

$$\sum_{a=1}^{2f} \mu_a = 2(\omega(f-2) - (n-1)(\tau_A + \tau_B - \omega)) \quad (3.23)$$

On the other hand the partition function for $U(n)$ SQCD with f pairs of fundamentals and anti-fundamentals and two adjoints X and Y is given by

$$\begin{aligned} Z_{U(n)}^f(\vec{\mu}; \vec{\nu}; \tau_X, \tau_Y; \xi) &= \frac{\Gamma_h(\tau_X)^n \Gamma_h(\tau_Y)^n}{\sqrt{-\omega_1 \omega_2}^{-n} n!} \int \prod_{i=1}^n d\sigma_i e^{-2i\pi\xi\sigma_i} \prod_{a=1}^f \Gamma_h(\sigma_i + \mu_a) \Gamma_h(-\sigma_i + \nu_a) \\ &\times \prod_{i < j} \frac{\Gamma_h(\pm(\sigma_i - \sigma_j) + \tau_X) \Gamma_h(\pm(\sigma_i - \sigma_j) + \tau_Y)}{\Gamma_h(\pm(\sigma_i - \sigma_j))} \end{aligned} \quad (3.24)$$

The parameter ξ is the FI, corresponding to the mass parameter for the topological $U(1)_T$ symmetry. The superpotential $W = X^{k+1} + XY^2$ fixes as $\tau_X = \frac{2}{k+1}\omega$ and $\tau_Y = \frac{k}{k+1}\omega$. In this case we can impose different constraints on the parameters, depending on the presence of a KK monopole superpotential or a linear monopole superpotential. The KK monopole imposes

$$\sum_{a=1}^f (\mu_a + \nu_a) = 2f\omega - n\tau_X \quad (3.25)$$

The linear monopole and anti-monopole superpotential imposes $\xi = 0$ and

$$\sum_{a=1}^f (\mu_a + \nu_a) = 2(\omega(f-2) - (n-1)(\tau_X + \tau_Y - \omega)) \quad (3.26)$$

while the linear monopole (or anti-monopole) superpotential imposes the constraint

$$\sum_{a=1}^f (\mu_a + \nu_a) = +(\text{or } -)2\xi + 2((f-2)\omega - (n-1)(\tau_X + \tau_Y - \omega)) \quad (3.27)$$

3.2 4d/3d reduction of $USp(2n)$ SQCD with two rank-two anti-symmetric tensors

In this section we derive the 3d dualities starting from the circle compactification of the one for $USp(2n)$ SQCD with two rank-two antisymmetric tensors. Before starting the analysis we have decided to simplify the reading by summarizing the final dualities in (3.28). We have specified the rank of the electric and of the magnetic gauge group, the electric and the magnetic superpotential and the paragraph where we have discussed the derivation of each duality.

G_{electric}	G_{magnetic}	W_{electric}	W_{magnetic}	Paragraph
$USp(2n)$	$USp(2(3kf - n - 4k - 2))$	(3.29)	(3.30)	3.2.1
$U(n)$	$U(3kf - n - 4k - 2)$	(3.18)	(3.19)	3.2.2
$U(n)$	$U(3kf - n - 2k - 1)$	(3.37)	(3.39)	3.2.3
$U(n)$	$U(3kf - n)$	(3.14)	(3.15)	3.2.4
$USp(2n)$	$USp(2(3kf - n - 2k - 1))$	(3.4)	(3.50)	3.2.5
$U(n)$	$U(3kf - n)$	(3.1) + (3.55)	(3.2) + (3.56)	3.3

(3.28)

3.2.1 $USp(2n)$ with KK monopole superpotential

The circle reduction of the 4d Brodie-Strassler duality for $USp(2n)$ with $2f$ fundamentals and two adjoints gives rise to the following 3d effective duality

- 3d $USp(2n)$ SQCD with $2f$ fundamentals Q and two rank-two antisymmetric tensors A and B

$$W = Tr A^{k+1} + Tr AB^2 + \eta Y_{USp} \quad (3.29)$$

- 3d $USp(2(3kf - n - 4k - 2))$ SQCD with $2f$ fundamentals q , two rank-two anti-symmetric tensors a and b and the dressed mesons $M_{rs}^{(j,\ell)} = Q_r A^j B^\ell Q_s$ symmetric (antisymmetric) for $j\ell$ odd (even) with $j = 0, \dots, k-1$ and $\ell = 0, 1, 2$. The superpotential of the dual phase is

$$W = Tra^{k+1} + Tr ab^2 + \sum_{j=0}^{k-1} \sum_{\ell=0}^2 M_{j\ell} q a^{k-j-1} b^{2-\ell} q + \tilde{\eta} y_{USp} \quad (3.30)$$

with k odd.

The monopole operators Y_{USp} and y_{USp} can be generated because the rank-two antisymmetric tensors do not carry new zero modes in the KK monopole background [79, 70].

The identity relating the superconformal indices of the 4d theory has been conjectured in [77]. Reducing the identity between the indices to an identity between the partition

functions can be done along the lines of the prescription given in [49]. Such prescription requires a re-definition of the fugacities p, q associated to the isometries of S^3 , of the fugacity u_a associated to the global symmetry and of the fugacity z_i associated to the gauge symmetry:

$$p = e^{2\pi i r \omega_1}, \quad q = e^{2\pi i r \omega_2}, \quad z = e^{2\pi i r \sigma}, \quad u = e^{2\pi i r m} \quad (3.31)$$

The 3d limit is taken as $r \rightarrow 0$, and it can be shown that the elliptic Gamma function become hyperbolic Gamma functions

$$\lim_{r \rightarrow 0} \Gamma_e(e^{2\pi i r z}) = e^{-\frac{i\pi}{6\omega_1\omega_2 r}(z-\omega)} \Gamma_h(z) \quad (3.32)$$

There is a divergent contribution associated to the gravitational anomalies, that cancels if one reduces an integral identity between 4d dual models. By applying this reduction to the identity between (3.11) and (3.13) we arrive at

$$\begin{aligned} Z_{U_{sp}(2n)}^{2f}(\vec{\mu}; \tau_A, \tau_B) &= Z_{USp(2(3kf-n-4k-2))}^{2f}(\tau_A - \tau_B - \vec{\mu}; \tau_A, \tau_B) \\ &\times \prod_{j=0}^{k-1} \prod_{\ell=0}^2 \prod_{1 \leq a < b \leq f} \Gamma_h(j\tau_A + \ell\tau_B + \mu_a + \mu_b) \\ &\times \prod_{q=0}^{k-1} \prod_{a=1}^f \Gamma_h((2q+1)\tau_A + \tau_B + 2\mu_a) \end{aligned} \quad (3.33)$$

with the constraint (3.23) among the mass parameters. This constraint descends from the 4d constraint (3.12). While this constraint corresponds to anomaly cancellations in 4d, in 3d it reflects the presence of the KK monopole superpotential, both in the electric and in the magnetic phase, preventing the generation of an axial symmetry. This is the crucial aspects underlining the reduction of 4d dualities to 3d, the presence of the KK monopoles generates new effective dualities on the circle, having the same global symmetries of the 4d ones. This guarantees that the 4d duality is preserved in the effective 3d description.

It is then possible to flow to other 3d dualities by consistently removing the KK monopole superpotential in both phases. This is in general non trivial because the real mass flow necessary to remove the monopole superpotential in the electric phase can require also a dual Higgsing in the magnetic one. On the partition function this translates into the cancellation of the divergent pre-factors emerging when integrating out the massive field in both sides of the identities. In the following we study some of these flows starting from the duality with the KK monopole superpotential and from the identity (3.33). In this way we obtain the other 3d dualities summarized in figure (3.1) (except for the $U(n)$ case with a KK monopole turned on, that will be discussed separately in Section 3.3).

3.2.2 $U(n)$ with linear monopole and anti-monopole superpotential

The first flow under investigation gives rise to the duality of [39] with linear monopole and anti-monopole superpotential reviewed in sub-section 3.1.2.

The flow consists of assigning a large positive real mass to f of the fundamentals and a large negative and opposite real mass to the remaining f fundamentals. This real mass flow is then combined with a Higgs flow, corresponding to a shift of the real scalars in the gauge group, equal (or equivalently opposite) to the one assigned to f fundamentals.

The electric theory becomes $U(n)$ with two adjoint and f pairs of fundamentals and antifundamentals, Q and \tilde{Q} . On the dual side the real scalars in the gauge group are shifted analogously, giving rise to an $U(3kf - n - 4k - 2)$ gauge theory with f pairs of fundamentals q and \tilde{q} and anti-fundamentals and two adjoints. In this case only the anti-symmetric contributions from the original mesons remains in the low energy spectrum and they correspond to the dressed mesons $M_{j,\ell}^{r,s} = Q^r X^j Y^\ell Q^s$.

The flow does not generate an axial and a topological symmetry, signaling the presence of the linear monopole and anti-monopole superpotential of [39].

This duality can be obtained also studying the flow on the partition function. In this case we assign the masses as

$$\begin{cases} \mu_a = m_a + s & a = 1, \dots, f \\ \mu_a = n_a - s & a = f + 1, \dots, 2f \end{cases}, \quad (3.34)$$

and we shift the integration variables $\sigma_i \rightarrow \sigma_i + s$ in both the electric and the magnetic phase.

By computing the large s limit and by canceling the common divergent pre-factors between the LHS and the RHS of the identity (3.33) we obtain a new identity

$$\begin{aligned} Z_{U(n)}^f(\vec{m}; \vec{n}, ; \tau_A, \tau_B; 0) &= Z_{U(3kf-n-4k-2)}^f(\tau_A - \tau_B - \vec{n}; \tau_A - \tau_B - \vec{n}; \tau_A, \tau_B; 0) \\ &\times \prod_{j=0}^{k-1} \prod_{\ell=0}^2 \prod_{a,b=1}^f \Gamma_h(j\tau_A + \ell\tau_B + m_a + n_b) \end{aligned} \quad (3.35)$$

with the constraint

$$\sum_{a=1}^f (m_a + n_b) = 2(\omega(f-2) - (n-1)(\tau_A + \tau_B - \omega)) \quad (3.36)$$

This is the expected identity for the duality with linear monopole and anti-monopole superpotential. The constraints imposed by the superpotential correspond indeed to the absence of an FI in (3.35) and to the constraint (3.36), as discussed in sub-section 3.1.3.

3.2.3 $U(n)$ with a single linear monopole superpotential term

The next step consist of integrating out one massive flavor from the last duality and flow to a new duality with a single one monopole (or anti-monopole) superpotential.

This flow requires some care in the magnetic sector, because it requires a dual higgsing in order to match the discrete anomalies.

If we consider $f + 1$ flavors on the electric side and assign large opposite real masses to the last pair on the dual side. The electric model becomes

$$W = TrXY^2 + TrX^{k+1} + V_{0,0}^+ \quad (3.37)$$

The linear monopole (anti-monopole) superpotential $W_{mon} = V_{0,0}^+$ survives the real mass flow. A completely analogous choice is give by linear superpotential for the anti-monopole, giving rise to $W_{mon} = V_{0,0}^-$. The sign depends on the choice of the sign of the

real mass assigned to the fundamental quarks.

In the magnetic theory, after the dual Higgsing, we have a $U(3kf - n - 2k - 1) \times U(k - 1)$ gauge group. There are f flavors q and \tilde{q} in the first gauge sector and 1 pair q_ρ and \tilde{q}_ρ in the magnetic one. There are also two pairs of adjoints, x and y in the $U(3kf - n - 2k - 1)$ sector and x_ρ and y_ρ in the $U(k - 1)$ sector. The superpotential is

$$\begin{aligned}
 W &= Trxy^2 + Trx^{k+1} + Trx_\rho y_\rho^2 + Trx_\rho^{k+1} + \tilde{V}_{0,0}^+ + \tilde{V}_{0,0}^+ \\
 &+ \sum_{j=0}^{k-1} \sum_{\ell=0}^2 \text{Tr}(\mathcal{M}^{j,\ell} q x^{k-1-j} y^{2-\ell} \tilde{q} + \mathcal{M}_\rho^{j,\ell} q_\rho x_\rho^{k-1-j} y_\rho^{2-\ell} \tilde{q}_\rho) + \\
 &+ \sum_{j=1}^{k-1} \tilde{V}_{j,0}^- \tilde{V}_{k-j,0}^- + \sum_{\ell=0}^2 \tilde{V}_{0,\ell}^- \tilde{V}_{0,2-\ell}^- + \sum_{q=0}^{\kappa=\frac{k-3}{2}} \tilde{W}_q^- \tilde{W}_{\kappa-q}^-
 \end{aligned} \tag{3.38}$$

where the singlets \mathcal{M} and \mathcal{M}_ρ are the light field that survive from the original mesons in the real mass flow. Furthermore the bare monopoles and anti-monopoles of the $U(k - 1)$ sector have been denoted as $\tilde{V}_{0,0}^\pm$ and $\tilde{W}_{0,0}^\pm$

Consistently with the assignation of the masses in the electric theory the linear monopole (anti-monopole) superpotential $W_{mon} = \tilde{V}_{0,0}^+ + \tilde{V}_{0,0}^+$ (or $W_{mon} = \tilde{V}_{0,0}^- + \tilde{V}_{0,0}^-$) remains in the superpotential. On the other hand the last line in (3.39) represents the AHW-like superpotential generated by the dual Higgsing between the monopole operators of the two gauge sectors.

We can consider this relation between the electric and the magnetic theory as a new duality for $U(n)$ SQCD with two adjoint and a single monopole turned on. Nevertheless here we are interested in a more conventional formulation of the dual model. This is achieved by conjecturing that the $U(k - 1)$ sector with two adjoints x_ρ and y_ρ interacting through $\tilde{W} = Trx_\rho^{k+1} + Trx_\rho y_\rho^2$ and one fundamental flavor identified with q_ρ and \tilde{q}_ρ is confining² in presence of a linear monopole superpotential, either $W_{mon} = \tilde{V}_{0,0}^+$ (or $W_{mon} = \tilde{V}_{0,0}^-$). In absence of further interactions the confining theory corresponds to a set of singlets identified with the dressed mesons $q_\rho x_\rho^{k-1-j} y_\rho^{2-\ell} \tilde{q}_\rho$ and with the monopoles $\tilde{V}_{j,\ell}^-$ (or $\tilde{V}_{j,\ell}^+$) with $j\ell = 0$ and \tilde{W}_q^- (or \tilde{W}_q^+) with $q = 0, \dots, \frac{k-3}{2}$.

This conjecture allows us to dualize the $U(k - 1)$ sector and the dual model becomes $U(3kf - n - 2k - 1)$ with superpotential

$$\begin{aligned}
 W &= Trxy^2 + Trx^{k+1} + \tilde{V}_{0,0}^+ + \sum_{j=0}^{k-1} \sum_{\ell=0}^2 \text{Tr}(\mathcal{M}^{j,\ell} q x^{k-1-j} y^{2-\ell} \tilde{q}) + \\
 &+ \sum_{j=1}^{k-1} \tilde{V}_{j,0}^- V_{k-j,0}^- + \sum_{\ell=0}^2 \tilde{V}_{0,\ell}^- V_{0,2-\ell}^- + \sum_{q=0}^{\kappa=\frac{k-3}{2}} \tilde{W}_q^- W_{\kappa-q}^-
 \end{aligned} \tag{3.39}$$

²Observe that in 4d the confining limiting case of Brodie duality has been studied in [80]. In 3d the number of confining limiting cases is expected to be larger, because of the possible presence of monopole superpotentials.

where in the last line we have identified the monopoles of the confining sector with some of the monopoles of the electric theory namely $V_{j,0}^+$, $V_{0,\ell}^+$ and W_q^+ .

We can translate the conjecture on the partition function side, conjecturing the following identity

$$\begin{aligned}
& Z_{U(k-1)}^1(m, m; \tau_A, \tau_B; 2(\tau_A - \tau_B - \omega - m)) = \\
& \times \prod_{j=0}^{k-1} \prod_{\ell=0}^2 \Gamma_h(2m + j\tau_A + \ell\tau_B) \prod_{q=0}^{\frac{k-3}{2}} \Gamma_h((2q+1)\tau_A - 4(m - \tau_A + \tau_B)) \\
& \times \prod_{j=0}^{k-1} \Gamma_h(j\tau_A - 2(m - \tau_A + \tau_B)) \prod_{\ell=1}^2 \Gamma_h(\ell\tau_B - 2(m - \tau_A + \tau_B)) \quad (3.40)
\end{aligned}$$

where the FI is fixed by the balancing condition (3.27), corresponding to the presence of the linear monopole superpotential, and k is odd. We are not aware of any mechanism to obtain this duality from other known dualities. Rather, in this Chapter we show that this conjecture, in particular in the s-confining case (3.40), allows us to consistently describe the various RG flows depicted in figure 3.1. It would be interesting to provide independent checks of this conjectured duality, for example by computing the superconformal index for low values of k [73].

The flow is triggered by considering the identity (3.35) with $f+1$ fundamental flavors and assigning a large mass parameter to the last pair as

$$\begin{cases} m_{f+1} = \mathbf{m} + s \\ n_{f+1} = \mathbf{m} - s \end{cases}, \quad (3.41)$$

On the dual side the gauge group $U(3kf - n - k - 2)$ is higgsed to $U(3kf - n - 2k - 1) \times U(k-1)$ by shifting $(k-1)$ integration variables as $\sigma_i \rightarrow \sigma_i - s$. Computing the large s limit on the identity (3.35) and eliminating the divergent part, that coincides on the electric and on magnetic side we end up with the relation

$$\begin{aligned}
Z_{U(n)}^f(\vec{m}, \vec{n}; \tau_A; \tau_B; -2(\mathbf{m} - \omega)) &= Z_{U(3kf-n-2k-1)}^f(\vec{n}, \vec{m}; \tau_A; \tau_B; 2(\mathbf{m} - \tau_B)) \\
&\times Z_{U(k-1)}^1(\vec{\mathbf{m}}, \vec{\mathbf{m}}; \tau_A, \tau_B; -2(\mathbf{m} - \omega)) \\
&\times \prod_{j=0}^{k-1} \prod_{\ell=0}^2 \prod_{a,b=1}^f \Gamma_h(j\tau_A + \ell\tau_B + m_a + n_b) \\
&\times \prod_{j=0}^{k-1} \prod_{\ell=0}^2 \prod_{a,b=1}^f \Gamma_h(j\tau_A + \ell\tau_B + 2m) e^{\frac{i\pi(k-1)}{2} \sum_{a=1}^f (m_a^2 - n_a^2)} \quad (3.42)
\end{aligned}$$

with $\vec{n} = \tau_A - \tau_B - \vec{n}$, $\vec{m} = \tau_A - \tau_B - \vec{m}$ and $\vec{\mathbf{m}} = \tau_A - \tau_B - \mathbf{m}$. There is also a constraint between the masses corresponding to

$$\sum_{a=1}^f (m_a + n_a) = 2((f-1)\omega - (n-1)(\tau_A + \tau_B - \omega)) - 2\mathbf{m} \quad (3.43)$$

that signals the presence of the monopole superpotential both in the $U(n)$ and in the $U(3kf - n - 2k - 1)$ sector. The monopole superpotential in the $U(k - 1)$ sector corresponds to the constraint on the FI in the second line of (3.42). The integral corresponding to the $U(k - 1)$ sector can then be computed using the conjectured relation (3.40). After eliminating the massive fields with the inversion formula for the hyperbolic gamma functions we obtain the relation

$$\begin{aligned}
Z_{U(n)}^f(\vec{m}, \vec{n}; \tau_A \ ; \ \tau_B; 2(\omega - \mathbf{m})) &= Z_{U(3kf - n - 2k - 1)}^f(\vec{n}, \vec{m}; \tau_A; \tau_B; 2(\mathbf{m} - \tau_B)) \\
&\times \prod_{j=0}^{k-1} \prod_{\ell=0}^2 \prod_{a,b=1}^f \Gamma_h(j\tau_A + \ell\tau_B + m_a + n_b) e^{\frac{i\pi(k-1)}{2} \sum_{a=1}^f (m_a^2 - n_a^2)} \\
&\times \prod_{\substack{j=0, \dots, k-1 \\ \ell=0, \dots, 2 \\ j\ell=0}} \Gamma_h((f-1)\omega - \frac{n-1}{2}\tau_A - \sum_{a=1}^f (m_a + n_a) + j\tau_A + \ell\tau_B) \\
&\times \prod_{q=0}^{\frac{k-3}{2}} \Gamma_h(2(f-1)\omega - (n-1)\tau_A - 2\sum_{a=1}^f (m_a + n_a) + (2q+1)\tau_A)
\end{aligned} \tag{3.44}$$

This relation reproduces, on the partition function, the duality that we have claimed on the field theory side. Furthermore the identity reduces to the one conjectured in formula (3.40) for $n = k - 1$, $f = 1$ and $m_1 = n_1$.

3.2.4 $U(n)$ without monopole superpotential

Another crucial sanity check of our construction consists of flowing to the pure 3d duality of [37]. This can be achieved by starting from the duality with linear monopole and anti-monopole superpotential with $f + 2$ flavors and assigning two large and opposite real masses to two pairs of fundamentals and antifundamentals.

In this case we have more freedom than above in the choice of the masses, and this gives rise to a free FI in both the electric and magnetic side. Furthermore on the magnetic side we have to consider the Higgsing to $U(3kf - n) \times U(k - 1)^2$. In the first sector there are f fundamental flavors while in the other two sectors there is a single fundamental flavor. Each sector contains two adjoints interacting through the usual power law binomial superpotential and there are interactions between the light singlets surviving the real mass flow and coming from the original meson and other combinations of fundamental and adjoint fields, generalizing the construction in (3.38). There linear monopole superpotentials for the $U(n)$ and the $U(3kf - n)$ sector are lifted, while there is still a single linear monopole superpotential in each $U(k - 1)$ sector. Furthermore the dressed monopole and the anti-monopoles of the $U(3kf - n)$ interact through an AHW-like superpotential with the ones of the two $U(k - 1)$ sectors (with the sign choice given by the sign choice of the large mass limit in the electric side). Proceeding as above we can dualize both the $U(k - 1)$ sectors and we end up with the duality of [37].

This construction can be reproduced on the partition function as well. The real masses

are chosen as

$$\begin{cases} m_{f+1} = \mathbf{m} + \frac{\xi}{2} + s \\ m_{f+2} = \mathbf{m} - \frac{\xi}{2} + s \\ n_{f+1} = \mathbf{m} + \frac{\xi}{2} - s \\ n_{f+1} = \mathbf{m} - \frac{\xi}{2} - s \end{cases}, \quad (3.45)$$

On the dual side the gauge group $U(3kf - n + 2k - 2)$ is higgsed to $U(3kf - n) \times U(k - 1) \times U(k - 1)$ by shifting $(k - 1)$ integration variables as $\sigma_i \rightarrow \sigma_i - s$ and $(k - 1)$ integration variables as $\sigma_i \rightarrow \sigma_i + s$. Computing the large s limit on the identity (3.35) and eliminating the divergent part, that coincides on the electric and on magnetic side we end up with the relation

$$\begin{aligned} Z_{U(n)}^f(\vec{m}; \vec{n}; \tau_A, \tau_B; \xi) &= Z_{U(3kf-n)}^f(\tau_A - \tau_B - \vec{n}; \tau_A - \tau_B - \vec{n}; \tau_A, \tau_B; -\xi) \\ &\times \prod_{j=0}^{k-1} \prod_{\ell=0}^2 \prod_{a,b=1}^f \Gamma_h(j\tau_A + \ell\tau_B + m_a + n_b) \\ &\times \prod_{\eta=\pm 1} Z_{U(k-1)}^1(\tilde{\mathbf{m}}_\eta, \tilde{\mathbf{m}}_\eta, \tau_A, \tau_B; 2\eta(\mathbf{m} - \omega) - \xi) \\ &\times \prod_{j=0}^{k-1} \prod_{\ell=0}^2 \prod_{a,b=1}^f \Gamma_h(j\tau_A + \ell\tau_B + m_a + n_b) \\ &\times \prod_{j=0}^{k-1} \prod_{\ell=0}^2 \prod_{a,b=1}^f \prod_{\eta=\pm 1} \Gamma_h(j\tau_A + \ell\tau_B + (2m + \eta\xi)) \end{aligned} \quad (3.46)$$

with $\tilde{\mathbf{m}}_\eta = \tau_A - \tau_B - \mathbf{m} + \frac{\eta\xi}{2}$. The constraint on the parameters reads

$$\sum_{a=1}^f (m_a + n_a) = 2(f\omega - (n - 1)(\tau_A + \tau_B - \omega)) - 4\mathbf{m} \quad (3.47)$$

In this case it signals the presence of the AHW interactions and it plays an important role in identifying the monopole operators of the confining sectors with the ones of the electric theory. On the other hand it does not play any role on the $U(n)$ and $U(3kf - n)$ sectors because we are in presence of an unconstrained FI ξ . It signals the absence of linear monopole deformations in these two gauge sectors.

Proceeding as above by dualizing the two $U(k - 1)$ sectors with the help of (3.40) and eliminating the massive fields with the help of the inversion formula for the hyperbolic

Gamma functions we end up with the relation

$$\begin{aligned}
Z_{U(n)}^f(\vec{m}; \vec{n}; \tau_A, \tau_B; \xi) &= Z_{U(3kf-n)}^f(\tau_A - \tau_B - \vec{n}; \tau_A - \tau_B - \vec{n}; \tau_A, \tau_B; -\xi) \\
&\times \prod_{j=0}^{k-1} \prod_{\ell=0}^2 \prod_{a,b=1}^f \Gamma_h(j\tau_A + \ell\tau_B + m_a + n_b) \\
&\times \prod_{q=0}^{\frac{k-3}{2}} \Gamma_h(\pm 2\xi + 2f\omega - (n-1)\tau_A - \sum_{a=1}^f (m_a + n_a) + (2q+1)\tau_A) \\
&\times \prod_{\substack{j=0, \dots, k-1 \\ \ell=0, \dots, 2 \\ j\ell=0}} \Gamma_h(\pm \xi + f\omega - \frac{n-1}{2}\tau_A - \frac{1}{2} \sum_{a=1}^f (m_a + n_a) + \ell\tau_B + j\tau_A)
\end{aligned} \tag{3.48}$$

with unconstrained parameters. More precisely the parameters m_a and n_a are constrained as $\sum_a m_a = \sum_a n_a = fm_A$ where m_A is the parameter associated to the axial symmetry. The relation (3.48) is the expected one between the electric and the magnetic side of the duality found in [37].

3.2.5 $Usp(2n)$ without monopole superpotential

Another duality that can be derived from the reduction of $Usp(2n)$ on the circle is obtained by eliminating the superpotentials ηY_{USp} and $\tilde{\eta} y_{Usp}$ in (3.4) and in (3.5). The flow in this case is engineered by considering $2(f+1)$ fundamentals and by assigning a large and opposite mass to two of them. On the dual side the gauge group is Higgsed to $USp(3k-n-2k-1) \times U(k-1)$, with $2f$ light fundamentals q in the symplectic sector and one fundamental flavor (p, \tilde{p}) in the $U(k-1)$ sector. Again the FI term generated in the $U(k-1)$ sector is constrained and it signals the presence of a linear monopole or anti-monopole superpotential (here the choice depends on the sign of the shift in the real scalar in the vector multiplet). In the $USp(3k-n-2k-1)$ sector there are two anti-symmetric rank-two tensors a and b while in the $U(k-1)$ sector there are two adjoints x and y . The superpotential of this dual model is

$$\begin{aligned}
W &= Tra^{k+1} + Trab^2 + Trx^{k+1} + Trxy^2 + V_{0,0}^+ + \\
&+ \sum_{j=0}^{k-1} \sum_{\ell=0}^2 (M_{j,\ell} q a^j b^\ell q + N_{j,\ell} p x^j y^\ell \tilde{p}) + \\
&+ \sum_{j=1}^{k-1} V_{j,0}^- \tilde{Y}_{k-j,0} + \sum_{\ell=0}^2 V_{0,\ell}^- \tilde{Y}_{0,2-\ell} + \sum_{q=0}^{\kappa=\frac{k-3}{2}} W_q^- \tilde{Z}_{\kappa-q}
\end{aligned} \tag{3.49}$$

where $\tilde{Y}_{j,\ell}$ and \tilde{Z}_q are dressed monopoles of the $USp(3kf-n-2k-1)$ sector with topological charge 1 and 2 respectively. They can be defined by radial quantization as in (3.16). Dualizing the $U(k-1)$ sector we arrive at the final formulation of the duality,

where the superpotential becomes

$$\begin{aligned}
W = & \text{Tr}a^{k+1} + \text{Tr}ab^2 + \sum_{j=0}^{k-1} \sum_{\ell=0}^2 (M_{j,\ell} q a^j b^\ell q) + \\
& + \sum_{j=1}^{k-1} Y_{j,0} \tilde{Y}_{k-j,0} + \sum_{\ell=0}^2 Y_{0,\ell} \tilde{Y}_{0,2-\ell} + \sum_{q=0}^{\kappa=\frac{k-3}{2}} Y_q \tilde{Z}_{\kappa-q}
\end{aligned} \tag{3.50}$$

where the monopoles arising from the $U(k-1)$ sectors are identified with the ones of the electric $USp(2n)$ gauge theory.

The global symmetry in this case is $SU(2f) \times U(1)_A \times U(1)_R$ and the fields and the monopoles transform under the gauge and global symmetries as follows:

Field	$USp(2n)$	$USp(2\tilde{n})$	$SU(2f)$	$U(1)_A$	$U(1)_R$
Q	n	1	$2f$	1	r
A	$n(2n-1)$	1	1	0	$\frac{2}{k+1}$
B	$n(2n-1)$	1	1	0	$\frac{k}{k+1}$
$Y_{j\ell}$	1	1	1	$-2f$	$2f(1-r) + \frac{2j+k\ell-2(n+k)}{k+1}$
Z_q	1	1	1	$-4f$	$4f(1-r) + \frac{2+4q-4(n+k)}{k+1}$
q	1	\tilde{n}	$2\bar{f}$	-1	$\frac{2-k}{k+1} - r$
a	1	$\tilde{n}(2\tilde{n}-1)$	0		$\frac{2}{k+1}$
b	1	$\tilde{n}(2\tilde{n}-1)$	1	0	$\frac{k}{k+1}$
$\mathcal{M}_{j0}(j=0,\dots,k-1)$	1	1	$f(2f-1)$	0	$2(1-r) + \frac{2j}{k+1}$
$\mathcal{M}_{2j1}(j=0,\dots,\frac{k-1}{2})$	1	1	$f(2f-1)$	2	$2(1-r) + \frac{4j+k}{k+1}$
$\mathcal{M}_{2j+11}(j=0,\dots,\frac{k-3}{2})$	1	1	$f(2f+1)$	2	$2(1-r) + \frac{4j+k+2}{k+1}$
$\mathcal{M}_{j2}(j=0,\dots,k-1)$	1	1	$f(2f-1)$	2	$2(1-r) + \frac{2j+2k}{k+1}$
$\tilde{Y}_{j\ell}$	1	1	1	$2f$	$2(f-1)r + \frac{k\ell+2(j+n+k+1)}{k+1}$
\tilde{Z}_q	1	1	1	$4f$	$4f(r-1) + \frac{4(q+n+k)+6}{k+1}$

(3.51)

We conclude the discussion by performing such a flow on the partition function. In this case we consider $2f+2$ mass parameters μ_a and assign the masses as

$$\begin{cases} \mu_{f+1} = \mathbf{m} + s \\ \mu_{f+2} = \mathbf{m} - s \end{cases}, \tag{3.52}$$

The dual higgsing corresponds to the shift $\sigma_i \rightarrow \sigma_i + s$ (or equivalently $\sigma_i \rightarrow \sigma_i + s$) for $k-1$ integration variables.

Computing the large s limit on the identity (3.33) and eliminating the divergent part, that coincides on the electric and on magnetic side, we end up with the relation

$$\begin{aligned}
 Z_{Usp(2n)}^{2f}(\vec{\mu}; \tau_A, \tau_B) &= Z_{Usp(2(3kf-n-2k-1))}^{2f}(\tau_A - \tau_B - \vec{\mu}; \tau_A, \tau_B) \\
 &\times \prod_{j=0}^{k-1} \prod_{\ell=0}^2 \prod_{1 \leq a < b \leq f} \Gamma_h(j\tau_A + \ell\tau_B + \mu_a + \mu_b) \\
 &\times \prod_{q=0}^{k-1} \prod_{a=1}^f \Gamma_h((2q+1)\tau_A + \tau_B + 2\mu_a) \\
 &\times Z_{U(k-1)}^1(\tilde{\mathbf{m}}, \tilde{\mathbf{m}}; \tau_A, \tau_B, -2(\omega - \mathbf{m})) \\
 &\times \prod_{j=0}^{k-1} \prod_{\ell=0}^2 \prod_{1 \leq a < b \leq f} \Gamma_h(j\tau_A + \ell\tau_B + 2\mathbf{m})
 \end{aligned} \tag{3.53}$$

with $\tilde{\mathbf{m}} = \tau_A - \tau_B - \mathbf{m}$ and the constraint

$$\sum_{a=1}^{2f} \mu_a = 2(\omega(f-1) - (n-1)(\tau_A + \tau_B - \omega)) - 2\mathbf{m} \tag{3.54}$$

Again this constraints does not affect the mass parameters on the electric side, signaling that the KK monopole superpotential has been lifted. On the dual side the constraint is crucial for the identification of the monopoles (or anti-monopoles) of the confining $U(k-1)$ sector with the ones of the electric $Usp(2n)$ model. The last step consists of integrating $Z_{U(k-1)}^1$ using the relation (3.40) and arrive to the equality

$$\begin{aligned}
 Z_{Usp(2n)}^{2f}(\vec{\mu} ; \tau_A, \tau_B) &= Z_{Usp(2(3kf-n-2k-1))}^{2f}(\tau_A - \tau_B - \vec{\mu}; \tau_A, \tau_B) \\
 &\times \prod_{j=0}^{k-1} \prod_{\ell=0}^2 \prod_{1 \leq a < b \leq f} \Gamma_h(j\tau_A + \ell\tau_B + \mu_a + \mu_b) \prod_{q=0}^{\frac{k-3}{2}} \prod_{a=1}^f \Gamma_h((2q+1)\tau_A + \tau_B + 2\mu_a) \\
 &\times \prod_{\substack{j=0, \dots, k-1 \\ \ell=0, \dots, 2 \\ j\ell=0}} \Gamma_h(j\tau_A + \ell\tau_B + 2f\omega - \tau_A(n+k) - \sum_{a=1}^{2f} \mu_a) \\
 &\times \prod_{q=0}^{\frac{k-3}{2}} \Gamma_h((2q+1)\tau_A + 4f\omega - 2\tau_A(n+k) - 2 \sum_{a=1}^{2f} \mu_a)
 \end{aligned}$$

3.3 Reconsidering the 4d/3d reduction of $U(n)$ SQCD with two adjoints

In this section we study the reduction of the 4d duality worked out in [45] and reviewed in sub-section 3.1.1 along the lines of [49].

Some comments are in order. First we consider a slight modification of the original the duality, by gauging the baryonic symmetry. The $SU(n)$ case can be studied similarly, even if it modifies the structure of the effective superpotential generated in the circle

reduction. It is nevertheless possible to recover the 3d limit of the $SU(n)$ duality by gauging the topological symmetry in the final step of our procedure. We will further comment on this possibility in the conclusions. A second comment regards the restriction to the case of odd k . A similar duality was also conjectured for the case of even k in [45]. The difference in such case is that the chiral ring is not truncated at classical level by the F-term constraints on the electric side and the proposal is that such truncation appears quantum mechanically. Here we will not elaborate further on this case and we restrict to the odd case.

The reduction of this duality to an *effective* duality on the circle has been studied in [37] by breaking the gauge group, and by reducing the duality only in $U(n_i)$ sectors without adjoints. Here we adopt a different strategy and leave the gauge group unbroken. The motivation underlining our analysis is that we want to follow the various steps at the level of the reduction of the 4d superconformal index to the 3d squashed three sphere partition function.

On the circle we obtain an *effective* duality relating

- 3d $U(n)$ SQCD with f flavors Q and \tilde{Q} with two adjoints X and Y interacting through the superpotential $W = (3.1) + W_\eta$ with

$$W = \text{Tr} X^{k+1} + \text{Tr} XY^2 + \eta \left(\sum_{j=1}^{k-1} V_{j,0}^+ V_{k-j,0}^- + \sum_{l=0}^2 V_{0,l}^+ V_{0,2-l}^- + \sum_{q=0}^{\kappa=\frac{k-3}{2}} W_q^+ W_{\kappa-q}^- \right) \quad (3.55)$$

- 3d $U(3kf - n)$ SQCD with f dual flavors q and \tilde{q} with two adjoints x and y interacting through the superpotential $W = (3.2) + W_{\tilde{\eta}}$

$$W_{\tilde{\eta}} = \tilde{\eta} \left(\sum_{j=1}^{k-1} \tilde{V}_{j,0}^+ \tilde{V}_{k-j,0}^- + \sum_{l=0}^2 \tilde{V}_{0,l}^+ \tilde{V}_{0,2-l}^- + \sum_{q=0}^{\kappa=\frac{k-3}{2}} \tilde{W}_q^+ \tilde{W}_{\kappa-q}^- \right) \quad (3.56)$$

The superpotentials W_η and $W_{\tilde{\eta}}$ break the axial symmetry, anomalous in the 4d case. The conventional 3d duality is obtained by a real mass flow, accompanied on the magnetic side by a dual Higgsing of the gauge group. Such real mass flow can be engineered on the electric side by considering $f + 2$ flavors and by assigning large (and opposite) real mass to two pairs of fundamentals and anti-fundamentals. On the magnetic side we can assign the same opposite shifts to the scalars in the vector multiplet by breaking $U(3k(f + 2) - n) \rightarrow U(3kf - n) \times U(3k)^2$. In the $U(3kf - n)$ gauge sector we have two adjoint x and y and f pairs of fundamental and anti-fundamental q and \tilde{q} . In the $U(3k)$ sectors we still have two adjoints, denoted respectively as x_ρ and y_ρ in the first sector and x_ξ and y_ξ in the second sector and one flavor, denoted (q_ρ, \tilde{q}_ρ) and (q_ξ, \tilde{q}_ξ) .

The superpotential of this model is

$$\begin{aligned}
W &= \text{Tr}xy^2 + \text{Tr}x^{k+1} + \text{Tr}x_\rho y_\rho^2 + \text{Tr}x_\rho^{k+1} + \text{Tr}x_\xi y_\xi^2 + \text{Tr}x_\xi^{k+1} \\
&+ \sum_{j=0}^{k-1} \sum_{\ell=0}^2 \text{Tr}(\mathcal{M}^{j,\ell} q x^{k-1-j} y^{2-\ell} \tilde{q} + \mathcal{M}_\rho^{j,\ell} q_\rho x_\rho^{k-1-j} y_\rho^{2-\ell} \tilde{q}_\rho + \mathcal{M}_\xi^{j,\ell} q_\xi x_\xi^{k-1-j} y_\xi^{2-\ell} \tilde{q}_\xi) \\
&+ \sum_{j=1}^{k-1} (\tilde{V}_{j,0}^+ \tilde{V}_{k-j,0}^- + \tilde{V}_{j,0}^- \tilde{V}_{k-j,0}^+ + \tilde{V}_{j,0}^+ \tilde{V}_{k-j,0}^-) \\
&+ \sum_{\ell=0}^2 (\tilde{V}_{0,\ell}^+ \tilde{V}_{0,2-\ell}^- + \tilde{V}_{0,\ell}^- \tilde{V}_{0,2-\ell}^+ + \tilde{V}_{0,\ell}^+ \tilde{V}_{0,2-\ell}^-) \\
&+ \sum_{q=0}^{\frac{k-3}{2}} (\tilde{W}_q^+ \tilde{W}_{\kappa-q}^- + \tilde{W}_q^- \tilde{W}_{\kappa-q}^+ + \tilde{W}_q^+ \tilde{W}_{\kappa-q}^-)
\end{aligned} \tag{3.57}$$

The first two lines of (3.57) correspond to the superpotential (3.2) in the gauge sectors of the dual theory, inherited from the original one after the real mass flow and the Higgs flow. The last three lines on the other hand correspond to an AHW-like superpotential generated between the monopole operators because of the dual Higgsing. We have denoted as \mathbf{V} and \mathbf{W} the monopoles of $U(3k)_\rho$ sector and \mathcal{V} and \mathcal{W} the monopoles of $U(3k)_\xi$ sector.

The last step consists of dualizing the $U(3k)$ sectors in terms of singlets. The duality that we have to use in this case corresponds to the limiting case of the 3d duality that we are looking for. This is a very standard phenomenon in the reduction of 4d dualities to 3d. In the case of SQCD such a limiting case was interpreted independently as local mirror symmetry, indeed the extra sectors correspond to SQED with one flavor, and the confining model could be regarded as local mirror symmetry. In the case with one adjoint such sector correspond to $U(k)$ with one adjoint and one flavor and $W = \text{Tr}X^{k+1}$. This model can be shown to be confining as well, even in absence of the adjoint superpotential, as discussed for example in [81, 69]. In both cases the confining duality corresponds to the limiting case of the duality that one is looking for.

Here we borrow the results obtained in sub-section 3.2.4 and dualize the two $U(3k)$ sectors with a fundamental flavor. From the superpotential (3.57) one can observe that the mesons $q_\xi x_\xi^{k-1-j} y_\xi^{2-\ell} \tilde{q}_\xi$ and $q_\rho x_\rho^{k-1-j} y_\rho^{2-\ell} \tilde{q}_\rho$ become massive and they can be integrated out at zero vev. In a similar fashion the monopoles $\tilde{V}_{j,\ell}^+$ and $\tilde{V}_{j,\ell}^-$ with $j\ell = 0$ and \tilde{W}_q^+ and \tilde{W}_q^- with $q = 0, \dots, \frac{k-3}{2}$ are singlets after confining the $U(3k)$ gauge groups and they become massive because of the superpotential (3.57). On the other hand the monopoles $\tilde{V}_{j,\ell}^-$ and $\tilde{V}_{j,\ell}^+$ with $j\ell = 0$ and \tilde{W}_q^- and \tilde{W}_q^+ with $q = 0, \dots, \frac{k-3}{2}$ are singlets of the $U(3f - n)$ gauge theory that interact with the monopoles $\tilde{V}_{j,\ell}^\pm$ and \tilde{W}_q^\pm . They can then be naturally identified with the monopoles $V_{j,\ell}^\pm$ and W_q^\pm of the electric theory acting as singlets in the dual phase. All in all we arrive at the dual superpotential (3.15) corresponding as expected to the one obtained in [37].

This analysis can be reproduced on the partition function as well. The first step consists

of reducing the identity of [77] between the 4d indices using the prescription of [49]. This gives an identity reproducing the effective duality on S^1 , with a constraint between the mass parameters signaling the presence of the KK monopole superpotential. The identity for the effective duality is

$$Z_{U(n)}^f(\vec{m}, \vec{n}; \tau_X, \tau_Y; \xi) = Z_{U(3kf-n)}^f(\vec{\tilde{m}}, \vec{\tilde{n}}; \tau_X, \tau_Y; -\xi) \times \prod_{j=0}^{k-1} \prod_{\ell=0}^2 \prod_{a,b=1}^f \Gamma_h(j\tau_X + \ell\tau_Y + m_a + n_b) \quad (3.58)$$

where $\tilde{m}_a = \tau_X - \tau_Y - m_a$ and $\tilde{n}_a = \tau_X - \tau_Y - n_a$. In this case the FI parameter is free while the constraint between the mass parameters corresponds to (3.25), preventing the generation of an axial symmetry.

Next we need to engineer the flow to the pure 3d duality. This flow can be constructed by considering $f + 2$ flavors and parameterizing the last two pairs as

$$\begin{cases} m_{f+1} = \mathbf{m} + s \\ m_{f+2} = \mathbf{m} - s \\ n_{f+1} = \mathbf{m} - s \\ n_{f+2} = \mathbf{m} + s \end{cases}, \quad (3.59)$$

On the dual side the gauge group $U(3k(f+2) - n)$ is higgsed to $U(3kf - n) \times U(3k) \times U(3k)$, by shifting $3k$ integration variables as $\sigma_i \rightarrow \sigma_i - s$ and $3k$ integration variables as $\sigma_i \rightarrow \sigma_i + s$. Computing the large s limit on the identity (3.35) and eliminating the divergent part, that coincides on the electric and on magnetic side we end up with the relation

$$Z_{U(n)}^f(\vec{m}, \vec{n}; \tau_X, \tau_Y; \xi) = Z_{U(3kf-n)}^f(\vec{\tilde{m}}, \vec{\tilde{n}}; \tau_X, \tau_Y; -\xi) \times \prod_{\eta=\pm 1} Z_{U(3k)}^1(\tilde{\mathbf{m}}, ; \tau_X, \tau_Y; 2\eta(\mathbf{m} - \omega) - \xi) \times \prod_{j=0}^{k-1} \prod_{\ell=0}^2 \prod_{a,b=1}^f \Gamma_h(j\tau_X + \ell\tau_Y + m_a + n_b) \Gamma_h(j\tau_X + \ell\tau_Y + 2\mathbf{m})^2 \quad (3.60)$$

where $\tilde{\mathbf{m}} = \tau_X - \tau_Y - \mathbf{m}$. The $U(3k)$ sectors are confining and the corresponding integrals can be computed using the results of the previous section. Indeed they correspond to the limiting case of the identity (3.48), because the rank of the dual gauge group vanishes if $n = 3k$ and $f = 1$. By computing these integrals, simplifying the massive fields and using the constraint

$$\sum_{a=1}^f (m_a + n_a) + 4\mathbf{m} = 2\omega(f+2) - n\tau_X \quad (3.61)$$

we arrive at the final relation, that coincides with (3.48) as expected.

3.4 Discussion and future developments

Many open questions arise from this work. First the prove of formula (3.40) is a necessary step to confirm the validity of our approach and corroborate the claims that we made for the new dualities. Another open question is related to the other duality³ discussed in [39], and reviewed in sub-section 3.1.2, involving linear superpotentials for the monopole operators with charge 2 under $U(1)_T$. It would be interesting to obtain such a duality by flowing from the ones discussed here.

Further classes of dualities can then be constructed starting from the ones proposed in our work, involving CS terms, a *chiral* matter content (i.e. a different number of fundamentals and anti-fundamentals) and/or $SU(n)$ gauge groups. The 3d analog of Brodie duality in presence of CS terms has been already proposed in [82]. It would be interesting to obtain this last duality by flowing from the ones without CS terms and then generalize the construction to the $Usp(2n)$ case as well. Also the cases with a chiral matter content can in principle be studied by opportune real mass flows, with possible dual Higgs flow, along the lines of [43, 83, 84, 85]. The analysis of $SU(n)$ dualities is in general less straightforward. This is due to the presence of quadratic monopole operators in many of the dual phases. The general prescription to obtain an $SU(n)$ gauge group starting from $U(n)$ consists of promoting the topological symmetry to a gauge symmetry; in presence of an FI term this gauging leads to a mass term between the dynamical photon of $U(1)_T$ and the original photon of $U(1) \subset U(n)$, through a mixed CS term. By integrating out the massive fields one is left, on the electric side, with an $SU(n)$ gauge group. On the other hand the presence of monopole operators in the dual phase does not allow the same operation in a straightforward manner, because there are extra fields charged under the gauged topological symmetry. The interpretation of the charge two monopole operators arising from the gauging of $U(1)_T$ is less clear than the one for the monopole with charge one under $U(1)_T$ and it is not obvious how to manage this new gauged sector in general. Anyway one could reverse the logic and start from the dualities that we have obtained here before applying any local confining duality on the extra $U(k-1)$ sectors. We hope to come back to this problem in the future. Other interesting lines of research involve the generalization of the construction to the other dualities with two rank-two tensors proposed in [46].

As a last comment we would like to stress that all the models discussed here refer to the case of odd k , being $k+1$ the exponent of the adjoint X and of the anti-symmetric A in all the $U(n)$ and $Usp(2n)$ SQCD superpotentials respectively. While this choice is motivated by anomaly matching for the $Usp(2n)$ gauge groups, $U(n)$ gauge theories with k -even are more tricky, because the chiral ring is supposed to truncate at quantum level, differently from the classical truncation taking place for k -odd (see [86, 87, 88] for further discussions on this issue). In three dimensions we have seen that the $U(n)$ dualities can be derived from the $Usp(2n)$ one, derived by circle reduction, only for odd k . It would be then interesting to understand if there is any connection between the quantum truncation of the chiral ring and the 4d/3d reduction.

³Observe that in [39] many other dualities are conjectured in presence of linear monopole deformations for the dressed monopole operators, in the case with a single adjoint. Similar results are then expected for the case with two adjoints. Here we have not addressed such an issue from the 4d perspective.

S-confinement in 3d $\mathcal{N} = 2$ SO/USp adjoint SQCD

In this Chapter we study s-confining 3d theories with $\mathcal{N} = 2$ supersymmetry. Compared to the 4d case, an ingredient that makes the classification of such theories more intricate and offers new examples of gauge theories with confining dynamics is given by the possibility of turning on monopole superpotentials. Many examples of 3d s-confining gauge theories have been studied in [49, 59, 60, 64, 89, 90, 71, 70, 91, 92, 93, 94, 95], where many checks of the new proposed dualities have been performed. In a recent paper [2] models with real gauge groups and adjoint matter have been studied and new confining dualities have been proposed. An interesting aspect of these cases is that the dualities can be proved by sequentially deconfining the adjoint (symmetric or antisymmetric tensors) in terms of other known dualities involving real gauge groups without any tensor. Such a deconfinement of two-index matter fields follows from the one originally worked out in 4d in [50] and then refined in [96] (see also the recent works [97, 51] where such deconfinement technique has been reconsidered in the 4d case). In 3d the structure of confining gauge theories is richer because of the possibility of turning on monopole superpotentials.

In this Chapter we elaborate on these results, showing the matching of the three-sphere partition function between the new dual phases proposed by [2]. We find that there is a straightforward proof of the hyperbolic integral identity that corresponds to the matching of the squashed three-sphere partition functions between the dual phases. The result follows from the identity relating $USp(2n)$ with the antisymmetric and four fundamentals without monopole superpotential and its description in terms of confined degrees of freedom. In this case by opportunely fixing the value of the mass parameters and by applying the *duplication formula* for the hyperbolic Gamma functions we observe that the identity can be manipulated into the expected ones for the new dualities proposed by [2].

This correspondence motivates us to make one step further, and to consider the case of $USp(2n)$ with the antisymmetric and six fundamentals, in presence of a monopole superpotential (see [67, 98, 66, 68, 99, 100, 101, 102, 103, 104, 105, 106] for recent examples of 3d $\mathcal{N} = 2$ gauge theories and dualities with monopole superpotential turned on). This model is confining as well and it admits the same manipulation referred above on the integral identity matching the squashed three-sphere partition functions. Again we obtain identities relating, in this case, the partition function of models with $USp(2n)$

or $SO(N)$ gauge groups with four fundamentals or three vectors and an adjoint matter field, and the partition function of models with (interacting) singlets.

We then analyze these models through sequentially deconfining the adjoint fields, obtaining a proof of the dualities. This last approach offers also an alternative derivation of the integral identities (obtained so far through the duplication formula), in terms of adjoint deconfinement. Indeed, as we will explicitly show below, each step discussed in the physical proof of the duality corresponds to the application of a known identity between hyperbolic integrals.

4.1 3d confining models with real gauge groups and adjoint matter

These dualities have been proved in [2] and they are the starting point of our analysis. Here we review the main properties of these dualities and briefly discuss their derivation.

The three classes of s-confining dualities with adjoint matter obtained in [2] are summarized in the following.

- In the first case the electric side of the duality involves an $USp(2n)$ gauge theory with adjoint S and two fundamentals p and q with superpotential $W = \text{Tr}(pSp)$. The dual model corresponds of a WZ model with $4n$ chiral multiplets. These $4n$ gauge fields corresponds to gauge invariant singlets of the electric theory. There are $2n$ dressed monopole operators, $Y_j = Y_{USp} \text{Tr} S^j$, $j = 0, \dots, 2n-1$, where Y_{USp} is the unit flux monopole of the $USp(2n)$ gauge theory. Then there are n dressed mesons $M_\ell = qS^{2\ell+1}q$ with $\ell = 0, \dots, n-1$ and eventually there are n singlets $\sigma_k = \text{Tr} S^{2k}$ with $k = 1, \dots, n$.
- The second case involves an $SO(2n)$ gauge theory with an adjoint A and a vector q , without superpotential. The dual theory is a WZ model with $4n$ chiral fields, corresponding to gauge invariant singlets of the electric theory. There are $2n-1$ dressed monopole operators, $Y_j^+ = Y_{SO}^+ \text{Tr} A^j$, $j = 0, \dots, 2n-2$, where Y_{SO}^+ is the unit flux monopole of the $SO(2n)$ gauge theory with positive charge with respect to the charge conjugation symmetry. Then there are n dressed mesons $M_\ell = qA^{2\ell}q$ with $\ell = 0, \dots, n-1$ and $n-1$ singlets $\sigma_k = \text{Tr} A^{2k}$ with $k = 1, \dots, n-1$. The last two chiral fields correspond to the baryon $\mathbb{B} \equiv \text{Pf} A$ and to the baryon monopole $Y_{A^{n-1}}^-$, obtained from the unit flux monopole of the $SO(2n)$ gauge theory with negative charge with respect to the charge conjugation symmetry.
- The third and last case involves an $SO(2n+1)$ gauge theory, again with an adjoint A , a vector q and vanishing superpotential. The dual theory is a WZ model with $4n+2$ chiral fields, corresponding to gauge invariant singlets of the electric theory. There are $2n$ dressed monopole operators, $Y_j^+ = Y_{SO}^+ \text{Tr} A^j$, $j = 0, \dots, 2n-1$, where Y_{SO}^+ is the unit flux monopole of the $SO(2n)$ gauge theory with positive charge with respect to the charge conjugation symmetry. Then there are n dressed mesons $M_\ell = qA^{2\ell}q$ with $\ell = 0, \dots, n-1$ and n singlets $\sigma_k = \text{Tr} A^{2k}$ with $k = 1, \dots, n$. The last two chiral fields correspond to the baryon $\mathbb{B} = \epsilon_{2n+1}(qA^n)$ and to the baryon monopole $Y_{qA^{n-1}}^-$.

As stressed in [2] the superpotential of the dual models correspond to polynomials of the singlets and with complexity that rapidly grows when the ranks of the gauge groups increase. Nevertheless by flipping the singlets σ_k , and the baryon and the baryon

monopole in the orthogonal cases, these superpotentials are given by cubic combinations of the remaining singlets.

Let us briefly sketch the strategy for proving these dualities. The first step consists of deconfining the adjoint field. In the symplectic case the adjoint is in the symmetric representation and it can be deconfined in terms of an orthogonal gauge group. On the other hand in the orthogonal case the adjoint is in the antisymmetric representation and it can be deconfined in terms of a symplectic gauge group. In each case this step requires to find a confining duality that reduces to the original model. After deconfining the adjoint one is then left with a two gauge node quiver gauge theory and one can then proceed by dualizing the original gauge node, by using a known duality. In the cases at hand this duality corresponds to a limiting case of an Aharony duality or a modification of it, with monopole superpotentials. This gives rise to another model with a real gauge group and adjoint matter and generically a more sophisticated superpotential. By repeating the procedure of rank-two tensor deconfinement and duality one is left with the original gauge group but with rank of one unit less and it allows to iterate the procedure and arrive to the desired WZ model at the end of such a cascading process.

By inspection it has been shown in [2] that the adjoint of the $USp(2n)$ case can be deconfined by an $SO(2n+1)$ gauge group and a superpotential flipping the monopole. After dualizing the $USp(2n)$ gauge theory one ends up with an $SO(2n+1)$ gauge theory with an adjoint and a dynamically generated superpotentials flipping both the monopole and the baryon monopole. In this case the adjoint can be deconfined by an $USp(2n-2)$ gauge group and a more intricate flavor structure. Indeed the $SO(2n+1)/USp(2n-2)$ gauge group have one extra vector/fundamental charged chiral fields and there is a superpotential interactions between these two fields and the $SO(2n+1) \times USp(2n-2)$ bifundamental. Furthermore there is a linear monopole superpotential for the $USp(2n)$ gauge node. By dualizing the $SO(2n+1)$ gauge node with $2n$ vectors one ends up with an $USp(2n-2)$ gauge theory, with two fundamentals and a non trivial superpotential. By opportunely flipping some of the singlets of the original model one can recast that the original $USp(2n)$, iterate the procedure and eventually prove the duality. Similar analysis have been used to prove the orthogonal dualities as well. In such cases after deconfining the antisymmetric in terms of $USp(2n-2)$ and dualizing the original orthogonal gauge group one is left with $USp(2n-2)$ and two fundamentals. Then the duality proven above for this case can be used to prove the duality for the orthogonal cases as well.

4.1.1 Confining theories and the three-sphere partition function

We are interested in two confining gauge with $USp(2n)$ gauge group and antisymmetric and six or four fundamentals. In the first case the theory has a monopole superpotential and it corresponds to the reduction of a 4d $\mathcal{N} = 1$ confining gauge theory. In the second case the theory with four fundamentals can be obtained by a real mass flow, it is still confining but in this case the superpotential is vanishing. Details on these models have been discussed in [70, 71].

In general the partition function of an $USp(2n)$ gauge theory with $2n_f$ fundamentals and

an antisymmetric tensor is

$$Z_{\tau, \vec{\mu}}^{USp(2n)} = \frac{\Gamma_h(\tau)^n}{(-\omega_1 \omega_2)^{\frac{n}{2}} 2^n n!} \int \prod_{a=1}^n dy_a \frac{\prod_{r=1}^{2n_f} \Gamma_h(\pm y_a + \mu_r)}{\Gamma_h(\pm 2y_a)} \prod_{1 \leq a < b \leq n} \frac{\Gamma_h(\pm y_a \pm y_b + \tau)}{\Gamma_h(\pm y_a \pm y_b)} \quad (4.1)$$

Where the parameters τ and μ_r are associated to the antisymmetric tensor and to the $2n_f$ fundamentals respectively. The two confining dualities discussed above for $2n_f = 6$ and $2n_f = 4$ correspond to the following identities

$$Z_{\tau, \mu_1, \dots, \mu_6}^{USp(2n)} = \prod_{j=0}^{n-1} \Gamma_h((j+1)\tau) \prod_{1 \leq r < s \leq 6} \Gamma_h(j\tau + \mu_r + \mu_s) \quad (4.2)$$

with the balancing condition

$$2(n-1)\tau + \sum_{a=1}^6 \mu_a = 2\omega \quad (4.3)$$

signaling the presence of a linear monopole superpotential, and

$$Z_{\tau, \mu_1, \dots, \mu_4}^{USp(2n)} = \prod_{j=0}^{n-1} \frac{\Gamma_h((j+1)\tau)}{\Gamma_h((2n-2-j)\tau + \sum_{r=1}^4 \mu_r)} \prod_{1 \leq r < s \leq 4} \Gamma_h(j\tau + \mu_r + \mu_s) \quad (4.4)$$

with unconstrained parameters, corresponding to the absence of any monopole superpotential.

These identities are the starting point of our analysis, and they contain all the mathematical information on the models with real gauge groups and adjoint matter.

In order to transform symplectic gauge groups into unitary one we will use a well known trick, already used in the literature [78, 107, 108, 43]. It consists of using the duplication formula [109, 110, 111]

$$\Gamma_h(2x) = \Gamma_h(x) \Gamma_h\left(x + \frac{\omega_1}{2}\right) \Gamma_h\left(x + \frac{\omega_2}{2}\right) \Gamma_h(x + \omega) \quad (4.5)$$

to modify the partition function of the vector multiplet of $USp(2n)$ into the partition function of the vector multiplet of $SO(2n)$ or $SO(2n+1)$.

This transformation requires to consider an $USp(2n)$ gauge theory with fundamental matter fields and assign to some of the mass parameters some specific value as $\mu = \pm \frac{\omega_i}{2}$ or $\mu = \omega$ or $\mu = 0$. Then by applying the duplication formula (and the reflection equation $\Gamma(x)\Gamma(2\omega - x) = 1$ when necessary) one can convert the contribution of $USp(2n)$ with fundamentals in the one of $SO(2n)$ or $SO(2n+1)$ with (few) vectors. Furthermore, by using the same mechanism, one can convert also the contribution of the $USp(2n)$ antisymmetric field into the one of an adjoint (for both the symplectic and the orthogonal cases).

To simplify the reading of the various steps of the derivation we conclude this section by summarizing the integral identities for $USp(2n)$ and $SO(N)$ s-confining SQCD, that

we have used in the analysis below. These identities are indeed necessary for translating into the language of the squashed three-sphere partition function the chain of adjoint deconfinements and dualities introduced above. In the table we indicate the gauge group, the matter content, the superpotential and the reference to the integral identity equating the partition function of each gauge theory with the one of its confined description .

Gauge group	Matter	Superpotential	Identity
$USp(2n)$	$2n + 4 \square$	$W = Y_{USp}$	(B.1)
$USp(2n)$	$2n + 2 \square$	$W = 0$	(A.2)
$SO(2n)$	$2n + 1 \square$	$W = Y_{SO} +$	(B.3)
$SO(2n)$	$2n - 1 \square$	$W = 0$	(A.3)
$SO(2n + 1)$	$2n + 2 \square$	$W = Y_{SO} +$	(B.2)
$SO(2n + 1)$	$2n \square$	$W = 0$	(A.1)

4.2 Proving known results

In this section we show how to obtain the integral identities for the three dualities reviewed in subsection (4.1) by applying the duplication formula (4.5) on the identity (4.4). Here and in the following section we will use three choice of masses, that are

$$\begin{aligned}
 \text{I. } \vec{\mu}_{n_f} &= \left(\frac{\tau}{2} + \frac{\omega_1}{2}, \frac{\tau}{2} + \frac{\omega_2}{2}, \frac{\tau}{2}, \vec{\mu}_{n_f-3} \right) \\
 \text{II. } \vec{\mu}_{n_f} &= \left(\frac{\omega_1}{2}, \frac{\omega_2}{2}, 0, \vec{\mu}_{n_f-3} \right) \\
 \text{III. } \vec{\mu}_{n_f} &= \left(\frac{\omega_1}{2}, \frac{\omega_2}{2}, \tau, \vec{\mu}_{n_f-3} \right)
 \end{aligned}$$

Here we did not specify the length n_f of the vector $\vec{\mu}$. In the following we will have $n_f = 4$ for the cases of [2] and $n_f = 6$ for the new dualities discussed here.

Case I: $USp(2n)$

We choose the masses μ_r as $\vec{\mu} = \left(\frac{\tau}{2} + \frac{\omega_1}{2}, \frac{\tau}{2} + \frac{\omega_2}{2}, \frac{\tau}{2}, m \right)$ and apply the duplication formula. Explicitly, the contribution of the quarks to the partition function becomes:

$$\begin{aligned}
 \prod_{a=1}^n \prod_{r=1}^4 \Gamma_h(\pm x_a + \mu_r) &\rightarrow \prod_{a=1}^n \Gamma_h\left(\pm x_a + \frac{\tau}{2} + \frac{\omega_1}{2}\right) \Gamma_h\left(\pm x_a + \frac{\tau}{2} + \frac{\omega_2}{2}\right) \\
 &\times \Gamma_h\left(\pm x_a + \frac{\tau}{2}\right) \Gamma_h(\pm x_a + m) \\
 &= \prod_{a=1}^n \Gamma_h(\pm 2x_a + \tau) \Gamma_h(\pm x_a + m) \Gamma_h\left(\pm x_a + \omega - \frac{\tau}{2}\right)
 \end{aligned} \tag{4.6}$$

where we used the duplication formula (4.5) with $x = \pm x_a + \tau/2$ and the reflection equation:

$$\Gamma_h\left(x_a + \omega - \frac{\tau}{2}\right) \Gamma_h\left(-x_a + \omega + \frac{\tau}{2}\right) = 1 \tag{4.7}$$

The LHS of (4.4) becomes

$$\begin{aligned} & \frac{\Gamma_h(\tau)^n}{(-\omega_1\omega_2)^{\frac{n}{2}} 2^n n!} \int_{C^n} \prod_{1 \leq j < k \leq n} \frac{\Gamma_h(\tau \pm x_j \pm x_k)}{\Gamma_h(\pm x_j \pm x_k)} \\ & \times \prod_{j=1}^n \frac{\Gamma_h(\tau \pm 2x_j) \Gamma_h(m \pm x_j) \Gamma_h(\omega - \frac{\tau}{2} \pm x_j)}{\Gamma_h(\pm 2x_j)} dx_j \end{aligned} \quad (4.8)$$

This corresponds to the partition function of $USp(2n)$ with an adjoint S , a fundamental p and a fundamental q with superpotential $W = Tr(pSp)$, where the constraint imposed by the superpotential corresponds to the presence of the parameter $\omega - \frac{\tau}{2}$ in the argument of the last hyperbolic gamma function in the numerator of (4.8).

On the other hand the RHS of (4.4) requires more care. Let us separate first the contributions of the three terms. By substituting the parameters μ_r and using the reflection equation we have

$$\begin{aligned} & \prod_{j=0}^{n-1} \Gamma_h(\omega - (2n - j - \frac{1}{2})\tau - m) \\ & \times \Gamma_h((j+1)\tau, (j+1)\tau + \frac{\omega_1}{2}, (j+1)\tau + \frac{\omega_2}{2}, (j+1)\tau + \omega) \\ & \times \Gamma_h((j + \frac{1}{2})\tau + \frac{\omega_1}{2} + m, (j + \frac{1}{2})\tau + \frac{\omega_2}{2} + m, (j + \frac{1}{2})\tau + m) \end{aligned} \quad (4.9)$$

where we used the shorthand notation $\Gamma_h(a, b) = \Gamma_h(a)\Gamma_h(b)$. By using the duplication formula it becomes

$$\prod_{j=0}^{n-1} \frac{\Gamma_h\left(\omega - (2n - j - \frac{1}{2})\tau - m, 2(j+1)\tau, (2j+1)\tau + 2m\right)}{\Gamma_h\left((j + \frac{1}{2})\tau + m + \omega\right)} \quad (4.10)$$

This last formula can be reorganized as

$$\prod_{j=0}^{2n-1} \Gamma_h\left(\omega - (2n - j - \frac{1}{2})\tau - m\right) \cdot \prod_{\ell=0}^{n-1} \Gamma_h((2\ell+1)\tau + 2m) \cdot \prod_{k=1}^n \Gamma_h(2k\tau) \quad (4.11)$$

The three terms in the argument of these hyperbolic Gamma function correspond to the ones expected from the duality. Indeed if we associate a mass parameter τ to the adjoint and two mass parameters $m_1 = m$ and $m_2 = \omega - \frac{\tau}{2}$ then the unit flux bare monopole $Y_{U_{sp}}$ has mass parameter $m_{Y_{U_{sp}}} = 2\omega - 2n\tau - m_1 - m_2$. The dressed monopole $Y_j = Y_{U_{sp}} S^j$ has mass parameter $m_{Y_j} = 2\omega - (2n - j)\tau - m_1 - m_2$. By using the constraint imposed by the superpotential on m_2 we then arrive at $m_{Y_j} = \omega - (2n - j - \frac{1}{2})\tau - m$, corresponding to the argument of the first hyperbolic Gamma function in (4.11). On the other hand the arguments of the second and of the third Gamma functions in (4.11) are straightforward and they correspond to the dressed mesons $M_\ell = qS^{2\ell+1}q$ and the to the singlets $\sigma_k = Tr S^{2k}$.

Case II: *SO*(2*n*)

In this case we choose the parameters μ_r as $\vec{\mu} = (\frac{\omega_1}{2}, \frac{\omega_2}{2}, 0, m)$ and apply the duplication formula. On the LHS of (4.4) we obtain

$$\frac{\Gamma_h(\tau)^n}{(-\omega_1\omega_2)^{\frac{n}{2}} 2^n n!} \int_{C^n} \prod_{1 \leq j < k \leq n} \frac{\Gamma_h(\tau \pm x_j \pm x_k)}{\Gamma_h(\pm x_j \pm x_k)} \prod_{j=1}^n \Gamma_h(m \pm x_j) dx_j \quad (4.12)$$

This corresponds to the partition function of *SO*(2*n*) with an adjoint *A* and a vector *q* with vanishing superpotential. Actually to correctly reproduce the expected partition function we need an extra factor of 2, in order to have 2^{n-1} in the denominator, that correctly reproduces the Weyl factor. This extra 2 will be generated when looking at the RHS as are going to explain.

The RHS of (4.4) can be studied as in the *USp*(2*n*) case above. In this case we obtain

$$\begin{aligned} & \frac{1}{2} \Gamma_h(n\tau) \cdot \Gamma_h(\omega - (n-1)\tau - m) \cdot \prod_{k=1}^{n-1} \Gamma_h(2k\tau) \\ & \times \prod_{\ell=0}^{n-1} \Gamma_h(2\ell\tau + 2m) \cdot \prod_{j=0}^{2n-2} \Gamma_h(\omega - (2n-2-j)\tau - m) \end{aligned} \quad (4.13)$$

where we used the duplication formula, the reflection equation and the relations $\Gamma_h(\frac{\omega_1}{2}) = \Gamma_h(\frac{\omega_2}{2}) = \frac{1}{\sqrt{2}}$. As anticipated above, the $\frac{1}{2}$ term can be moved on the LHS reproducing the Weyl factor of *SO*(2*n*). The other contributions correspond to the 4*n* singlets of [2]. Let us discuss them in detail. Again we associate a mass parameter τ to the adjoint and a mass parameters *m* to the vector. The unit flux bare monopole Y_{SO}^+ has mass parameter $m_{Y_{SO}^+} = \omega - 2(n-1)\tau - m$. The dressed monopoles $Y_j^+ = Y_{SO}^+ \text{Tr } A^j$ have mass parameter $m_{Y_j^+} = \omega - (2n-2-j)\tau - m$, corresponding to the last term in the second line of (4.13). The mass parameter associated to the baryon monopole is obtained by adding $(n-1)\tau$ to $m_{Y_{SO}^+}$. This gives $m_{Y_{SO}^{A^{n-1}}} = \omega - (n-1)\tau - m$ and it corresponds to the second term in the first line of (4.13). The first term of (4.13), with mass parameter $n\tau$ corresponds to the baryon $\mathbb{B} \equiv \text{Pf } A$. The dressed mesons $M_\ell = qA^{2\ell}q$ and the singlets $\sigma_k = \text{Tr } A^{2k}$ are associated to the combinations $m_{M_\ell} = 2\ell\tau + 2m$ and $m_{\sigma_k} = 2k\tau$ respectively.

Case III: *SO*(2*n* + 1)

In this case we choose the parameters μ_r as $\vec{\mu} = (\frac{\omega_1}{2}, \frac{\omega_2}{2}, \tau, m)$ and apply the duplication formula. On the LHS of (4.4) we obtain

$$\frac{\Gamma_h(\tau)^n}{(-\omega_1\omega_2)^{\frac{n}{2}} 2^n n!} \int_{C^n} \prod_{1 \leq j < k \leq n} \frac{\Gamma_h(\tau \pm x_j \pm x_k)}{\Gamma_h(\pm x_j \pm x_k)} \prod_{j=1}^n \frac{\Gamma_h(\tau \pm x_j) \Gamma_h(m \pm x_j)}{\Gamma_h(\pm x_j)} dx_j \quad (4.14)$$

This corresponds to the partition function of *SO*(2*n* + 1) with an adjoint *A* and a vector *q* with vanishing superpotential. Actually we are still missing a contribution $\Gamma_h(m)$ coming from the zero modes of the vector. As in the *SO*(2*n*) case discussed above, the extra

term comes from the RHS, that in this case becomes

$$\begin{aligned} & \frac{\Gamma_h(\omega - n\tau)\Gamma_h(n\tau + m)}{\Gamma_h(m)} \prod_{k=1}^n \Gamma_h(2k\tau) \prod_{\ell=0}^{n-1} \Gamma_h(2\ell\tau + 2m) \\ & \times \prod_{j=0}^{2n-1} \Gamma_h(\omega - (2n - 1 - j)\tau - m) \end{aligned} \quad (4.15)$$

As anticipated above the denominator can be moved on the LHS and it is necessary to reproduce the zero mode of the chiral fields in the vectorial representation of the $SO(2n + 1)$ gauge group. The other $4n + 2$ Gamma functions correspond to the singlets discussed in [2]. Let us discuss them in detail. Again we associate a mass parameter τ to the adjoint and a mass parameters m to the vector. The unit flux bare monopole Y_{SO}^+ has mass parameter $m_{Y_{SO}^+} = \omega - (2n - 1)\tau - m$. The dressed monopoles $Y_j^+ = Y_{SO}^+ \text{Tr } A^j$ have mass parameter $m_{Y_j^+} = \omega - (2n - 1 - j)\tau - m$, corresponding to the term in the second line of (4.13). The baryon monopole $Y_{qA^{n-1}}^-$ is obtained by adding $(n - 1)\tau + m$ to the contribution of $m_{Y_{SO}^+}$. This gives $m_{Y_{qA^{n-1}}^-} = \omega - (n - 1)\tau$, and this gives raise to the first term in the first line of (4.15). The second term in the first line of (4.15), with mass parameter $n\tau + m$ corresponds to the baryon $\epsilon_{2n+1}(qA^n)$. The dressed mesons $M_\ell = qA^{2\ell}q$ and the singlets $\sigma_k = \text{Tr } A^{2k}$ are associated to the combinations $m_{M_\ell} = 2\ell\tau + 2m$ and $m_{\sigma_k} = 2k\tau$ respectively.

4.3 New results

In this section we propose three new dualities, that generalize the ones reviewed above, in presence of two more fundamentals (or vectors) and of a monopole superpotential.

Here we propose such dualities by reversing the procedure adopted so far. We start from the integral identity (4.2), that has a clear physical interpretation, because it gives the mathematical version of the confinement of $USp(2n)$ with an antisymmetric, six fundamentals and the monopole superpotential.

Then we use the duplication formula and we obtain three new relations as discussed above in terms of $USp(2n)$ ($SO(N)$) with an adjoint S (A), four (three) fundamentals (vectors) and $W = pSp$ ($W = 0$). In each case the masses are constrained because the choice of parameters necessary to apply the duplication formula leaves us with a constraint, corresponding to the leftover of (4.3).

By applying the three choices of mass parameters discussed in Section 4.2 we arrive at the following three identities

Case I: $USp(2n)$

The first choice corresponds to choosing $\vec{\mu} = (\frac{\tau}{2} + \frac{\omega_1}{2}, \frac{\tau}{2} + \frac{\omega_2}{2}, \frac{\tau}{2}, \mu_1, \mu_2, \mu_3)$. Substituting in (4.2) it gives raise to the following identity

$$\begin{aligned} & \frac{\Gamma_h(\tau)^n}{(-\omega_1\omega_2)^{\frac{n}{2}} 2^n n!} \int_{C^n} \prod_{1 \leq j < k \leq n} \frac{\Gamma_h(\tau \pm x_j \pm x_k)}{\Gamma_h(\pm x_j \pm x_k)} \prod_{j=1}^n \frac{\Gamma_h(\tau \pm 2x_j) \prod_{r=1}^4 \Gamma_h(\mu_r \pm x_j)}{\Gamma_h(\pm 2x_j)} dx_j \\ = & \prod_{k=1}^n \Gamma_h(2k\tau) \cdot \prod_{j=0}^{n-1} \prod_{r=1}^3 \Gamma_h((2j+1)\tau + 2\mu_r) \cdot \prod_{j=0}^{2n-1} \prod_{1 \leq r < s \leq 3} \Gamma_h(j\tau + \mu_r + \mu_s) \quad (4.16) \\ = & \prod_{k=1}^n \Gamma_h(2k\tau) \cdot \prod_{j=0}^{n-1} \left(\prod_{1 \leq r \leq s \leq 3} \Gamma_h((2j+1)\tau + \mu_r + \mu_s) \cdot \prod_{1 \leq r < s \leq 3} \Gamma_h(2j\tau + \mu_r + \mu_s) \right) \end{aligned}$$

with the conditions

$$2n\tau + \sum_{a=1}^4 \mu_a = 2\omega \quad \& \quad 2\mu_4 + \tau = 2\omega \quad (4.17)$$

Schematically this corresponds to:

$Sp(2n)$ w/ adjoint S and 4 fundamentals $q_{1,2,3}, p$ $W = Y_{USp} + \text{Tr}(pSp)$	\iff	Wess-Zumino w/ 10n chirals $\sigma_k = \text{Tr} S^{2k}, \quad k = 1, \dots, n$ $\mathcal{A}_{rs}^{(2\ell)} \equiv q_r S^{2\ell} q_s, \quad r < s$ $\mathcal{S}_{rs}^{(2\ell+1)} \equiv q_r S^{2\ell+1} q_s, \quad r \leq s$
--	--------	---

where $\ell = 0, \dots, n-1$ and $r, s = 1, 2, 3$. The dual (confined) model corresponds to a set of singlets, $\sigma_k = \text{Tr} S^{2k}$, with $k = 1, \dots, n$, and dressed mesons. These are in the antisymmetric and in the symmetric representation of the flavor symmetry group that rotates $q_{1,2,3}$ and they can be defined as $\mathcal{A}_{rs}^{(2\ell)} \equiv q_r S^{(2\ell)} q_s$ and $\mathcal{S}_{rs}^{(2\ell+1)} \equiv q_r S^{2\ell+1} q_s$ respectively. By flipping the singlets σ_k we modify the electric theory, adding the superpotential terms $\Delta_{W_{ele}} = \sum_{k=1}^n \rho_k \text{Tr} S^{2k}$. In the dual theory we are left with the cubic superpotential

$$\begin{aligned} W = & \sum_{\ell_1 + \ell_2 + \ell_3 = 2n-2} \epsilon^{r_1 r_2 r_3} \epsilon^{s_1 s_2 s_3} \mathcal{S}_{s_1, r_1}^{(2\ell_1+1)} \mathcal{S}_{s_2, r_2}^{(2\ell_2+1)} \mathcal{S}_{s_3, r_3}^{(2\ell_3+1)} \\ & + \sum_{\ell_1 + \ell_2 + \ell_3 = 2n-1} \epsilon^{r_1 r_2 r_3} \epsilon^{s_1 s_2 s_3} \mathcal{A}_{s_1, r_1}^{(2\ell_1)} \mathcal{A}_{s_2, r_2}^{(2\ell_2)} \mathcal{S}_{s_3, r_3}^{(2\ell_3+1)} \quad (4.19) \end{aligned}$$

On the identity (4.16) the effect of such a flip corresponds to moving the terms $\Gamma_h(2k\tau)$ on the LHS and taking them to the numerator by using the reflection equation, giving raise to the contribution $\Gamma_h(2\omega - 2k\tau)$, corresponding to the singlets ρ_k .

Case II: $SO(2n)$

The second choice corresponds to choosing $\vec{\mu} = (\frac{\omega_1}{2}, \frac{\omega_2}{2}, 0, \mu_1, \mu_2, \mu_3)$. Substituting in (4.2) gives rise to the following identity

$$\begin{aligned} & \frac{\Gamma_h(\tau)^n}{(-\omega_1\omega_2)^{\frac{n}{2}} 2^{n-1}n!} \int_{C^n} \prod_{1 \leq j < k \leq n} \frac{\Gamma_h(\tau \pm x_j \pm x_k)}{\Gamma_h(\pm x_j \pm x_k)} \prod_{j=1}^n \prod_{r=1}^3 \Gamma_h(\mu_r \pm x_j) dx_j = \Gamma_h(n\tau) \\ & \prod_{k=1}^{n-1} \Gamma_h(2k\tau) \prod_{j=0}^{n-1} \prod_{r=1}^3 \Gamma_h(2j\tau + 2\mu_r) \prod_{1 \leq r < s \leq 3} \Gamma_h((n-1)\tau + \mu_r + \mu_s) \prod_{j=0}^{2n-2} \Gamma_h(j\tau + \mu_r + \mu_s) \end{aligned} \quad (4.20)$$

with the condition

$$2(n-1)\tau + \sum_{r=1}^3 \mu_r = \omega \quad (4.21)$$

This corresponds to the duality:

$$\begin{aligned} & \begin{array}{l} SO(2n) \text{ w/ adjoint } A \\ \text{and 3 vectors } q_{1,2,3} \\ W = Y_{SO}^+ \end{array} \iff \begin{array}{l} \text{Wess-Zumino w/ } 10n + 3 \text{ chirals} \\ \sigma_k = \text{Tr } A^{2k} \\ \mathcal{A}_{rs}^{(2\ell+1)} \equiv q_r A^{2\ell+1} q_s \quad r < s \\ \mathcal{S}_{rs}^{(2\ell)} \equiv q_r A^{2\ell} q_s \quad r \leq s \\ \mathbb{B} = \text{Pf } A \\ \mathbb{B}_r = \epsilon_{rst} \epsilon_{2n} (A^{n-1} q_s q_t) \end{array} \end{aligned} \quad (4.22)$$

with $k = 1, \dots, n-1$, $\ell = 0, \dots, n-1$ and $r, s = 1, 2, 3$. The dual description consists of a set of chiral fields identified with mesons and baryons of the electric theory. The baryon $\mathbb{B} = \text{Pf } A$ is reproduced on the partition function by $\Gamma_h(n\tau)$ while the baryons $\mathbb{B}_r = \epsilon_{rst} \epsilon_{2n} (A^{n-1} q_s q_t)$ are reproduced on the partition function by $\Gamma_h((n-1)\tau + \mu_r + \mu_s)$. There is also a tower of singlets σ_k associated to the singlets $\text{Tr } A^{2k}$ contributing to the partition function as $\prod_{k=1}^{n-1} \Gamma_h(2k\tau)$.

The mesons are in the antisymmetric and in the symmetric representation of the flavor symmetry group that rotates the three vectors and they can be defined as $\mathcal{A}_{rs}^{(2\ell+1)} \equiv q_r A^{2\ell+1} q_s$ and $\mathcal{S}_{rs}^{(2\ell)} \equiv q_r A^{2\ell} q_s$ respectively. By flipping the singlets σ_k and the baryons we are left, in the dual theory, with the cubic superpotential

$$\begin{aligned} W &= \sum_{\ell_1 + \ell_2 + \ell_3 = 2n-2} \epsilon^{r_1 r_2 r_3} \epsilon^{s_1 s_2 s_3} \mathcal{S}_{s_1, r_1}^{(2\ell_1)} \mathcal{S}_{s_2, r_2}^{(2\ell_2)} \mathcal{S}_{s_3, r_3}^{(2\ell_3)} \\ &+ \sum_{\ell_1 + \ell_2 + \ell_3 = 2n-3} \epsilon^{r_1 r_2 r_3} \epsilon^{s_1 s_2 s_3} \mathcal{A}_{s_1, r_1}^{(2\ell_1+1)} \mathcal{A}_{s_2, r_2}^{(2\ell_2+1)} \mathcal{S}_{s_3, r_3}^{(2\ell_3)} \end{aligned} \quad (4.23)$$

Again we can reproduce the effect of the flip on the partition function by moving the relative Gamma function on the LHS of (4.20) and using the reflection equation.

$SO(2n + 1)$

The third choice corresponds to choosing $\vec{\mu} = (\frac{\omega_1}{2}, \frac{\omega_2}{2}, \tau, \mu_1, \mu_2, \mu_3)$. Substituting in (4.2) gives rise to the following identity

$$\begin{aligned}
 & \frac{\Gamma_h(\tau)^n \prod_{r=1}^3 \Gamma_h(\mu_r)}{(-\omega_1 \omega_2)^{\frac{n}{2}} 2^n n!} \int_{C^n} \prod_{1 \leq j < k \leq n} \frac{\Gamma_h(\tau \pm x_j \pm x_k)}{\Gamma_h(\pm x_j \pm x_k)} \\
 & \times \prod_{j=1}^n \frac{\Gamma_h(\tau \pm x_j) \prod_{r=1}^3 \Gamma_h(\mu_r \pm x_j)}{\Gamma_h(\pm x_j)} dx_j = \Gamma_h(\omega - n\tau) \prod_{r=1}^3 \Gamma_h(n\tau + \mu_r) \\
 & \times \prod_{k=1}^n \Gamma_h(2k\tau) \prod_{j=0}^{n-1} \prod_{r=1}^3 \Gamma_h(2j\tau + 2\mu_r) \prod_{j=0}^{2n-1} \prod_{1 \leq r < s \leq 3} \Gamma_h(j\tau + \mu_r + \mu_s)
 \end{aligned} \tag{4.24}$$

with the condition

$$(2n - 1)\tau + \sum_{a=1}^3 \mu_a = \omega \tag{4.25}$$

This corresponds to:

$$\begin{array}{l}
 \text{Wess-Zumino w/ } 10n + 4 \text{ chirals} \\
 \sigma_k = \text{Tr } A^{2k} \\
 SO(2n + 1) \text{ w/ adjoint } A \\
 \text{and 3 vectors } q_{1,2,3} \\
 W = Y_{SO}^+
 \end{array} \iff \begin{array}{l}
 \mathcal{A}_{rs}^{(2\ell+1)} \equiv q_r A^{2\ell+1} q_s \quad r < s \\
 \mathcal{S}_{rs}^{(2\ell)} \equiv q_r A^{2\ell} q_s \quad r \leq s \\
 \mathbb{B} \equiv \epsilon_{2n+1} A^{n-1} q_1 q_2 q_3 \\
 \mathbb{B}_i \equiv \epsilon_{2n+1} A^n q_i
 \end{array} \tag{4.26}$$

with $k = 1, \dots, n - 1$, $\ell = 0, \dots, n$ and $r, s = 1, 2, 3$. The dual description consists of a set of chiral fields identified with symmetric and antisymmetric mesons as above, the baryons $\mathbb{B} \equiv \epsilon_{2n+1} A^{n-1} q_1 q_2 q_3$ and $\mathbb{B}_i \equiv \epsilon_{2n+1} A^n q_i$ and the singlets $\sigma_k = \text{Tr } A^{2k}$. On the partition function such fields correspond to $\Gamma_h(\omega - n\tau)$, $\Gamma_h(n\tau + \mu_r)$ and $\prod_{k=1}^n \Gamma_h(2k\tau)$ respectively. Again by flipping the singlets and leaving only the mesons on the dual side we are left with the superpotential (4.23). We can reproduce the effect of such flip on the partition function by moving the relative Gamma function on the LHS of (4.24) and using the reflection equation.

4.3.1 A consistency check: flowing to the cases of [2]

Here we show that by giving large masses to two of the fundamentals (or two of the vectors in the theories with orthogonal group) the dualities (4.16), (4.20) and (4.24) reduce respectively to the dualities (5.1), (5.2) and (5.3) of [2].

Case I: $USp(2n)$

We consider the real mass flow triggered by giving large real masses (of opposite signs) to two of the quarks, say q_1 and q_2 . On the electric side we are left with a $USp(2n)$ theory with two quarks $q = q_3$ and p , one adjoint and $W = pSp$. The linear monopole superpo-

tential is lifted in the mass flow. On the magnetic side the dressed mesons $\mathcal{A}_{3r}^{(2\ell)}$, $\mathcal{S}_{3r}^{(2\ell+1)}$ and $\mathcal{S}_{rr}^{(2\ell+1)}$ with $r = 1, 2$ become massive and are integrated out in the IR. The dressed mesons $\mathcal{A}_{12}^{(2\ell)}$ and $\mathcal{S}_{12}^{(2\ell+1)}$ are massless and are identified with the dressed monopoles Y_j of the electric theory. More precisely we identify $\mathcal{A}_{12}^{(2\ell)}$ with $Y_{2\ell}$ and $\mathcal{S}_{12}^{(2\ell+1)}$ with $Y_{2\ell+1}$ for $\ell = 0, \dots, n-1$. The leftover dressed mesons $\mathcal{S}_{33}^{2\ell+1}$ correspond to M_ℓ , for $\ell = 0, \dots, n-1$. The superpotential (4.19) reduces to the one of [2] when the singlets σ_k are flipped. Indeed the only superpotential terms surviving the real mass flow are

$$\begin{aligned} W &\propto \sum_{\ell_1+\ell_2+\ell=2n-2} S_{1,2}^{(2\ell_1+1)} S_{1,2}^{(2\ell_2+1)} S_{3,3}^{(2\ell+1)} + \sum_{\ell_1+\ell_2+\ell=2n-1} A_{1,2}^{(2\ell_1)} A_{1,2}^{(2\ell_2)} S_{3,3}^{(2\ell+1)} \\ &= \sum_{j_1, j_2, \ell} Y_{j_1} Y_{j_2} M_\ell \delta_{j_1+j_2+2\ell-4n+2} \end{aligned} \quad (4.27)$$

We can follow this real mass flow on the partition function in the following way. We parametrize the mass parameters as:

$$\mu_1 = \nu + s, \quad \mu_2 = \nu - s, \quad \mu_3 = m \quad (4.28)$$

and we take the limit $s \rightarrow \infty$. The constraint from the monopole superpotential reads:

$$2\nu = \omega - 2n\tau + \frac{\tau}{2} - m \quad (4.29)$$

On the RHS of (4.16) the Gamma functions with finite argument in the $s \rightarrow \infty$ limit are:

$$\begin{aligned} &\prod_{\ell=0}^{n-1} \Gamma_h((2\ell+1)\tau + 2m) \prod_{\ell=0}^{2n-1} \Gamma_h(\ell\tau + 2\nu) \\ &= \prod_{\ell=0}^{n-1} \Gamma_h((2\ell+1)\tau + 2m) \prod_{j=0}^{2n-1} \Gamma_h\left(\omega + j\tau - 2n\tau + \frac{\tau}{2} - m\right) \end{aligned} \quad (4.30)$$

which correspond to the singlets M_ℓ and Y_j . On the LHS it corresponds to the partition function of $USp(2n)$ with 2 fundamentals p, q , one adjoint S , n singlets ρ_k and superpotential $W = \sum_{k=1}^n \rho_k \text{Tr} S^{2k} + pSp$ as expected. The Gamma functions with divergent argument can be written as an exponential using (2.11), that we report here:

$$\lim_{z \rightarrow \pm\infty} \Gamma_h(z) = \zeta^{-\text{sgn}(z)} \exp\left(\frac{i\pi}{2\omega_1\omega_2} \text{sgn}(z)(z - \omega)^2\right) \quad (4.31)$$

where $\zeta = \exp\left(2\pi i \frac{\omega_1^2 + \omega_2^2}{48\omega_1\omega_2}\right)$. The resulting phase on the LHS is then (we omit the prefactor $\frac{i\pi}{2\omega_1\omega_2}$):

$$\sum_{j=1}^n (s + \nu \pm x_j - \omega)^2 - (-s + \nu \pm x_j - \omega)^2 = 8sn(\nu - \omega) \quad (4.32)$$

while on the RHS it is:

$$\begin{aligned}
 & \sum_{\ell=1}^n \left(((2\ell-1)\tau + 2\nu + 2s - \omega)^2 - ((2\ell-1)\tau + 2\nu - 2s - \omega)^2 \right) \\
 & + \sum_{\ell=0}^{2n-1} \left((\ell\tau + m + \nu + s - \omega)^2 - (\ell\tau + m + \nu - s - \omega)^2 \right) \\
 & = 4ns(6\nu + 2m - 4\omega + (4n-1)\tau)
 \end{aligned} \tag{4.33}$$

Under the constraint (4.29) the divergent phases cancel between the RHS and the LHS. We are then left with an equation which corresponds to the identity between the partition functions of the theories of the duality (5.1) of [2].

Case II: $SO(2n)$

We can flow from the duality (4.20) to (5.2) of [2] by giving a large mass of opposite sign to two vectors. Indeed the only mesons that survive the projection are the ones labeled by $\mathcal{A}_{12}^{(2\ell+1)}$, $\mathcal{S}_{12}^{(2\ell)}$ and $\mathcal{S}_{33}^{(2\ell)}$. The first two are associated to the dressed monopoles Y_j^+ as $\mathcal{A}_{12}^{(2\ell+1)} = Y_{2\ell+1}^+$ and $\mathcal{S}_{12}^{(2\ell)} = Y_{2\ell}^+$ for $\ell = 0, \dots, n-1$. The leftover dressed mesons $\mathcal{S}_{33}^{2\ell}$ correspond to M_ℓ . After the real mass flow the superpotential (4.23) reduces to the one of [2] when the singlets σ_k , $Y_{A^{n-1}}^-$ and Y_j^+ are flipped:

$$\begin{aligned}
 W & \propto \sum_{\ell_1+\ell_2+\ell=2n-2} \mathcal{S}_{1,2}^{(2\ell_1)} \mathcal{S}_{1,2}^{(2\ell_2)} \mathcal{S}_{3,3}^{(2\ell)} + \sum_{\ell_1+\ell_2+\ell=2n-3} \mathcal{A}_{1,2}^{(2\ell_1+1)} \mathcal{A}_{1,2}^{(2\ell_2+1)} \mathcal{S}_{3,3}^{(2\ell)} \\
 & = \sum_{j_1, j_2, \ell} Y_{j_1}^+ Y_{j_2}^+ M_\ell \delta_{j_1+j_2+2\ell-4n+4}
 \end{aligned} \tag{4.34}$$

In order to follow the real mass flow on the partition function we parametrize the masses as:

$$\mu_1 = \nu + s, \quad \mu_2 = \nu - s, \quad \mu_3 = m \tag{4.35}$$

The constraint reads:

$$2(n-1)\tau + 2\nu + m = \omega \tag{4.36}$$

Taking the limit $s \rightarrow \infty$ the LHS becomes the partition function for $SO(2n)$ with one vector and one adjoint multiplied by a divergent phase. The singlets on the RHS of (4.20) that remain massless are:

$$\begin{aligned}
 & \Gamma_h(n\tau) \prod_{k=1}^{n-1} \Gamma_h(2k\tau) \prod_{\ell=1}^{n-1} \Gamma_h(2\ell\tau + 2m) \Gamma_h(\omega - (n-1)\tau - m) \\
 & \times \prod_{j=0}^{2n-1} \Gamma_h(\omega + j\tau - m - 2(n-1)\tau)
 \end{aligned} \tag{4.37}$$

which correspond respectively to the singlets \mathbb{B} , σ_k , M_ℓ , $Y_{A^{n-1}}^-$ and Y_j^+ discussed above. Along the lines of the computation done in the previous case one can show that the divergent phases cancel between the LHS and the RHS. The limit $s \rightarrow \infty$ then gives the identity between the partition functions of the dual theories (5.2) of [2].

Case III: $SO(2n + 1)$

When we give large masses to two of the vectors this duality reduces to the duality (5.3) of [2]. Analogously to the $SO(2n)$ case the the superpotential reduces to the one of [2] when the singlets σ_k , Y_j^+ and $Y_{qA^{n-1}}^-$ are flipped.

We parametrize the real masses as in (4.35). The constraint reads:

$$(2n - 1)\tau + 2\nu + m = \omega \quad (4.38)$$

The LHS becomes the partition function for a $SO(2n + 1)$ gauge theory with one vector q and one adjoint A multiplied by a divergent phase. The singlets on the RHS of (4.24) that remain massless are:

$$\begin{aligned} & \Gamma_h(\omega - n\tau) \Gamma_h(n\tau + m) \prod_{k=1}^n \Gamma_h(2k\tau) \prod_{\ell=0}^{n-1} \Gamma_h(2\ell\tau + 2m) \\ & \times \prod_{j=0}^{2n-1} \Gamma_h(\omega + j\tau - m - (2n - 1)\tau) \end{aligned} \quad (4.39)$$

which correspond respectively to the singlets $Y_{qA^{n-1}}^-$, \mathbb{B} , σ_k , M_ℓ and Y_j^+ discussed above. The divergent phases cancel between the LHS and the RHS. The resulting identity corresponds to the duality (5.3) of [2].

4.3.2 Proving the new dualities through adjoint deconfinement

The dualities read above from the matching of the three-sphere partition functions can be proved along the lines of [2] by deconfining the adjoints as reviewed in sub-section 4.1. Even if the logic is very similar the presence of more fundamentals/vectors and the constraints imposed by the monopole superpotentials modify the analysis and it is worth to study explicitly the mechanism. Furthermore when translated to the three-sphere partition function this process offers an alternative derivation of the mathematical identities (4.16), (4.20) and (4.24) from a physical perspective. In Figure 4.1 we show schematically the confinement/deconfinement procedure we used to prove the confinement of the $USp(2n)$ model with monopole superpotential.

Case I: $USp(2n)$

The $USp(2n)$ model with an adjoint S , four fundamentals $\{q_{1,2,3}, p\}$ and superpotential (4.18) is dual to the $USp(2n) \times SO(2n)$ quiver given in Figure 4.2. As discussed above the analysis is made easier by flipping the singlets $\text{Tr } S^{2k}$ with $k = 1, \dots, n$. On the physical side this corresponds to adding singlets ρ_k to the original USp theory with superpotential:

$$\delta W = \sum_{k=1}^n \rho_k \text{Tr} \left(S^{2k} \right) \quad (4.40)$$

while mathematically it corresponds to moving the tower $\Gamma_h(2k\tau)$ on the LHS of (4.16) and by using the reflection equation we are left with $\Gamma_h(2\omega - 2k\tau)$. The superpotential

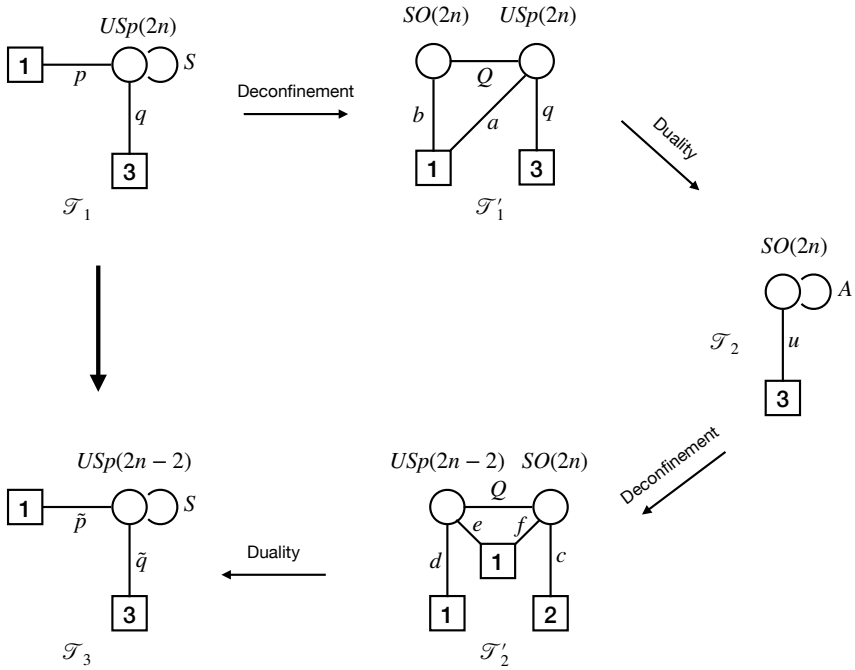


Figure 4.1 Schematic representation of one step of the deconfinement procedure used to prove the confinement of the $USp(2n)$ model with monopole superpotential. The superpotential and three-sphere partition function of each model in Figure are:

	\mathcal{T}_1	\mathcal{T}'_1	\mathcal{T}_2	\mathcal{T}'_2	\mathcal{T}_3
W	(4.18)	(4.41)	(4.52)	(4.54)	(4.60)
\mathcal{Z}_{S^3}	(4.16)	(4.50)	(4.53)	(4.58)	(4.62)

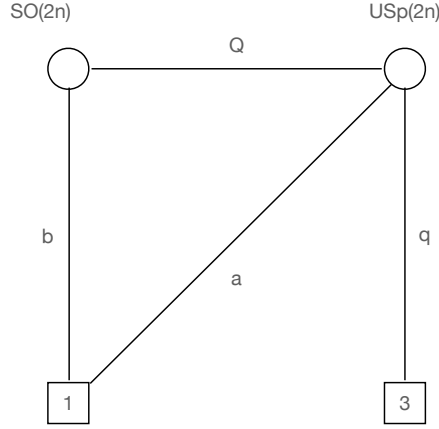


Figure 4.2 Quiver description of the deconfinement of the adjoint S of the $USp(2n)$ model with superpotential (4.18). In this and in the following quivers we decided to omit to represent the various singlets.

associated to the quiver in Figure 4.2 is then¹:

$$W = Y_{USp} + Y_{SO}^+ + \text{Tr}(abQ) + s_1 \epsilon_{2n} (Q^{2n}) + \sum_{k=1}^{n-1} \rho_k \text{Tr} \left((QQ)^{2k} \right) \quad (4.41)$$

Indeed by confining the $SO(2n)$ gauge node of this quiver we arrive at the original model. This can be proved thanks to a confining duality reviewed in the appendix B. By confining the $SO(2n)$ node the superpotential becomes

$$\begin{aligned} W &= Y_{USp} + \text{Tr}(aM_{bQ}) + \sum_{k=1}^{n-1} \rho_k \text{Tr} \left(S^{2k} \right) + s_1 q_b + pSp \\ &+ M_{bb} q_b^2 + M_{bQ} q_b p + \det \begin{pmatrix} S & M_{bQ} \\ M_{bQ} & M_{bb} \end{pmatrix} \end{aligned} \quad (4.42)$$

where the duality map for the meson of $SO(N)$ is

$$\begin{pmatrix} QQ & bQ \\ bQ & bb \end{pmatrix} \equiv \begin{pmatrix} S & M_{bQ} \\ M_{bQ} & M_{bb} \end{pmatrix} \quad (4.43)$$

¹In $\epsilon_{2n} Q^{2n}$ the USp indices of Q are contracted using $J = \begin{pmatrix} 0 & \mathbb{1}_n \\ -\mathbb{1}_n & 0 \end{pmatrix}$ and the SO indices are contracted with ϵ_{2n} , explicitly $\epsilon_{2n} Q^{2n} = \epsilon_{i_1 j_1 \dots i_n j_n} Q_{i_1}^{a_1} J^{a_1 b_1} Q_{j_1}^{b_n} \dots Q_{i_n}^{a_n} J^{a_n b_n} Q_{j_n}^{b_n}$. Similarly $\text{Tr}(S^n)$ is a shorthand notation for $\text{Tr}((S \cdot J)^n)$. In the rest of this Chapter we omit the matrix J , which is always understood whenever we contract the indices of a symplectic group.

while the baryons are $q_b \equiv \epsilon_{2n}(Q^{2n})$ and $p \equiv \epsilon_{2n}(Q^{2n-1}b)$. The field S is in the adjoint of $USp(2n)$ while the field p is the fourth fundamental of $USp(2n)$ (the other three fundamentals $q_{1,2,3}$ are spectator when confining $SO(2n)$). By evaluating the F-terms of the massive fields we end up with the original $USp(2n)$ gauge theory, with an adjoint, four fundamentals and superpotential

$$W = Y_{USp} + pSp + \sum_{k=1}^{n-1} \rho_k \text{Tr}(S^{2k}) + M_{bb} \det(S) \quad (4.44)$$

We can expand the determinant of S in terms of traces²:

$$\det(S) \propto \text{Tr}(S^{2n}) + \text{multi-traces} \quad (4.45)$$

By dropping the multi-trace terms and by comparing with the superpotential $W = (4.18) + (4.40)$ of the $USp(2n)$ model we started with, we identify $M_{bb} = \rho_n$.

On the partition function the mass parameters for the fields appearing in this $USp(2n) \times SO(2n)$ quiver are related to the ones of the original $USp(2n)$ model (i.e. μ_r and τ in formula (4.16)) by the following set of relations

$$\sum_{r=1}^3 \mu_r + 2n\mu_Q + \mu_a = 2\omega, \quad 2n\mu_Q + \mu_b = \omega, \quad \mu_Q + \mu_b + \mu_a = 2, \quad \mu_{s_1} + 2n\mu_Q = 2 \quad (4.47)$$

where μ_r are the three mass parameter for the fields $q_{1,2,3}$. Furthermore we can map these parameters to the ones in the confined $SO(2n)$ model by imposing $\mu_Q = \frac{\tau}{2}$. In this way we arrive at the following identifications

$$\mu_{s_1} = 2\omega - n\tau, \quad \mu_b = \omega - n\tau, \quad \mu_a = 2\omega - \sum_{r=1}^3 \mu_r - n\tau \quad (4.48)$$

with the constraint

$$2n\tau - \frac{\tau}{2} + \sum_{r=1}^3 \mu_r = \omega \quad (4.49)$$

The duality between the original $USp(2n)$ model and the quiver with the deconfined adjoint can be checked on the partition function by using the identity (B.3). This can be

²For a $2n \times 2n$ symmetric matrix S :

$$\det(S) = \det(S \cdot J) = \frac{1}{(2n)!} B_{2n}(s_1, \dots, s_{2n}), \quad s_k = (-1)^{k-1} (k-1)! \text{Tr}((S \cdot J)^k) \quad (4.46)$$

where B_n are Bell polynomials $B_l(s_1, \dots, s_l) = s_l + \dots$

shown explicitly by considering the partition function of the quiver, i.e.

$$\begin{aligned}
Z_{USp(2n) \times SO(2n)} &= \frac{\prod_{k=1}^{n-1} \Gamma_h(2\omega - 2k\tau) \Gamma_h(\mu_{s_1})}{(-\omega_1 \omega_2)^n 2^{2n-1} (n!)^2} \int \prod_{i=1}^n dx_i \frac{\Gamma_h(\pm x_i + \mu_b)}{\Gamma_h(\pm x_i)} \\
&\times \prod_{\alpha=1}^n dy_\alpha \frac{\Gamma_h(\pm y_\alpha + \mu_a) \prod_{r=1}^3 \Gamma_h(\pm y_\alpha + \mu_r)}{\Gamma_h(\pm 2y_\alpha)} \\
&\times \frac{\prod_{i=1}^n \prod_{\alpha=1}^n \Gamma_h(\pm x_i \pm y_\alpha + \mu_Q)}{\prod_{i < j} \Gamma_h(\pm x_i \pm x_j) \prod_{\alpha < \beta} \Gamma_h(\pm y_\alpha \pm y_\beta)} \quad (4.50)
\end{aligned}$$

and then by using the relation (B.3). This is possible because the mass parameters of the $2n + 1$ vectors in the $SO(2n)$ model are related, due to the linear monopole superpotential, by

$$\sum_{\alpha=1}^n (\pm y_\alpha + \mu_Q) + \mu_b = 2n\mu_Q + \mu_b = \omega \quad (4.51)$$

By applying (B.3) and by using the reflection equation we end up with the first line of (4.16), finding the expected result.

Next we can dualize the $USp(2n)$ node with the linear monopole superpotential turned on. We are left with an $SO(2n)$ SQCD with an adjoint A and superpotential

$$W = Y_{SO}^+ + \sum_{k=1}^{n-1} \rho_k \text{Tr} A^{2k} + \epsilon_{rst} (M_{rs} v_t P f A + v_r \epsilon (A^{n-1} u_s u_t)) + s_1 P f A \quad (4.52)$$

In this case the fields are mapped to the ones in the $USp(2n) \times SO(2n)$ quiver as $u_r = Q q_r$, $A = Q Q$, $M_{rs} = q_r q_s$ and $v_r = a q_s$. The fields u_r are three vectors while A is in the adjoint of $SO(2n)$. The fields M_{rs} and v_r are singlets. The term $\epsilon_{rst}(\dots)$ in the superpotential originates from the Pfaffian of the generalized meson, built up by contracting the fundamentals of the $USp(2n)$ gauge node, after integrating out the massive component $M_{Qa} = Qa$.

The partition function is obtained by the limiting case of the identity given in **Proposition 5.3.4** of [56] and we report it in formula (B.1). It corresponds to the confining duality for $USp(2n)$ with $2n + 4$ fundamentals and linear monopole superpotential turned on. This identity was obtained also in [49] from the reduction of the integral identity relating the superconformal indices of the 4d duality of [17]. The partition function obtained after confining the $USp(2n)$ gauge node is

$$\begin{aligned}
Z_{SO(2n)} &= \frac{\prod_{r < s} \Gamma_h(\mu_r + \mu_s) \prod_{r=1}^3 \Gamma_h(\omega + n\tau - \frac{\tau}{2} + \mu_r) \Gamma_h(2\omega - n\tau) \prod_{k=1}^{n-1} \Gamma_h(2\omega - 2k\tau)}{(-\omega_1 \omega_2)^{\frac{n}{2}} 2^{n-1} (n!)} \\
&\times \int \prod_{i=1}^n dx_i \prod_{r=1}^3 \Gamma_h\left(\pm x_i + \mu_r + \frac{\tau}{2}\right) \prod_{1 \leq i < j \leq n} \frac{\Gamma_h(\pm x_i \pm x_j + \tau)}{\Gamma_h(\pm x_i \pm x_j)} \quad (4.53)
\end{aligned}$$

As a consistency check we can now use formula (4.20) on the integral (4.53) because the mass parameters are constrained as in (4.21). After some rearranging we eventually checked that the integral reduces to the LHS of (4.16). This signals the consistency of the various steps done so far and motivated us to further deconfine the adjoint of $SO(2n)$ in

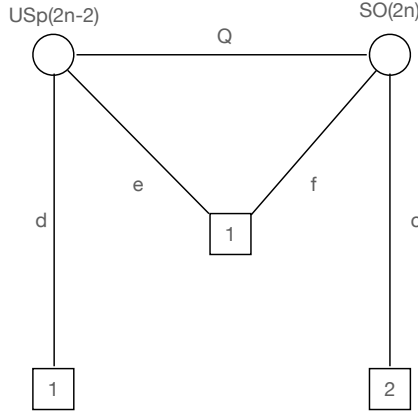


Figure 4.3 Quiver representation of the $SO(2n)$ model after the adjoint field has been deconfined

order to produce a new quiver with a symplectic and an orthogonal node.

The $SO(2n)$ model with adjoint and three fundamentals is equivalent to the $USp(2n - 2) \times SO(2n)$ quiver given in Figure 4.3 with superpotential

$$\begin{aligned}
 W = & Y_{USp} + Y_{SO}^+ + \sum_{k=1}^{n-1} \rho_k \text{Tr}(QQ)^{2k} + \text{Tr}(Qef) + v_1 \epsilon_{2n}(Q^{2n-2}c_2c_3) \\
 & + v_3 \text{Tr}(fc_2) + v_2 \text{Tr}(fc_3) + \epsilon_{2n}(Q^{2n})(\text{Tr}(de) + \epsilon_{rst}M_{rs}v_t)
 \end{aligned}
 \tag{4.54}$$

The duality map reflects on the following relations between the mass parameters in the partition function

$$\mu_{c_{2,3}} = \mu_{2,3} + \frac{\tau}{2}, \quad \mu_{d_1} = \mu_1, \quad \mu_Q = \frac{\tau}{2}
 \tag{4.55}$$

Furthermore the superpotential imposes the following relations on the other parameters

$$\mu_f = \omega - \mu_2 - \mu_3 - n\tau, \quad \mu_e = 2\omega - n\tau - \mu_1
 \tag{4.56}$$

and the usual constraint

$$2n\tau - \frac{\tau}{2} + \sum_{r=1}^3 \mu_a = \omega
 \tag{4.57}$$

We can see that this model reduces to the $SO(2n)$ model discussed above when the $USp(2n - 2)$ node with $2n + 2$ fundamentals and a linear monopole superpotential confines. Again the confinement of the $USp(2n - 2)$ symplectic gauge group gives raise to a superpotential term proportional to the Pfaffian of the generalized meson. By integrat-

ing out the massive fields and substituting in the Pfaffian we recover the superpotential (4.52). The partition function of the $USp(2n-2) \times SO(2n)$ model is

$$\begin{aligned}
Z_{SO(2n) \times USp(2n-2)} &= \frac{\prod_{r < s} \Gamma_h(\mu_r + \mu_s) \prod_{r=1}^3 \Gamma_h(\omega + n\tau - \frac{\tau}{2} + \mu_r) \prod_{k=1}^{n-1} \Gamma_h(2\omega - k\tau)}{(-\omega_1 \omega_2)^{\frac{2n-1}{2}} 2^{2n-2} (n!(n-1)!)} \\
&\times \int \prod_{i=1}^n dx_i \frac{\Gamma_h(\pm x_i + \mu_f) \prod_{\ell=2}^3 \Gamma_h(\pm x_i + \mu_{c_\ell})}{\Gamma_h(\pm x_i)} \\
&\times \prod_{a=1}^{n-1} dy_a \frac{\Gamma_h(\pm y_a + \mu_d) \Gamma_h(\pm y_a + \mu_e)}{\Gamma_h(\pm 2y_a)} \\
&\times \frac{\prod_{i=1}^n \prod_{a=1}^{n-1} \Gamma_h(\pm x_i \pm y_a + \mu_Q)}{\prod_{i < j} \Gamma_h(\pm x_i \pm x_j) \prod_{a < b} \Gamma_h(\pm y_a \pm y_b)} \tag{4.58}
\end{aligned}$$

One can check that the partition functions for the $SO(2n)$ model and that for the $USp(2n-2) \times SO(2n)$ quiver are equal by applying the identity for the confining USp node with $2n+2$ fundamentals discussed above. The last step consists in performing a confining duality on the $SO(2n)$ gauge node with $2n+1$ vectors and linear monopole superpotential turned on. This gives rise to an $USp(2n-2)$ gauge theory with an adjoint, four fundamentals and a series of singlets. The mesonic and baryonic operators associated to the $SO(2n)$ gauge group are

$$\mathcal{M} = \begin{pmatrix} S \equiv Q^2 & M_{Q,f} \equiv Qf & M_{Q,c_1} \equiv Qc_1 \\ M_{Q,f}^T & M_{ff} \equiv ff & M_{f,c_1} \equiv fc_1 \\ M_{Q,c_1}^T & M_{f,c_1}^T & M_{c_1,c_m} \equiv c_1c_m \end{pmatrix}, \quad \mathcal{Q} = \begin{pmatrix} q \equiv \epsilon_{2n}(Q^{2n-3}fc_2c_3) \\ q_f \equiv \epsilon_{2n}(Q^{2n-2}c_2c_3) \\ q_{c_2} \equiv \epsilon_{2n}(Q^{2n-2}fc_3) \\ q_{c_3} \equiv \epsilon_{2n}(Q^{2n-2}fc_2) \end{pmatrix} \tag{4.59}$$

with $l, m = 2, 3$ and where S is in the adjoint of the $USp(2n-2)$ gauge group, while $M_{Q,f}, M_{Q,c_1}, M_{Q,c_2}$ and q are four fundamentals of $USp(2n-2)$. There are also two extra fundamentals of $USp(2n-2)$ corresponding to the fields d and e of the previous model, which are not modified by the duality on the $SO(2n)$ gauge node. The superpotential of the dual $USp(2n-2)$ adjoint SQCD is then

$$\begin{aligned}
W &= Y_{USp} + \sum_{k=1}^{n-1} \rho_k \text{Tr} S^{2k} + \mathcal{M} \mathcal{Q} \mathcal{Q}^T + \det \mathcal{M} + e M_{Q,f} + v_1 q_f \\
&+ v_3 M_{f,c_2} + v_2 M_{f,c_3} + \text{Tr}(S^n) (de + \epsilon_{rst} M_{rs} v_t) \tag{4.60}
\end{aligned}$$

The determinant can be evaluated as

$$\begin{aligned}
W_{\det \mathcal{M}} &= \det S \det \begin{pmatrix} M_{ff} & M_{f,\vec{c}} \\ M_{f,\vec{c}}^T & M_{\vec{c},\vec{c}} \end{pmatrix} + \epsilon_{2n-2} \epsilon_{2n-2} \left(S^{2n-3} (M_{Q,f} M_{c_2,c_3} + M_{Qc_2} M_{f,c_3} \right. \\
&+ M_{Qc_3} M_{f,c_2})^2 + S^{2n-4} (M_{Q,f} M_{Q,c_2} M_{Q,c_3} (M_{Q,f} M_{c_2,c_3} + M_{Qc_2} M_{f,c_3} \\
&+ M_{Qc_3} M_{f,c_2}) + S^{2n-5} (M_{Q,f} M_{Q,c_2} M_{Q,c_3})^2 \left. \right) \tag{4.61}
\end{aligned}$$

We can then integrate out the massive fields $\{e, M_{Q,f}, \vec{v}, q_f, M_{f,\vec{c}}\}$ and we are left with

USp($2n - 2$) adjoint SQCD with four fundamentals. There is a rather rich structure of singlets that we do not report here but that can be read by computing the F -terms of (4.60). We can now iterate this procedure by alternating adjoint deconfinement and duality in order to arrive to the final step and eventually prove the duality.

As anticipated this procedure can be used on the mathematical side to prove the identity (4.16) from a physical perspective. In order to complete the proof we need to consider the partition function obtained so far after the final duality on the *SO*($2n$) node (B.3). It is

$$\begin{aligned}
 Z_{USp(2n-2)} &= \frac{\prod_{l,m=1,2} \Gamma_h(\mu_{c_l} + \mu_{c_m}) \prod_{l=1}^2 \Gamma_h(\omega - \mu_{c_l}) \Gamma_h(2\mu_a) \prod_{r<s}^3 \Gamma_h(\mu_r + \mu_s)}{(-\omega_1\omega_2)^{\frac{n-1}{2}} 2^{n-1} (n-1)!} \\
 &\times \prod_{k=1}^{n-1} \Gamma_h(2\omega - 2k\tau) \int \prod_{\alpha=1}^{n-1} dy_\alpha \frac{\prod_{r=1}^4 \Gamma_h(\pm y_\alpha + \tilde{\mu}_r)}{\Gamma_h(\pm 2y_\alpha)} \prod_{1 \leq \alpha < \beta \leq n-1} \frac{\Gamma_h(\pm y_\alpha \pm y_\beta + \tau)}{\Gamma_h(\pm y_\alpha \pm y_\beta)}
 \end{aligned} \tag{4.62}$$

Where the masses $\tilde{\mu}_r$ are:

$$\vec{\tilde{\mu}} = \left\{ \mu_1, \mu_2 + \tau, \mu_3 + \tau, \omega - \frac{\tau}{2} \right\} \tag{4.63}$$

Notice that the superpotential constraint reads:

$$2(n-1)\tau + \sum_{r=1}^4 \tilde{\mu}_r = 2\omega \quad \& \quad 2\tilde{\mu}_4 + \tau = 2\omega \tag{4.64}$$

which is equivalent in form to the original superpotential constraint (4.17).

The contribution of the singlets can be written as:

$$\begin{aligned}
 &\prod_{k=1}^{n-1} \Gamma_h(2\omega - 2k\tau) \prod_{r<s}^3 \Gamma_h(\mu_r + \mu_s) \prod_{r=2}^3 \Gamma_h(\mu_r + \mu_1(2n-1)\tau) \\
 &\times \Gamma_h(\mu_2 + \mu_3 + \tau) \prod_{r=2}^3 \Gamma_h(2\mu_r + \tau) \Gamma_h(2\mu_1 + \tau(2n-1))
 \end{aligned} \tag{4.65}$$

We can prove the confining duality for *USp*($2n$) with four fundamental and linear monopole superpotential by iterating this procedure n times. In each step we obtain a new set of singlets as in (4.65), with the exception that the tower of $\Gamma_h(2\omega - 2k\tau)$ reduces of one unit. Furthermore in each step the rank of the gauge group decreases by one and the real masses are redefined as in (4.63), so that the fundamentals of *USp*($2(n-h)$) obtained after h steps are related to the original ones by:

$$\vec{\mu}_{h\text{-th step}} = \left\{ \mu_1, \mu_2 + h\tau, \mu_3 + h\tau, \omega - \frac{\tau}{2} \right\} \tag{4.66}$$

Thus iterating this procedure n times each term in (4.65) gives a tower of singlets of the final confined phase. Schematically:

$$\prod_{r < s}^3 \Gamma_h(\mu_r + \mu_s) \rightarrow \begin{cases} \prod_{\ell=0}^{n-1} \prod_{r=2}^3 \Gamma_h(\ell\tau + \mu_1 + \mu_r) \\ \prod_{\ell=0}^{n-1} \Gamma_h(2\ell\tau + \mu_2 + \mu_3) \end{cases} \quad (4.67)$$

$$\prod_{r=2}^3 \Gamma_h(\mu_r + \mu_1(2n-1)\tau) \rightarrow \prod_{\ell=n}^{2n-1} \prod_{r=2}^3 \Gamma_h(\ell\tau + \mu_1 + \mu_r) \quad (4.68)$$

$$\Gamma_h(\mu_2 + \mu_3 + \tau) \rightarrow \prod_{\ell=0}^{n-1} \Gamma_h((2\ell+1)\tau + \mu_2 + \mu_3) \quad (4.69)$$

$$\prod_{r=2}^3 \Gamma_h(2\mu_r + \tau) \rightarrow \prod_{\ell=0}^{n-1} \prod_{r=2}^3 \Gamma_h(2\mu_r + (2\ell+1)\tau) \quad (4.70)$$

$$\Gamma_h(2\mu_1 + \tau(2n-1)) \rightarrow \prod_{\ell=0}^{n-1} \Gamma_h(2\mu_1 + \tau(2\ell+1)) \quad (4.71)$$

while the contribution of the tower $\prod_{k=1}^{n-1} \Gamma_h(2\omega - 2k\tau)$ reduces of one unit at each step, and eventually disappear. Together these reproduce the formula (4.16).

Case II: $SO(2n)$

Now we prove the confining duality for $SO(2n)$ with one adjoint A , three vectors $q_{1,2,3}$ and monopole superpotential (4.20) by deconfining the adjoint. The mass parameters for the three vectors q_r are referred as μ_r with $r = 1, 2, 3$ and the one for the adjoint is referred as τ . The $SO(2n)$ model is equivalent to the $USp(2n-2) \times SO(2n)$ quiver in Figure 4.3, but this time the superpotential is

$$W = Y_{USp} + Y_{SO}^+ + g \text{Tr}(de) + \text{Tr}(Qef) \quad (4.72)$$

The duality map is:

$$\mu_{c_{2,3}} = \mu_{2,3}, \quad \mu_d = \mu_1 - \frac{\tau}{2}, \quad \mu_Q = \frac{\tau}{2} \quad (4.73)$$

The other parameters are fixed by the constraints given by the superpotential:

$$\mu_e = 2\omega - n\tau - \mu_1 + \frac{\tau}{2}, \quad \mu_f = \omega - \mu_2 - \mu_3 - (n-1)\tau = (n-1)\tau + \mu_1, \quad \mu_g = n\tau \quad (4.74)$$

with the constraint given by the monopole superpotential:

$$2(n-1)\tau + \sum_{r=1}^3 \mu_r = \omega \quad (4.75)$$

The partition function of the quiver is:

$$\begin{aligned}
 Z_{SO(2n) \times USp(2n-2)} &= \frac{\Gamma_h(\mu_g)}{(-\omega_1 \omega_2)^{\frac{2n-1}{2}} 2^{2n-2} (n!(n-1)!)} \\
 &\times \int \prod_{i=1}^n dx_i \frac{\Gamma_h(\pm x_i + \mu_f) \prod_{\ell=2}^3 \Gamma_h(\pm x_i + \mu_{c_\ell})}{\Gamma_h(\pm x_i)} \\
 &\times \prod_{a=1}^{n-1} dy_a \frac{\Gamma_h(\pm y_a + \mu_d) \Gamma_h(\pm y_a + \mu_e)}{\Gamma_h(\pm 2y_a)} \\
 &\times \frac{\prod_{i=1}^n \prod_{a=1}^{n-1} \Gamma_h(\pm x_i \pm y_a + \mu_Q)}{\prod_{i < j} \Gamma_h(\pm x_i \pm x_j) \prod_{a < b} \Gamma_h(\pm y_a \pm y_b)} \tag{4.76}
 \end{aligned}$$

Now we dualize the node with orthogonal group, this results in a $USp(2n - 2)$ model with four fundamentals and superpotential:

$$W = Y_{USp} + h \text{Tr}(de) + \text{Tr}(M_Q f e) + \det \mathcal{M} + \text{Tr} \mathcal{Q} \mathcal{M} \mathcal{Q} \tag{4.77}$$

where \mathcal{M} and \mathcal{Q} are given by (4.59). Due to the rather complicated structure of such superpotential we decide to proceed by adding some interactions in the original theory. We turn on the extra superpotential term

$$\delta W_{SO(2n)} = \sum_{k=1}^{n-1} \rho_k \text{Tr} A^{2i} + \beta \text{Pf} A + \epsilon_{rst} \alpha_r \epsilon_{2n} (A^{n-1} q_s q_t) \tag{4.78}$$

On the partition function this removes the contributions of $\Gamma_h(n\tau)$, $\prod_{r < s} \Gamma_h((n-1)\tau + \mu_r + \mu_s)$ and $\prod_{k=1}^n \Gamma_h(2k\tau)$ from the RHS of (4.20) giving raise to the contributions $\Gamma_h(2\omega - n\tau)$, $\prod_{r=1}^3 \Gamma_h(\omega + (n-1)\tau + \mu_r)$ and $\prod_{k=1}^n \Gamma_h(2\omega - 2k\tau)$ on the LHS. Mathematically this is achieved by applying the reflection equation and the balancing condition (4.75) and it does not spoil the integral identity (4.20). Furthermore (4.72) becomes

$$\begin{aligned}
 W &= Y_{USp} + Y_{SO}^+ + \sum_{k=1}^{n-1} \rho_k \text{Tr} Q^{2k} + \text{Tr}(Qef) \\
 &+ \alpha_1 \epsilon_{2n} (Q^{2n-2} c_2 c_3) + \alpha_2 \text{Tr}(f c_2) + \alpha_3 \text{Tr}(f c_3) \tag{4.79}
 \end{aligned}$$

In this way we can dualize the $USp(2n - 2)$ node integrating out M_{Qe} and f and identify β with M_{de} . The final result coincides to the original model with the superpotential deformation (4.78).

We can proceed by confining the $SO(2n)$ node with $2n + 1$ fundamentals and linear monopole superpotential after we have added the contributions of $\alpha_{1,2,3}$ and β . The

partition function for the $USp(2n-2)$ model is

$$Z_{USp(2n-2)} = \frac{\prod_{k=1}^{n-1} \Gamma_h(2\omega - 2k\tau) \prod_{2 \leq l \leq m \leq 3} \Gamma_h(\mu_{c_l} + \mu_{c_m}) \prod_{l=2}^3 \Gamma_h(\omega - \mu_{c_l}) \Gamma_h(2\mu_f)}{(-\omega_1 \omega_2)^{\frac{n-1}{2}} 2^{n-1} (n-1)!} \\ \times \int \prod_{a=1}^{n-1} dy_a \frac{\prod_{r=1}^4 \Gamma_h(\pm y_a + \tilde{\mu}_r)}{\Gamma_h(\pm 2y_a)} \prod_{1 \leq a < b \leq n-1} \frac{\Gamma_h(\pm y_a \pm y_b + \tau)}{\Gamma_h(\pm y_a \pm y_b)} \quad (4.80)$$

Where the masses are:

$$\vec{\mu} = \left\{ \mu_1 - \frac{\tau}{2}, \mu_2 + \frac{\tau}{2}, \mu_3 + \frac{\tau}{2}, \omega - \frac{\tau}{2} \right\} \quad (4.81)$$

If we now ignore the singlets we observe that the contribution of the $USp(2n-2)$ gauge sector to this partition function corresponds to the LHS of the identity (4.16). The duality associated to such a sector was proven in the previous section. We can then use this duality to confine the $USp(2n-2)$ theory, resulting in a WZ model with partition function:

$$\prod_{2 \leq l \leq m \leq 3} \Gamma_h(\mu_{c_l} + \mu_{c_m}) \cdot \Gamma_h(2\mu_f) \cdot \prod_{\ell=0}^{n-2} \prod_{r=1}^2 \Gamma_h(2(\ell+1)\tau + 2\mu_r) \Gamma_h(2\ell\tau + 2\mu_1) \\ \times \prod_{l=2}^3 \Gamma_h(\omega - \mu_{c_l}) \cdot \prod_{\ell=0}^{2n-3} (\Gamma_h((\ell+1)\tau + \mu_2 + \mu_3)) \cdot \prod_{r=1}^2 \Gamma_h(\ell\tau + \mu_1 + \mu_r) \quad (4.82)$$

which reproduces the RHS of (4.20) once the contributions of the baryons $\text{Pf } A$ and $\epsilon_{2n-2}(A^{n-1} q_r q_s)$ and of the singlets $\text{Tr } A^{2k}$ are removed.

Case III: $SO(2n+1)$

The $SO(2n+1)$ model with adjoint A and three fundamentals $q_{1,2,3}$ is equivalent to the $USp(2n) \times SO(2n+1)$ quiver given in Figure 4.4. The superpotential of this quiver is given by

$$W = Y_{USp} + Y_{SO}^+ + \text{Tr}(abQ) + f_1 \text{Tr}(c_1 a) + f_2 \text{Tr}(c_2 a) + g \text{Tr}(c_2 c_3) \quad (4.83)$$

The mass parameters in the partition function are

$$\mu_{c_{2,3}} = \mu_{2,3} - \frac{\tau}{2}, \quad \mu_Q = \frac{\tau}{2}, \quad \mu_d = \mu_1, \quad \mu_a = 2\omega - \mu_2 - \mu_3 - n\tau + \frac{\tau}{2} \\ \mu_b = \omega - \mu_1 - n\tau, \quad \mu_g = 2\omega - \mu_2 - \mu_3 - \tau, \quad \mu_{f_{2,3}} = \mu_{3,2} + n\tau \quad (4.84)$$

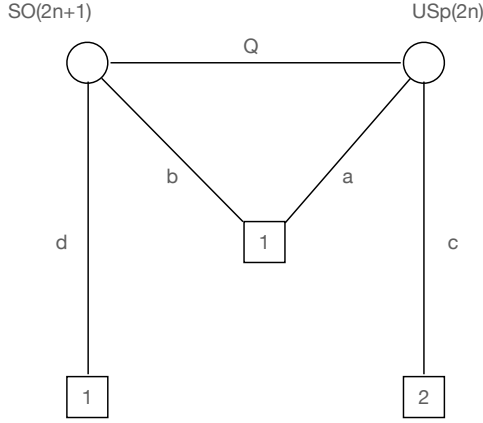


Figure 4.4 Quiver representation of the $SO(2n + 1)$ model after the adjoint field has been deconfined

with the constraint (4.25). The partition function of the $SO(2n + 1) \times USp(2n)$ quiver is given by

$$\begin{aligned}
 Z_{SO(2n+1) \times USp(2n)} &= \frac{\Gamma_h(\mu_g) \prod_{m=2,3} \Gamma_h(\mu_{f_m}) \Gamma_h(\mu_d) \Gamma_h(\mu_b)}{(-\omega_1 \omega_2)^{\frac{2n}{2}} 2^{2n} (n!)^2} \\
 &\times \int \prod_{i=1}^n dx_i \frac{\Gamma_h(\pm x_i + \mu_d) \Gamma_h(\pm x_i + \mu_b)}{\Gamma_h(\pm x_i)} \\
 &\times \prod_{\alpha=1}^n dy_\alpha \frac{\Gamma_h(\pm y_\alpha + \mu_a) \prod_{m=2}^3 \Gamma_h(\pm y_\alpha + \mu_{c_m}) \Gamma_h(\pm y_\alpha + \mu_Q)}{\Gamma_h(\pm 2y_\alpha)} \\
 &\times \frac{\prod_{i=1}^n \prod_{\alpha=1}^n \Gamma_h(\pm x_i \pm y_\alpha + \mu_Q)}{\prod_{i < j} \Gamma_h(\pm x_i \pm x_j) \prod_{\alpha < \beta} \Gamma_h(\pm y_\alpha \pm y_\beta)} \tag{4.85}
 \end{aligned}$$

Next we have to confine the $SO(2n + 1)$ sector with $2n + 2$ vectors and a linear monopole superpotential and we end up with $USp(2n)$. The problem consists of understanding the interaction among the various singlets from the confining dynamics of $SO(2n + 1)$. Again we can simplify the problem by modifying the original $SO(2n + 1)$ model by considering the superpotential

$$W = Y_{SO}^+ + \sum_{k=1}^n \rho_k \text{Tr} A^{2k} + \beta \epsilon_{2n+1} (A^{n-1} q_1 q_2 q_3) + \sum_{r=1}^3 \alpha_r \epsilon_{2n+1} (A^n q_r) \tag{4.86}$$

corresponding to remove the baryons and the singlets $\text{Tr} A^{2k}$ from the confined phase and add the new singlets $\alpha_{1,2,3}$ and β in the original model. On the partition function this removes the contributions of $\Gamma_h(\omega - n\tau)$, $\prod_{r=1}^3 \Gamma_h(n\tau + \mu_r)$ and $\prod_{k=1}^n \Gamma_h(2k\tau)$ from

the RHS of (4.24) giving raise to the contributions $\Gamma_h(\omega + n\tau)$, $\prod_{r=1}^3 \Gamma_h(2\omega - n\tau - \mu_r)$ and $\prod_{k=1}^n \Gamma_h(2\omega - 2k\tau)$ on the LHS. Mathematically this is achieved by applying the reflection equation and it does not spoil the integral identity (4.24). By deconfining the adjoint A the superpotential (4.83) is modified as well. The new superpotential is

$$W = Y_{USp} + Y_{SO}^+ + Tr(abQ) + gTr(c_2c_3) + \beta Tr bd + \alpha_1 \epsilon_{2n+1}(Q^{2n}d) \quad (4.87)$$

We can proceed by confining the $SO(2n+1)$ node. By integrating out the massive fields we arrive to an $USp(2n)$ gauge theory with an adjoint S , three fundamentals, identified by d and the two mesonic composites Qc_2 and Qc_3 , and a fourth fundamental corresponding to $u = \epsilon_{2n+1}(Q^{2n-1}bd)$, interacting with the adjoint through a superpotential term $W \propto uSu$. There is also a linear monopole superpotential and many more interactions with the singlets that we do not report here, but that can be obtained by evaluating the determinant $\det S$ and the superpotential contraction of S with the baryons of the confined $SO(2n+1)$ node. The partition function of the model is

$$\begin{aligned} Z_{USp(2n)} &= \frac{\Gamma_h(\tau)^n \prod_{k=1}^n \Gamma_h(2\omega - 2k\tau) \Gamma_h(2\mu_1) \Gamma_h(\omega - \mu_1) \Gamma_h(\omega + \mu_1 + 2n\tau) \Gamma_h(2\mu_b)}{(-\omega_1\omega_2)^{\frac{n}{2}} 2^n (n!)} \\ &\times \int \prod_{a=1}^n dy_a \frac{\prod_{r=1}^4 \Gamma_h(\pm y_i + \tilde{\mu}_r)}{\Gamma_h(\pm 2y_a)} \prod_{1 \leq a < b \leq n} \frac{\Gamma_h(\pm y_a \pm y_b + \tau)}{\Gamma_h(\pm y_a \pm y_b)} \end{aligned} \quad (4.88)$$

with $\vec{\mu} = \{\mu_1 - \frac{\tau}{2}, \mu_2 + \frac{\tau}{2}, \mu_3 + \frac{\tau}{2}, \omega - \frac{\tau}{2}\}$ and the constraints $\sum_{\ell=1}^4 \tilde{\mu}_\ell + 2n\tau = 2\omega$ and $2\tilde{\mu}_4 + \tau = 2\omega$. Also in this case we can borrow the results of the previous sections. Indeed if we ignore the singlets we observe that the contribution of the gauge $USp(2n-2)$ sector to this partition function corresponds to the LHS of the identity (4.16). The duality associated to such a sector was proven in the previous section. We can then use this duality to confine the $USp(2n-2)$ theory and prove the confining duality for the $SO(2n+1)$ model.

4.4 Discussion

In this Chapter we exploited the *duplication formula* to study 3d $\mathcal{N} = 2$ confining gauge theories with real USp/SO gauge groups, with fundamentals/vectors and adjoint matter. We were able to show that the cases of [2], with two fundamentals and one vector respectively, can be studied by the squashed three-sphere localization by applying the *duplication formula* for the hyperbolic Gamma function of another s-confining model, namely $USp(2n)$ with an antisymmetric and four fundamentals. By applying the same strategy we derived three new integral identities involving symplectic and orthogonal adjoint SQCD, with four fundamentals and three vector respectively and a monopole superpotential.

There are several directions where this approach can be applied. For example one can apply the *duplication formula* to the integral identities for $USp(2n)$ theories with an antisymmetric and eight fundamentals, where the A_7 global symmetry enhances to E_7 . This case has been deeply investigated in the mathematical [56] and then in the physical literature [70, 71] and it may be interesting to understand if similar enhancements or new dualities appear for models with adjoint matter as well.

Another interesting family of models that may deserve some further investigation are models with power law superpotential for the two index tensor. In this case the starting

point of the analysis are the integral identities discussed in [112] for $USp(2n)$ with antisymmetric and adjoint matter fields. Again applying the duplication formula in such cases could lead to new relations between these models and to new results for the orthogonal cases.

A deeper question that we have not addressed here consists of the physical interpretation, if any, of the *duplication formula*. As observed in the literature this formula allows to switch from the integral identities for the $USp(2n)$ duality with fundamentals to the integral identities for the $SO(n)$ dualities with vectors. This has been discussed in [108] for the superconformal index of 4d dualities and in [43] for the squashed three-sphere partition function of 3d dualities. In presence of monopole superpotential this issue is more delicate, because in some cases it can lead to a singular behavior that requires more care. In any case, when the procedure gives rise to a finite result, also in presence of monopole superpotential, the constraints imposed by anomalies (in 4d) and by monopole superpotential (in 3d) translate in a consistent way into the new identities, and the latter can be interpreted as new physical dualities (or in new examples of s-confining theories). It should be then important to have a physical interpretation of the *duplication formula*.

Part II

Exploring Conformal Manifolds of 4d SCFTs

Conformal S-dualities from O-planes

In this Part of thesis we will consider 4d QFTs obtained from stacks of D3 branes in Type IIB string theory probing a toric Calabi-Yau singularity in the presence of orientifolds, following [113]. Two different CY singularity correspond, in the low energy limit capturing the worldvolume theory of the D3 branes, to different 4d theories. When on top of the CY singularity we also consider an orientifold projection it is possible for two different singularity to have the same IR dynamics. More precisely, it is possible that two QFTs obtained as the low energy limit of different CY singularities with an orientifold to be related by exactly marginal deformations.

This phenomenon has been studied in great detail in a recent paper [9], where it has been observed that there are infinite families of examples in which models that are unrelated by any IR duality before the projection turn out to share the same central charges and superconformal indices in the IR after it. This generalizes a previous construction [12] for oriented chiral quivers. The equivalence of these quantities led to a natural duality conjecture among these oriented models, but this duality cannot be always obtained by applying the usual rules of Seiberg duality on the quiver.

In Chapter 6 and 7 we construct many examples of toric theories which, in the presence of an orientifold, engineer conformally dual theories. The examples studied in Chapter 6 are a generalization of the models studied in [9], and consist in \mathbb{Z}_2 orbifolds of the singularities considered in [9] in the presence of orientifolds. The examples studied in 7 generalize the duality of [12] between orientifolds of the PdP 3_b and PdP 3_c singularities.

As motivation for the following two Chapters let us briefly review the examples of conformal dualities between orientifolds of toric theories considered in [9].

5.1 Conformal dualities from Type IIA elliptic models with orientifolds

Let us consider the models studied in [9]. For these theories an alternative construction in terms of elliptic models in Type IIA is available, and involves D4 branes wrapped on a compact direction, NS5 branes and orientifold planes. Some of these models (corresponding to pairs of O6 and pairs of O6'-planes) were studied in [3, 4] where a Type IIB T-dual description was also constructed. The directions wrapped by the branes are

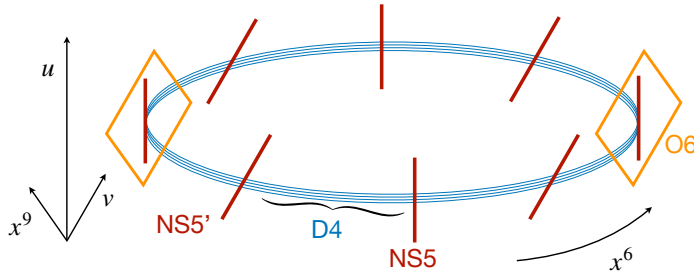


Figure 5.1 IIA picture of an elliptic model with O6-planes. The low-energy effective quiver theory can have orthogonal and/or symplectic gauge groups.

summarized in the following table:

	0	1	2	3	4	5	6	7	8	9
D4	—	—	—	—	·	·	—	·	·	·
NS5	—	—	—	—	—	—	·	·	·	·
NS5'	—	—	—	—	·	·	·	—	—	·
O6	—	—	—	—	·	·	·	—	—	—
O6'	—	—	—	—	—	—	·	·	·	—

The presence of both primed and non-primed branes breaks supersymmetry to $\mathcal{N} = 1$: a pair of nearby NS-NS' gives infinite mass to the scalar in the $\mathcal{N} = 2$ vector multiplet breaking supersymmetry to $\mathcal{N} = 1$, while an NS-O6'-NS (NS'-O6-NS') configuration brings $\mathcal{N} = 1$ chiral multiplets in conjugate tensorial representations other than the adjoint. Again we do not consider models which need additional flavor D6-branes. NS5-branes must be tilted in pairs, according to the \mathbb{Z}_2 quotient. A possible configuration is shown in figure 5.1.

The classification of possible configuration of O6-planes and NS5-branes (coincident with the O6-planes) is shown in table 5.2. There, the resulting quiver theories are shown schematically with the leftmost and rightmost gauge groups together with their tensorial matter. The other nodes have unitary gauge groups with (without) adjoint if the corresponding NS5-branes are parallel (non-parallel). Additionally, the real groups may have either an adjoint, or a tensorial representation other than the adjoint or may not have any tensorial matter at all. The type of tensorial matter for the real groups depends on the orientation of the corresponding O6-plane, while the presence of tensorial matter depends on the orientation of the two nearest NS5-branes. Quivers without tensorial matter for the real groups can be engineered by considering O6-planes at an angle in the (4578) space, but we do not consider this possibility here.

Following the notation of [3], there are four families of quivers distinguished by the leftmost and rightmost gauge group. In the following we consider configurations which correspond to quivers with $n_g + 1$ nodes. The amount of NS5-branes needed to obtain such theories depends on the family.¹ The i -th node has an adjoint if $i \in I$, where I is a

¹For family *i*) one needs $2n_g$ NS5's, for families *ii*) and *iii*) one needs $2n_g + 1$ NS5's, and for family *iv*) one needs $2n_g + 2$ NS5's. Furthermore observe that the number of regular D4-branes corresponds to $2(\tilde{N}_c - n_g)$

with two antisymmetric A, \tilde{A} for the rightmost gauge group and superpotential

$$W = \phi_1 X_{12} X_{21} + \sum_{i \in I} \phi_i (X_{i,i-1} X_{i-1,i} - X_{i,i+1} X_{i+1,i}) + \sum_{i \notin I} (\pm X_{i,i-1} X_{i-1,i} X_{i,i+1} X_{i+1,i}) + \phi_{n_g+1} A \tilde{A}. \quad (5.4)$$

where the i -th node has an adjoint iff $i \in I$. We will refer to this family as theory \mathcal{A} .

- iii) This is realized when an NS5 intersects the $O6^+$ and there are no NS5's intersecting the $O6^-$. The quiver is:

$$S, \tilde{S} \quad \begin{array}{cccc} SU(2N_c) & SU(2N_c - 2) & SU(2N_c - 4) & USp(2(N_c - n_g)) \\ \circ & \circ & \circ & \cdots \circ \end{array} \quad (5.5)$$

with two conjugate symmetric tensors S and \tilde{S} for the leftmost gauge group and superpotential

$$W = \phi_1 S \tilde{S} + \sum_{i \in I} \phi_i (X_{i,i-1} X_{i-1,i} - X_{i,i+1} X_{i+1,i}) + \sum_{i \notin I} (\pm X_{i,i-1} X_{i-1,i} X_{i,i+1} X_{i+1,i}) + \phi_{n_g+1} X_{n_g, n_g+1} X_{n_g+1, n_g}. \quad (5.6)$$

where the i -th node has an adjoint iff $i \in I$. We will refer to this family as theory \mathcal{B} . S-duality maps model \mathcal{A} to model \mathcal{B} in the $\mathcal{N} = 2$ case.

- iv) This is realized when both $O6^-$ -planes have an NS5 on top. The quiver is:

$$S, \tilde{S} \quad \begin{array}{cccc} SU(N_c) & SU(N_c - 2) & SU(N_c - 4) & SU(N_c - 2n_g) \\ \circ & \circ & \circ & \cdots \circ \end{array} A, \tilde{A} \quad (5.7)$$

with two antisymmetric A, \tilde{A} for the rightmost gauge group and two symmetric S, \tilde{S} for the leftmost gauge group. The superpotential is

$$W = S \tilde{S} \phi_1 + \sum_{i \in I} \phi_i (X_{i,i-1} X_{i-1,i} - X_{i,i+1} X_{i+1,i}) + \sum_{i \notin I} (\pm X_{i,i-1} X_{i-1,i} X_{i,i+1} X_{i+1,i}) + \phi_{n_g+1} A \tilde{A}, \quad (5.8)$$

where the i -th node has an adjoint iff $i \in I$. In this case the models are not in general self-dual under S-duality.² For example when $n_g = 0$ the S-dual models have been found in [114, 115]. However for higher values of n_g one can still have shift and permutation symmetries for the NS5-branes that are not placed on top of the O-planes.

(In the above survey we have described the case where the leftmost and rightmost

²We are grateful to I. García-Etxebarria for comments on this point.

groups have an adjoint ϕ_1, ϕ_{n_g+1} , or either an adjoint or a tensor for the real groups. If they do not have such two-index matter field, the corresponding superpotential term must be replaced with a quartic term, in a straightforward way.)

Given an $\mathcal{N} = 1$ model from one of the families above, for fixed n_g , one can show that the vanishing of the beta functions fixes the R-charge of the adjoint matter to be equal to 1. Then a mass term for the adjoint fields is a marginal deformation, and a further analysis of the global charges of the adjoints, following [16], shows that this deformation is exactly marginal. Then two theories differing for the number of adjoint fields can be connected by adding a large mass to some of the adjoint fields and integrating them out, which is a marginal deformation. This provides infinite families of examples of the phenomenon that we are interested in: two different elliptic models, which correspond to different CY singularities in the dual Type IIB construction, give rise to *conformally dual* theories in the presence of orientifolds.

An interesting duality also exists between models in families *ii)* and *iii)*, i.e. model \mathcal{A} and \mathcal{B} respectively where some of the NS5-branes are non-parallel. In [9, 10] it was shown that this can be considered as an example of inherited S-duality from the corresponding $\mathcal{N} = 2$ models where all NS5 branes are parallel. We will not discuss this topic further, but we summarize the results of [9, 10] in Table 5.2.

	\mathcal{N}	Theory \mathcal{B}	Theory \mathcal{A}
= O6 = NS5 = D4			
$O6^+-O6^-$	 2 S, \tilde{S} SU SU A, \tilde{A}	 S, \tilde{S} SU USp ϕ	 ϕ SO SU A, \tilde{A}
$O6^+-O6'^-$	 flavor	 S, \tilde{S} SU USp A	 flavor
$O6'^+-O6^-$	 flavor	 flavor	 flavor
$O6'^+-O6'^-$	 flavor	 flavor	 flavor

Table 5.2 Elliptic models with O6-planes and corresponding quivers. Models connected by \leftrightarrow are S-dual. Configurations denoted by ‘flavor’ need additional flavor hypermultiplets in order to make all the β function vanish. The dashed line in the middle of the quiver corresponds to the intermediate $n_g - 1$ nodes with unitary gauge groups. In this table we have assumed that all the NS5-branes are in the (012345) directions; the generalization to non-parallel branes is straightforward. Models in the first row were considered in [3]; models in the fourth row were considered in [4].

$\mathcal{N} = 1$ conformal dualities from unoriented chiral quivers

In this Chapter we generalize the phenomenon described in Chapter 5, where specific orientifold models not only give rise to conformal fixed points at strong coupling in the infrared (IR), but also that these models belong to the same conformal manifold. The mechanism was first identified and discussed in [12, 9] and then extended in [10] to non-chiral $L^{a,b,a}$ quiver gauge theories, a subfamily of the $L^{p,q,r}$ models [116, 117, 118] characterized by the presence of orbifold singularities. The models admit both a brane tiling description and a Hanany–Witten one [72] in type IIA string theory in terms of N D4-branes, extended along the directions x^{0123} and compactified along one direction, say x^6 , and n_G NS5-branes extended along x^{012345} and separated along x^6 . We described the Hanany-Witten setup in more details in Chapter 5. Such non-chiral models, known as elliptic models [119, 120], have n_G $SU(N)$ gauge groups¹ and $\mathcal{N} = 2$ supersymmetry if $a = 0$, otherwise $\mathcal{N} = 1$. Pairs of six-dimensional orientifold planes with opposite charge ($O6^\pm$) extended along $x^{0123457}$ can be placed symmetrically on the circle without breaking further supersymmetry. For the case with extended supersymmetry this description has been extensively studied in [3], where four families of models have been identified. The classification depends on the presence of an odd or even number n_G of gauge groups and on the possibility of placing, or not placing, an $O6^+$ and/or an $O6^-$ on top of an NS5-brane. Breaking supersymmetry down to $\mathcal{N} = 1$ in presence of orientifold planes and suitable choices of fractional branes has been shown to lead to models with conjugate pairs of chiral multiplets with R -charge $R = 1$ in tensor representations of the gauge group [121, 9, 10]. Supersymmetry is broken in general by tilting some of the NS5-branes and/or $O6$ -planes, such that the orientifold projection can be still applied consistently.²

From the perspective of brane tilings associated to $L^{a,b,a}$, we can visualize the process with orientifolds acting with fixed loci on the tiling, as discussed in [113]. Proper choices of fractional branes, often dictated by the constraints on the β -functions, lead to models with the same central charges and superconformal index after integrating out the chiral fields with R -charge $R = 1$ [9, 10]. The mass terms for these fields have indeed R -charge $R = 2$ and they are exactly marginal deformations. From a purely field theory perspective, a similar situation occurs when breaking $\mathcal{N} = 2$ by a mass term for the adjoint field, given an $\mathcal{N} = 1$ description. The resulting theory develops a quartic term

¹The $U(1)_{\text{center-of-mass}}$ is free while the other $U(1)$'s decouple in the IR.

²In the IIA elliptic engineering of $L^{a,b,a}$, $a + b$ corresponds to the total number of untilted NS5-branes, whereas a to that of the tilted NS5's. When $a = 0$ we are left with $b = n_G$ NS5's and $\mathcal{N} = 2$ supersymmetry.

in the superpotential and the Seiberg dual theory has mesons with a marginal mass term, so that these mesons can be integrated out. In this context, Seiberg duality relates strongly-coupled and weakly-coupled regimes of theories whose matter content differs only for mesons with marginal mass [122, 123], inheriting the action of S -duality from the mother $\mathcal{N} = 2$ theory.³

Observe that parent theories L^{a_1, b_1, a_1} , described either by elliptic models or brane tilings, admit relevant mass terms [125] that deform the model into an L^{a_2, b_2, a_2} with $a_1 + b_1 = a_2 + b_2$ and $b_1 > b_2$. Clearly, they are not Seiberg dual to each other, as can be seen from the fact that their toric geometry is different. The novel aspect here is the presence of the orientifold, because once we reach $\mathcal{N} = 1$, all projected models with constant $a + b$ have the same number of gauge groups and of non-anomalous $U(1)$'s but differ only by the presence of fields, tensors or adjoints, that admit marginal mass terms. Therefore, the consequence of the orientifold projection is that the two theories flow to the same conformal manifold. For this reason, we borrow nomenclature from the literature [24] and say that certain orientifolds of $L^{a, b, a}$ with constant $a + b$ are *conformally dual*. They are not Seiberg dual, for they cannot be related by Seiberg dualities known in the literature [9, 10], but they inherit part of the S -duality action on the marginal masses from the mother $\mathcal{N} = 2$ models through the mechanism of inherited duality introduced in [126, 127].

It is natural to wonder whether the mechanism discussed so far can be generalized to other $\mathcal{N} = 1$ models, extending the notion of conformal dualities to toric quiver gauge theories with a chiral field content. The first necessary ingredient in the recipe is the presence of internal points in the toric diagram. Indeed these are associated to anomalous $U(1)$ global (baryonic) symmetries and they require the presence of a chiral field content, i.e. there are bi-fundamental fields connecting two nodes of the quiver, without the corresponding anti-bifundamental [128]. Another necessary ingredient is the presence of points on the perimeter of the toric diagram, because this allows to RG flow from one model to another even before the orientifold projection, through a mass deformation [125].

A natural set of models where to look for a generalization of the mechanism of conformal duality in presence of orientifolds consists of $L^{a, b, a}/\mathbb{Z}_2$ orbifolds, leading generically to a chiral field content (with the exception of $L^{0, 2, 0}$ and $L^{1, 1, 1}$) – see Fig. 6.1 for examples of such orbifolds on the toric diagram. In this Chapter we will see that such orbifolds admit a generalization of the mechanism of conformal duality similar to the one obtained for the four $\mathcal{N} = 2$ families of [3] broken to $\mathcal{N} = 1$. We will distinguish two out of these four families (corresponding to families **i**) and **iv**) of [3]) allowing for the presence of marginal mass terms. Another difference with the construction presented in [9, 10], briefly review in Chapter 5, is that here we will observe that in some cases fractional branes will not be required. Observe also that in these $L^{a, b, a}/\mathbb{Z}_2$ models the type IIA description is not readily available and the orientifold projection can be performed on the dimer model with the techniques of [113] and the recent extension of [129] in terms of a Klein bottle. This is the other main novelty of the construction performed here. We will observe that the projections are implemented on the brane tiling either in terms of fixed points and fixed lines or by maps on the dimer without fixed points that lead to Klein bottles.

³Or better, being η the coupling of the quartic term, there is a line of conformal theories described by the equation $\gamma(g, \eta) = -1/2$ and Seiberg duality relates opposite regimes on this line, see [124].

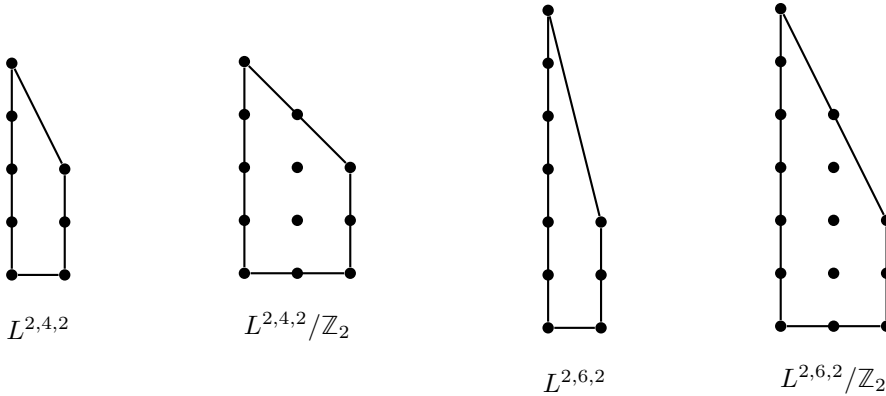


Figure 6.1 Examples of chiral orbifolds for the $L^{a,b,a}$ family.

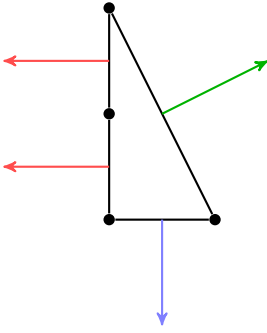
6.1 Orientifolds and conformal duality

The aim of this section is to summarize the results of [12, 9, 10], where specific $\mathcal{N} = 1$ supersymmetric gauge theories obtained as orientifold projections of toric quivers were shown to be related to one another by conformal duality. We will first concentrate on the simplest models wherein this occurs, namely the orientifold of $\mathbb{C}^2/\mathbb{Z}_2 \times \mathbb{C}$ and the orientifold of the conifold, obtained by mass deformation of the former [130]. This example contains all relevant information and, as we will see, it can be naturally generalized to the more elaborate models discussed in [12, 9, 10].

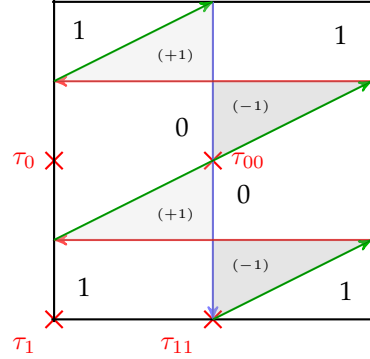
6.1.1 A picture of five-branes

A toric diagram in a \mathbb{Z}^d lattice encodes the information about a d -dimensional complex toric variety, admitting the action of a complex torus $(\mathbb{C}^*)^d$ [131, 132, 133, 134]. For toric CY threefolds (i.e. $d = 3$) it is enough to focus on a two-dimensional diagram, thanks to the vanishing of the first Chern class [132]. The toric data can be translated into a well defined supersymmetric gauge theory in four dimensions, using a five-brane diagram as an intermediate step, from which the corresponding brane tiling or dimer can be immediately drawn [135, 136, 137, 138, 139, 140, 141, 142]. More explicitly, one identifies the vectors with coordinates (p, q) that are dual (outgoing normal) to the sides of the toric diagram and represents them as one-cycles of a two-dimensional torus with (p, q) winding numbers. The resulting five-brane diagram owes its name to the fact that in the IIB picture, whereby D3-branes are T-dualized into D5-branes wrapping the two-torus, the one-cycles are NS5-branes that emerge from T-dualizing the toric singularity. As an example, see the toric diagram of $\mathbb{C}^3/\mathbb{Z}_2$ and the associated five-brane diagram in Figs. 6.2a-6.2b.

The one-cycles divide the planar graph in different regions, highlighted in white, gray or black in Fig. 6.2b. White regions are $SU(N)$ gauge factors, whereas bifundamental fields X_{ab} , where a, b are labels for the gauge factors, correspond to arrows crossing the white regions a and b at the intersection points. The direction of the arrows determines if a field transforms as a fundamental (out) or antifundamental (in) of a gauge factor. Gray and black regions are encircled by the arrows in clockwise (+1) or counterclockwise (-1) direction, respectively. They correspond to gauge-invariant interaction terms,



(a) The toric diagram of $\mathbb{C}^2/\mathbb{Z}_2 \times \mathbb{C}$ and the vectors orthogonal to the edges.



(b) The five-brane diagram of $\mathbb{C}^2/\mathbb{Z}_2 \times \mathbb{C}$, with the four fixed points of the orientifold projection.

that involve all the fields surrounding the region and give rise to a trace-like ‘mesonic’ operator. In our example, the five-brane diagram in Fig. 6.2b gives two gauge factors, which have been labelled by 0 and 1. The bifundamental fields are

$$\begin{aligned} X_{01}^1 &= (\square_0, \bar{\square}_1)^1 & , & & X_{10}^1 &= (\square_1, \bar{\square}_0)^1 \\ X_{01}^2 &= (\square_0, \bar{\square}_1)^2 & , & & X_{10}^2 &= (\square_1, \bar{\square}_0)^2 \\ X_{00} &= \phi_0 = (\square_0, \bar{\square}_0) & , & & X_{11} &= \phi_1 = (\square_1, \bar{\square}_1) \end{aligned} \quad (6.1)$$

where the latter two fields are adjoints and the upper index labels different fields with the same transformation rules. The superpotential reads

$$W_{\mathbb{C}^2/\mathbb{Z}_2 \times \mathbb{C}} = \epsilon_{ij} \left(\phi_1 X_{10}^i X_{01}^j + \phi_0 X_{01}^i X_{10}^j \right) . \quad (6.2)$$

As a final step one turns the five-brane diagram into the brane tiling or dimer by shrinking the gray and black regions into points, white points for (+1) and black for (-1), and connects white points to black ones by edges, so as to obtain a bipartite graph. This is in a sense dual to the five-brane diagram, as the edges represent the bifundamental fields. The brane tiling encodes the information about the toric CY geometry and completely defines the dual gauge theory in the sense of the AdS/CFT correspondence. The brane tiling of $\mathbb{C}^2/\mathbb{Z}_2 \times \mathbb{C}$ is drawn in Fig. 6.3.

To sum up, in a toric variety the geometry is encoded in a toric diagram whose discrete data allows to construct the brane tiling, which translates geometric information into a 4d gauge theory. The dictionary of this bipartite graph is as follows. Each face represents a gauge group factor $SU(N)_a$, each edge represents a bifundamental field X_{ab} transforming under the adjacent faces, with an orientation given by the direction black to white, each node represents a gauge-invariant term in the superpotential. The gauge factors and matter fields can be translated from the five-branes to a quiver representation in form of nodes and arrows, respectively. The legend in Fig. 6.4 shows the various matter fields that appear in subsequent sections.

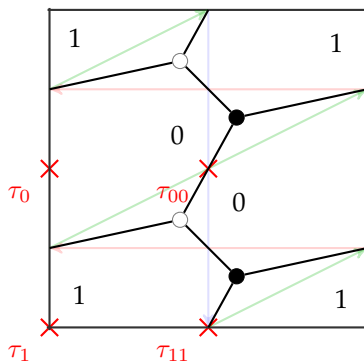


Figure 6.3 The brane tiling of $\mathbb{C}^2/\mathbb{Z}_2 \times \mathbb{C}$ with the four fixed points of the orientifold projection.

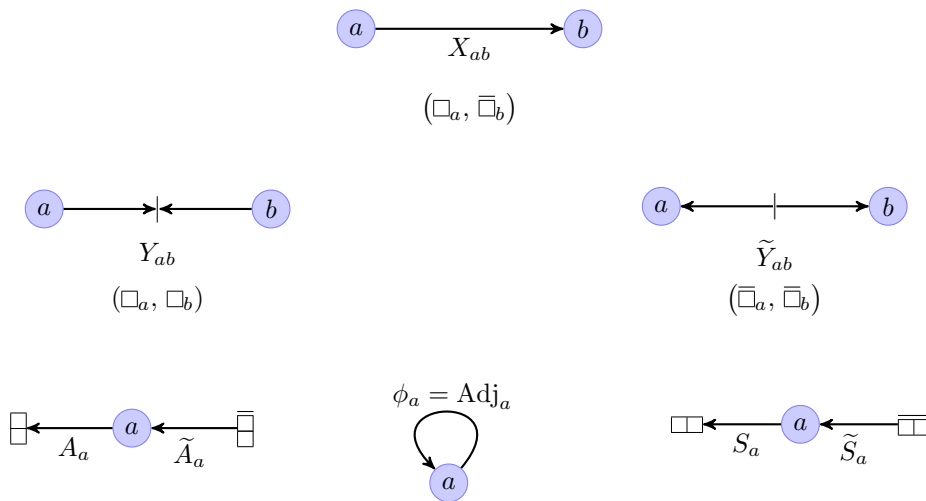


Figure 6.4 The various matter fields and their representations that we will use in quiver diagrams. We draw multiple arrows for multiple fields connecting the same pair of nodes. When nodes are both SO and/or USp groups, we drop the arrow and connect them with an edge, signaling the fact that representations are real. For tensor representations, when not specified if they are symmetric or antisymmetric, we simply denote them by T_a .

6.1.2 Inherited S -duality

The quiver of $\mathbb{C}^2/\mathbb{Z}_2 \times \mathbb{C}$ is drawn on the top left of Fig. 6.5, where the red dashed line highlights the orientifold projection. (Let us call the projection Ω .) On the brane tiling, the projection is realized by four fixed points, whose charges are encoded in a vector $\vec{\tau} = (\tau_0, \tau_{00}, \tau_1, \tau_{11})$ and project in turn the gauge group $SU(N_0)$, the field ϕ_0 , the gauge group $SU(N_1)$ and the field ϕ_1 . Positive τ 's give either orthogonal groups or symmetric representations, while negative τ 's give either symplectic groups or antisymmetric representations. The product of the τ 's is constrained by the condition [113]

$$\prod \tau = (-1)^{\frac{N_W}{2}}, \quad (6.3)$$

where N_W is the number of terms in the superpotential of the parent theory. In the present $\mathbb{C}^2/\mathbb{Z}_2 \times \mathbb{C}$ case $N_W = 4$, thus the product of the τ 's is $+1$. The superpotential reads

$$W_{\mathbb{C}^2/\mathbb{Z}_2 \times \mathbb{C}}^\Omega = -T_0 X_{01} X_{10} + T_1 X_{10} X_{01}. \quad (6.4)$$

We observe that in the five-brane diagram in Fig. 6.2b, the fixed points that project the adjoint fields are located at the intersections between the 'vertical' (blue) brane and the 'oblique' (green) brane, and the two 'horizontal' (red) branes are identified by the orientifold.

Given the above orientifold, the field content of the model can easily be read from the linear quiver either on the top right or bottom of Fig. 6.5, the two representing two different choices for $\vec{\tau}$. We can find out whether the model has a conformal fixed point by analyzing the beta functions. Let us identify the R -charges R_{01} and R_{10} of the two bifundamental fields, while imposing $R(W) = 2$ that identifies the R -charges R_0 and R_1 of the two projected fields. This gives the condition $r_0 + 2r_{01} = -1$, where

$$r = R - 1 \quad (6.5)$$

is the R -charge of the fermion in the chiral multiplet.⁴ Together with the condition that the β -functions of the two gauge group vanish, we have

$$\begin{aligned} r_0(m + 2\tau_{00}) &= -(m - 2\tau_0), \\ r_0(m - 2\tau_{11}) &= -(m + 2\tau_1), \end{aligned} \quad (6.6)$$

where $m = N_0 - N_1$. We now study the solutions to these equations for the different possible choices of the τ 's.

It is straightforward to see that there is a choice that preserves $\mathcal{N} = 2$ supersymmetry, choosing $\tau_{00} = -\tau_0$ and $\tau_{11} = -\tau_1$, and we denote it as $\vec{\tau}_A$. (Let us call Ω_A the associated orientifold projection.) In this case the solution demands $m = 2\tau_0$ and $\tau_1 = -\tau_0$, so that $\vec{\tau}_A = (\pm, \mp, \mp, \pm)$. These conditions leave r_0 undetermined, and we find that at large N the value of r_0 that maximizes the central charge a is $r_0 = -\frac{1}{3}$. Hence, at large N the R -charges of all the fields are $\frac{2}{3}$, and the central charge

$$a_{\mathbb{C}^2/\mathbb{Z}_2 \times \mathbb{C}}^{\Omega_A} = \frac{1}{4}N^2 \quad (6.7)$$

⁴ $R = 2/3$ is the 'canonical' R -charge of a free field.

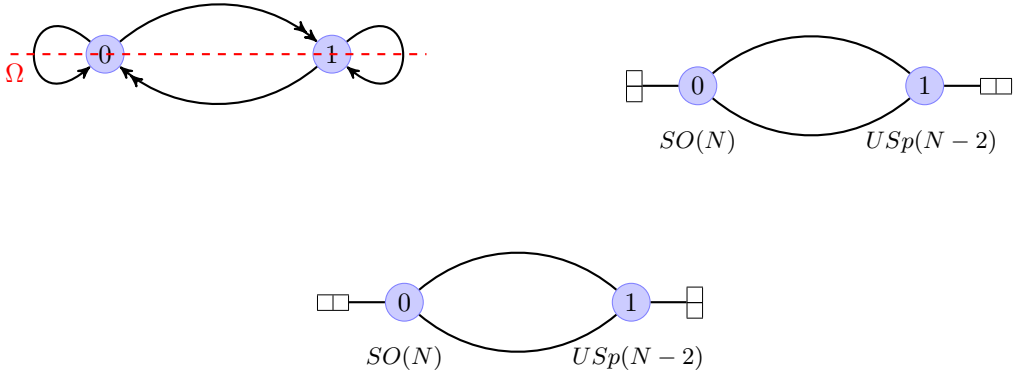


Figure 6.5 The quiver diagram for $\mathbb{C}^2/\mathbb{Z}_2 \times \mathbb{C}$ with the orientifold projection Ω on the top left, while on the top right the associated (linear) ‘unoriented’ quiver after the $\mathcal{N} = 2$ choice for the orientifold and the $\mathcal{N} = 1$ choice at the bottom.

is half the value of the central charge of the parent theory. To summarize, and choosing without loss of generality $\tau_0 = 1$, one gets the gauge groups $SO(N)$ and $USp(N - 2)$,⁵ with projected fields A_0 and S_1 in the adjoint of each group.

There are however other possible solutions to Eq. (6.6). These are $\mathcal{N} = 1$ solutions with $\tau_{00} = \tau_0, \tau_{11} = \tau_1$ and $\tau_1 = -\tau_0$, which we denote as $\vec{\tau}_B = (\pm, \pm, \mp, \mp)$ giving

$$\begin{aligned}
 r_{00} &= -\frac{m - 2\tau_0}{m + 2\tau_0}, \\
 r_{01} &= -\frac{2\tau_0}{m + 2\tau_0}.
 \end{aligned}
 \tag{6.8}$$

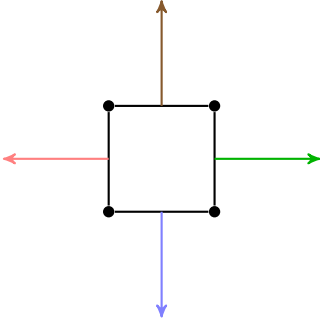
In general for these solutions one should worry about the presence of gauge-invariant composite operators that hit the unitarity bound $R = 2/3$ and decouple. This analysis was performed in [9] and it was shown that in the range $1 < m < 10$ this cannot occur. There is a particular value of m in this range, namely $m = 2\tau_0$, that gives $R_0 = 1$ and $R_{01} = 1/2$. We observe that the value of m is the same as the one of the $\mathcal{N} = 2$ preserving orientifold, i.e. $\tau_0 = -\tau_{00} = -\tau_1 = \tau_{11}$, and the value of the central charge $a = \frac{3}{32}(3\text{Tr}R^3 - \text{Tr}R) \sim c$ at large N is

$$a_{\mathbb{C}^2/\mathbb{Z}_2 \times \mathbb{C}}^{\Omega_B} = \frac{27}{128}N^2,
 \tag{6.9}$$

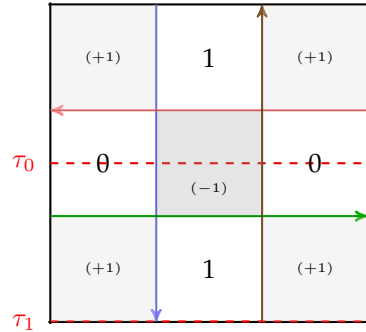
which is $\frac{27}{32}$ times the central charge of the $\mathcal{N} = 2$ orientifold. Again, choosing $\tau_0 = 1$ gives the gauge groups $SO(N)$ and $USp(N - 2)$, but now the projected fields are S_0 and A_1 and both have $R = 1$, while the bifundamental fields have $R = 1/2$. We observe that the fields with $R = 1$ do not contribute to the central charge.

The other value for m in Eq. (6.6) we are interested in is $m = 4\tau_0$, which gives $R_{00} = R_{01} = 2/3$ as in the $\mathcal{N} = 2$ model, and as a consequence gives also the same central charge at large N , although the difference between the ranks at finite N is not the same,

⁵Here $N_0 = N$, which is assumed to be even. The ranks of the two groups are $N/2$ and $N/2 - 1$.



(a) The toric diagram of the conifold \mathcal{C} and the vectors orthogonal to the edges.



(b) The five-brane diagram of the conifold \mathcal{C} with the fixed lines of the Ω projection.

and the projected fields are not in the adjoint. As we will see, the presence of this kind of solution will be systematic in the models discussed in this Chapter.

The central charge of the $\mathcal{N} = 1$ model with $m = 2\tau_0$ coincides (exactly, that is even at finite N) with the central charge of the orientifold of the conifold \mathcal{C} . This can be quickly shown by determining the central charges and the difference of the ranks of the two gauge groups at the conformal fixed point. For completeness, we draw in Figs. 6.6a and 6.6b the toric diagram and the five-brane diagram of the conifold. We also draw in Fig. 6.7 the corresponding quiver. In this case the orientifold projection cannot be realized on the five-brane diagram by fixed points, but instead by fixed lines. Identifying the R -charges of all the fields, the superpotential of the parent theory

$$W_c = \epsilon_{ab\epsilon_{cd}} X_{01}^a X_{10}^c X_{01}^b X_{10}^d \quad (6.10)$$

implies that they are all equal to $1/2$, and they do not change after the orientifold projection. Denoting as before τ_0 and τ_1 the orientifold charges that project the two gauge groups, the condition that the β -functions vanish gives $m = 2\tau_0$ and $\tau_1 = -\tau_0$, where again we denote with m the difference $N_0 - N_1$. Choosing $\tau_0 = +1$, we end up again with the gauge groups $SO(N)$ and $USp(N - 2)$, while the bifundamental fields have $R = 1/2$.⁶ Hence, apart from the absence of the fields S_0 and A_1 , we get exactly the same ranks and the same R -charges as the $\mathcal{N} = 1$ $\mathbb{C}^2/\mathbb{Z}_2 \times \mathbb{C}$ orientifold with $m = 2\tau_0$, implying that we get exactly the same central charge in Eq. (6.9).

As is well-known [130], if one deforms the $\mathbb{C}^2/\mathbb{Z}_2 \times \mathbb{C}$ parent theory by adding a mass term for the two adjoint fields, this generates a flow that in the IR reaches the conifold model. This explains why the ratio of the central charges of the two parent theories is $27/32$ [146]. This picture is preserved by the orientifold: starting with the $\mathcal{N} = 2$ $\mathbb{C}^2/\mathbb{Z}_2 \times \mathbb{C}$ orientifold and mass deforming, one ends up with the orientifold of the conifold, and again this explains the value of the ratio of the central charges. The fact that the orientifold of the conifold and the $\mathcal{N} = 1$ orientifold $\vec{\tau}_B$ of $\mathbb{C}^2/\mathbb{Z}_2 \times \mathbb{C}$ with $m = 2\tau_0$ have

⁶The same solution for the orientifold of the conifold has been constructed in [143, 144, 145], where the first reference observes that seven-branes should not be present in the type IIB configuration due to the lack of $1/N$ corrections to the a -anomaly, and the other two construct a configuration with one $O3^+$ and one $O3^-$ that wrap two homologically different two-cycles, both coming from a fractional $O5$.

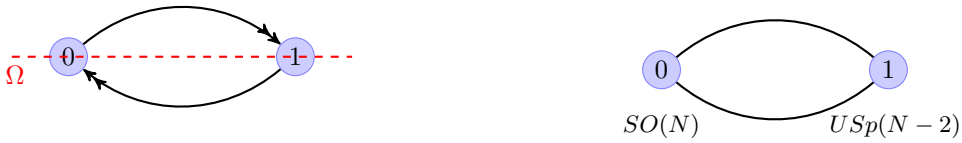


Figure 6.7 On the left, the quiver diagram for \mathcal{C} , where the red line represents the orientifold projection. On the right, the linear ‘unoriented’ quiver for the theory after the orientifold [1].

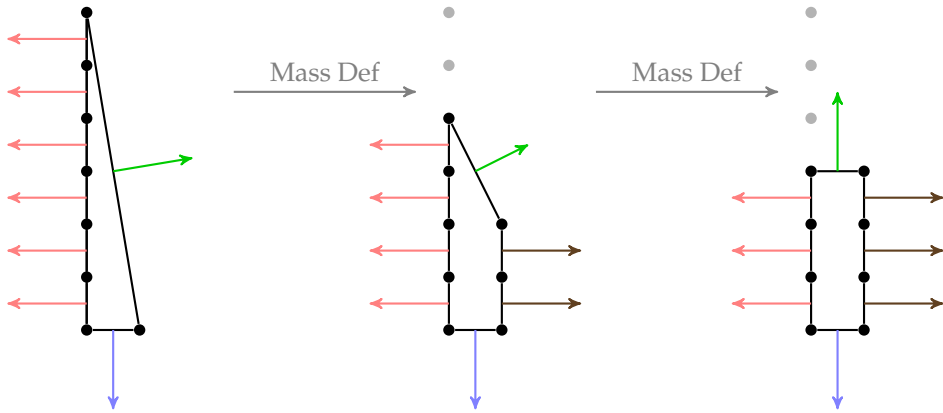


Figure 6.8 The chain of toric diagrams connected by mass deformation for $n = 6$: $\mathbb{C}^2/\mathbb{Z}_6 \times \mathbb{C} \rightarrow L^{2,4,2} \rightarrow L^{3,3,3}$, the number of points remains $n + 2 = 8$ all along. It holds also with the orientifold projection, mutatis mutandis.

the same central charge suggests that the two theories are conformally dual, meaning that they flow to the same conformal manifold, and indeed they are connected by turning on a mass term for the projected fields, which is an exactly marginal deformation because these fields have $R = 1$ and the mass operator is not charged under any other global factors.

The results of [9, 10] are a natural generalization of the mechanism described above to the infinite class of $L^{a,b,a}$ theories ($a \leq b$). The parent $L^{a,n-a,a}$ toric models can all be obtained by mass deformations of $L^{0,n,0}$, which is the $\mathcal{N} = 2$ orbifold $\mathbb{C}^2/\mathbb{Z}_n \times \mathbb{C}$. Specifically, starting from $L^{0,n,0}$, one can add a mass to a pair of adjoints⁷ of gauge groups that are connected in the quiver, and integrating out this mass term gives the $L^{1,n-1,1}$ theory [125]. This can be iterated to produce a chain that ends with $L^{\frac{n}{2},\frac{n}{2},\frac{n}{2}}$ for n even and $L^{\frac{n-1}{2},\frac{n+1}{2},\frac{n-1}{2}}$ for n odd. We represent some steps of this chain for $n = 6$ in Fig. 6.8. In fact, these theories can be embedded in IIA elliptic models, where stacks of D4-branes are wrapped around a circle and their worldvolume is divided by orthogonal NS5’s. The rotation of the five-branes describes the mass deformation, see for example Fig. 6.9. This construction holds also in presence of orientifold planes.

For the orientifold of $L^{0,n,0}$ theory one can choose the ranks in such a way that the choice of τ ’s preserving $\mathcal{N} = 2$ supersymmetry has a fixed point with ‘canonical’ R -charges

⁷Giving mass to pairs is necessary but not sufficient to preserve toricity [125].

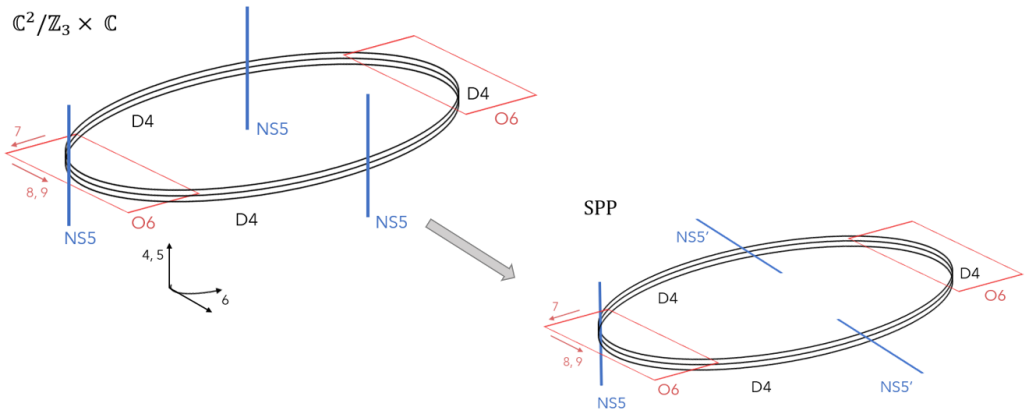


Figure 6.9 The theories $\mathbb{C}^2/\mathbb{Z}_3 \times \mathbb{C}$ and suspended pinch point (SPP) represented via IIA elliptic models. Rotating NS5 branes results in mass deforming the theory.

$2/3$ and half the central charge of the parent theory at large N . On the other hand, for all such theories it is also possible to perform an $\mathcal{N} = 1$ orientifold projection, with the same ranks of the gauge groups, and such that all the adjoints and projected fields have $R = 1$ and all the bifundamental fields have $R = 1/2$.

Note also that, for higher values of n , the $L^{a,n-a,a}$ theory admits different toric phases, which means different ways of integrating out pairs of adjoints, compatible with the orientifold. These correspond to different ways of accommodating the horizontal branes in the five-brane diagram, see Fig. 6.12 for an example.

For a family with n even, there are orientifold projections that generalize the ones of $\mathbb{C}^2/\mathbb{Z}_2 \times \mathbb{C}$ and the conifold, corresponding to the fixed points in Fig. 6.2b and the fixed lines in Fig. 6.6b. As an example, we represent in Fig. 6.10 the $n = 6$ case. The five-brane diagrams are constructed from the toric diagrams in Fig. 6.8. The parent theories describe six gauge groups, with vector-like bifundamentals connecting group i and $i + 1$. In the first and second diagram, the fixed points with charge τ_0 and τ_3 project the groups 0 and 3, while τ_{00} and τ_{33} project the adjoints of these groups. The $L^{1,5,1}$ theory is missing in the chain because it does not allow this orientifold. Indeed, in $L^{1,5,1}$ we would have five horizontal red branes (pointing towards the left) and one horizontal brown brane (pointing towards the right), and there is no way to accommodate them compatibly with the desired orientifold. Finally, the last diagram represents the orientifold of the non-chiral \mathbb{Z}_3 orbifold of the conifold, which is realized by fixed lines that project groups 0 and 3. In general, given a generic even n , all of the $\mathcal{N} = 1$ orientifold theories in the family have the same central charge a , 't Hooft anomalies and superconformal index of the orientifold of the orbifold of the conifold, which is the theory at the end of the chain. The value of the central charge is always $27/32$ the value of the $\mathcal{N} = 2$ theory. This was shown originally in [9] for $n = 3p$ studying the orientifold of the non-chiral orbifold SPP/\mathbb{Z}_p , i.e. the $L^{p,2p,p}$ theory and, then generalized in [10] to any even n .

For n even another orientifold projection is allowed, with all of the four fixed points lying on the intersections between NS5-branes, i.e. generating two conjugate pairs of tensor matter fields. In this way, all gauge factors remain unitary. We can construct such an orientifold by shifting the fixed points by a quarter of a period in the five-brane

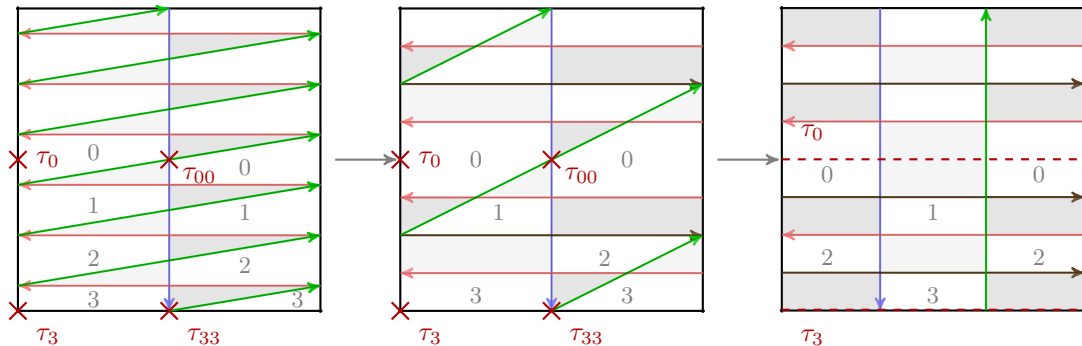


Figure 6.10 The chain of five-brane diagrams connected by mass deformation for $n = 6$: $\mathbb{C}^2/\mathbb{Z}_6 \times \mathbb{C} \rightarrow L^{2,4,2} \rightarrow L^{3,3,3}$, the number of vectors remains $n + 2 = 8$ all along. It holds also with the orientifold projection, provided a \mathbb{Z}_2 symmetry is preserved.

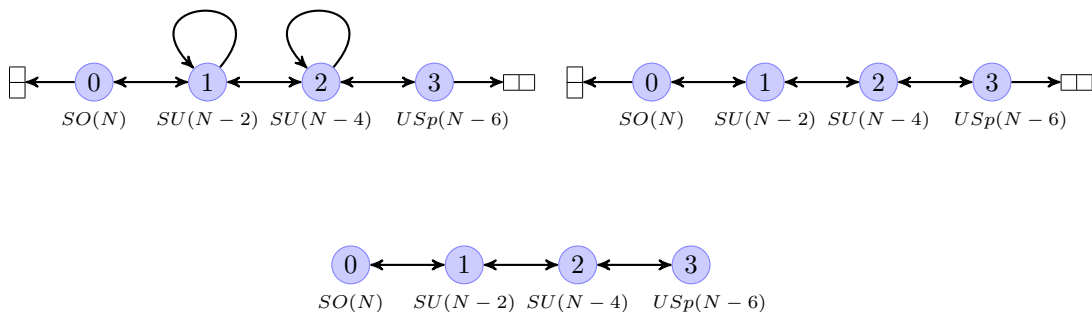


Figure 6.11 The chain of linear quiver diagrams after the orientifold connected by mass deformation for $n = 6$: $\mathbb{C}^2/\mathbb{Z}_6 \times \mathbb{C} \rightarrow L^{2,4,2} \rightarrow L^{3,3,3}$.

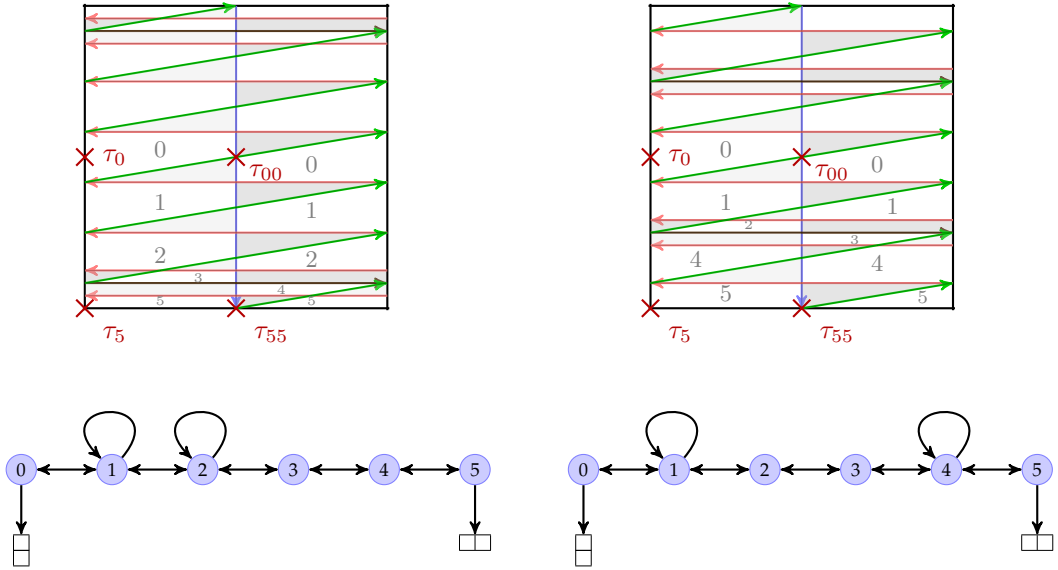


Figure 6.12 The two inequivalent ways of accommodating the horizontal branes for $L^{2,8,2}$ and the associated linear quivers.

diagram (see Fig. 6.13 for the $L^{2,4,2}$ example). These orientifolds were also analyzed in [10], and shown to realize the same mechanism as the models above. Note that when the toric diagram is a rectangle, such a projection cannot be obtained either with fixed points or with fixed lines, which implies that in order to include the last step of the chain the orientifold projection must be realized differently on the five-brane diagram. As we will see in the next section, this occurs for a chain of $L^{a,b,a}/\mathbb{Z}_2$ models with a particular orientifold projection introduced in [129] known as *glide orientifold*. This will play an important role in the remainder.

In the case of n odd the process is similar, but at the end of the chain a single adjoint field remains, corresponding to the $L^{\frac{n-1}{2}, \frac{n+1}{2}, \frac{n-1}{2}}$ toric model. We show in Fig. 6.14 the example of SPP, that is $L^{1,2,1}$, obtained by a mass deformation of $\mathbb{C}^2/\mathbb{Z}_3 \times \mathbb{C}$. The figure

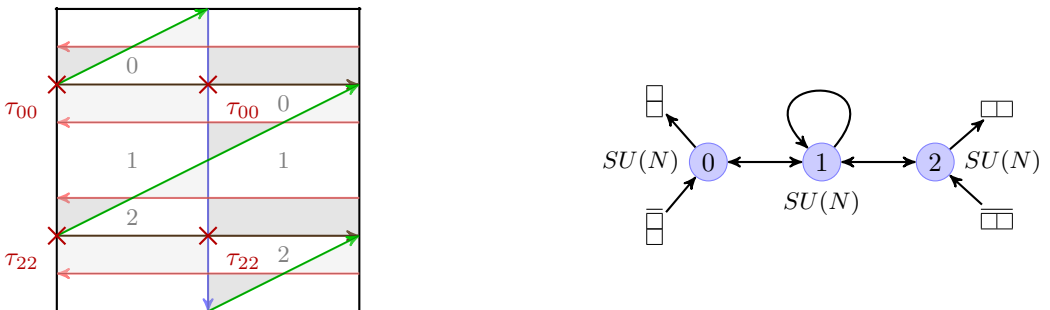


Figure 6.13 The orientifold projection of $L^{2,4,2}$ with four fixed points that yields unitary groups and pairs of conjugate tensor fields and the choice $\tau_{00} = -1, \tau_{22} = +1$.

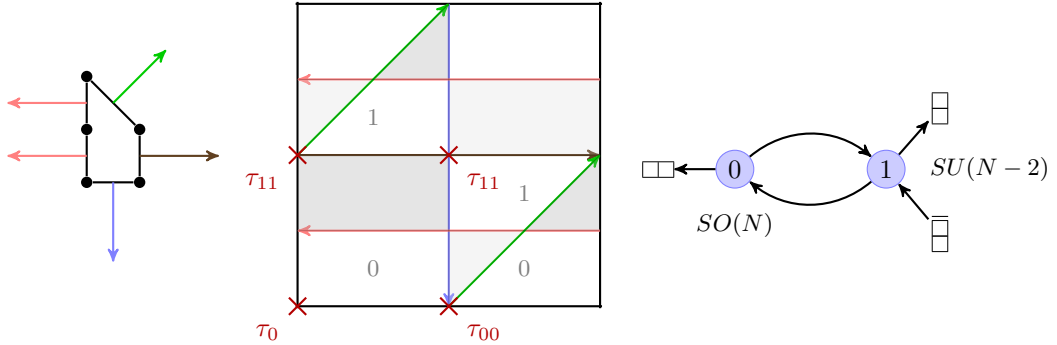


Figure 6.14 An example with n odd obtained from mass deformation of $\mathbb{C}^2/\mathbb{Z}_3 \times \mathbb{C}$ and the orientifold projection with fixed points. On the left, the toric diagram of $L^{1,2,1}$ or SPP, center its five-brane and on the right the quiver after the orientifold with $\tau_0 = +1$, $\tau_{00} = +1$, $\tau_{11} = -1$.

reveals the general feature of these orientifolds, in which one group and its adjoint are projected, while the other two τ 's give two conjugate fields which are symmetric or antisymmetric under a unitary group. In [9] these models were studied for $n = 3p$ and generalized in [10] to any n , showing that again the same mechanism occurs.

Finally, [10] shows that the conformal duality discussed above is an ‘inherited S -duality’ from the mother $\mathcal{N} = 2$ theory that is subsequently mass-deformed.

In the rest of this Chapter we will show how the same construction works for another infinite class of toric models, which are \mathbb{Z}_2 chiral orbifolds of the models of this section. In particular, the next section is devoted to the description of the models in terms of five-brane diagrams.

6.2 Glide orientifold and $L^{a,b,a}/\mathbb{Z}_2$ models

In this section we are going to introduce the class of orientifold models $L^{a,b,a}/\mathbb{Z}_2$, which we will focus on hereafter. In the first subsection we discuss the glide orientifold projection introduced in [129], which we will perform in the case $a = b$. The second subsection is devoted to a description of the models involved and the results. The following two sections will then contain a detailed analysis of such models.

6.2.1 Orientifolds and Klein bottles

Among the \mathbb{Z}_2 involutions of a torus, there are some choices that do not leave fixed points. This is interesting, as the five-brane diagram and the brane tiling are embedded in a torus and the orientifold projection is realized as a \mathbb{Z}_2 involution. While the past literature mostly focuses on projections with fixed loci, the case of a glide orientifold was recently analyzed in [129]. This involution maps a point to another by combining a shift by half a period of the fundamental cell with a reflection about one of its axes, see Fig. 6.15b. The topology obtained after this involution is that of a Klein bottle. This operation does not leave any fixed points and this can be understood by the fact that the net orientifold charge in the system is zero. As a consequence, the glide orientifold yields only $SU(N)$ gauge factors and tensor representations, if any, in conjugate pairs.

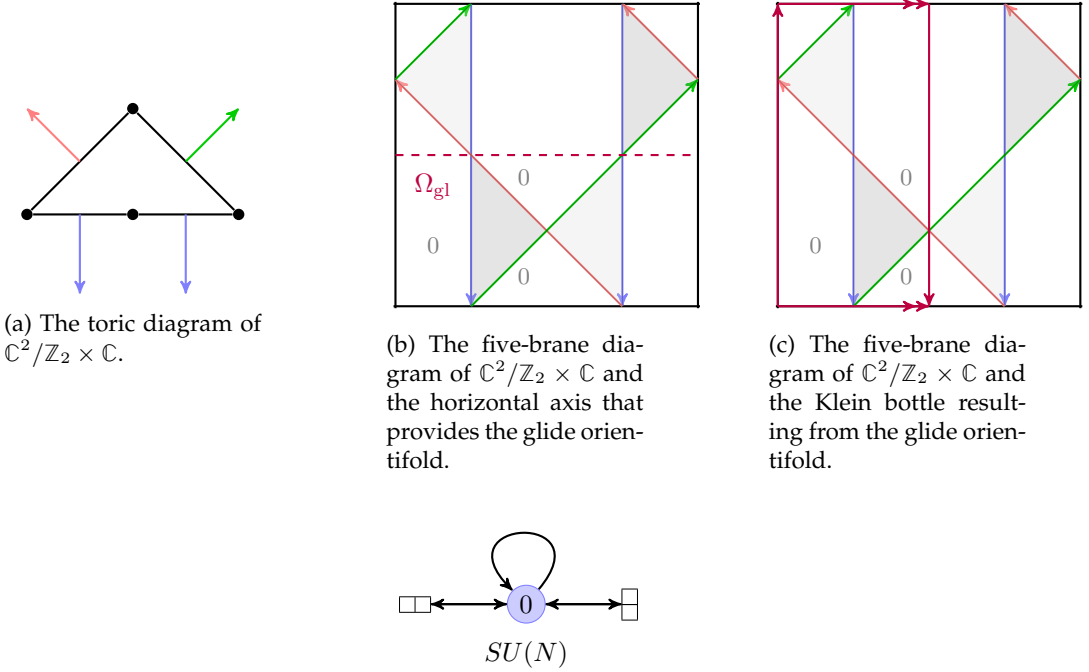


Figure 6.16 The linear quiver resulting from the glide orientifold of $\mathbb{C}^3/\mathbb{Z}_2$.

Hence, the resulting model is automatically free of any gauge anomaly. We denote this projection by Ω_{g1} .

As an example, consider again the original orbifold $\mathbb{C}^2/\mathbb{Z}_2 \times \mathbb{C}$. First, we need to move to a different toric phase by means of an $SL(2, \mathbb{Z})$ transformation, since the toric diagram needs to be symmetric about an axis that crosses at least two points of the toric diagram. In other words, if one consider the vectors dual to the sides of the toric diagram, an even number of them must be parallel to the symmetry axis of the glide. For our example, we choose the phase displayed in Fig. 6.15a, whose associated five-brane and its symmetry axis is drawn in Fig. 6.15b. Finally, the Klein bottle is explicitly displayed in Fig. 6.15c. The parent theory has two gauge factors, labelled by 0 and 1. The projection maps one factor into the other, while representation are conjugate. Moreover, the glide projection maps fields $\phi_0 \rightarrow \phi_1$, $X_{01}^1 \rightarrow X_{01}^2$ and $X_{10}^1 \rightarrow X_{10}^2$, so the upper index can be dropped. Since $\square_1 \rightarrow \bar{\square}_0$, we can split $X_{01} = (\square_0, \bar{\square}_1)$ in $\bar{\square}_0 = A$, $\square_0 = S$, and $X_{10} = (\square_1, \bar{\square}_0)$ in $\bar{\square}_0 = \tilde{A}$, $\square_0 = \tilde{S}$. The linear quiver that summarizes this matter content is drawn in Fig. 6.16. Finally, the superpotential reads

$$W_{\mathbb{C}^2/\mathbb{Z}_2 \times \mathbb{C}}^{\Omega_{g1}} = \phi_0 \tilde{A} \tilde{S} - \phi_0 \tilde{S} A . \tag{6.11}$$

6.2.2 Families of orientifolds of $L^{a,b,a}/\mathbb{Z}_2$

In the previous section we argued about a conformal duality between projected non-chiral toric theories, connected by a deformation that changes the shape of the toric

diagram while preserving the number of points [125]. We constructed a chain of toric polygons that belong to the $L^{a,b,a}$ family, where a and b can take generic values with $a \leq b$.

In order to generalize the duality to chiral theories, we consider the \mathbb{Z}_2 orbifold $L^{a,b,a}/\mathbb{Z}_2$ of that family, and infer some general behaviors that may be useful for a complete classification of the phenomenon of conformal duality among toric quivers after an orientifold projection. Indeed we observe that all such models are chiral, except for $L^{0,2,0}$ and $L^{1,1,1}$. Note that in order to have chiral theories, we lose the elliptic model description of these model. Perhaps, one could still construct a similar one along the lines of [129].

Moreover, for constructing a chain of toric diagrams as before, the number of external points of the toric diagram, i.e. on the perimeter, and the number of internal points must separately coincide. This implies that the models before the projection have the same number of gauge nodes and of non-anomalous $U(1)$ symmetries. This imposes constraints on the possible orbifold that we can use to generate an infinite family of dual models. Interestingly the conformally dual models discussed in [12], that are not related by an $R = 2$ mass deformation, respect these constraints as well. It may be a hint to a more general phenomenon whereby the conformally dual models obtained after orientifold projections are related by non-quadratic superpotential deformations.

In the following we identify three families in terms of the parity of a and b and in terms of the type of projection that we will realize on the five-brane web, though we will focus only on the first two.

Family \mathcal{A}

The first family that we study is the orientifold projection of $L^{a,b,a}/\mathbb{Z}_2$ with $a + b$ even that leads to quiver gauge theories with only unitary gauge groups and two pairs of conjugate tensor matter fields at the extremal gauge nodes, and we call it *family \mathcal{A}* . This is the generalization of family *i*) of [10] and we analyze it in Section 6.3. Imposing $a + b = 2k$, two extreme possibilities are $L^{0,2k,0}/\mathbb{Z}_2$ and $L^{k,k,k}/\mathbb{Z}_2$. As anticipated above, the case with $k = 1$ has a non-chiral field content before the orientifold projection, while for $k > 1$ internal points on the toric diagram necessarily arise. A generic model in the family is $L^{2p,2k-2p,2p}/\mathbb{Z}_2$ with $4k - 4p$ hexagons and $4p$ squares. We can construct a chain of toric diagrams that describe, upon orientifold projection, theories connected by conformal duality, i.e. a quadratic exactly marginal deformation:

$$L^{0,2k,0}/\mathbb{Z}_2 \rightarrow L^{2,2(k-1),2}/\mathbb{Z}_2 \dots \rightarrow L^{2p,2k-2p,2p}/\mathbb{Z}_2 \rightarrow \dots \rightarrow L^{k,k,k}/\mathbb{Z}_2, \quad (6.12)$$

where $p = 1, \dots, \lfloor \frac{k}{2} \rfloor$. Along the chain, pairs of vector-like fields with $R = 1$ are integrated out thanks to quadratic marginal deformation, until the last step where tensor fields are deformed. Note that the number of vector-like fields is $k - 1$, so when k is even the last step requires that one remaining vector-like field is integrated out together with the tensors.

In all steps but the last the orientifold projection is given by fixed points. On the five-brane, these lie at the intersection between a vertical brane and a skew brane. On the other hand, the last step requires a glide orientifold. An example of a chain of models, upon orientifold, is showed in Fig. 6.17-6.18, and the quiver in Fig. 6.19.

Note that the orientifold projection allows also for another configuration with four tensor

fields at four different nodes, associated to five-branes where the four fixed points lie at the intersection of the green vectors and horizontal red ones. In this way, orientifolds of $L^{p,2k-p,p}/\mathbb{Z}_2$ are also allowed. However, such a configuration does not feature the R -charges and dualities we want to discuss here, at least for the first examples we worked out, hence we will not consider it in the following.

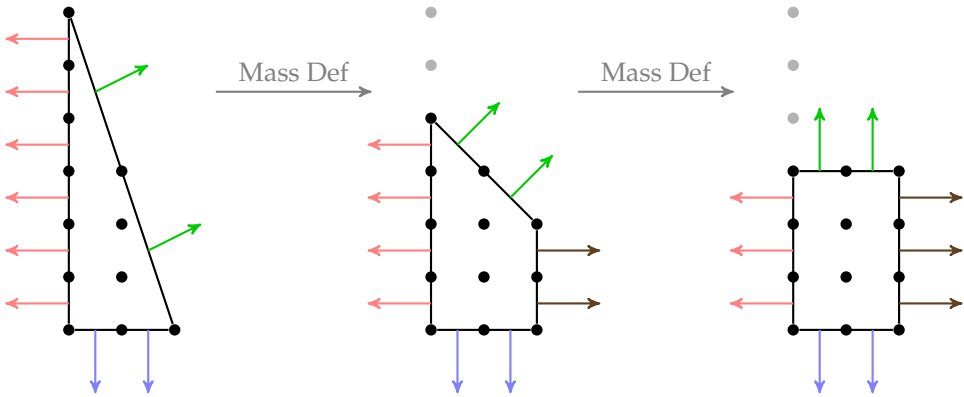


Figure 6.17 An example of a chain of toric diagrams of family \mathcal{A} connected by mass deformation for $k = 3$: $L^{0,6,0}/\mathbb{Z}_2 \rightarrow L^{2,4,2}/\mathbb{Z}_2 \rightarrow L^{3,3,3}/\mathbb{Z}_2$. It holds also with the orientifold projection, mutatis mutandis.

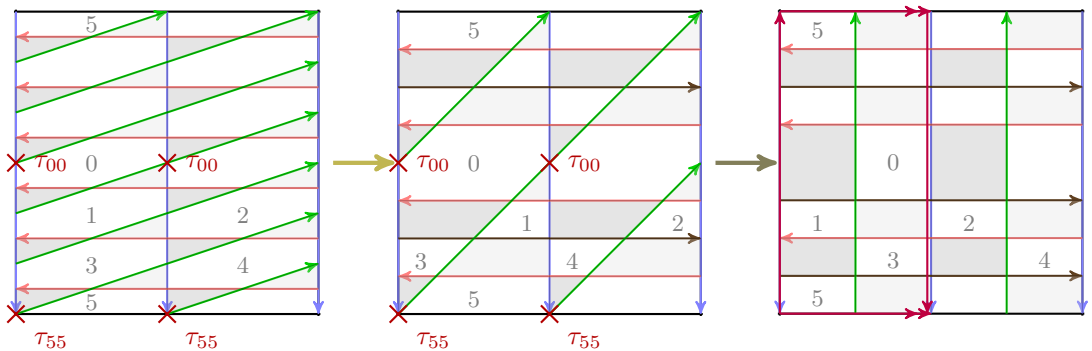


Figure 6.18 The chain of five-brane diagrams of family \mathcal{A} connected by mass deformation for $k = 3$: $L^{0,6,0}/\mathbb{Z}_2 \rightarrow L^{2,4,2}/\mathbb{Z}_2 \rightarrow L^{3,3,3}/\mathbb{Z}_2$. It holds also with the orientifold projection, provided a \mathbb{Z}_2 symmetry is preserved.

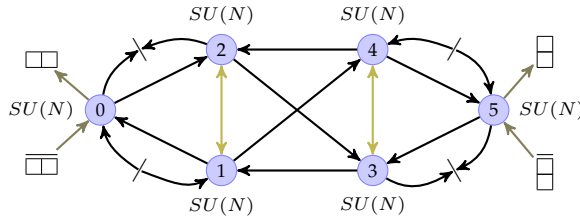


Figure 6.19 The quiver for the orientifold theory of $L^{0,6,0}/\mathbb{Z}_2 \rightarrow L^{2,4,2}/\mathbb{Z}_2 \rightarrow L^{3,3,3}/\mathbb{Z}_2$ in Family \mathcal{A} with choice $(\tau_{00} = +, \tau_{55} = -)$. Colored fields represent the pairs that are mass deformed in the chain, the color match the chain of five-branes in Fig. 6.18.

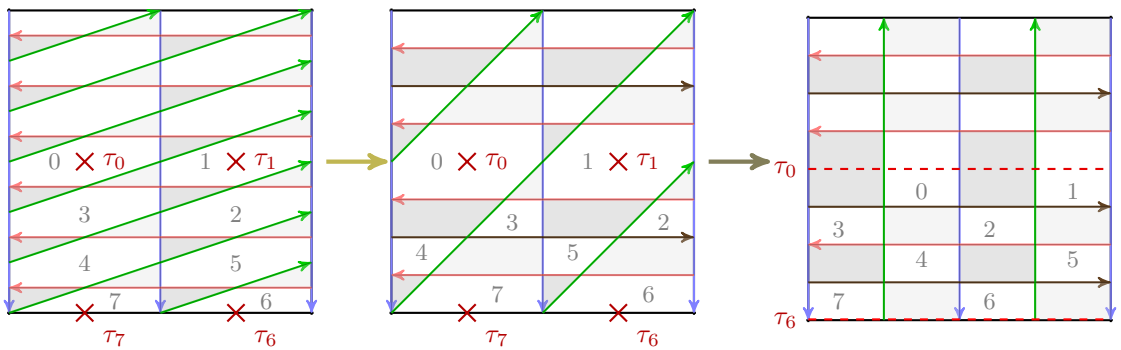


Figure 6.20 The chain of five-brane diagrams of family \mathcal{B} connected by mass deformation for $k = 3$: $L^{0,6,0}/\mathbb{Z}_2 \rightarrow L^{2,4,2}/\mathbb{Z}_2 \rightarrow L^{3,3,3}/\mathbb{Z}_2$. It holds also with the orientifold projection, provided a \mathbb{Z}_2 symmetry is preserved.

Family \mathcal{B}

We will refer to the second family as *family \mathcal{B}* , which generalizes family *iv)* of [10]. Also in this case $a + b = 2k$, but the orientifold projection acts either with fixed points or with fixed lines, lying on top of the faces of the five-brane, either hexagons or squares depending on the fixed loci. Contrary to the previous family, four gauge factors are now real groups,⁸ SO or USp depending on the signs of the fixed loci. The chain of toric diagrams is the same as in the previous family, Eq. (6.12), but the orientifold projection is realized differently on the five-branes, as we need to move the fixed points by a quarter period, see for example Fig. 6.20 and the associated quiver in Fig. 6.21. The extremal cases are $L^{0,2k,0}/\mathbb{Z}_2$ and $L^{k,k,k}/\mathbb{Z}_2$. Moreover, the last model in the chain is projected by fixed lines. As we will observe in Section 6.4, in this family marginal quadratic superpotential deformations with $R = 2$ can be generated only with a specific shift between the ranks of the gauge factors.

⁸We loosely refer to $SO(N)$ or $USp(N)$ as real gauge groups since, contrary to $SU(N)$, they do not admit complex representations. Complex spinors do not appear in perturbative open string constructions.

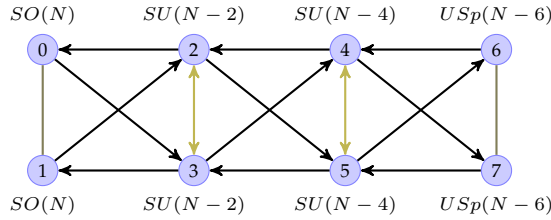


Figure 6.21 The quiver for the orientifold theory of $L^{0,6,0}/\mathbb{Z}_2 \rightarrow L^{2,4,2}/\mathbb{Z}_2 \rightarrow L^{3,3,3}/\mathbb{Z}_2$ in Family \mathcal{B} with choice $(\tau_0 = \tau_1 = +, \tau_6 = \tau_7 = -)$. Colored fields represent the pairs that are mass deformed in the chain, the color match the chain of five-branes in Fig. 6.20.

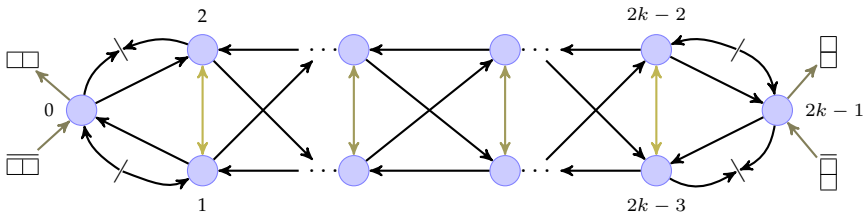


Figure 6.22 The generic quiver of family \mathcal{A} models. Colored fields are the mass deformed pairs. All gauge nodes are $SU(N)$.

6.3 Family \mathcal{A}

In this section we study in detail the conformal duality for the $L^{a,b,a}/\mathbb{Z}_2$ models (with $a + b = 2k$) after an orientifold projection that induces only unitary gauge groups. The generic quiver of this family of models is given in Fig. 6.22, where colored fields have $R = 1$ and they are progressively integrated out by mass deformations that generate the chain of conformally dual models in Eq. (6.12). We realize the orientifolds as fixed points on the five-brane for $a \neq b$ and both even, while for $a = b$ the gauge theory is realized as a glide orientifold [129].

The analysis is based on the computation and comparison of the central charges of the different $L^{a,b,a}/\mathbb{Z}_2$ orientifolds, which we denote as $a_{a,b,a}^\Omega$. We first analyze in detail the cases with $k = 1$ and $k = 2$ and then discuss the generalization to any k .

6.3.1 Orbifold with $k = 1$

The case $k = 1$ is the only non-chiral one among the models we discuss in this section. The $L^{0,2,0}/\mathbb{Z}_2$ model is $\mathbb{C}^3/(\mathbb{Z}_2 \times \mathbb{Z}_2)$ with charges $(0, 1, 1) \times (1, 0, 1)$, while $L^{1,1,1}/\mathbb{Z}_2$ is the non-chiral \mathbb{Z}_2 orbifold of the conifold \mathcal{C} .

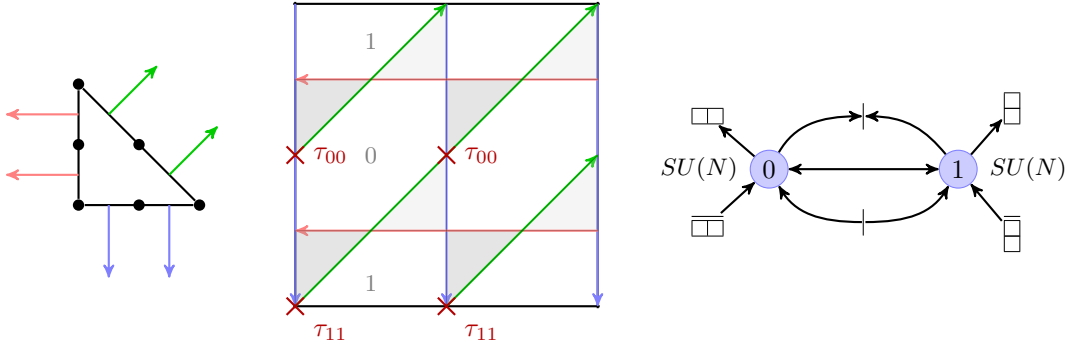


Figure 6.23 The model $L^{0,2,0}/\mathbb{Z}_2$. On the left the toric diagram is drawn, at the center the five-brane and its orientifold projection with fixed points, on the right the quiver resulting from the orientifold projection.

Orientifold projection of $L^{0,2,0}/\mathbb{Z}_2$ with fixed points

We study the orientifold projections with fixed points of $L^{0,2,0}/\mathbb{Z}_2$. After the projection, the gauge group is $G = SU(N_0) \times SU(N_1)$, whereas the field content is given by

$$\begin{aligned}
 X_{01} &= (\square_0, \bar{\square}_1) , & X_{10} &= (\square_1, \bar{\square}_0) \\
 Y_{01} &= (\square_0, \square_1) , & \tilde{Y}_{01} &= (\bar{\square}_0, \bar{\square}_1) \\
 T_{00} &= (\square_0, \square_0) , & \tilde{T}_{00} &= (\bar{\square}_0, \bar{\square}_0) \\
 T_{11} &= (\square_1, \square_1) , & \tilde{T}_{11} &= (\bar{\square}_1, \bar{\square}_1) ,
 \end{aligned}
 \tag{6.13}$$

where fields Y_{01} and \tilde{Y}_{01} arise at the intersection between red and blue vectors on the five-brane diagram in Fig. 6.23, while the particular representation of the tensor fields $T_{00}, \tilde{T}_{00}, T_{11}$ and \tilde{T}_{11} depends on the signs of the charges $\vec{\tau}$. Since $N_W/2 = 4$, the product of these charges must be positive. Another constraint for the charges $\vec{\tau}$ comes from gauge anomaly cancellation that requires the presence of conjugate pairs of tensor representations, hence $\tau_{00} = \tilde{\tau}_{00}$ and $\tau_{11} = \tilde{\tau}_{11}$. We denote the inequivalent choices of $\vec{\tau} = (\tau_{00}, \tilde{\tau}_{00}, \tau_{11}, \tilde{\tau}_{11})$ as $\vec{\tau}_A = (\pm, \pm, \mp, \mp)$ and $\vec{\tau}_B = (\pm, \pm, \pm, \pm)$. The resulting quiver is drawn in Fig. 6.23, while the superpotential reads

$$W_{0,2,0}^\Omega = X_{01}T_{11}\tilde{Y}_{01} - Y_{01}\tilde{T}_{11}X_{10} + X_{10}T_{00}\tilde{Y}_{01} - Y_{01}\tilde{T}_{00}X_{01} .
 \tag{6.14}$$

Imposing that the β -functions all vanish one obtains

$$\begin{aligned}
r_{00} + \tilde{r}_{00} &= r_{11} + \tilde{r}_{11} , \\
r_{01} + \tilde{r}_{00} + r_Y &= -1 , \\
r_{10} + r_{00} + \tilde{r}_Y &= -1 , \\
(r_{00} + \tilde{r}_{00}) + (r_{01} + r_{10}) + (r_Y + \tilde{r}_Y) &= -2 , \\
(r_{00} + \tilde{r}_{00})(m + 2\tau_{00}) &= -2m , \\
(r_{00} + \tilde{r}_{00})(m - 2\tau_{11}) &= -2m ,
\end{aligned} \tag{6.15}$$

where $m = N_0 - N_1$ and $\vec{\tau}_A$ is selected. Note that with $m = 0$, the choice on $\vec{\tau}$ is no longer constrained.⁹ Further imposing that R -charges of conjugate pairs are the same, i.e. $r_{01} = r_{10}$ and $r = \tilde{r}$ we get

$$\begin{aligned}
r_{00} = \tilde{r}_{00} = r_{11} = \tilde{r}_{11} &= -\frac{m}{m + 2\tau_{00}} , \\
r_{01} + r_{00} + r_Y &= -1 ,
\end{aligned} \tag{6.16}$$

We can select equal ranks by imposing $m = 0$, as opposed to the orientifold projection studied in [9, 10], meaning that this model does not require the presence of fractional branes. This holds for the whole family \mathcal{A} . At large N , we have

$$\begin{aligned}
\text{Tr}R &= 0 , \\
\text{Tr}R^3 &= 2N^2 \left(r_{01}^3 + (-1 - r_{01})^3 + 1 \right) ,
\end{aligned} \tag{6.17}$$

and the central charge is maximized at

$$\begin{aligned}
r_{00} = \tilde{r}_{00} = r_{11} = \tilde{r}_{11} &= 0 , \\
r_{01} = r_{10} = r_Y = \tilde{r}_Y &= -\frac{1}{2} , \\
a_{0,2,0}^{\Omega_{m=0}} &= \frac{27}{64}N^2 ,
\end{aligned} \tag{6.18}$$

implying superconformal $R = 1$ for the tensor fields, and $R = 1/2$ for the remaining ones.

Finally, note that for $m = \tau_{01}$, we have that all the fields have $R = 2/3$, and the value of the central charge is

$$a_{0,2,0}^{\Omega_{m=\tau_{01}}} = \frac{1}{2}N^2 . \tag{6.19}$$

Remarkably, shifting the ranks of the unitary groups, which means that a fractional brane is present in the system, yields the R -charge of free fields. This solution is present for all orbifold of flat space $(L^{0,2k,0}/\mathbb{Z}_2)^\Omega$. Surprisingly, the ratio between the two central

⁹The fact that $\vec{\tau}_B$ works here is due to $R = 1$. Similarly, in family *ii*) and *iii*) of [10] one can engineer a configuration of O6-planes that yields pairs of tensors that transform in the same way. The point is that they can still be integrated out.

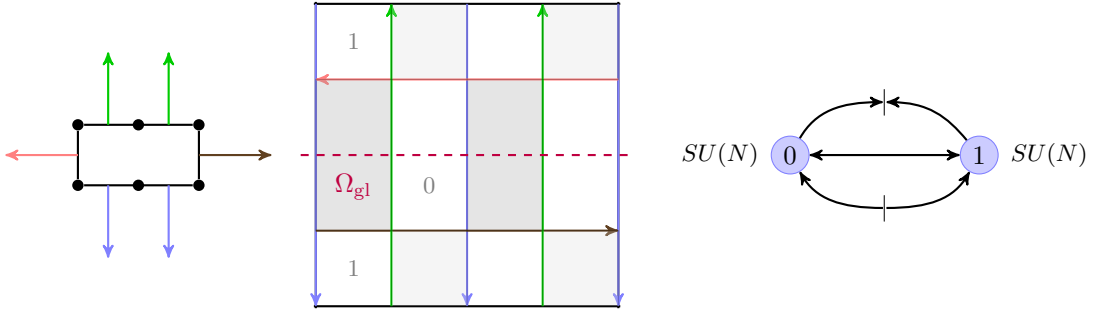


Figure 6.24 The model $L^{1,1,1}/\mathbb{Z}_2$. On the left the toric diagram is drawn, at the center the five-brane and its glide projection, on the right the quiver resulting from the orientifold projection.

charges in Eqs. (6.18)-(6.19) is $27/32$. This is supposed to happen when $\mathcal{N} = 2$ is broken, via mass deformation, down to $\mathcal{N} = 1$ [146]. We briefly discuss the role of this solution in section 7.5.

Glide orientifold of $L^{1,1,1}/\mathbb{Z}_2$

We study the glide orientifold of $L^{1,1,1}/\mathbb{Z}_2$, whose field content is

$$\begin{aligned} X_{01} &= (\square_0, \bar{\square}_1) , & X_{10} &= (\square_1, \bar{\square}_0) \\ Y_{01} &= (\square_0, \square_1) , & \tilde{Y}_{01} &= (\bar{\square}_0, \bar{\square}_1) , \end{aligned} \tag{6.20}$$

which is similar to Eq. (6.13) except for the tensor fields. The projection yields a theory with gauge group $G = SU(N_0) \times SU(N_1)$ and superpotential

$$W_{1,1,1}^{\Omega_{g1}} = X_{01} X_{10} Y_{01} \tilde{Y}_{01} - X_{10} X_{01} Y_{01} \tilde{Y}_{01} , \tag{6.21}$$

as can be read from Fig. 6.24. The set of constraints for the superconformal R -charges, together with $r_{01} = r_{10}$ yields

$$\begin{aligned} N_0 &= N_1 = N , \\ r_{01} + r_Y &= -1 , \end{aligned} \tag{6.22}$$

and at large N we retrieve Eqs. (6.17) and at the local maximum

$$\begin{aligned} r_{01} = r_{10} = r_Y = \tilde{r}_Y &= -\frac{1}{2} , \\ a_{1,1,1}^{\Omega_{g1}} &= \frac{27}{64} N^2 . \end{aligned} \tag{6.23}$$

The central charge, 't Hooft anomalies and the superconformal index are the same for the orientifold projection with fixed points of $L^{0,2,0}/\mathbb{Z}_2$ and the two orientifold theories are conformally dual.

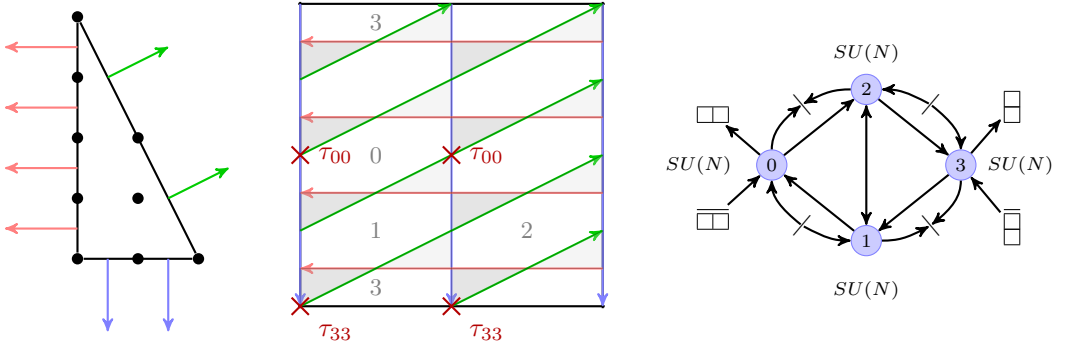


Figure 6.25 The model $L^{0,4,0}/\mathbb{Z}_2$. On the left the toric diagram is drawn, at the center the five-brane and its orientifold projection with fixed points, on the right the quiver resulting from the orientifold projection.

6.3.2 Orbifold with $k = 2$

We now discuss models with $a + b = 4$. The parent theories are chiral and their toric diagrams are reflexive polygons, having one internal point [147]. As already mentioned above, we restrict ourselves on orientifolds of models with even a (and b), because in the case of a, b odd the projection does not give a theory with the the desired features, as we will explicitly see for $L^{1,3,1}/\mathbb{Z}_2$.

Orientifold projection of $L^{0,4,0}/\mathbb{Z}_2$ with fixed points

We study the orientifold of $L^{0,4,0}/\mathbb{Z}_2$ with fixed points such that $\prod \tau = +1$ the projection yields gauge groups $G = SU(N_0) \times SU(N_1) \times SU(N_2) \times SU(N_3)$. The toric diagram of the parent theory, the five-brane and the quiver of the resulting projected theory are shown in Fig 6.25. The field content is

$$\begin{aligned}
 X_{02} &= (\square_0, \bar{\square}_2) , & X_{10} &= (\square_1, \bar{\square}_0) \\
 X_{12} &= (\square_1, \bar{\square}_2) , & X_{21} &= (\square_2, \bar{\square}_1) \\
 X_{23} &= (\square_2, \bar{\square}_3) , & X_{31} &= (\square_3, \bar{\square}_1) \\
 Y_{02} &= (\square_0, \square_2) , & \tilde{Y}_{01} &= (\bar{\square}_0, \bar{\square}_1) \\
 Y_{13} &= (\square_1, \square_3) , & \tilde{Y}_{23} &= (\bar{\square}_2, \bar{\square}_3) \\
 T_{00} &= (\square_0, \square_0) , & \tilde{T}_{00} &= (\bar{\square}_0, \bar{\square}_0) \\
 T_{33} &= (\square_3, \square_3) , & \tilde{T}_{33} &= (\bar{\square}_3, \bar{\square}_3)
 \end{aligned}
 \tag{6.24}$$

and the superpotential reads

$$\begin{aligned}
 W_{0,4,0}^\Omega &= T_{00} \tilde{Y}_{01} X_{10} - X_{10} X_{02} X_{21} + \tilde{T}_{00} X_{02} Y_{02} - Y_{02} \tilde{Y}_{01} X_{12} \\
 &+ X_{12} X_{23} X_{31} + Y_{13} \tilde{Y}_{23} X_{21} - T_{33} \tilde{Y}_{23} X_{23} - \tilde{T}_{33} X_{31} Y_{13} .
 \end{aligned}
 \tag{6.25}$$

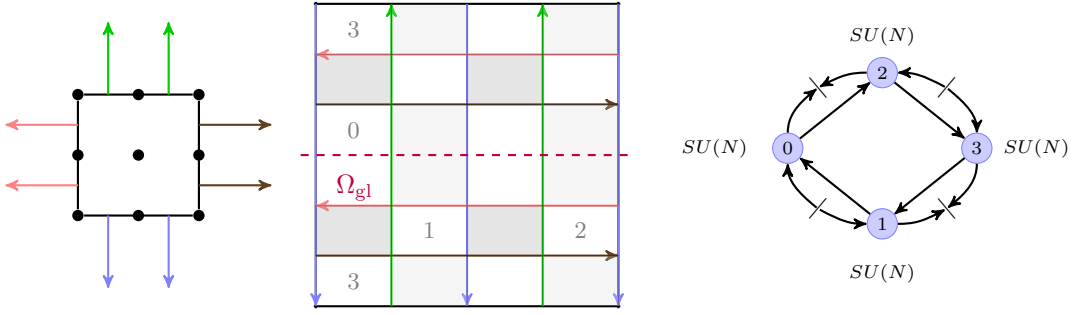


Figure 6.26 The model $L^{2,2,2}/\mathbb{Z}_2$. On the left the toric diagram is drawn, at the center the five-brane and its glide orientifold, on the right the quiver resulting from the projection.

Cancellation of gauge-anomalies requires that

$$N_1 - N_2 = 2(\tau_{00} - \tilde{\tau}_{00}) . \tag{6.26}$$

Proceeding as before, we find the condition for β -functions to vanish and $R(W) = 2$, together with demanding that the R -charges of conjugate pairs are equal. Imposing that all ranks are equal, $N_a = N \forall a$, we find

$$\begin{aligned} r_{00} = \tilde{r}_{00} = r_{33} = \tilde{r}_{33} = r_{12} = r_{21} = 0 , \\ r_{Y_{02}} = r_{10} , \quad r_{Y_{13}} = r_{23} , \\ r_{02} = \tilde{r}_{Y_{01}} = -1 - r_{10} , \quad r_{31} = \tilde{r}_{Y_{23}} = -1 - r_{23} , \end{aligned} \tag{6.27}$$

in terms of two R -charges r_{10} and r_{23} . This solution gives at large N

$$\begin{aligned} \text{Tr}R = 0 , \\ \text{Tr}R^3 = 2N^2 \left[r_{10}^3 + (-1 - r_{10})^3 + r_{23}^3 + (-1 - r_{23})^3 + 2 \right] , \end{aligned} \tag{6.28}$$

which is symmetric under the exchange $r_{10} \leftrightarrow r_{23}$. The resulting global anomaly is twice the one of $(L^{0,2,0}/\mathbb{Z}_2)^\Omega$ and the local maximum stays at

$$\begin{aligned} r_{10} = r_{23} = -\frac{1}{2} , \\ a_{0,4,0}^\Omega = \frac{27}{32}N^2 , \end{aligned} \tag{6.29}$$

so that the R -charges of tensor fields and vector-like fields is $R = 1$ and they do not contribute to 't Hooft anomalies and the superconformal index, while the remaining ones have $R = 1/2$.

Glide orientifold of $L^{2,2,2}/\mathbb{Z}_2$

We now study the glide orientifold of $L^{2,2,2}/\mathbb{Z}_2$, which yields a theory with gauge group $G = SU(N_0) \times SU(N_1) \times SU(N_2) \times SU(N_3)$. The toric diagram of the parent theory, the

five-brane and the quiver resulting from the projection are drawn in Fig. 6.26. The field content is

$$\begin{aligned}
X_{10} &= (\square_1, \bar{\square}_0) , & X_{02} &= (\square_0 \bar{\square}_2) \\
X_{23} &= (\square_2, \bar{\square}_3) , & X_{31} &= (\square_3 \bar{\square}_1) \\
Y_{02} &= (\square_0, \square_2) , & \tilde{Y}_{23} &= (\bar{\square}_2, \bar{\square}_3) ; \\
Y_{13} &= (\square_1, \square_3) , & \tilde{Y}_{01} &= (\bar{\square}_0, \bar{\square}_1) ,
\end{aligned} \tag{6.30}$$

whereas the superpotential is

$$\begin{aligned}
W_{2,2,2}^{\Omega_{\text{gl}}} &= X_{10} Y_{02} (X_{02})^T \tilde{Y}_{01} - X_{10} X_{02} X_{23} X_{31} + X_{31} Y_{13} (X_{23})^T \tilde{Y}_{23} \\
&\quad - \tilde{Y}_{01} Y_{13} \tilde{Y}_{23} Y_{02} + \tilde{Y}_{23} X_{23} Y_{13} (X_{31})^T + Y_{02} (X_{10})^T \tilde{Y}_{01} X_{02} .
\end{aligned} \tag{6.31}$$

The field content is similar to Eq. (6.24) except for the tensor and the vector-like fields. We notice that in this case it is not enough to mass deform the pairs of tensor fields from $(L^{0,4,0}/\mathbb{Z}_2)^\Omega$, but we need to mass deform also X_{12}, X_{21} . This happens when the number $k-1$ of vector-like fields is odd, hence for k even.

The set of constraints for the superconformal R -charges, together with cancellation of gauge-anomaly and the \mathbb{Z}_2 -symmetry of the quiver yields

$$\begin{aligned}
N_0 &= N_1 = N_2 = N_3 = N , \\
r_{23} &= r_{10} , & r_{02} &= r_{31} = -1 - r_{10} , \\
r_{Y_{13}} &= r_{Y_{02}} , & \tilde{r}_{Y_{23}} &= \tilde{r}_{Y_{01}} = -1 - r_{Y_{02}} ,
\end{aligned} \tag{6.32}$$

expressed in terms of the two charges r_{10} and $r_{Y_{02}}$. At large N , the global anomalies read

$$\begin{aligned}
\text{Tr} R &= 0 , \\
\text{Tr} R^3 &= 2N^2 \left[r_{10}^3 + (-1 - r_{10})^3 + r_{Y_{02}}^3 + (-1 - r_{Y_{02}})^3 + 2 \right] ,
\end{aligned} \tag{6.33}$$

whose share the same form and local maximum of $(L^{0,4,0}/\mathbb{Z}_2)^\Omega$ in Eqs. (6.28)-(6.29), as

$$\begin{aligned}
r_{10} &= r_{Y_{02}} = -\frac{1}{2} , \\
a_{0,4,0}^\Omega &= \frac{27}{32} N^2 ,
\end{aligned} \tag{6.34}$$

The two models orientifold of $L^{0,4,0}/\mathbb{Z}_2$ and of $L^{2,2,2}/\mathbb{Z}_2$ are conformally dual, connected by quadratic marginal deformations.

L^{131}/\mathbb{Z}_2 and general feature of odd a

The set of parent theories $L^{a,b,a}/\mathbb{Z}_2$ with $a+b=4$ involves also the case $a=1$ and $b=3$, i.e. both odd numbers. The orientifold of $L^{1,3,1}/\mathbb{Z}_2$ with four fixed points yields a theory that does not belong to the chain of conformally dual projected theories, i.e. cannot be

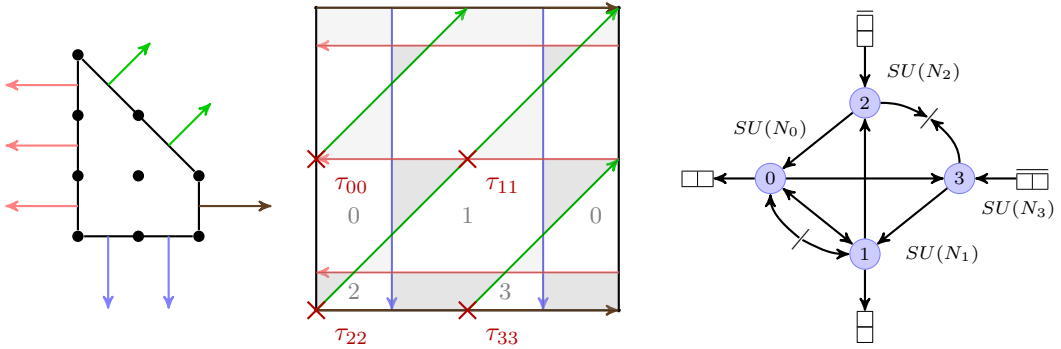


Figure 6.27 The model $L^{1,3,1}/\mathbb{Z}_2$. On the left the toric diagram is drawn, at the center the five-brane and its orientifold projection with fixed points, on the right the quiver resulting from a choice of orientifold projection consistent with gauge anomalies. This does not belong to family \mathcal{A} .

connected to other models by an exactly marginal deformation that integrates out pairs of conjugate fields, as we instead showed in the previous sections and works [9, 10]. We can see this clearly from Fig. 6.27. In particular, from the quiver we see that the four tensor fields transform under four different groups, hence they cannot be mass deformed as for the theories in family \mathcal{A} . Moreover, cancellation of gauge anomalies gives

$$\begin{aligned}
 N_0 - N_1 - N_2 + N_3 + 4\tau_{00} &= 0, \\
 -N_0 + N_1 + N_2 - N_3 + 4\tau_{11} &= 0, \\
 N_0 - N_1 - N_2 + N_3 - 4\tau_{22} &= 0, \\
 -N_0 + N_1 + N_2 - N_3 - 4\tau_{33} &= 0
 \end{aligned} \tag{6.35}$$

and all ranks equal is not a solution, as it is for family \mathcal{A} .

From the point of view of the five-brane diagram, when a and b are both odd, the \mathbb{Z}_2 involution of the orientifold imposes that two horizontal vectors, one oriented to the right and one to the left, pass through two fixed points. See for example Fig. 6.27, where a red vector oriented to the left lies on τ_{00} and τ_{11} , while a brown vector oriented to the right lies on τ_{22} and τ_{33} . Since only two five-branes can meet on a point,¹⁰ we need to move either the skew green vectors or the vertical blue vectors. The consequence is that the four fixed points project fields transforming in four different groups. This is general, for all odd a and b , and therefore they do not belong to the family \mathcal{A} .

Finally, one can easily see that from the five-brane in Fig. 6.27 the models do not admit a glide orientifold.

¹⁰Or better, in those cases one can describe strongly coupled sectors following [148].

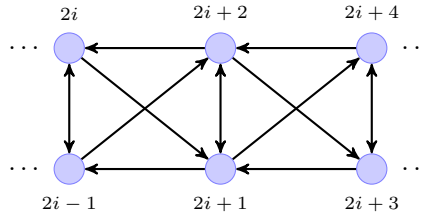


Figure 6.28 A portion of generic quiver of the orientifold of $L^{0,2k,0}/\mathbb{Z}_2$ from node $2i$.

6.3.3 Generalization

In this section we want to show the previous results are general and hold for the whole chain

$$L^{0,2k,0}/\mathbb{Z}_2 \rightarrow L^{2,2(k-1),2}/\mathbb{Z}_2 \dots \rightarrow L^{2p,2k-2p,2p}/\mathbb{Z}_2 \rightarrow \dots \rightarrow L^{k,k,k}/\mathbb{Z}_2, \quad (6.36)$$

where $p = 1, \dots, \lfloor \frac{k}{2} \rfloor$. Let us begin with the orientifold of $L^{0,2k,0}/\mathbb{Z}_2$, the generic quiver is drawn in Fig. 6.22, with all vector-like fields. From the five-brane, we can write down the superpotential as

$$\begin{aligned} W_{0,2k,0}^\Omega &= T_{00}\tilde{Y}_{01}X_{10} + \tilde{T}_{00}X_{02}Y_{02} - X_{02}X_{21}X_{10} - Y_{02}\tilde{Y}_{01}X_{12} \\ &\quad - T_{2k-1,2k-1}\tilde{Y}_{2k-2,2k-1}X_{2k-2,2k-1} - \tilde{T}_{2k-1,2k-1}X_{2k-1,2k-3}Y_{2k-3,2k-1} \\ &\quad + X_{2k-2,2k-1}X_{2k-1,2k-3}X_{2k-3,2k-2} + Y_{2k-3,2k-1}\tilde{Y}_{2k-2,2k-1}X_{2k-2,2k-3} \\ &\quad + \sum_{i=1}^{k-2} (X_{2i-1,2i}X_{2i,2i+1}X_{2i+1,2i-1} + X_{2i,2i-1}X_{2i-1,2i+2}X_{2i+2,2i}) \\ &\quad - \sum_{i=1}^{k-2} (X_{2i+1,2i+2}X_{2i+2,2i}X_{2i,2i+1} + X_{2i+2,2i+1}X_{2i+1,2i-1}X_{2i-1,2i+2}) . \end{aligned} \quad (6.37)$$

We need to impose the conditions $R(W) = 2$ and that all β -functions vanish, with all ranks equal, $N_a = N \forall a$. Consider a section of the quiver from node $2i$, as in Fig. 6.28 and the related superpotential terms, whose constraints imply

$$\begin{aligned} r_{2i,2i-1} &= -1 - (r_{2i-1,2i+2} + r_{2i+2,2i}), \\ r_{2i-1,2i} &= -1 - (r_{2i,2i+1} + r_{2i+1,2i-1}), \end{aligned} \quad (6.38)$$

as well as the same equations with $i \rightarrow i + 2$. The sum of this four equations gives:

$$m_{2i,2i-1} + m_{2i+2,2i+1} = -4 - (r_{2i-1,2i+2} + r_{2i+2,2i} + r_{2i,2i+1} + r_{2i+1,2i-1} + \{i \rightarrow i + 2\}) . \quad (6.39)$$

where $m_{2i,2i-1} = r_{2i,2i-1} + r_{2i-1,2i}$. Vanishing of the beta functions on the nodes $2i + 2$ and $2i + 1$ imply:

$$m_{2i+2,2i+1} = -2 - (r_{2i+2,2i} + r_{2i-1,2i+2} + r_{2i+4,2i+2} + r_{2i+2,2i+3}) , \quad (6.40)$$

$$m_{2i+2,2i+1} = -2 - (r_{2i+1,2i-1} + r_{2i,2i+1} + r_{2i+1,2i+4} + r_{2i+3,2i+1}) . \quad (6.41)$$

The combination of Eqs. (6.40) + (6.41) – (6.39) gives

$$m_{2i,2i-1} = m_{2i+2,2i+1} , \quad i = 1, \dots, (k - 2) . \quad (6.42)$$

Similarly one can show that

$$r_{00} + \tilde{r}_{00} = r_{2k-1,2k-1} + \tilde{r}_{2k-1,2k-1} = m_{2i,2i-1} , \quad i = 1, \dots, (k - 2) . \quad (6.43)$$

Finally the beta equation for the node $i = 0$ and the superpotential terms that include the tensor fields T_{00} and \tilde{T}_{00} yield

$$(r_{00} + \tilde{r}_{00})2\tau_{00} = 0 \quad (6.44)$$

Together with (6.43) this implies that the combinations $T_{00}\tilde{T}_{00}$, $T_{2k-1,2k-1}\tilde{T}_{2k-1,2k-1}$ and $X_{2i,2i-1}X_{2i-1,2i}$ have fermionic R -charge $r = 0$ (bosonic R -charge $R = 2$) and they are marginal deformations. If we impose that conjugate fields have the same R -charge, this also means that tensor fields and vector-like have r -charge $r = 0$. The quadratic marginal operators written above give mass to the fields and we can integrate them out. The resulting effective theory is the orientifold of $L^{2p,2k-2p,2p}/\mathbb{Z}_2$, where p is the number of pairs of conjugate fields that have been integrated out. The conformal mass terms for the pairs of conjugate fields is marginal and does not trigger an RG flow. Another way to see this is that the superpotential of the orientifold of $L^{2p,2k-2p,2p}/\mathbb{Z}_2$ imposes the same constraints in the r -charges as the theory $(L^{0,2k,0}/\mathbb{Z}_2)^\Omega$. Indeed from the last two lines of the superpotential in Eq (6.37), using $i \rightarrow (i + 2)$ for the first term in each line, we can write

$$\begin{aligned} r_{2i+2,2i+3} + r_{2i+3,2i+1} + r_{2i+1,2i-1} + r_{2i-1,2i+2} &= -2 , \\ r_{2i+2,2i} + r_{2i,2i+1} + r_{2i+1,2i+4} + r_{2i+4,2i+2} &= -2 , \end{aligned} \quad (6.45)$$

where we also used (6.44). These are exactly the constraints from the quartic terms after the quadratic deformation. This is due to the fact that one integrates the pairs of conjugate fields out plugging their F -terms into the superpotential. Therefore, all we need to study is the first model of the chain in Eq. (6.36). From the superpotential and the β -functions we have now

$$\begin{aligned} r_{00} = \tilde{r}_{00} = r_{2k-1,2k-1} = \tilde{r}_{2k-1,2k-1} = r_{2i,2i-1} = r_{2i-1,2i} &= 0 , \\ r_{2i-1,2i+2} + r_{2i+2,2i} &= -1 , \\ r_{2i,2i+1} + r_{2i+1,2i-1} &= -1 . \end{aligned} \quad (6.46)$$

All superpotential terms are generated sequentially shifting $i \rightarrow (i + 2)$ from the quiver combining a vertical arrow, which does not contribute now, an horizontal one and a diagonal one. Compare Fig. 6.19 and Eq. (6.37) in order to see that. Moreover, the generic

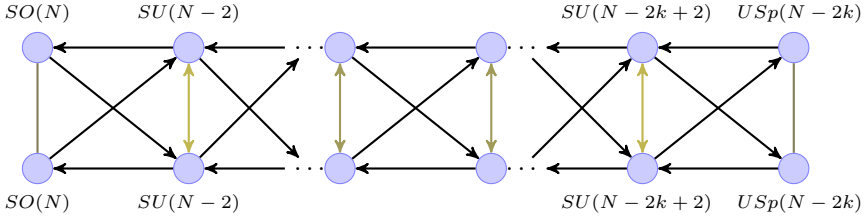


Figure 6.29 The general quiver of family \mathcal{B} models. Colored fields are the mass deformed pairs.

quiver has a \mathbb{Z}_2 symmetry. Hence, we can impose

$$r_{10} = r_{02} = r_{2k-2,2k-1} = r_{2k-1,2k-3} = r_{2i,2i+1} = r_{2i-1,2i+2} = \dots \{i \rightarrow (i+2)\},$$

$$r_{Y_{02}} = \tilde{r}_{Y_{01}} = r_{Y_{2k-2,2k-1}} = \tilde{r}_{Y_{2k-3,2k-1}} = r_{2i+2,2i} = r_{2i+1,2i-1} = \dots \{i \rightarrow (i+2)\}, \quad (6.47)$$

so that we can express 't Hooft anomalies only in terms of four R -charges, r_{10} , $(-1 - r_{10})$, $r_{Y_{02}}$ and $(-1 - r_{Y_{02}})$, and we have a number k of each of them. The central charge reads

$$a_{0,2k,0}^\Omega = \frac{9}{32} N^2 k \left[r_{10}^3 + (-1 - r_{10})^3 + r_{Y_{02}}^3 + (-1 - r_{Y_{02}})^3 + 2 \right], \quad (6.48)$$

whose local maximum is

$$r_{10} = r_{Y_{02}} = -\frac{1}{2},$$

$$a_{0,2k,0}^\Omega = \frac{27}{64} N^2 k, \quad (6.49)$$

and the same holds for the orientifold of $L^{2p,2k-2p,2p}/\mathbb{Z}_2$ and $L^{k,k,k}/\mathbb{Z}_2$, as they only differ by fields with $r = 0$. Since the quiver is the same and these fields enter in conjugate pairs, 't Hooft anomalies and superconformal index match along the chain of quadratic marginal deformation.

6.4 Family \mathcal{B}

As already anticipated in section 6.2, the second family of conformally dual models that we consider are orientifolds of the chiral \mathbb{Z}_2 orbifolds of $L^{a,b,a}/\mathbb{Z}_2$ (with fixed $a + b = 2k$) that give rise to four real gauge groups. As shown in Fig. 6.20, for $a \neq b$ (and again both a and b even) the orientifold projection is realized on the five-brane diagram by means of fixed points that are shifted horizontally by a quarter of a period with respect to the case of family \mathcal{A} , while for $a = b$ the projection is realized by means of fixed lines. The resulting quiver is drawn in Fig. 6.29, where as in the previous case the colored fields have unit R -charge and they are progressively integrated out along the chain.

Again, the results are based on the computation and comparison of the central charges, that we denote as $a_{a,b,a}^\Omega$ as in the previous section.¹¹ We will discuss in more detail the

¹¹Given that these models are not compared to the models in the previous sections, we assume that this will not cause any confusion to the reader.

$k = 1$ and $k = 2$ cases, showing that the central charges of the orientifolds of $L^{0,2,0}/\mathbb{Z}_2$ and $L^{1,1,1}/\mathbb{Z}_2$ coincide. The analysis reveals a direct analogy with the models in family \mathcal{A} , and as a consequence the generalization to any k will be given with fewer details.

6.4.1 Orbifold with $k = 1$

Orientifold projection of $L^{0,2,0}/\mathbb{Z}_2$ with fixed points

We draw in Fig. 6.30 the toric diagram of the parent $L^{0,2,0}/\mathbb{Z}_2$ theory, the five-brane diagram with the location of the fixed points and the resulting quiver. Imposing that the superpotential has R -charge 2 gives the constraints

$$\begin{aligned} r_{03} + r_{01} + r_{13} &= -1 \\ r_{03} + r_{02} + r_{23} &= -1 \\ r_{12} + r_{01} + r_{02} &= -1 \\ r_{12} + r_{13} + r_{23} &= -1. \end{aligned} \tag{6.50}$$

We assign the same τ 's and the same ranks on the groups 0 and 1 and the groups 2 and 3 respectively, so that the quiver possesses a \mathbb{Z}_2 symmetry under flip with respect to a horizontal axis, which implies that $r_{02} = r_{13}$ and $r_{03} = r_{12}$. As a consequence, Eqs. (6.50) are reduced to two independent equations implying $r_{01} = r_{23}$, and plugging this into the condition that the β -function vanishes for each gauge group gives

$$r_{01} = \frac{N_2 - N_0 + 2\tau_0}{N_0 - N_2} = \frac{N_2 - N_0 - 2\tau_2}{N_0 - N_2}. \tag{6.51}$$

This condition clearly imposes $\tau_0 = -\tau_2$, and we can set $\tau_0 = 1$ to get the groups in Fig. 6.30. If we also assign the ranks as in the figure,¹² Eq. (6.51) gives $r_{01} = 0$. Therefore the fields X_{01} and X_{23} have R -charge equal to 1, and maximizing the a central charge one can show that the other R -charges are all equal to $\frac{1}{2}$, which can also be more directly deduced observing that the quiver has an additional symmetry under flip of the nodes 2 and 3. The value of the central charge at large N is

$$a_{0,2,0}^\Omega = \frac{27}{64} N^2. \tag{6.52}$$

As an aside, we observe that once again there is a different assignment of the ranks of the gauge groups, namely $N_2 = N_0 - 3$, which results in a conformal field theory with all R -charges equal to $\frac{2}{3}$, and central charge equal to $\frac{1}{2}N^2$. This corresponds to two $SO(N)$ and two $USp(N - 3)$ gauge groups.¹³ The occurrence of these orientifolds is a feature of all $L^{0,2k,0}/\mathbb{Z}_2$ models.

¹²This implies that N must be even.

¹³Obviously N must be odd in this case.

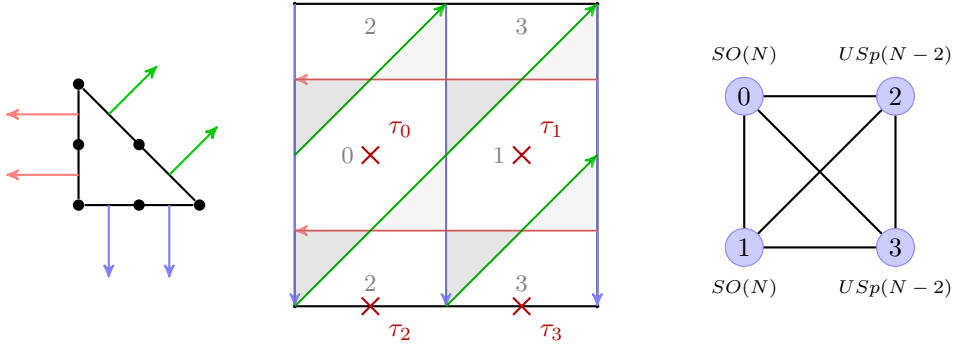


Figure 6.30 The model $L^{0,2,0}/\mathbb{Z}_2$. On the left the toric diagram is drawn, at the center the five-brane and its orientifold projection with fixed points, on the right the quiver resulting from the orientifold projection.

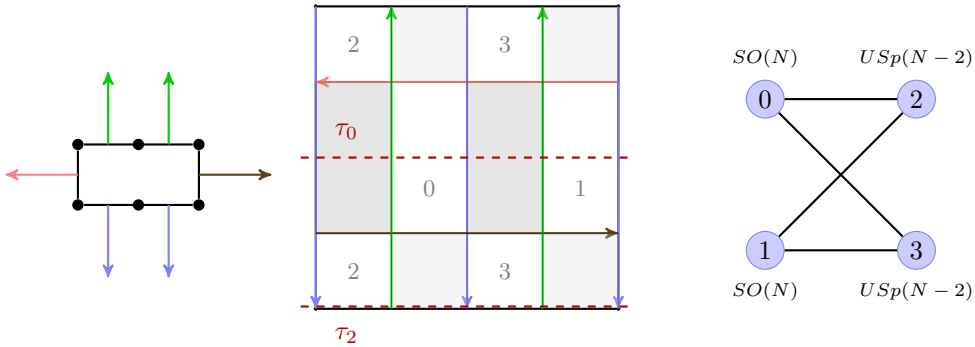


Figure 6.31 The model $L^{1,1,1}/\mathbb{Z}_2$. On the left the toric diagram is drawn, at the center the five-brane and its orientifold with fixed lines, on the right the quiver resulting from the orientifold projection.

Orientifold projection of $L^{1,1,1}/\mathbb{Z}_2$ with fixed lines

The second and last orientifold in the $k = 1$ chain is the $L^{1,1,1}/\mathbb{Z}_2$ orientifold described in Fig. 6.31. This theory has a quartic superpotential which leads to the constraints

$$\begin{aligned}
 r_{02} + r_{12} &= -1 \\
 r_{03} + r_{13} &= -1 \\
 r_{03} + r_{02} &= -1 \\
 r_{13} + r_{12} &= -1,
 \end{aligned}
 \tag{6.53}$$

and substituting them in the β -function conditions implies the τ 's and the rank assignment that can be read from the quiver. Imposing a -maximization one can show that the R charges must all be equal to $\frac{1}{2}$, as one could also easily deduce by symmetry arguments. This results in a central charge identical to the one in Eq. (6.52).

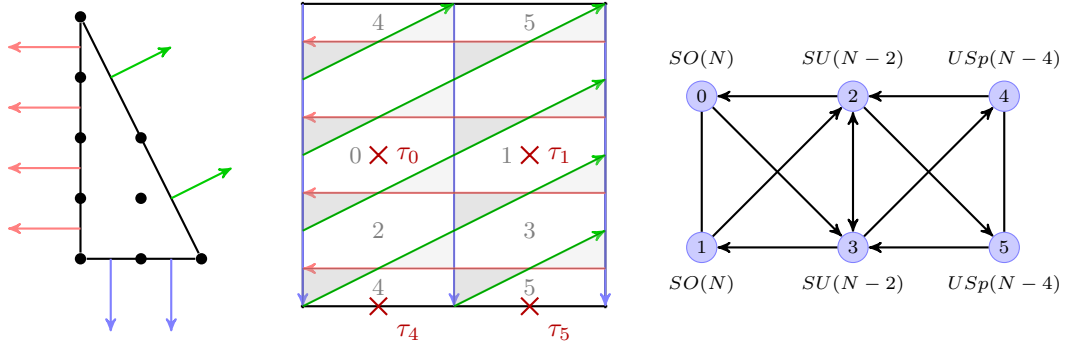


Figure 6.32 The model $L^{0,4,0}/\mathbb{Z}_2$. On the left the toric diagram is drawn, at the center the five-brane and its orientifold projection with fixed points, on the right the quiver resulting from the orientifold projection.

6.4.2 Orbifold with $k = 2$

Orientifold projection of $L^{0,4,0}/\mathbb{Z}_2$ with fixed points

The next model we consider is the $L^{0,4,0}/\mathbb{Z}_2$ orientifold, whose five-brane diagram and quiver, together with the toric diagram of the parent theory, are drawn in Fig. 6.32. We assign the same rank to the groups 0 and 1, 2 and 3 and 4 and 5, and we also require $\tau_0 = \tau_1$ and $\tau_4 = \tau_5$. Again, this implies a symmetry under flip with respect to an horizontal axis. Imposing that the superpotential has R -charge 2 then implies $r_{01} = r_{23} = r_{45}$, and requiring that the β -functions vanish gives

$$r_{01} = \frac{N_2 - N_0 + 2\tau_0}{N_0 - N_2} = \frac{N_4 - N_2 - 2\tau_4}{N_2 - N_4} \tag{6.54}$$

together with the further condition on the ranks

$$N_2 = \frac{N_0 + N_4}{2} . \tag{6.55}$$

One can then immediately notice that the rank and τ assignment in the quiver in Fig. 6.32 implies that X_{01} , X_{23} and X_{45} have R -charge 1, while all the remaining fields have R -charge $\frac{1}{2}$. The value of the central charge at large N is

$$a_{0,4,0}^\Omega = \frac{27}{32} N^2 . \tag{6.56}$$

From Eqs. (6.54) and (6.55) we deduce that imposing instead that there is a shift of 3 in the ranks, i.e. $N_2 = N_0 - 3$ and $N_4 = N_2 - 3$, results in a conformal model in which all the R -charges are equal to $\frac{2}{3}$ and the central charge is equal to N^2 at large N .

Orientifold projection of $L^{2,2,2}/\mathbb{Z}_2$ with fixed lines

For the sake of completeness, we also briefly discuss the other model with $k = 2$, namely the $L^{2,2,2}/\mathbb{Z}_2$ orientifold with fixed lines. The toric diagram of the parent theory, together with the projected five-brane diagram and quiver, are given in Fig. 6.33, and as usual we

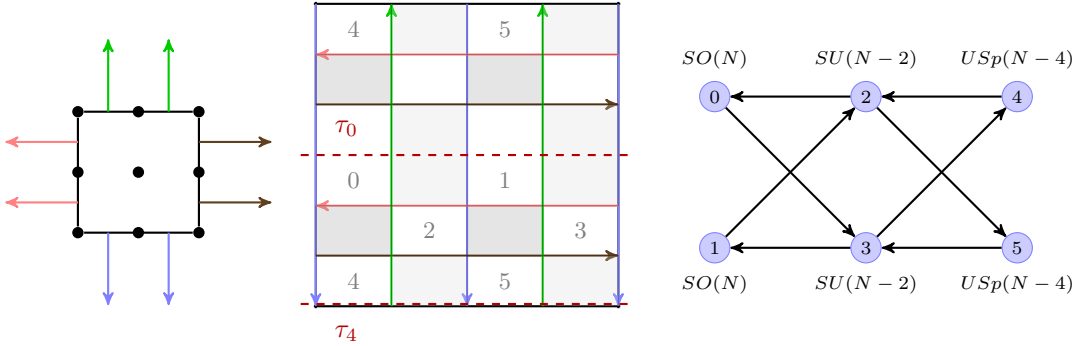


Figure 6.33 The model $L^{2,2,2}/\mathbb{Z}_2$. On the left the toric diagram is drawn, at the center the five-brane and its orientifold with fixed lines, on the right the quiver resulting from the projection.

assign the ranks so that the quiver possesses a symmetry with respect to the horizontal axis. This fully constrains the model, because imposing the relations on the R -charges coming from the superpotential and requiring that the β -functions vanish give

$$N_2 = N_0 - 2\tau_0 \quad N_2 = \frac{N_0 + N_4}{2} \quad N_4 = N_2 + 2\tau_2 . \tag{6.57}$$

From this we read that the τ 's must be opposite, and choosing for instance $\tau_0 = 1$ one gets $N_2 = N_0 - 2$ and $N_4 = N_2 - 2$, which gives precisely the groups and their corresponding ranks as in the quiver in Fig. 6.33. One can finally realize that the central charge $a_{2,2,2}^\Omega$ matches exactly, i.e. at all orders in N , the central charge in Eq. (6.56).

6.4.3 Generalization

In the following we generalize the set of constraints for the R -charges in order to find a superconformal point. Since the line of reasoning follows closely section 6.3.3, we show the generic solution in a more compact way. In this family of models the τ 's of the four fixed points project four of the $(2k + 2)$ gauge factor as $(\tau_0, \tau_1, \tau_{2k}, \tau_{2k+1})$, which must be equal in pairs as (\pm, \pm, \mp, \mp) , in order to yield the same theory of the last model in the family with fixed lines. Let us use the upper signs without loss of generality and consider $L^{0,2k,0}/\mathbb{Z}_2$. All interactions are cubic and the generic terms read

$$\pm X_{2j+2,2j} X_{2j,2j+3} X_{2j+3,2j+2} \mp X_{2j+3,2j+1} X_{2j+1,2j+2} X_{2j+2,2j+3} . \tag{6.58}$$

Using Fig. 6.29, we choose the ranks such that they are symmetric around the horizontal axis, i.e. $N_{2i} = N_{2i+1}$ with $i = 0, \dots, k$. Moreover, all fields enter iteratively in the superpotential and we call the R -charge of the fermions r_x for all horizontal fields, r_y for all diagonal ones and r_z for all vertical one. The latter are precisely the fields that are integrated out in the chain Eq. 6.12.¹⁴ Note that the choices we made corresponds to require that the non-anomalous baryonic symmetries do not contribute at the fixed

¹⁴With the choice of the orientifold of family \mathcal{B} .

point. The condition from the superpotential together with the beta functions impose

$$\begin{aligned} r_x + r_y + r_z &= -1, \\ N_{2i} - N_{2i+2} &= \frac{2}{r_z + 1}. \end{aligned} \tag{6.59}$$

We see that choosing a pattern for the ranks fixes the R -charge of the vertical fields in Fig. 6.29. For instance, with $N_{2i+2} = N_{2i} - 2$,¹⁵ $r_z = 0$ and the mechanism described in the previous sections arises, as we can integrate out the vertical fields. The crucial point is that their mass term is exactly marginal. The resulting theory is the orientifold of $L^{2p, 2k-2p, 2p}/\mathbb{Z}_2$ with quartic terms in the superpotential that give $2r_x + 2r_y = -2$. Therefore, the solution for $L^{0, 2k, 0}/\mathbb{Z}_2$ still holds.

Finally, there are $2k$ fields with fermionic R -charge r_x and $2k$ with $r_y = -1 - r_x$, so at large N the local maximum of the central charge reads

$$\begin{aligned} r_x &= -\frac{1}{2}, \\ a_{0, 2k, 0}^\Omega &= \frac{27}{64} k N^2. \end{aligned} \tag{6.60}$$

If we use instead $N_{2i+2} = N_{2i} - 3$, we find the solution where $R_X = R_Y = R_Z = 2/3$, that holds only for $L^{0, 2k, 0}/\mathbb{Z}_2$, i.e. the orbifolds of flat space, since the R -charges are not compatible with a marginal mass term.

6.5 Discussion and conclusions

In this Chapter we have generalized the mechanism studied in [9, 10] to chiral \mathbb{Z}_2 orbifolds of $L^{a, b, a}$ models. The $L^{a, b, a}$ family exhausts the class of non-chiral toric models. However there exists one (and only one) non-chiral orbifold which does not belong to this infinite class, corresponding to the $\mathbb{C}^3/(\mathbb{Z}_2 \times \mathbb{Z}_2)$ theory studied in section 6.3. We have observed that the fixed point orientifold of this theory is conformally dual to the glide orientifold of $L^{2, 2, 2}$, corresponding to the non-chiral \mathbb{Z}_2 orbifold of the conifold (i.e. $L^{1, 1, 1}/\mathbb{Z}_2$). The presence of the glide orientifold is the key ingredient that has allowed us to generalize the above construction to an infinite family of dualities analogous to the case of $L^{a, b, a}$ studied in [9, 10]. We explicitly verified that this is not possible for the $L^{a, b, a}$ non-chiral theories studied in [9, 10], so the additional \mathbb{Z}_2 orbifold is a necessary condition for the new infinite family to exist.

With the exception of the “seed” duality between the non-chiral $\mathbb{C}^3/(\mathbb{Z}_2 \times \mathbb{Z}_2)$ orbifold and $L^{1, 1, 1}/\mathbb{Z}_2$, this generalization involves chiral models such as $\mathbb{C}^3/(\mathbb{Z}_2 \times \mathbb{Z}_{2k}) = L^{0, 2k, 0}/\mathbb{Z}_2$ and $L^{k, k, k}/\mathbb{Z}_2$. For $k \geq 2$ we have observed the presence of intermediate models $L^{2p, 2k-2p, 2p}/\mathbb{Z}_2$ with fixed point projections. They altogether form a family of dual projected models that we named family \mathcal{A} in section 6.3. The field theory interpretation of the duality is the presence of an exactly marginal quadratic deformation. In the $L^{a, b, a}$ case such deformation is realized by a pairing of (conjugate) two-index tensor fields with $R = 1$ [9, 10]. In the orientifolded $L^{a, b, a}/\mathbb{Z}_2$ chiral orbifolds studied here we have observed the possibility of realizing the quadratic deformation via a pair of conjugate bifundamentals. Note that

¹⁵Which is the choice in Fig. 6.29.

a different glide orientifold, i.e. around the other axis (see figure 6.26 for example) does not give rise to conformally dual models.

By considering a different fixed point projection of $L^{2p,2k-2p,2p}/\mathbb{Z}_2$ with $0 \leq p < \lfloor k/2 \rfloor$ we have found the existence of a second family, dubbed family \mathcal{B} in section 6.4, involving the fixed line orientifold of $L^{k,k,k}/\mathbb{Z}_2$. This represents a more conventional family of dualities from the perspective of [9, 10] since it does not involve a glide orientifold.

Another difference between family \mathcal{A} and \mathcal{B} is that in the former all gauge group ranks are equal, whereas in the latter the ranks are assigned in a way that resembles what done in the non-chiral cases of [9, 10]. Moreover, in the orientifold models of [9, 10] there is always an $\mathcal{N} = 2$ mother theory with the same choice of the ranks that flows, upon adding a relevant deformation, to the $\mathcal{N} = 1$ models. This is the reason why those dual models inherit part of the action of S -duality. We have not been able to identify the mother counterpart for the theories studied here, neither the origin of their duality. However, in both families \mathcal{A} and \mathcal{B} , the extremal case $L^{0,2k,0}/\mathbb{Z}_2$ has always a different rank assignment such that $R = 2/3$ for all fields and all β -functions vanish. This choice has two interesting features. First, it is always a shift by one unit w.r.t the rank choice that yields the conformal duality discussed here. It is unclear if this can be understood in terms of fractional branes present in the system, and if there exists any relevant deformation that connects to the conformally dual models. Second, its central charge is always $27/32$ times smaller than the central charge of the conformally dual theories, which usually happens when supersymmetry is broken via mass deformation from $\mathcal{N} = 2$ to $\mathcal{N} = 1$ [146]. Clearly, this is not the case here, but an explanation is that the Cartan of $SU(2)_R$ survives the extra orbifold \mathbb{Z}_2 and enters in the combination with the $U(1)_R$ as in [146].

In all orientifold models studied so far, both here and in [9, 10], there are empirical rules at the level of toric diagrams which are necessary but not sufficient to have a conformal duality, namely that the numbers of internal and external points are separately equal and that all internal points sit on a line. The geometric deformation that allow us to pass from a toric diagram to another with these rules is associated to the quadratic deformation on the field theory side, which integrates out fields with $R = 1$.

Another pair of toric quiver gauge theories describing different singularities before the orientifold projection but that give rise to a pair of chiral models on the same conformal manifold has been obtained in [12], relating a fixed line projection of PdP_{3b} to a fixed point projection of PdP_{3c} . In this case there is no notion of geometric deformation, i.e. the possibility of deforming the superpotential by an exactly marginal massive chiral operator. Even though PdP_{3c} is actually $L^{1,2,1}/\mathbb{Z}_2$, it does not belong to any of the families studied here, because the sum $a + b$ is odd. Nevertheless the model of [12] behaves as the models studied here from the toric perspective, i.e. the toric diagrams in the two phases have separately the same number of internal and external points. For this reason, the models of [12] represent a seed for another infinite family of dual orientifold models. In a forthcoming publication we are planning to show the generalization of this model, similarly to the cases discussed here.

Finally, let us discuss some interesting avenues of future investigation. A possible generalizations involve orientifolds in presence of extra flavors. In [149] different projections of the same orbifold result in dual unoriented theories. One may also ask if dualities similar to the ones studied here exist in lower or higher dimensional SCFTs. In lower dimensions it would also be interesting to apply the orientifold projections, denoted as $Spin(7)$ orientifolds in [150, 151], which break holomorphy while preserving some su-

persymmetry.

Another aspect that we would like to stress is that differently from the pure $L^{a,b,a}$ cases, where four families have been identified [10], here for the chiral $L^{a,b,a}/\mathbb{Z}_2$ orbifolds we only found two families giving rise to a conformal duality. The two missing families correspond to the S-dual quivers studied in [10]. Here, by inspection, we have not found the generalization of models with both real gauge groups and tensor matter. If they do not exist, we would like to understand why.

It would be desirable to have a geometric interpretation of the conformal duality from the perspective of the 10d string setup and/or the holographic dual. For instance for the conformal dualities of non-chiral $L^{a,b,a}$ models one can understand them as being inherited from S-duality of the $\mathcal{N} = 2$ parent theories. (See [10, Sec. 4.2].) The latter are engineered as type IIA elliptic models of D4's, NS5's and O6-planes, where by tilting some of the NS5-branes (or the O6-planes) one can halve supersymmetry. In turn, by lifting the $\mathcal{N} = 2$ models to M-theory one can understand S-duality relating two type IIA configurations as two different classical degenerations of the M-theory torus [3]. Having at hand a similar picture for the $\mathcal{N} = 1$ dualities studied here would clarify their string theory origin. A possible starting point is the conformal duality between one of the fixed point orientifolds of $\mathbb{C}^3/\mathbb{Z}_2$ and the fixed line orientifold of $L^{1,1,1}$, i.e. the conifold. For the latter, both type IIB and IIA (elliptic) configurations have been constructed in [144] without relying on the brane tiling technology. One would then need to construct the type IIA engineering of the former, and lift the two IIA setups to M-theory to try to understand the addition of the exactly marginal quadratic deformation in field theory (responsible for the $\mathcal{N} = 1$ conformal duality) via a chain of string dualities.

Lastly, another promising piece of geometric technology is K-stability [152, 153] of the SCFT [154, 155, 156, 157, 158, 159, 160], which can be understood as a criterion to check whether the SCFT is stable in the IR against certain deformations of its superpotential, captured by the chiral ring. In favorable situations (such as for toric theories, but also for classes of non-toric ones) these deformations can be classified, and are related to complex deformations of the hypersurface singularity probed by the N D3-branes. It would be interesting to study whether the conformal dualities of this paper admit an interpretation in terms of deformations of the chiral ring of the SCFTs.

Multi-planarizable quivers, orientifolds, and conformal dualities

In this Chapter we study further instances of conformally dual theories obtained from Type IIB string theory setups in the presence of orientifolds. The examples worked out in [9, 10, 11] and reviewed in Chapter 5 and 6, corresponding to orientifolds of L^{aba} and L^{aba}/\mathbb{Z}_2 , provide examples of conformally dual theories engineered in string theories. The parent models (i.e. before the orientifold projection) describe stacks of D3-branes probing different Calabi–Yau threefolds (CY₃'s) and, only after the projection and for suitable choices of ranks, the models have the same conformal and 't Hooft anomalies and superconformal indices. The claim is that the models are also conformally dual and the marginal deformations that relate them are associated to quadratic superpotential deformations.¹ Then, by integrating out such *conformal masses*, the final models become identical.

Another similar behavior was anticipated in [12]. In this case the two models before the projection are associated to D3-branes probing two different singularities, namely (cones over) the pseudo del Pezzo surfaces PdP_{3b} and PdP_{3c}. After a fixed-line and fixed-point projection respectively, again with a suitable choice of ranks, it turns out that the two models have the same quiver structure, field content, anomalies and index. These models differ only by the superpotential interactions, i.e. they differ only by the point on the conformal manifold that they describe, or equivalently there is an exactly marginal deformation connecting them. This notion of conformal duality between these two models generalizes the one found for the L^{aba} and L^{aba}/\mathbb{Z}_2 orientifolds discussed in [9, 10, 11] (see Chapters 5 and 6), even though in the former there is not any (explicit) *conformal mass* connecting the two theories.

Motivated by this example, in this Chapter we look for a generalization of this behavior for infinite families of toric quiver gauge theories. We note that the crucial property at the core of the relation between PdP_{3b} and PdP_{3c} is that the two models can be represented with the same quiver even before the orientifold projection. The quiver admits two different planarizations, corresponding to the two inequivalent toric descriptions. We then look for families of quivers admitting multiple planarizations, referring to quivers of such type as *multi-planarizable*. We find an infinite family of models of such type: toric diagrams described by three parallel lines connecting the integer point lattices, two on

¹Note that these mass terms are relevant in the parent theories [125, 121], but become marginal after the orientifold projection.

the perimeter and a central one (see Fig. 7.9). We observe that there always exist coincident quivers (in some Seiberg/toric dual phase) associated to different toric diagrams in this family. The recipe to obtain such quivers corresponds to moving one or more lattice points from one external line to the other.

We then study orientifold projections of these models, and by inspection we identify a subfamily that generalizes the construction discussed above for PdP_{3b} and PdP_{3c} . This subfamily corresponds to the case where there is an even number of points on the perimeter.

We show that after the orientifold (by fixed lines or fixed points, depending on the toric diagram) the models differ only by exactly marginal deformations. Furthermore we observe that acting with Seiberg duality and global symmetries we can always find a phase where the difference between these models corresponds to a sign or a set of signs in some superpotential interaction.

7.1 Toy models for conformal dualities

In this section we construct pairs of $\mathcal{N} = 1$ toy models that differ only by a marginal deformation on the conformal manifold. In particular, given a unique quiver we turn on different interaction terms such that the models are not the same. We begin with SQCD in the conformal window, and introduce singlets and interactions so that the global symmetry contains (at least) an $SU(2)$ factor. Turning on further interactions breaks this $SU(2)$ and yields different models. We find a behavior that resembles β -deformations in $\mathcal{N} = 4$ SYM [122], as the models differ only by a sign flip in a subset of terms.

We exhibit examples with unitary and real gauge factors, which will be embedded in string models in later sections.

7.1.1 SQCD with singlets

The simplest toy model in which the mechanism of conformal duality described above can be found is SQCD with a single unitary gauge group $SU(N)$ and F flavors. We can break the flavor group $SU(F)$ in different patterns, by introducing singlets and turning on interactions. Let us start from the quiver drawn in Fig. 7.1a with F quarks q , F anti-quarks \tilde{q} and no interaction, and choose F such that the theory stays inside the conformal window, i.e. $F = 2N$. Now break the non-abelian global symmetry from $SU(F) \times SU(F)$ into the pattern in Fig. 7.1b, $SU(F_1) \times SU(F_2) \times SU(G_1) \times SU(G_2)$ with $F_1 + F_2 = G_1 + G_2 = F$. The quarks q_1, q_2 transform under $SU(F_1) \times SU(F_2)$, whereas the anti-quarks \tilde{q}_1 and \tilde{q}_2 under $SU(G_1) \times SU(G_2)$. Note that with no gauge singlets and $W = 0$ the non-abelian global symmetry of this quiver is actually enhanced back to $SU(F) \times SU(F)$. In order to effectively break the flavor, we introduce gauge singlets M_{11}, M_{12}, M_{21} and M_{22} , which interact with the quarks via a cubic superpotential. Denoting the color indices with a and flavor indices with f_ℓ, g_j ($\ell, j = 1, 2$), we can write

$$W = h_{\ell j} (M_{\ell j})_{f_j}{}^{g_\ell} (\tilde{q}_\ell)_{g_\ell}{}^a (q_j)_a{}^{f_j}, \quad (7.1)$$

so that we can control the actual global symmetry by turning on subsets of $h_{\ell j}$ and imposing conditions on the ranks of the flavor groups. Henceforth we will omit color and flavor indices for clarity. For instance, the theory with only $h_{11} \neq 0$ and $h_{12} = h_{21} =$

$h_{22} = 0$ has superpotential given by

$$W = h_{11} M_{11} \tilde{q}_1 q_1, \quad (7.2)$$

and if we require further that $F_1 = G_1$ and $F_2 = G_2$, we obtain the quiver of Fig. 7.1c. This model is studied in [161], where it is shown that it is dual to the case with $h_{11} = 0$ and $h_{12}, h_{21}, h_{22} \neq 0$ with a bifundamental singlet, an adjoint singlet on the second node and the same requirement for the ranks of the flavor groups.

An interesting case is the one given by $h_{11}, h_{22} \neq 0$ and $h_{12} = h_{21} = 0$, thus the interaction has the form

$$W = h_{11} M_{11} \tilde{q}_1 q_1 + h_{22} M_{22} \tilde{q}_2 q_2, \quad (7.3)$$

where two out of four couplings are non-zero. Requiring that $G_1 = G_2, F_1 = F_2$ and identifying singlets $M_{11} = M_{22} = M$ and couplings $h_{11} = h_{22} = h$, the resulting quiver is drawn in Fig. 7.1d and the superpotential simplifies to

$$W = h M \tilde{q}_1 q_1 + h M \tilde{q}_2 q_2. \quad (7.4)$$

Note that we can rotate the quarks q_1, q_2 and the anti-quarks \tilde{q}_1, \tilde{q}_2 , signaling an $SU(2) \times SU(2)$ global symmetry that emerges only under the required condition. Rotating both quarks and anti-quarks gives the same superpotential, while rotating only one species is equivalent to choosing h_{12}, h_{21} to be non-zero and the diagonal terms to be zero.

The final case has $h_{\ell j} \neq 0 \forall \ell, j$. We can require that either $F_1 = F_2, G_1 = G_2$ so that there are four bifundamental singlets, or $F_1 = G_1, F_2 = G_2$ resulting in two conjugated bifundamental singlets and one adjoint singlets at each node [161].

All patterns of global symmetry breaking discussed above are summarized in Tab. 7.1.

Couplings	Superpotential	Global Symmetry
$h_{ij} = 0$	$W = 0$	$SU(F) \times SU(F)$, Fig. 7.1a
$h_{11} \neq 0$	$W = h_{11} M_{11} \tilde{q}_1 q_1$	$SU(F_1)^2 \times SU(F_2)^2$, Fig. 7.1c
$h_{11} = h_{22} = h \neq 0$	$W = h M (\tilde{q}_1 q_1 + \tilde{q}_2 q_2)$	$SU(F_1) \times SU(G_1 = F_1) \times SU(2)^2$, Fig. 7.1d
$h_{\ell j} \neq 0$	$W = h_{\ell j} M_{\ell j} \tilde{q}_\ell q_j$	$SU(F_1) \times SU(F_2) \times$ $SU(G_1) \times SU(G_2)$, Fig. 7.1b

Table 7.1 The various patterns for breaking the global symmetry $SU(F) \times SU(F)$ of SQCD introducing four singlets $M_{\ell j}$ and four couplings $h_{\ell j}, \ell, j = 1, 2$, referring to Fig. 7.1b with $F_1 + F_2 = F = G_1 + G_2$.

Consider now the case with two couplings turned on, either $h_{11} = h_{22} = h \neq 0$ or $h_{12} = h_{21} = h \neq 0$. In particular, from the quiver in Fig. 7.1d we focus on two models, obtained by turning on the first pair or the second one. Denoting them as model *A* and *B* respectively, their superpotentials read

$$\begin{aligned} W_A &= h M (\tilde{q}_1 q_1 + \tilde{q}_2 q_2), \\ W_B &= h M (\tilde{q}_1 q_2 + \tilde{q}_2 q_1). \end{aligned} \quad (7.5)$$

As mentioned above, we can move from one model to the other by rotating the pairs of quarks, thanks to the $SU(2)$ global symmetry. It is useful for later purposes to change basis for the quarks as

$$\begin{aligned} q_1 &\rightarrow (Q_+ + Q_-) , \\ q_2 &\rightarrow (Q_+ - Q_-) , \end{aligned}$$

so that the superpotentials in the two models become

$$\begin{aligned} W_A &\rightarrow h M [\tilde{q}_1(Q_+ + Q_-) + \tilde{q}_2(Q_+ - Q_-)] , \\ W_B &\rightarrow h M [\tilde{q}_1(Q_+ - Q_-) + \tilde{q}_2(Q_+ + Q_-)] , \end{aligned} \quad (7.6)$$

and we can redefine the field $Q_- \rightarrow -Q_-$ in W_A so that the two interactions match. We add further flavors to this construction, in order to turn on additional interactions. In Fig. 7.1d, add e.g. $SU(F_3)^2 \times SU(G_3)^2$, bifundamental matter fields p, \tilde{p} , bifundamental singlets $l, r, f_1, f_2, \tilde{f}_1, \tilde{f}_2$ landing us onto the model in Fig. 7.2. Note that the ranks of the flavor groups must be chosen such that $2F_1 + F_3 = 2G_1 + G_3$ for the theory to be free of gauge anomalies. Another interaction can be turned in both model A and B , namely

$$W_\lambda = \lambda pl\tilde{q}_1 + \lambda r\tilde{p}q_1 + \lambda \tilde{q}_2 p f_1 f_2 + \lambda \tilde{p} q_2 \tilde{f}_2 \tilde{f}_1 , \quad (7.7)$$

where λ is the coupling.² This interaction breaks the $SU(2)$ global symmetry, as we cannot rotate the quarks anymore. In the basis chosen earlier, we have

$$\begin{aligned} W_A + W_\lambda &\rightarrow hM [\tilde{q}_1(Q_+ + Q_-) + \tilde{q}_2(Q_+ - Q_-)] \\ &\quad + \lambda pl\tilde{q}_1 + \lambda r\tilde{p}(Q_+ + Q_-) + \lambda \tilde{q}_2 p f_1 f_2 + \tilde{p}(Q_+ - Q_-) \tilde{f}_2 \tilde{f}_1 , \\ W_B + W_\lambda &\rightarrow hM [\tilde{q}_1(Q_+ - Q_-) + \tilde{q}_2(Q_+ + Q_-)] \\ &\quad + \lambda pl\tilde{q}_1 + \lambda r\tilde{p}(Q_+ + Q_-) + \lambda \tilde{q}_2 p f_1 f_2 + \tilde{p}(Q_+ - Q_-) \tilde{f}_2 \tilde{f}_1 , \end{aligned} \quad (7.8)$$

and, if we proceed as before, the additional transformation $Q_- \rightarrow -Q_-$ does not send one model into the other. The new interaction is crucial as there is no field redefinition that transforms the two superpotentials into the same form. However, the two models preserve the same global symmetry. In particular, the constraints for the R -charges are compatible and if a conformal point exists for one model, the same happens for the other, where one of the couplings has acquired a minus sign. As long as the ranks of the gauge group and of the flavor groups are chosen such that the β -functions vanish, we expect that they live on the same conformal manifold.

In order to see that, let us choose the ranks of the flavour groups as

$$\begin{aligned} G_1 &= N + 2 , & F_3 &= N + 4 , \\ F_1 &= N - 2 , & G_3 &= N - 4 , \end{aligned} \quad (7.9)$$

and let us turn on the interaction terms one by one, following the flow at every step.

²In principle, there may be two different couplings, $\lambda_{(3)}$ for cubic terms and $\lambda_{(4)}$ for quartic, and the argument still holds. We pick $\lambda_{(3)} = \lambda_{(4)} = \lambda$ for the sake of brevity.

When $W = 0$ all of the fields are free, i.e. $R = 2/3$, the central charge is $a = 11/24$ and the cubic interaction W_A is marginal, while the quartic operators in W_λ are irrelevant. Requesting that the β -functions of all the couplings vanish leads to a new conformal fixed point, whose central charge a has decreased to $a \simeq 0.305$. The R -charges of gauge-invariant operators stay above the unitarity bound, so no accidental symmetries are generated along the flow. The story is repeated exactly with W_B , and both $W_A + W_\lambda$ and $W_B + W_\lambda$ have the same central charge. At this conformal point, the non-anomalous global symmetry of the two models match as well, with the same charges for the matter fields, see Tab. 7.2 and therefore the 't Hooft anomalies match. One can see that W_B (W_A) is classically marginal at the fixed point of model A (B). Furthermore, from Tab. 7.2, we can see that W_B (W_A) is not charged under any of the global symmetries, hence it is exactly marginal [16] for the model A (B). This identifies a direction on the conformal manifold along which we can move from one model to the other by turning on exactly marginal operators.

	q_1	q_2	\tilde{q}_1	\tilde{q}_2	M	p	\tilde{p}	l	r	f_1	f_2	\tilde{f}_1	\tilde{f}_2
$U(1)_B$	1	1	-1	-1	0	1	-1	0	0	0	0	0	0
$U(1)_1$	1	1	0	0	-1	$-\frac{1}{2}$	$-\frac{3}{2}$	$\frac{1}{2}$	$\frac{1}{2}$	0	$\frac{1}{2}$	0	$\frac{1}{2}$
$U(1)_2$	2	2	-1	-1	-1	$\frac{1}{2}$	$-\frac{5}{2}$	$\frac{1}{2}$	$\frac{1}{2}$	1	$-\frac{1}{2}$	1	$-\frac{1}{2}$
$U(1)_3$	0	0	0	0	0	0	0	0	0	1	-1	1	-1

Table 7.2 The global symmetry charges for the matter fields, both for $W_A + W_\lambda$ and for $W_B + W_\lambda$.

Furthermore, we shall see that the quiver in Fig. 7.2 can be embedded in a dimer construction, where one can read off the low-energy gauge theory associated to a particular toric singularity. To be more precise, the flavor factors would be gauged and further interactions arise, since each field must appear twice in the superpotential with opposite sign,³ as a consequence of the strong constraints given by the toric condition. We notice that in each case considered below, any pairs of superpotentials of conformally dual models, obtained along these lines, do not admit any field redefinitions transforming one into another.

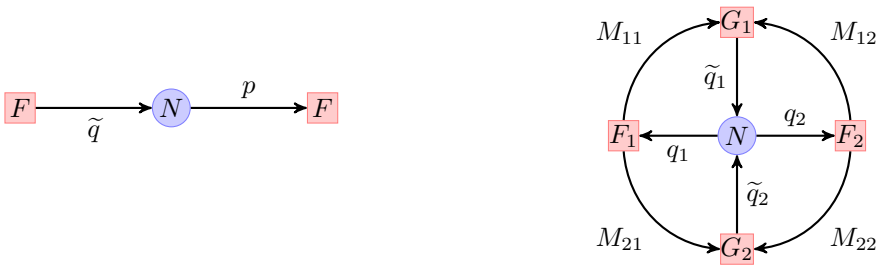
7.1.2 Real gauge groups

The previous mechanism of conformal duality can occur also in the case of a real gauge group. In order to see that, consider a single gauge group, either $SO(N)$ or $USp(N)$,⁴ with $2F$ flavors and a singlet in a tensor representation of the flavor group $SU(F)$. Let us choose the tensor to be symmetric for orthogonal gauge groups and antisymmetric for symplectic ones. The quiver associated to this theory is drawn in Fig. 7.4a,⁵ where q_1 and q_2 are the fundamental flavors, T is the tensor, and the real group is drawn as a diamond (see Fig. 7.3 for a legend about our notation for quivers.). We can turn on two

³This can be accounted for by inserting a factor $(-1)^{\ell+1}$ in front of the superpotential in Eq. (7.1) and the subsequent ones.

⁴In our convention $USp(2) \cong SU(2)$, hence in $USp(N)$ N is even.

⁵Even though the gauge group is real, we keep drawing arrows for the bifundamental matter fields to show the chirality under $SU(F)$.



(a) The quiver for SQCD with gauge group $SU(N)$, non-abelian global symmetry $SU(F) \times SU(F)$ and $W = 0$.

(b) The quiver for SQCD with gauge group $SU(N)$, non-abelian global symmetry $SU(F_1) \times SU(F_2) \times SU(G_1) \times SU(G_2)$, with $F_1 + F_2 = F = G_1 + G_2$, singlets M_{ij} and $W = h_{ij} M_{ij} \tilde{q}_i q_j$.



(c) The quiver for SQCD with gauge group $SU(N)$, global symmetry $SU(F_1)^2 \times SU(F_2)^2$, adjoint singlet M_{11} and interaction $W = h_{11} M_{11} \tilde{q}_1 q_1$.

(d) The quiver for SQCD with gauge group $SU(N)$, non-abelian global symmetry $SU(F_1) \times SU(G_1 = F_1) \times SU(2)^2$, bi-fundamental singlet $M_{11} = M_{22} = M$ and interaction $W = hM(\tilde{q}_1 q_1 + \tilde{q}_2 q_2)$.

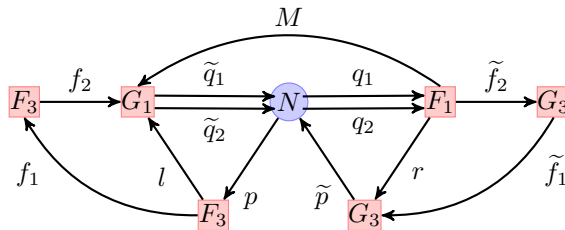


Figure 7.2 The quiver for SQCD with singlets with gauge group $SU(N)$ and non-abelian global symmetry $SU(F_1) \times SU(G_1) \times SU(F_3)^2 \times SU(G_3)^2$.

$$\begin{array}{ccc}
\textcircled{N} \text{ gauge } SU(N) & & \textcircled{N} \text{ gauge } SO/USp(N) \\
\\
\textcolor{red}{\square} F \text{ flavor } SU(F) & &
\end{array}$$

Figure 7.3 The notation we use for quivers: a blue circle for a $SU(N)$ gauge factor, a blue diamond for a $SO(N)$ or $USp(N)$ gauge factor and a red square for a flavor factor.

interaction terms

$$W_A = h \frac{1}{2} T(q_1^2 + q_2^2), \quad (7.10)$$

$$W_B = h T q_1 q_2, \quad (7.11)$$

where h is the coupling, and we refer to the theory with W_A (W_B) turned on as model A (B). The constraints for the R -charges given by these interactions are compatible with each other. Redefine the fields as

$$\begin{aligned}
q_1 &\rightarrow \frac{1}{\sqrt{2}} (Q_+ + Q_-), \\
q_2 &\rightarrow \frac{1}{\sqrt{2}} (Q_+ - Q_-),
\end{aligned} \quad (7.12)$$

so that the interaction terms become

$$\begin{aligned}
W_A &= h \frac{1}{2} T(q_1^2 + q_2^2) \rightarrow \frac{1}{2} T(Q_+^2 + Q_-^2), \\
W_B &= h T(q_1 q_2) \rightarrow \frac{1}{2} T(Q_+^2 - Q_-^2),
\end{aligned} \quad (7.13)$$

and they differ only by a relative sign. As before, we can still perform a second transformation on W_A that acts as $Q_- \rightarrow iQ_-$ and the two theories end up having the same interaction. Hence, they are equivalent and we can move from one to the other with simple field redefinitions, similarly to the previous case.

Let us add two flavour groups and four bifundamental fields, w, v, f_1 and f_2 as in Fig. 7.4b. We can turn on an additional interaction in both models, as

$$W_\lambda = \lambda q_1 w v - \lambda q_2 w v + \lambda q_1 w f_1 f_2 + \lambda q_2 w f_1 f_2, \quad (7.14)$$

so that model A has superpotential $W_A + W_\lambda$ and model B has $W_B + W_\lambda$. We note that the constraints for the R -charges are compatible, similarly as before, and we ask whether the two theories are equivalent. If we perform again the two transformations, i.e. Eq. (7.12)

for both models and subsequently $Q_- \rightarrow iQ_-$ for model A , we obtain

$$\begin{aligned}
 W_A + W_\lambda &\rightarrow h \frac{1}{2} T (Q_+^2 - Q_-^2) + \lambda \left[\frac{1}{\sqrt{2}} (Q_+ + iQ_-) - \frac{1}{\sqrt{2}} (Q_+ - iQ_-) \right] wv \\
 &\quad + \frac{1}{\sqrt{2}} (Q_+ + iQ_-) w f_1 f_2 + \frac{1}{\sqrt{2}} (Q_+ - iQ_-) w f_1 f_2 , \\
 W_B + W_\lambda &\rightarrow h \frac{1}{2} T (Q_+^2 - Q_-^2) + \lambda \left[\frac{1}{\sqrt{2}} (Q_+ + Q_-) - \frac{1}{\sqrt{2}} (Q_+ - Q_-) \right] wv \\
 &\quad + \frac{1}{\sqrt{2}} (Q_+ + iQ_-) w f_1 f_2 + \frac{1}{\sqrt{2}} (Q_+ - iQ_-) w f_1 f_2 , \tag{7.15}
 \end{aligned}$$

and the two models are no longer trivially connected by a simple field redefinition, due to the presence of additional interactions. As before, the two theories preserve the same global symmetry, including the abelian R -symmetry and if a conformal point exists, e.g. by choosing ranks such that the β -functions vanish, it exists for both models. Let us choose the ranks as

$$F = N - 2, \quad \bar{F} = N - 4, \tag{7.16}$$

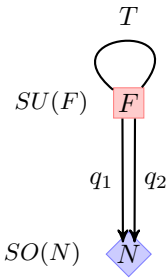
and study, as before, the dynamics of operators turning interactions one by one. With no interactions, all of the fields are free and the central charge is $a = 11/48$. Around this conformal point, the cubic operators are marginal and quartic ones are irrelevant. As in the previous section, it exists a consistent conformal point in the IR where the β -functions for all the couplings vanish, with $a \simeq 0.153$, reached by both $W_A + W_\lambda$ and $W_B + W_\lambda$. No accidental symmetries are generated along the flow. Again, the two models share the same global symmetry and the charges match, see Tab 7.3, and W_A is exactly marginal for model B , and viceversa. As before, the two models live on the same conformal manifold, even though they they flow to different points on the conformal manifold.

	q_1	q_2	w	v	T	f_1	f_2
$U(1)_1$	1	1	-3	2	-2	0	2
$U(1)_2$	0	0	-1	1	0	1	0

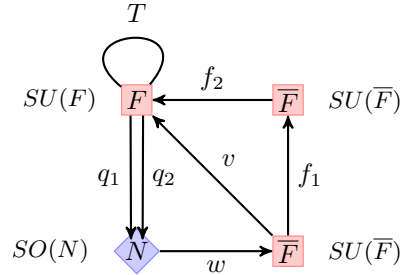
Table 7.3 The global symmetry charges for the matter fields, both for $W_A + W_\lambda$ and for $W_B + W_\lambda$.

7.1.3 Duality frames

When the models we introduced in the previous subsections are embedded in larger quivers, the resulting theory contains more gauge group factors, fields and interactions. At any rate, two models that differ only by superpotential terms of the form W_A and W_B are in fact the same theory, but if an interaction that breaks explicitly the rotation among the quarks in both models is present, then they live on the same conformal manifold, at separate points where one of the couplings (or a subset thereof) has changed sign. However, the presence of extra structure can hide the superpotential mechanism we showed earlier. While the computation of protected quantities such as anomalies and indices



(a) The quiver model with a single real gauge and global symmetry $SU(2F)$.



(b) The quiver model with a single real gauge and global symmetry $SU(F) \times SU(\bar{F})^2$.

would undoubtedly signal that the two theories end up on the same conformal manifold, it can be unclear whether they are actually the same theory or different points on the same manifold [12]. One would need to compare and map gauge-invariant operators of the models. In this regard, finding the proper duality frame can make the comparison easier.

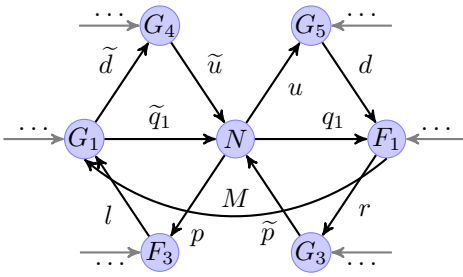
Below we will show prototypical examples that we will encounter in the rest of the Chapter. The idea is that after some duality operation, the superpotential can be brought to the form of Eqs. (7.8)-(7.15). Even though there are more gauge factors, the underlying message is the same as long as all factors lie in the conformal window. For instance, it may happen that the $SU(2)$ is not explicit, namely \tilde{q}_2 and q_2 are not present in the theory, but a composite operator will take their place. There is a Seiberg-dual frame in which this is a fundamental field of the theory and one only needs to find this dual description. A common situation occurs as follows. Suppose we have the quiver in Fig. 7.5a, part of two larger models A and B with superpotential

$$\begin{aligned}
 W_A &= h M \tilde{q}_1 q_1 + h M \tilde{d} \tilde{u} u d + \lambda p l \tilde{d} \tilde{u} + \lambda \tilde{p} u d r + \dots, \\
 W_B &= h M \tilde{q}_1 u d + h M \tilde{d} \tilde{u} q_1 + \lambda p l \tilde{d} \tilde{u} + \lambda \tilde{p} u d r + \dots,
 \end{aligned}
 \tag{7.17}$$

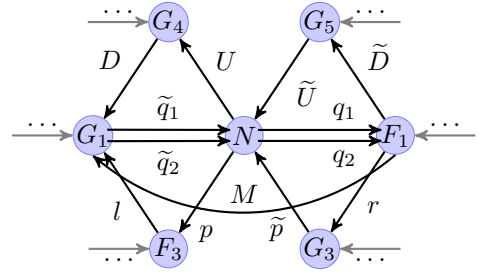
where the dots indicate the part of the superpotential that does not contain \tilde{d} , d , \tilde{u} or u and it is shared by models A and B . Note that all the nodes in the quiver are gauge factors. If we dualize both nodes G_4 and G_5 in models A and B , the dual quiver results in the one of Fig. 7.5b, where the dual quarks are $D, U, \tilde{U}, \tilde{D}$ and the mesons $ud = q_2$, $\tilde{d}\tilde{u} = \tilde{q}_2$. As there will be more fields transforming under the nodes G_4 and G_5 , more mesons will be present and other interaction terms will arise, but they do not spoil the argument. The superpotentials of the Seiberg-dual phases read

$$\begin{aligned}
 W_A &= h M \tilde{q}_1 q_1 + h M \tilde{q}_2 q_1 + \lambda p l \tilde{q}_2 + \lambda \tilde{p} q_2 r + q_2 \tilde{D} \tilde{U} + \tilde{q}_2 U D + \dots, \\
 W_B &= h M \tilde{q}_1 q_2 + h M \tilde{q}_2 q_1 + \lambda p l \tilde{q}_2 + \lambda \tilde{p} q_2 r + q_2 \tilde{D} \tilde{U} + \tilde{q}_2 U D + \dots,
 \end{aligned}
 \tag{7.18}$$

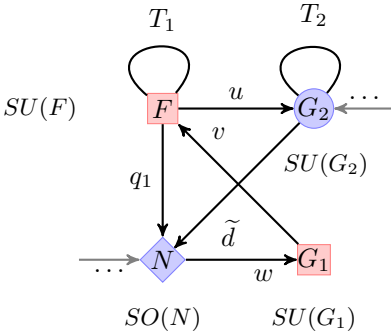
and the quarks q_i and \tilde{q}_j can be rotated as in Eq. (7.6), hence, with the proper choice of ranks such that the two theories stay inside the conformal window, they live on the same conformal manifold. Looking back at the original phase (i.e. before dualization), despite the fact that the interactions differ in the two models (a cubic and a quintic in model A ,



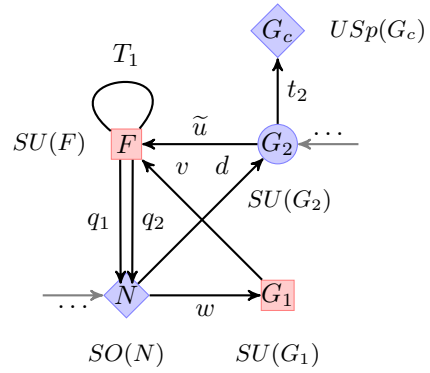
(a) Quiver for a part of a larger model. The connection to the remaining part is indicated by the dots.



(b) The quiver after dualization of nodes $SU(G_4)$ and $SU(G_5)$.



(a) The quiver with tensors, part of a larger model.



(b) The quiver with tensors, part of a larger model, where tensor T_2 has been deconfined into $(t_2)^2$ and the gauge node $SU(G_2)$ has been dualized.

and two quartic terms in model B), the two models flow to the same conformal manifold.

It may also happen that we need to dualize only one model, if the interaction in the other one is already in the form of Eq. (7.18).⁶ As a consequence, we have two interesting types of conformal duality: either a pair of models with two cubic terms in A and two quartic terms in B , or a pair of models with one cubic term and one quintic term in A and two cubic terms in B .

Deconfinement of tensors

The last case of interest concerns the presence of tensor fields. Suppose we have the quiver of Fig. 7.6a, part of two larger models A and B with superpotentials

$$\begin{aligned}
 W_A &= h \frac{1}{2} T_1 \left(q_1^2 + u^2 \tilde{d}^2 \right) + \lambda w v q_1 + \dots, \\
 W_B &= h T_1 q_1 u \tilde{d} + \lambda w v q_1 + \dots.
 \end{aligned}
 \tag{7.19}$$

⁶We need to be careful that the new phase does not exhibit any global symmetry enhancement.

We may proceed as before, but we need to dualize the node with the tensor field T_2 . In order to do that, we need first to deconfine the tensor field [50, 162, 96], which is seen as the result of the confinement of a real group. At this step, we need to be careful not to add extra gauge-invariant operators, which may arise due to the presence of the confining gauge factor. In particular, when T_2 is an antisymmetric tensor of $SU(\overline{G})$ and \overline{G} is even, the confining gauge factor is symplectic⁷ and we may need to add the Pfaffian operator $W_{T_2} = \text{Pf}(T_2)$ to the superpotential, so that it is forced to vanish. However, the complete structure of the interaction may already impose this constraint, so a case-by-case analysis is actually needed.⁸

After having deconfined, we are allowed to dualize the node $SU(G_2)$, resulting in the meson $u\tilde{d} = q_2$, possibly among other composite operators that become fundamental in the dual phase. The dual theory has the quiver shown in Fig. 7.6b and the superpotentials of the two models read

$$\begin{aligned} W_A &= h \frac{1}{2} T_1 (q_1^2 + q_2^2) + \lambda w v q_1 + q_2 \tilde{D}U + \dots, \\ W_B &= h T_1 q_1 q_2 + \lambda w v q_1 + q_2 \tilde{D}U + \dots. \end{aligned} \quad (7.20)$$

We realize we are back to the models described in Sec. 7.1.2, hence the same argument holds. In this case, model A with a cubic interaction and a quintic interaction, involving a tensor field, flows to the same conformal manifold of model B with a quartic term involving a tensor field.

7.2 Gauging the flavor: PdP_{3b} vs. PdP_{3c} and their orientifolds

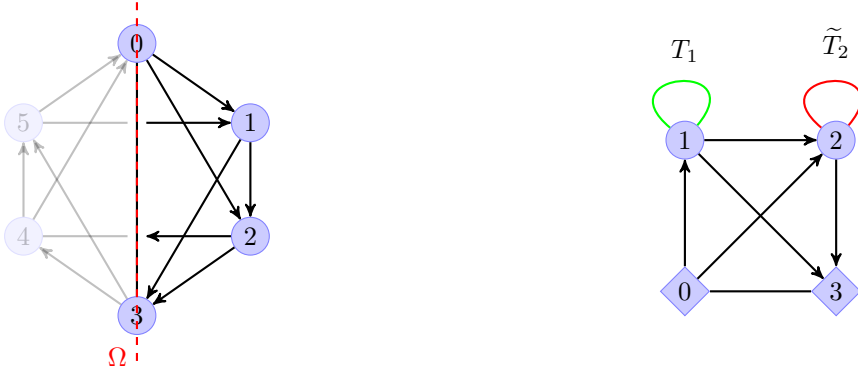
In this section we discuss gauging of global symmetries in the toy models studied above, focusing on a detailed example. On one hand, this section is a bridge that allows us to fix the notation necessary for the more general analysis of the conformal dualities for multi-planarizable quivers studied below. On the other hand we will be able to give an explanation for the results obtained in [12]. The models that we present here correspond indeed to stacks of D3-branes probing the complex cone over the pseudo del Pezzo surfaces PdP_{3b} and PdP_{3c} with appropriate orientifold projections, over specific toric phases that enjoy the \mathbb{Z}_2 needed for the projection. The final models can be constructed by gauging the global symmetries of the toy models discussed above, by further requiring the cancellation of gauge anomalies and the vanishing of the beta functions.

As observed in [12] the quivers associated to the PdP_{3b} and PdP_{3c} coincide, and are given in Fig. 7.7a. However the two models have different superpotentials. Explicitly:

$$\begin{aligned} W_b &= X_{01} X_{13} X_{30} - X_{13} X_{35} X_{51} + X_{35} X_{50} X_{03} - X_{50} X_{01} X_{12} X_{24} X_{45} \\ &+ X_{12} X_{23} X_{34} X_{45} X_{51} + X_{24} X_{40} X_{02} - X_{02} X_{23} X_{30} - X_{40} X_{03} X_{34} \end{aligned} \quad (7.21)$$

⁷In the case of a symmetric tensor, the auxiliary gauge factor that confines is orthogonal. The moduli space of such a gauge theory must be studied carefully, since the origin may not be smoothed out [18]. Whenever we need to deconfine a symmetric tensor, we restrict ourselves to the case in which the auxiliary gauge factor $SO(N+4)$ confines, generating a symmetric tensor of $SU(N)$.

⁸In this Chapter we will study cases where those operators are irrelevant.



(a) The quiver of theories PdP_{3b} and PdP_{3c} , with the orientifold represented with the dashed red line.

(b) The quiver of theories PdP_{3b} and PdP_{3c} after the orientifold projection.

and

$$\begin{aligned}
 W_c = & X_{01} X_{13} X_{30} - X_{13} X_{34} X_{45} X_{51} + X_{35} X_{50} X_{03} - X_{40} X_{01} X_{12} X_{24} \\
 & + X_{12} X_{23} X_{35} X_{51} - X_{24} X_{45} X_{50} X_{02} - X_{02} X_{23} X_{30} + X_{40} X_{03} X_{34} . \quad (7.22)
 \end{aligned}$$

This difference gives rise to two different dimers and thus two different toric diagrams. As a consequence the two models are *not* related by any IR duality.

As discussed in the introduction in this case we refer to the quiver as multi-planarizable, because there exist two inequivalent periodic planar quivers (and consequently dimers), i.e. there are two different consistent choices of toric data for the quiver in Fig. 7.7a. In absence of orientifolds this degeneration does not have further implications for the gauge theories associated to the two singularities.

The situation is more interesting if one studies orientifold projections. When orientifolds are added to the previous brane setups symplectic and orthogonal gauge groups and two index symmetric and antisymmetric representations naturally arise after the projections and the quivers become unoriented. This is a consequence of the fact that the orientifolds reverse the orientation of the strings, giving rise to a \mathbb{Z}_2 involution on the gauge theory [163, 164, 165, 166, 167, 168]. On the brane tiling these projections can be represented by the general fixed points/fixed lines procedure spelled out in [113, 169, 170] (recently also projections that involve the Klein bottle have been considered [129]). Orientifolds have many applications in various sectors, both at theoretical level [171, 172, 173, 174, 175, 176, 177, 178] and at phenomenological one [179, 180, 181, 182, 183, 184, 185].

Here we will not review the whole construction and refer the reader to [113, 170] for more details and notations. The idea is that one considers the action of the orientifold by looking at identifications on the dimer in terms of fixed points and fixed lines. The charges carried by the orientifolds reflect in consistent choices of charges associated to the fixed points and fixed lines. As discussed in [12], the non-trivial statement is that there exists a fixed-line projection on PdP_{3b} that has the same quiver as a fixed-point projection of PdP_{3c} . The action of such projections on the dimer is explicitly represented in Fig. 7.8. The final quiver after the projection corresponds to the unshaded one in Fig. 7.7a, which results in the quiver in Fig. 7.7b. The net effect of the projection is

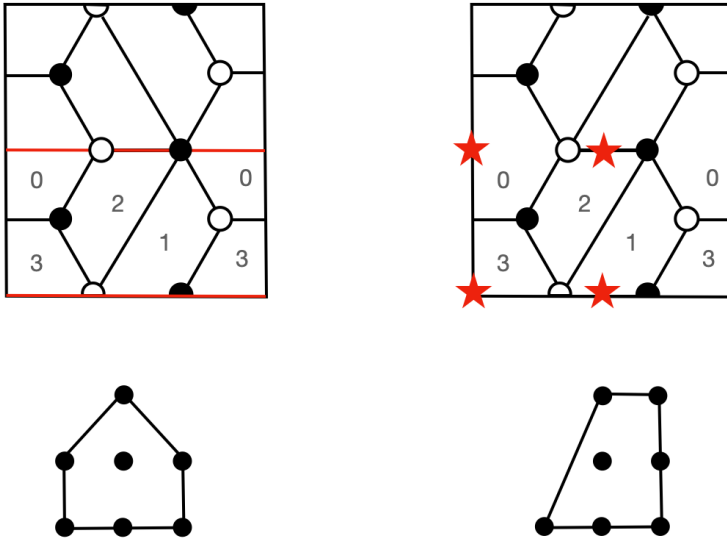


Figure 7.8 The dimers of Pseudo del Pezzo 3b and 3c with the fixed lines and fixed points projections, drawn in red.

then to identify the gauge groups $SU(N_1)$ with $SU(N_5)$ and $SU(N_2)$ with $SU(N_4)$. As a consequence, bifundamental fields X_{51} and X_{24} are projected to two-index tensor representations, drawn in red and green. Finally, the remaining two gauge groups $SU(N_0)$ and $SU(N_3)$ are projected to USp or SO depending on the choice of charges associated to the fixed points. We use to draw the real gauge nodes as diamonds on the quiver. Observe that the quiver in Fig. 7.7b is the simplest model that one can construct by gauging the flavour in the model discussed in Sec. 7.1.2 and Fig. 7.6a.

In the case of the fixed-point orientifold there are four charges, denoted with τ and labeled from 1 to 4 as in Fig. 7.8. These charges are either $+1$ or -1 and then, from now on, we will associate to them the value $\tau_i = \pm 1$ with $i = 1, \dots, 4$. In the case at hand, τ_1 projects the bifundamental X_{51} to the conjugate tensor \tilde{T}_{11} , τ_2 projects the bifundamental X_{42} to the tensor T_{22} , τ_3 acts on the gauge factor $SU(N_3)$ and τ_4 acts on the factor $SU(N_0)$. As discussed in [12] the product of these charges is constrained as $\prod_{i=1}^4 \tau_i = (-1)^{n_W/2}$ where n_W is the number of superpotential terms. We thus have $\prod_{i=1}^4 \tau_i = 1$. The further requirement that PdP_{3c} and PdP_{3b} have the same quiver after the projections imposes that $\tau_1 = \tau_4$ and $\tau_2 = \tau_3$, as these are the charges of the two fixed lines. The choices of τ_i consistent with the vanishing of the beta functions are constrained by $\tau_1 + \tau_2 = 0$. This requirement further fixes the gauge ranks properly. There are two possible choices for $\tau_1 = \pm 1$, but they are equivalent because of the \mathbb{Z}_2 reflection symmetry of the quiver. In general, for the more complicated cases that we will analyze below, this property does not hold anymore and the two choices for τ_1 will give rise to different models.

Let us fix $\tau_1 = 1$ for concreteness. In this case we are left with an

$$SO(N_0 = n) \times SU(N_1 = n - 2) \times SU(N_2 = n - 2) \times USp(N_3 = n - 4) \quad (7.23)$$

gauge theory. Each pair of nodes is connected by a bifundamental field, where the representations are inherited from the parent theory consistently with the projection. Furthermore there are two tensors for the unitary gauge groups. In the $SU(N_1)$ case there is a conjugate antisymmetric tensor, denoted T_{11} and colored in green in Fig. 7.7b. In the $SU(N_2)$ case there is a symmetric tensor that we denote T_{22} and color in red in Fig. 7.7b. The same colors are used in the rest of the Chapter. In the general analysis in the following sections we will not specify the value of τ_1 . For this reason in this section we are using the same notation T for symmetric and antisymmetric tensors. This implies that in each case the correct representation will be specified by the choice of sign for τ_1 .⁹ On the other hand we distinguish with a tilde the conjugate representation, because it is independent of the choice of sign for τ_1 .

The superpotentials (7.21) and (7.22) are projected as

$$\begin{aligned} W_{3b}^{\Omega_{fl.}} &= X_{01}X_{13}X_{30} - X_{02}X_{23}X_{30} + \frac{1}{2}T_{22}X_{02}^2 \\ &\quad - \frac{1}{2}T_{22}(X_{01}X_{12})^2 - \frac{1}{2}\tilde{T}_{11}X_{13}^2 + \frac{1}{2}\tilde{T}_{11}(X_{12}X_{23})^2 \end{aligned} \quad (7.24)$$

by fixed lines, and

$$W_{3c}^{\Omega_{fp.}} = X_{01}X_{13}X_{30} - X_{02}X_{23}X_{30} + T_{22}X_{12}X_{01}X_{02} - \tilde{T}_{11}X_{13}X_{12}X_{23} \quad (7.25)$$

by fixed points. Observe that, as in Sec. 7.1, in these formulas and in the rest of the Chapter all the gauge contractions will be understood.

Let us make an important remark regarding the factors of $1/2$ in formula (7.24). The presence of such factors has not been discussed in the original references on orientifolds and dimers [113], because the authors were not interested in the structure of the exactly marginal deformations. Here we observe that these factors appear each time a fixed line crosses some superpotential interaction in the dimer, which in turn arises from a disk amplitude in the five-brane picture and whose volume is halved by the fixed line. As we discussed above, they are crucial in our discussion about the conformal duality. The analysis of the fixed point via a -maximization was performed in [12]. This analysis has shown that the two models differ only by exactly marginal deformations.

Here we analyze the fixed points of the two models by turning on the superpotential terms one by one. We stress that a similar analysis can be performed in the other models considered in next sections. We start from $W = 0$, where a fixed point exists with central charge $a \simeq 0.650$, and the unitarity bound is not violated. Let us first focus on the PdP_{3b} . At this point, at large N , the cubic operators without tensors in Eq. (7.24) are marginal, the quintic operators are irrelevant and the cubic operators with tensors are relevant. We turn on the cubic operators and find a new fixed point with $a \simeq 0.609$, where the unitarity bound is satisfied. At this new fixed point, the quintic operators are marginal.

Studying the model PdP_{3c} , at the fixed point with $W = 0$ the cubic operators in Eq. (7.25) are marginal and the quartic operators, which involve tensors, are irrelevant. By

⁹We are confident this will not generate any confusion in the attentive reader.

turning on these operators we find a new fixed point with central charge $a \simeq 0.609$, the same value we just found for PdP_{3b}. The unitarity bound is satisfied and we see that the central charge has decreased. This suggests that the quartic operators are dangerously irrelevant. At this fixed point the operators appearing in the superpotential of PdP_{3b} are classically marginal. One can check, from Tab. 7.4, that these operators are in fact exactly marginal, therefore the two theories live on the same conformal manifold.

	X_{01}	X_{02}	X_{12}	X_{13}	X_{23}	X_{30}	\tilde{T}_{11}	T_{22}
$U(1)_1$	0	1	1	1	0	-1	-2	-2
$U(1)_2$	1	0	-1	0	1	-1	0	0

Table 7.4 The global symmetry charges for the matter fields, at large N , both for PdP_{3b} and for PdP_{3c}.

Here we will go one step further by applying a chain of tensor deconfinement ‘tricks’ and Seiberg dualities to show that the two superpotentials are actually identical up to some sign factors. The interpretation of the conformal duality in this sense is more natural and fits with the general behaviors discussed in Sec. 7.1. Observe that the simplest example of such a conformal duality is the case of $\mathcal{N} = 4$ SYM in presence of a β -deformation [122]. More generally the β -deformation is always an exactly marginal deformation for any toric quiver gauge theory [186, 187]. Starting from the superpotential $W = hW_0$ of a toric quiver gauge theory the beta deformed superpotential is $W = hW_0 + \beta W_\beta$, where W_β corresponds to the toric superpotential but this time taken with all plus signs. In this sense a model with $W = hW_0$ is conformally dual to a model with $W = hW_\beta$. Here we will consider exactly marginal deformations of this type, but only by flipping the sign of a subset of superpotential interactions.

The next step consists in finding an auxiliary quiver without tensors. This corresponds to deconfining the symmetric tensor with an $SO(N_A = n + 2)$ gauge node and the conjugate antisymmetric tensor with an $USp(N_B = n - 6)$ gauge node. The new bifundamentals X_{A1} and X_{2B} will appear quadratically in the superpotentials, i.e. we substitute $T_{22} \rightarrow X_{2B}^2$ and $\tilde{T}_{11} \rightarrow X_{A1}^2$. (Indeed by confining these nodes the theory comes back to the original one with the tensor.) There are in addition non-perturbative contributions for the tensors but for generic N they are irrelevant and we can ignore them. In the deconfined model we can Seiberg dualize the unitary gauge nodes. In this way we want to explicitly see the conformal duality applying the ideas and the construction discussed in Sec. 7.1.

The models share two cubic superpotential terms, hence the chain of dualities we are going to discuss will affect them in the same way, for this reason we prefer to keep the discussion simple by not showing them in the following. Seiberg duality on $SU(N_2 = n - 2)$ gives an $SU(\tilde{N}_2 = n)$ gauge node with dual superpotential

$$W_{\text{dual}} = M_{1B}Y_{B2}Y_{21} + M_{13}Y_{32}Y_{21} + M_{0B}Y_{B2}Y_{20} + M_{03}Y_{32}Y_{20} , \quad (7.26)$$

where M are the mesons of this duality and Y are the dual (bi-)fundamentals. The remaining superpotentials in the two cases are

$$W_{3b} = M_{03}X_{30} - X_{02}X_{23}X_{30} + \frac{1}{2}M_{0B}^2 - \frac{1}{2}M_{1B}^2X_{01}^2 + \frac{1}{2}X_{A1}^2M_{13}^2 - \frac{1}{2}X_{A1}^2X_{13}^2 \quad (7.27)$$

and

$$W_{3c} = M_{03}X_{30} - X_{02}X_{23}X_{30} + M_{0B}M_{1B}X_{01} - X_{A1}^2M_{13}X_{13} . \quad (7.28)$$

By integrating out the massive fields (only M_{03} and X_{30} for the moment)

$$M_{03}X_{30} - X_{02}X_{23}X_{30} + M_{03}Y_{32}Y_{20} \rightarrow -X_{01}X_{13}Y_{32}Y_{20} , \quad (7.29)$$

we have

$$\begin{aligned} W_{3b} &= M_{1B}Y_{B2}Y_{21} + M_{13}Y_{32}Y_{21} + M_{0B}Y_{B2}Y_{20} \\ &- X_{01}X_{13}Y_{32}Y_{20} + \frac{1}{2}M_{0B}^2 - \frac{1}{2}M_{1B}^2X_{01}^2 + \frac{1}{2}X_{A1}^2M_{13}^2 - \frac{1}{2}X_{A1}^2X_{13}^2 \end{aligned} \quad (7.30)$$

and

$$\begin{aligned} W_{3c} &= M_{1B}Y_{B2}Y_{21} + M_{13}Y_{32}Y_{21} + M_{0B}Y_{B2}Y_{20} \\ &- X_{01}X_{13}Y_{32}Y_{20} + M_{0B}M_{1B}X_{01} - X_{A1}^2M_{13}X_{13} \end{aligned} \quad (7.31)$$

Next we can dualize node 2. Seiberg duality on $SU(N_1 = n-2)$ gives an $SU(\tilde{N}_1 = 2n-4)$ gauge node. Using the letter N for the mesons of this duality and Z for the dual quarks, the dual superpotential of the gauge node reads

$$\begin{aligned} W_{\text{dual}} &= \sum_{i=1,2} N_{23}^{(i)} Z_{31}^i Z_{12} + N_{A3}^{(i)} Z_{31}^i Z_{2A} + N_{03}^{(i)} Z_{31}^i Z_{10} + \\ &+ N_{0B} Z_{B1} Z_{10} + N_{2B} Z_{B1} Z_{10} + N_{AB} Z_{B1} Z_{1A} , \end{aligned} \quad (7.32)$$

where the index i refers to the mesons constructed from X_{13} ($i = 1$) or M_{13} ($i = 1$). The remaining superpotentials in the two cases are

$$\begin{aligned} W_{3b,\text{def}} &= M_{0B}Y_{B2}Y_{20} + Y_{32}N_{23}^{(2)} + Y_{B2}N_{2B}^{(2)} - N_{03}^{(1)}Y_{32}Y_{20} + W_{\text{dual}} \\ &+ \frac{1}{2}(M_{0B}^2 - N_{0B}^2 + N_{A3}^{(1)2} - N_{A3}^{(2)2}) \end{aligned} \quad (7.33)$$

and

$$\begin{aligned} W_{3c,\text{def}} &= M_{0B}Y_{B2}Y_{20} + Y_{32}N_{23}^{(2)} + Y_{B2}N_{2B}^{(2)} - N_{03}^{(1)}Y_{32}Y_{20} + W_{\text{dual}} \\ &+ M_{0B}N_{0B} + N_{A3}^{(1)}N_{A3}^{(2)} . \end{aligned} \quad (7.34)$$

We can see that the difference between the two models corresponds then to the last line in (7.33) and (7.34) respectively.

By rotating the fields M_{0B} and N_{0B} and the fields $N_{A3}^{(1)}$ and $N_{A3}^{(2)}$ we arrive at a situation similar to the one discussed in Sec. 7.1. The main difference in this case is that the difference between the models resides in mass terms and not in cubic interactions. Nevertheless we can proceed by rotating these fields as discussed above and then integrate them out in both phases.¹⁰ The final difference then resides only in the sign of some of the superpotential terms as in the discussion in Sec. 7.1.

¹⁰Observe that there are other massive terms that can be integrated out as well but they behave identically between the two phases.

Observe that we can rotate fields only if they carry the same charges under the global symmetry, otherwise we will generate non-marginal terms and break the global symmetry explicitly. As stressed in Sec. 7.1, in addition to sharing the same quiver the models need to have the same global anomalies in order to be conformally dual. This is crucial, as it determines which theories that share the same quiver flow to the same conformal manifold. For example, the parent theories PdP_{3b} and PdP_{3c} , without the orientifold projection, still share the same quiver but are not conformally dual because cancellation of the β -functions requires different solutions. In this sense, the action of the orientifold is pivotal to ensure anomaly matching.

7.3 Embedding in string theory

In this section we give a general description of the 4d $\mathcal{N} = 1$ toric quiver gauge theories that generalize the duality between PdP_{3b} and PdP_{3c} after the fixed-line/fixed-point orientifold projections. The key fact that lends itself to a natural generalization is that both PdP_{3b} and PdP_{3c} can be represented by the same quiver. However the two models have different superpotentials that correspond to the two inequivalent planarizations of the quiver and they cannot be related by any low-energy duality. This reflects in the fact that the two toric diagrams are not related by any $SL(2, \mathbb{Z})$ transformation. In general we are looking for examples of such type: pairs (or sets) of models sharing the same quiver but with inequivalent planarizations. This is a necessary but not sufficient condition in our construction of conformally dual models. We refer to such quivers as multi-planarizable. After obtaining classes of models with this property we discuss general aspects of their orientifold projections that give rise to conformal dualities.

7.3.1 Multi-planarizable quivers

In most cases, given a planarizable quiver the latter admits a unique planarization in terms of plaquettes and therefore a unique dimer and tiling. However here we are interested in families of models with the same quiver but different planarizations. We identify such families in terms of their toric diagrams, that are inequivalent also up to $SL(2, \mathbb{Z}_2)$ transformations. From the toric diagram we then identify the brane tiling using the inverse algorithm. This step is not unique, because toric dual phases can emerge by different choices of the intersections of the five-branes in the brane tilings that preserve the zig-zag paths. Nevertheless we observe that it is always possible to choose these brane tilings for pairs of inequivalent toric diagrams, in order to obtain an identical quiver. This implies that the quivers obtained by this procedure are the multi-planarizable quivers that we are looking for. The simplest realization of models with such property corresponds to the case of PdP_{3b} and PdP_{3c} .

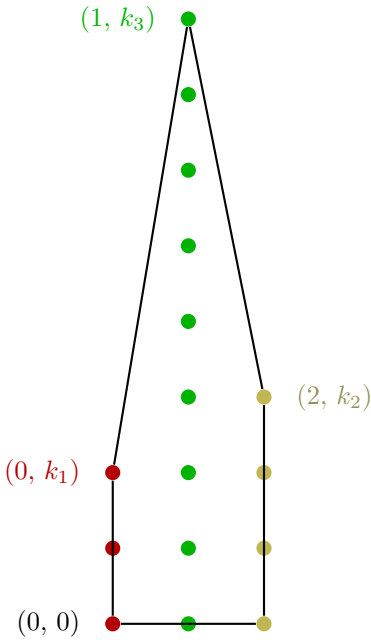


Figure 7.9 Generic toric diagram labeled by (k_1, k_2, k_3) .

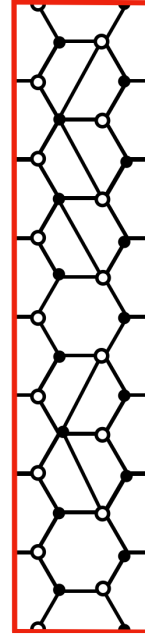


Figure 7.10 Fundamental cell of the (k_1, k_2, k_3) model.

Let us start by identifying the toric diagrams: they are drawn in Fig. 7.9. In general we label these toric diagrams by three integers (k_1, k_2, k_3) , where k_1 and k_2 represent the number of points in the two external lines and k_3 is the number of points in the central one, excluding the points at the base. Equivalently, k_1 and k_2 represent the length of the external lines, while k_3 the length of the central line.

It is possible to show that such toric diagrams always admit a dimer with a fundamental cell given in Fig. 7.10. This dimer has $2k_1$ squares obtained by cutting hexagons with the NW-SE orientation and $2k_2$ with the NE-SW orientation. Then, there are $k_3 - k_2 - k_1$ hexagons in the central part of the fundamental cell. The other column is on the other hand made of k_3 hexagons. We have to require $k_3 \geq k_2 + k_1$, which is saturated when there are only squares in the central column. With this notation, the examples in the previous section correspond to $(1, 1, 2)$ for PdP_{3b} and $(0, 2, 2)$ for PdP_{3c} .

Here is the key observation that allows us to construct multiplanarizable quivers. We consider the flip in figure 7.11, where a hexagon cut by a diagonal with the NW-SE orientation is transformed into a NE-SW oriented one, while relabeling the faces as in Fig. 7.11. This flip does not give in general a new consistent brane tiling, and in many cases the flipped dimer shows one of the inconsistencies discussed in [188]. However this is not the case for the models labeled by (k_1, k_2, k_3) considered here. Indeed in such cases the flip does not modify the quiver even if it is associated in general to a consistent but inequivalent model. In fact the latter has a different toric diagram. Labeling the original toric diagram with the triple (k_1, k_2, k_3) , the new toric diagram after such a flip

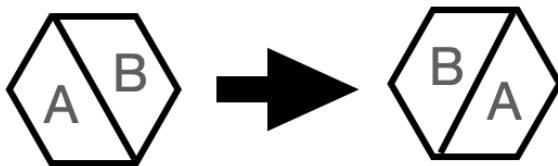


Figure 7.11 In this picture we represent the flip on the dimer that preserves the quiver. We consider a pair of faces A and B obtained by cutting an hexagon with a NW-SE diagonal and we flip it into a NE-SW one. By relabeling the faces one can see that the quiver remains identical even if in general it is associated to a different toric diagram.

is given by the new triple $(k_1 + 1, k_2 - 1, k_3)$. In general we can iterate the flip described above and conclude that two models (k_1, k_2, k_3) and (k'_1, k'_2, k'_3) have the same quiver but different toric data if $k'_3 = k_3$ and $k_1 + k_2 = k'_1 + k'_2$ (observe that the choice $k_1 = k'_2$ is trivial in this sense).

7.3.2 Orientifold projections

In this sub-section we add the orientifolds to the previous brane setups and we focus on the relation between the orientifolds and the conformal symmetry. Typically when O-planes are considered it is not straightforward to preserve the conformal symmetry for stacks of N D3- branes probing the singularity. On the field theory side suitable choices of gauge ranks have to be considered.

As discussed in [12] there are three possible scenarios if one considers the fate of conformal invariance after the projection. The first scenario corresponds to the case in which there is a fixed point after the projection and there are $\mathcal{O}(1/N)$ corrections on the physical observables due to the presence of the orientifold. The second scenario corresponds to the case in which the theory obtained after the projection does not have any conformal fixed point. The third possible scenario corresponds to the case in which there is a new fixed point in the unoriented model, but the corrections are not of order $\mathcal{O}(1/N)$ anymore.

In the example of [12] it was shown that there is an interplay between the first and the third scenario in the orientifold projections of the two inequivalent models. Here we will extend this relation in the models parameterized by (k_1, k_2, k_3) . Namely we will find a general assignment of gauge ranks such that some unoriented conformal theories will belong to the first scenario and some other to the third scenario. We checked that the central charges of these orientifold models match and that only the cases with $k_1 = k_2$ belong to the first scenario. Furthermore we claim that by applying the orientifold and assigning such ranks to pairs of inequivalent models sharing the same quiver we obtain unoriented theories differing only by exactly marginal deformations as in the case studied in [12] that we have reviewed above.

Concretely, by analyzing a large amount of models, we have indeed observed that the conformal duality obtained in [12] can be generalized by requiring that the final models have two real gauge groups (and equivalently two two-index tensors for two of the

unitary groups). This restricts the possibilities, implying that $k_1 + k_2 = 2k$ with k integer, and $k_3 \geq 2k$. We have explicitly seen that relaxing this condition allows for models which are not conformally dual, but it is not clear, at least for the moment, what is the reason behind it, both from the field theory perspective and from the string theory side. In this way one of the possible models is always $(k, k, k_3 \geq 2k)$, that admits a fixed-line projection. This fixes also the possible signs of the fixed-point projections in the other models in the same family of conformally dual theories. In order to construct a family of fixed-point conformally dual orientifolds we proceed as follows. First we identify the model with $(0, 2k, k_3)$ as the seed of the family. This model and the (k, k, k_3) model must be chosen in a Seiberg dual phase that allows the fixed-point or fixed-line projections to give rise to the same final quiver. Such a phase is not unique, there can also be other phases that give rise to the same final quiver, and there can be also other (inequivalent) choices. As we will discuss, those inequivalent choices are no longer related by chains of Seiberg dualities after the orientifold projection. Once this is fixed we can increase k_1 using the flip in figure 7.11 by two units preserving the sum $k_1 + k_2$. A generic model in this case is $(2p + 1, 2k - 2p - 1, k_3)$. Depending on the parity of k the sequence of flips terminates with (k, k, k_3) or $(k - 1, k + 1, k_3)$. We will give evidence that all of the models constructed by fixed-point orientifolds in this way are conformally dual to the fixed-line¹¹ orientifold of (k, k, k_3) (i.e. that there is at least one Seiberg dual phase that gives rise to such a conformally dual theory, once the gauge ranks are suitably chosen). Observe that the minimal $k = 1$ corresponds to the case studied in [12], where indeed there are only two possibilities $(1, 1, k_3 = 2)$ and $(0, 2, k_3 = 2)$. Furthermore, the case $k = 2$ cannot give rise to any intermediate case either, since only $(2, 2, k_3 = 4)$ and $(0, 4, k_3 = 4)$ are allowed, while $(1, 3, k_3 = 4)$ does not admit any toric dual phases that can be projected consistently with the other two cases. Hence, the first non-trivial case with more than two models has necessarily $k = 3$.

By inspection we have also observed that there is a unique assignation of ranks that gives rise to the generalization of the conformal duality found in the original PdP_{3b/c} case. This choice is explained as follows. Consider the limiting case with $k_1 = k_2$ and its fixed-line orientifold projection, so that there are only two charges whose signs are τ_1 and τ_2 . On the reduced fundamental cell delimited by the fixed lines, τ_1 is the charge associated to the line at the top, while τ_2 at the bottom, as in Fig. 7.12. The vanishing of the beta functions always requires that $\tau_1 = -\tau_2 = \tau$, consistently with the prototypical case of PdP models. Consider the case in which the gauge factors projected by the top line and the bottom lines lie on the side of the dimer, and label them with 0 and $3k$, respectively. The hexagons on the sides of the reduced cell are labelled with 3ℓ , $\ell = 0, \dots, k$. As a consequence, gauge factors from the central line in the reduced cell of the dimer are labelled with $3\ell + 1$ and $3\ell + 2$ for a pair of squares, $3\ell + 1$ (or $3\ell + 2$ equivalently) for hexagons. Having set up the notation for the labels, we assign rank $N_0 = n$ to the first gauge factor¹² and the choice of the ranks is summarized as

$$N_{3\ell} = n - 4\ell \tau_1, \quad (7.35)$$

$$N_{3\ell+1} = N_{3\ell+2} = n - 2 - 4\ell \tau_1, \quad (7.36)$$

¹¹For odd k , the (k, k, k_3) case admits also a fixed-point projection. We will see in the examples below that this choice has to be considered as well because it can give rise to new types of conformally dual models. Observe that there are also other choices of signs if (k, k, k_3) has fixed points but we will not discuss such possibility below.

¹²Or better, the zeroth one.

with $\ell = 0, \dots, k$, where the shifts are understood as in Fig. 7.12.

If the projected gauge factors lie on the central part of the dimer instead, we only need to shift the labels by 3, with $\ell \rightarrow \ell + 1$, and the rank assignment remains as in Eq. (7.35) for the gauge factors on the side of the dimer, and Eq. (7.36) for the gauge factors on the central part of the dimer. Colored fields in red and green represent tensors and conjugated tensors, while diamond nodes are real gauge groups. Finally, the general quiver is drawn as in Fig. 7.13 and wherever there are hexagons in the central line of the dimer, their contribution to the quiver is drawn in an example in Fig. 7.14, where we may think of it as part of the diagram has been folded.

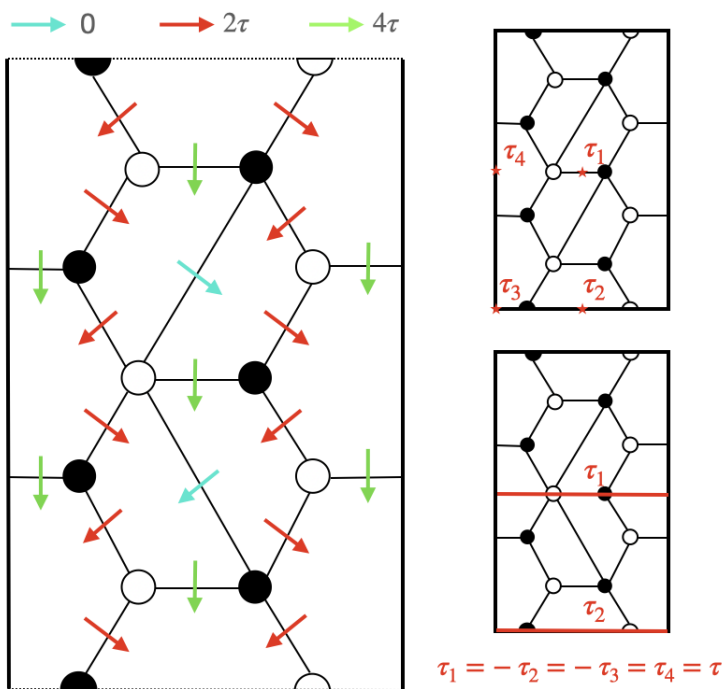


Figure 7.12 On the LHS we summarize the general rank assignment on the dimer that we have considered in the whole Chapter. We start by considering the same rank for each node and then we shift the ranks by $j\tau$ where $j = 0, 2, 4$ following the coloring of the arrows in the figure. On the RHS we consider the choices of the charges τ for a generic fixed line and fixed point projection.

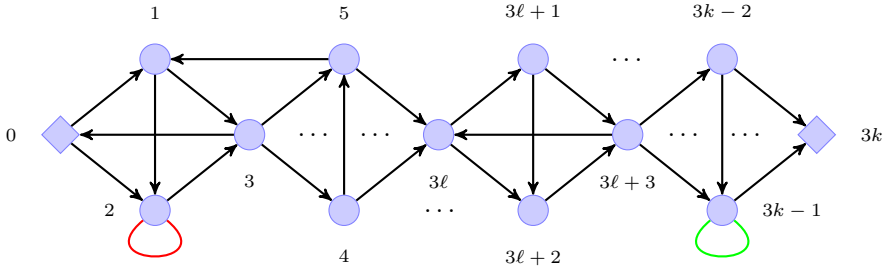


Figure 7.13 The generic quiver associated to a toric theory with (k_1, k_2, k_3) and $k_3 = k_1 + k_2 = 2k$ and $\ell = 0, \dots, k$.

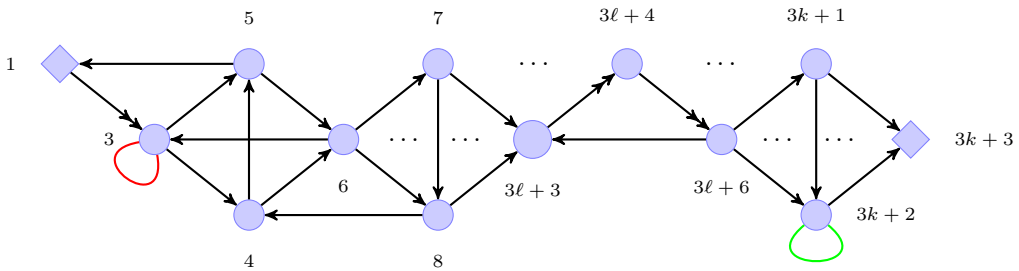


Figure 7.14 The generic quiver associated to a toric theory with (k_1, k_2, k_3) and $k_3 > k_1 + k_2 = 2k$ and $\ell = 1, \dots, (k + 1)$.

7.4 Case study

In this section we apply the construction discussed above for obtaining conformally dual models by suitable orientifold projections of multi-planarizable toric quiver gauge theories. We will discuss explicitly two cases, both with $k = 2$, where all the properties and possibilities discussed in Sec. 7.1 show up. A larger set of examples is included in App. C. In the following analysis we will keep the same conventions for the quivers and for the projections discussed in the previous sections. We checked, by following the same analysis discussed for the toy models and the PdPs, that each model has a fixed point that satisfies the unitarity bound. We will then show in each case that, by applying chains of tensor matter deconfinements, dualities and rotations, all the conformally dual models can be transformed into models with the same superpotential up to some signs in the interactions, making the conformal duality completely explicit.

7.4.1 $(2, 2, 5)$ vs. $(0, 4, 5)$

Let us start the analysis with the dimers and the toric diagrams depicted in Fig. 7.15. There are three dimers associated to the $(2, 2, 5)$ model and one dimer associated to the $(0, 4, 5)$ model. Even if the three dimers associated to $(2, 2, 5)$ are Seiberg dual before the orientifold, we will analyze the various possibilities because the conformal duality model emerges in different ways.

While in the $(0, 4, 5)$ case we have only a single fixed-point orientifold projection that adapts to our goals, in the $(2, 2, 5)$ case there are three orientifold projections that we can

consider. Two of them are fixed-line projections while the last is one by fixed points.

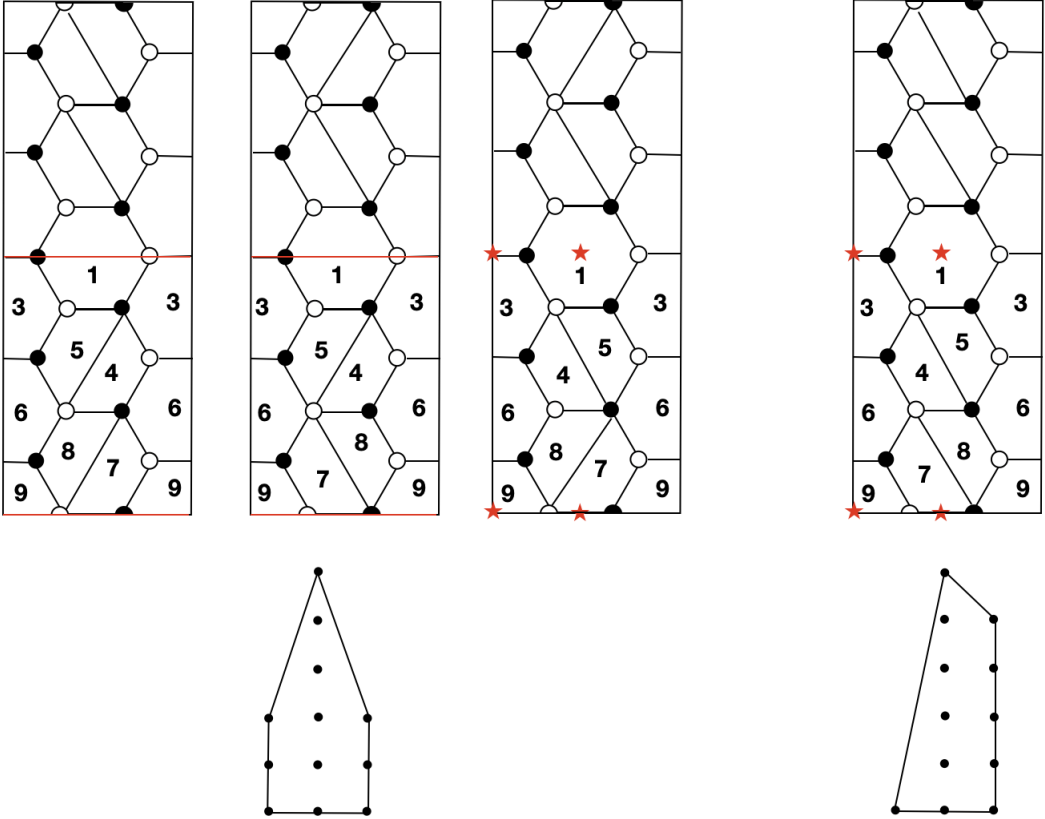


Figure 7.15 The dimers representing the orientifold projection of toric diagrams $(2, 2, 5)$, on the left, and $(0, 4, 5)$ on the right. For $(2, 2, 5)$, there are both fixed lines and fixed points projections.

The projections give rise to different superpotentials. For the first fixed-line projection of the $(2, 2, 5)$ model we have

$$\begin{aligned}
 W_{(2,2,5)}^{\Omega_{f_1}^1} &= \frac{1}{2} T_{33}(X_{13}^2 - Y_{13}^2) + Y_{13} X_{35} Y_{51} - X_{13} X_{34} X_{45} X_{51} \\
 &+ X_{34} X_{46} X_{63} - X_{35} X_{56} X_{63} + X_{56} X_{68} X_{84} X_{45} - X_{46} X_{67} X_{78} X_{84} \\
 &+ X_{67} X_{79} X_{96} - X_{68} X_{89} X_{96} + \frac{1}{2} \tilde{T}_{77}(X_{78}^2 X_{89}^2 - X_{79}^2), \tag{7.37}
 \end{aligned}$$

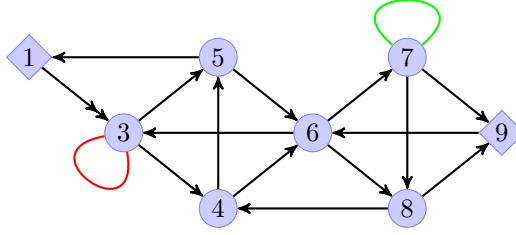


Figure 7.16 The quiver for the theories $(2, 2, 5)$ and $(0, 4, 5)$, after the orientifold projection.

while the second fixed-line projection of the $(2, 2, 5)$ model we have

$$\begin{aligned}
 W_{(2,2,5)}^{\Omega_{\text{fl}}^2} &= \frac{1}{2} T_{33} (X_{13}^2 - Y_{13}^2) + Y_{13} X_{35} Y_{51} - X_{13} X_{34} X_{45} X_{51} \\
 &\quad + X_{34} X_{46} X_{63} - X_{35} X_{56} X_{63} + X_{56} X_{67} X_{78} X_{84} X_{45} - X_{46} X_{68} X_{84} \\
 &\quad + X_{68} X_{89} X_{96} - X_{67} X_{79} X_{96} + \frac{1}{2} \tilde{T}_{77} (X_{79}^2 X_{78}^2 - X_{89}^2) . \tag{7.38}
 \end{aligned}$$

On the other hand the fixed-point projection of the $(2, 2, 5)$ model gives

$$\begin{aligned}
 W_{(2,2,5)}^{\Omega_{\text{fp}}} &= \frac{1}{2} T_{33} X_{13} Y_{13} + Y_{13} X_{34} X_{45} X_{51} - X_{13} X_{35} Y_{51} \\
 &\quad + X_{35} X_{56} X_{63} - X_{34} X_{46} X_{63} + X_{46} X_{68} X_{84} - X_{56} X_{67} X_{78} X_{84} X_{45} \\
 &\quad + X_{67} X_{79} X_{96} - X_{68} X_{89} X_{96} + \tilde{T}_{77} X_{79} X_{78} X_{89} . \tag{7.39}
 \end{aligned}$$

Lastly, the fixed-point projection for the $(0, 4, 5)$ model gives

$$\begin{aligned}
 W_{(0,4,5)}^{\Omega_{\text{fp}}} &= T_{33} X_{13} Y_{13} + Y_{13} X_{34} X_{45} X_{51} - X_{13} X_{35} Y_{51} \\
 &\quad + X_{35} X_{56} X_{63} - X_{34} X_{46} X_{63} + X_{46} X_{67} X_{78} X_{84} - X_{56} X_{68} X_{84} X_{45} \\
 &\quad + X_{68} X_{89} X_{96} - X_{67} X_{79} X_{96} + \tilde{T}_{77} X_{78} X_{89} X_{79} . \tag{7.40}
 \end{aligned}$$

The ranks of the gauge groups consistent with the anomaly cancellations and the existence of a conformal fixed point are

$$\begin{aligned}
 N_1 &= n, N_3 = n - 2\tau, N_4 = N_5 = n - 4\tau, \\
 N_6 &= n - 6\tau, N_7 = N_8 = n - 8\tau, N_9 = n - 10\tau . \tag{7.41}
 \end{aligned}$$

Let us remind the reader that the two possible choices of sign $\tau = \pm 1$ give rise to two different quivers, that in this case are inequivalent and need to be studied separately.

The two different projections indeed yield either $SO(N_1)$ and $USp(N_9)$ or $USp(N_1)$ and $SO(N_9)$. Furthermore the tensors T_{33} and \tilde{T}_{77} are either symmetric and conjugate anti-symmetric or conjugate symmetric and anti-symmetric, respectively.

We have checked that both choices of τ give consistent SCFT by a -maximizing with the ranks in formula (7.41). Furthermore we have computed the various 't Hooft anomalies and have seen that they coincide between the models. The relation between these models is then very similar to one between the projections of PdP_{3b} and PdP_{3c}.

In the following we will see that indeed, by applying the general analysis of Sec. 7.1, we can distinguish (in some Seiberg dual phase) the models only by some superpotential signs.

Let us begin by comparing the superpotential of the two fixed-line projections of the model $(2, 2, 5)$, Eqs. (7.37)-(7.38). They differ only in the last terms in the second line and the first two terms in the last line. While the latter two can be reabsorbed by a change of sign in X_{96} , the former two can not, and we proceed as follow. Observe that before the orientifold projection the two theories represent two different Seiberg dual phases associated with the same toric geometry. After the projection they are conformally dual, and one might think they are actually Seiberg dual. We shall see that this is *not* the case. Performing Seiberg duality on the gauge node labeled by 5, the superpotentials become¹³

$$\begin{aligned} W_{(2,2,5)}^{\Omega_{i1}^1} &= (\dots) + M_{46}X_{68}X_{84} - X_{46}X_{67}X_{78}X_{84} , \\ W_{(2,2,5)}^{\Omega_{i1}^2} &= (\dots) + M_{46}X_{67}X_{78}X_{84} - X_{46}X_{68}X_{84} , \end{aligned} \quad (7.42)$$

where we have highlighted only the unequal terms and where M_{46} is one of the mesons in the duality. If we consider the combinations $N_{46}^{(\pm)} = X_{46} \pm M_{46}$ we can see that the two superpotentials differ only in a sign, as discussed in Sec. 7.1. Hence, the theories after the orientifold projection are conformally dual but not Seiberg dual (as one could expect, since usually the orientifold does not “commute” with Seiberg duality).¹⁴ However, in larger dimer structures there may be chains of Seiberg dualities preserved by the orientifold projection, as we show in App. C. Observe that one can equivalently deconfine the tensor \tilde{T}_{77} and dualize node 7, obtaining the same result.

If we compare the orientifold projection with fixed points on the model $(2, 2, 5)$ to the fixed-line ones, we see from Eqs. (7.39)-(7.37) that we need to act upon the terms with the tensors and the same pair of terms of the previous case, hence the discussion holds in the same way. Furthermore, Eqs. (7.39)-(7.38) differ only in the terms where tensors appear, and we are back to the case studied in Sec. 7.1.2.

These three theories obtained by projecting the $(2, 2, 5)$ models can also be related to the fixed-point projection of the $(0, 4, 5)$ case corresponding to the superpotential (7.40). The proof is straightforward because it uses the same dualities and field redefinitions discussed already in the $(2, 2, 5)$ case.

The models discussed in this subsection summarize the core of the mechanism of conformal duality as it is introduced in Sec. 7.1, i.e. no field redefinition reabsorbs the relative

¹³Also, some fields become massive in both models and are integrated out, but their F -terms do not affect the terms we are interested in.

¹⁴This happens when one performs Seiberg duality on a gauge factor “close” to the fixed locus. On the brane tiling, Seiberg duality corresponds to moving NS5-branes across each other. This operation does not commute with the orientifold projection when one needs to cross the orientifold plane. On the other hand, before and after the projection the duality is preserved when the NS5-branes do not cross the orientifold plane and the same operation is performed on the NS5's on the other side, preserving the \mathbb{Z}_2 symmetry.

sign between parts of a pair of superpotential and transform one into the other. It is the flip move, introduced in Sec. 7.3 from one dimer to the other that generates the sign flips. Some of them can be fixed by the redefinition of an horizontal edge (X_{96} in (7.37)-(7.38)), but this is not enough to fix the whole superpotential. The reason is that the orientifold theory inherits the structure of the interaction from the parent theory and the pattern of the signs is strongly constrained by the toric condition.

7.4.2 (2, 2, 6) vs. (0, 4, 6)

We conclude this section with a second example. The two models before the projections correspond to the toric diagrams identified by $(k_1, k_2, k_3) = (2, 2, 6)$ and $(k_1, k_2, k_3) = (0, 4, 6)$. We refer to the projections considered here as “first case”, because there is a second possibility discussed in the App. C. The models and the projections are summarized in Fig. 7.17.

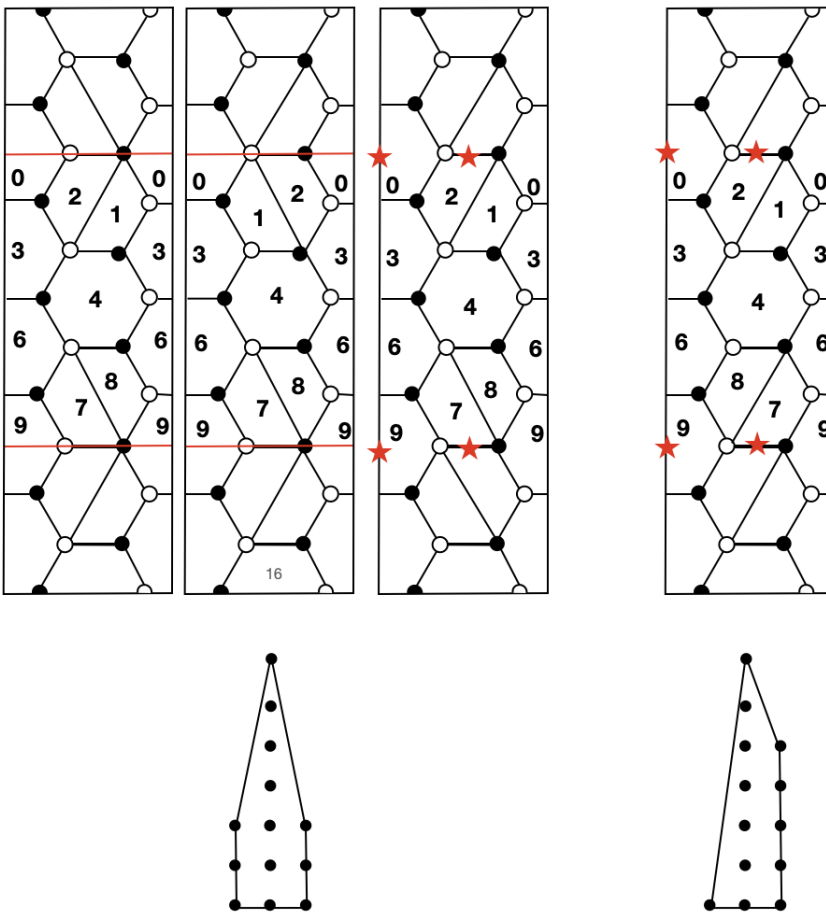


Figure 7.17 The dimers representing the orientifold projection of toric diagrams (2, 2, 6), on the left, and (0, 4, 6) on the right. For (2, 2, 6), there are both fixed-line and fixed-point projections.

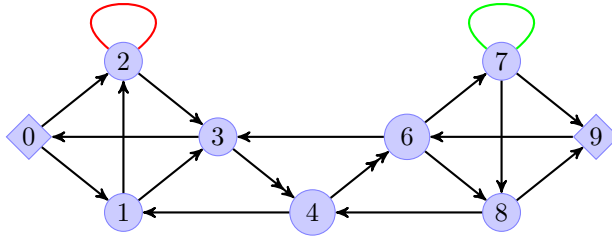


Figure 7.18 The quiver for the theories $(2, 2, 6)$ and $(0, 4, 6)$, after the orientifold projection.

The projections give rise to different superpotentials. For the first fixed-line projection of the $(2, 2, 6)$ model we have

$$\begin{aligned}
 W_{(2,2,6)}^{\Omega_{i.l.}^1} &= \frac{1}{2} T_{22} \left(X_{02}^2 - X_{01}^2 X_{12}^2 \right) + X_{01} X_{13} X_{30} - X_{02} X_{23} X_{30} \\
 &+ X_{23} Y_{34} X_{41} X_{12} - X_{13} X_{34} X_{41} + X_{34} X_{46} X_{63} - Y_{34} Y_{46} X_{63} \\
 &+ Y_{46} X_{67} X_{78} X_{84} - X_{46} X_{68} X_{84} + X_{68} X_{89} X_{96} - X_{67} X_{79} X_{96} \\
 &+ \frac{1}{2} \tilde{T}_{77} \left(X_{79}^2 - X_{78}^2 X_{89}^2 \right), \tag{7.43}
 \end{aligned}$$

while the second fixed-line projection of the $(2, 2, 6)$ model we have

$$\begin{aligned}
 W_{(2,2,6)}^{\Omega_{i.l.}^2} &= \frac{1}{2} T_{22} \left(X_{01}^2 X_{12}^2 - X_{02}^2 \right) + X_{02} X_{23} X_{30} - X_{01} X_{13} X_{30} \\
 &+ X_{13} Y_{34} X_{41} - X_{23} X_{34} X_{41} X_{12} + X_{34} X_{46} X_{63} - Y_{34} Y_{46} X_{63} \\
 &+ Y_{46} X_{67} X_{78} X_{84} - X_{46} X_{68} X_{84} + X_{68} X_{89} X_{96} - X_{67} X_{79} X_{96} \\
 &+ \frac{1}{2} \tilde{T}_{77} \left(X_{79}^2 - X_{78}^2 X_{89}^2 \right). \tag{7.44}
 \end{aligned}$$

On the other hand the fixed-point projection of the $(2, 2, 6)$ model gives

$$\begin{aligned}
 W_{(2,2,6)}^{\Omega_{i.p.}} &= T_{22} X_{02} X_{01} X_{12} + X_{01} X_{13} X_{30} - X_{02} X_{23} X_{30} \\
 &+ X_{23} Y_{34} X_{41} X_{12} - X_{13} X_{34} X_{41} + X_{34} X_{46} X_{63} - Y_{34} Y_{46} X_{63} \\
 &+ Y_{46} X_{67} X_{78} X_{84} - X_{46} X_{68} X_{84} + X_{68} X_{89} X_{96} - X_{67} X_{79} X_{96} \\
 &+ \tilde{T}_{77} X_{79} X_{78} X_{89}. \tag{7.45}
 \end{aligned}$$

Lastly, the fixed-point orientifold projection for the $(0, 4, 6)$ model yields

$$\begin{aligned}
W_{(0,4,6)}^{\mathcal{O}_P} &= T_{22}X_{01}X_{12}X_{02} + X_{01}X_{13}X_{30} - X_{02}X_{23}X_{30} \\
&+ X_{23}Y_{34}X_{41}X_{12} - X_{13}X_{34}X_{41} + X_{34}X_{46}X_{63} - Y_{34}Y_{46}X_{63} \\
&+ Y_{46}X_{68}X_{84} - X_{46}X_{67}X_{78}X_{84} + X_{67}X_{79}X_{96} - X_{68}X_{89}X_{96} \\
&+ \tilde{T}_{77}X_{79}X_{78}X_{89} .
\end{aligned} \tag{7.46}$$

The ranks of the gauge groups consistent with the anomaly cancellations and the existence of a conformal fixed point are

$$\begin{aligned}
N_0 &= n, N_1 = N_2 = n - 2\tau, N_3 = n - 4\tau \\
N_4 &= n - 6\tau, N_6 = n - 8\tau, N_7 = N_8 = n - 10\tau, N_9 = n - 12\tau .
\end{aligned} \tag{7.47}$$

Again the two possible choices of sign $\tau = \pm 1$ give two different quivers, that in this case are inequivalent and need to be studied separately. The two different projections indeed give either $SO(N_0)$ and $USp(N_9)$ or $USp(N_0)$ and $SO(N_9)$. Furthermore the tensors T_{22} and \tilde{T}_{77} are either symmetric and conjugate anti-symmetric or conjugate symmetric and anti-symmetric, respectively. We have checked that both choices of τ give a consistent SCFT by maximizing the a central charge with the ranks in formula (7.47). Furthermore we have computed the various 't Hooft anomalies and we have seen that they coincide among the models.

Similarly to the previous example we can study the conformal duality between these four models by applying the discussion in Sec. 7.1. Again the first three cases are toric dual before the projections and even if such a duality is broken by the projections the models remain conformally dual.

Let us discuss the map between each pair of superpotentials explicitly. The superpotentials of the two fixed-line projections, given in formulae (7.43) and (7.44), differ by a sign¹⁵ by considering the combinations $N_{34}^{(\pm)} = X_{34} \pm Y_{34}$. The superpotentials of the two fixed-point projections, given in formula (7.45) and (7.46), differ by a sign by considering the combinations $N_{46}^{(\pm)} = X_{46} \pm Y_{46}$. The map among one of the superpotentials obtained by a fixed-line projection and one obtained from a fixed-point projection requires also to apply one Seiberg duality on node $SU(N_1)$ and one on node $SU(N_8)$.

The transformations of the two superpotentials obtained by a fixed-line projection after this duality corresponds to

$$\begin{aligned}
\frac{1}{2}T_{22}(X_{02}^2 - X_{01}^2X_{12}^2) &\rightarrow \frac{1}{2}T_{22}(X_{02}^2 - M_{02}^2) , \\
\frac{1}{2}\tilde{T}_{55}(X_{79}^2 - X_{78}^2X_{89}^2) &\rightarrow \frac{1}{2}\tilde{T}_{55}(X_{79}^2 - M_{79}^2) ,
\end{aligned} \tag{7.48}$$

while those of the two superpotentials obtained by a fixed-point projection after this

¹⁵Also by a sign in the first line, but this can be reabsorbed redefining X_{30} and T_{22} , similarly as in the previous section.

duality corresponds to

$$\begin{aligned} T_{22}X_{01}X_{12}X_{02} &\rightarrow T_{22}M_{02}X_{02} , \\ \tilde{T}_{77}X_{79}X_{78}X_{89} &\rightarrow \tilde{T}_{77}X_{79}M_{79} . \end{aligned} \tag{7.49}$$

After applying these dualities we consider the combinations of fields $X_{02} \pm M_{02}$ and $X_{79} \pm M_{79}$. We can see explicitly that combining these operations and the field redefinitions $X_{46} \pm Y_{46}$ and $X_{34} \pm Y_{34}$ when necessary, each superpotential obtained by a fixed-line projection differs only in sign choices from the superpotentials obtained by a fixed-point projection.

This concludes the analysis for this case, showing indeed that the conformal duality can be reformulated along the lines of the discussion in Sec. 7.1.

We have studied many other examples, and they all behave as the two examples studied here. For completeness we briefly discuss these models in App. C.

7.5 Discussion and conclusions

In this Chapter we have generalized the result obtained in [12], where it was shown that two quiver gauge theories describing stacks of D3-branes probing different toric CY_3 singularities reside on the same conformal manifold once suitable orientifold projections are considered. The two singularities studied in [12] are the PdP_{3b} and PdP_{3c} surfaces and the orientifolds are implemented by a fixed-line and a fixed-point projection on the dimer, respectively.

The key point allowing for a natural generalization of this conformal duality is that the two models share the same quiver even before considering the orientifold. These quivers have different superpotentials however, and this gives rise to different dimers and toric diagrams. Nonetheless there exists a “flip” on the dimer (see Fig. 7.11) that can be used to transform one toric diagram into the other, by reversing the orientation of one zig-zag path in a consistent way. We have found infinite families of dimers associated to different toric diagrams but sharing the same quiver by the application of this flip. It is enough to require that the flip does not spoil the quiver structure and that the zig-zag paths intersect consistently. We have referred to quivers with this property as multi-planarizable, i.e. the same quiver admits different planar periodic quivers associated, in general, to different CY singularities. We have then studied the orientifold projections in terms of fixed-line and fixed-point identifications on the dimer. By analyzing a large set of models we have found infinite classes of models that behave as the ancestral case of PdP_{3b} and PdP_{3c} . These models are specified by the reflection symmetry property of the toric diagram, in the phase projected by fixed lines.

We have further studied the conformal dualities among the models obtained after the projection by iterative applications of ordinary Seiberg dualities. Our strategy consists in considering two conformally dual phases and applying the same dualities on both. This procedure preserves the fact that the two models have the same quivers and that all the fields have the same global charges. We have found that a judicious application of Seiberg dualities transforms the superpotential interactions of the two phases in a remarkable way. There always exists a phase where two conformally dual models have the same quiver and the same superpotential interaction. The only difference regards the sign of the coupling: some of these may indeed have a different sign. This sign

difference cannot be reabsorbed in a phase for the fields and thus represents a genuine exactly marginal deformation connecting the two models.

We left open many questions and possible directions of future investigation. Here we have found infinite families of quivers that admit different periodic planar descriptions. It is natural to wonder if these families exhaust (up to Seiberg or toric dualities) the possible quivers with this peculiar property. If other such models exist then one should check if there are orientifold projections giving rise to conformally dual models for suitable and consistent choices of gauge ranks. One may also add flavor branes to the configuration along the lines of [1], which will provide an even richer structure on the gauge theory and more freedom for the choice of the gauge ranks, but at the same time one would lose the description of the orientifold projection from the dimer construction.

One can also wonder whether there are quivers that coincide only after the orientifold projection. If true, it should be possible to find other conformal dualities for these cases as well.

In general it is worth mentioning that all the conformally dual models found in this Part and in [12, 9, 10, 11] share a similar property when looking at their toric diagrams, i.e. they have the same number of internal and external points. This signals that the gauge theories have the same number of gauge groups and of non-anomalous global symmetries. The role of the orientifold is to further break the global symmetry, and to identify the 't Hooft anomalies of the surviving ones. This idea can be used to generalize the construction to more general cases. One may in principle find examples of conformal dualities with different Lagrangians and quivers by studying orientifolds of models with the same number of gauge groups and global symmetries. The final goal of this program consists in finding a predictive stringy recipe for obtaining conformal dualities in presence of orientifolds. One may think of such a top-down approach as complementary to the bottom-up one used in [24] to find conformal dualities. A key role in their setup seems related to the presence of orientifolds, since most of the examples feature real gauge groups and tensor matter fields.

One last natural question regards the holographic interpretation of the dualities found here.¹⁶ In particular, it is necessary to understand the role played by exactly marginal deformations in the gravity dual. As we stressed in the discussion the marginal deformation connecting the models obtained here is related to the β -deformation of SYM, because it can always be reformulated as a sign flip of some superpotential terms. Observe that, despite the similarities among models related by such a sign flip, there are non-trivial differences. For example they differ in the spectrum of chiral primary operators [190, 191]. See also [192, 193] for an analysis of the chiral matter superfield propagator in the β -deformed case. The holographic dual mechanism for the case of the β -deformed $\mathcal{N} = 4$ SYM was originally interpreted in [194] as a TsT transformation on the AdS side. Here we are considering more complicated cases, because the sign change involves only a subset of couplings and because we are in presence of orientifolds. A general discussion on the gravitational origin of marginal deformations for toric quiver gauge theories appeared in [187]. In absence of orientifolds, the intimate relations between the marginal deformations and the zig-zag paths recently obtained in [195, 196] may provide a useful guideline to address the problem from the gravity side. Generalizing such constructions in presence of orientifolds represents a first step to investigate in this direction.

Finally it would be desirable to find the origin of the conformal dualities in terms of

¹⁶See also the recent reference [189] for related comments.

string dualities, starting from two inequivalent CY_3 singularities and considering orientifolds of those which are known to give rise to conformally dual gauge theories.

Part III

Generalized Symmetries, S-folds and $\mathcal{N} = 2$ SCFTs

In this Part of this thesis we consider superconformal theories (SCFTs) in 4d. In particular we will be interested in SCFTs with $\mathcal{N} \geq 2$, that is conformal theories which preserve at least 8 supercharges (plus the 8 conformal partners of the supercharges). We will study the 1-form symmetry groups of these theories, which are global symmetries that act trivially on local operators but act non-trivially on line operators. Furthermore we will develop some consistency conditions for these CFTs based on the rank, the geometry of the space of vacua and the electromagnetic charges of local operators. We analyze a class of $\mathcal{N} = 3$ SCFTs called S-fold SCFTs [197], that we briefly review in Section 8.1. In general, theories with $\mathcal{N} = 3$ supersymmetry have not been deeply investigated so far. Such models have been predicted in [198], and then found in [197]. Many generalizations have been then studied by using various approaches [199, 200, 201, 202, 203, 204, 205, 5], we will be interested in particular in the theories called exceptional S-fold SCFTs introduced in [200].

Our interest in studying CFTs arises from their role as fixed points of the RG flow, making CFTs a basic building block of our understanding of quantum field theories. Alongside CFTs obtained as IR fixed points of Lagrangian theories a large and interesting class of interacting CFTs can be obtained from string/M-theory, either through dimensional compactification or geometric engineering. Many of these theories lack a conventional Lagrangian description, therefore the study of their dynamics should involve an analysis of their stringy construction, aided by field theoretical constraints, for example those originating by symmetries.

When, on top of the conformal symmetry, a CFT also enjoys supersymmetry then field theoretical results can strongly constrain a theory. As an example it is widely believed that in 4d with 16+16 conserved supercharges all the CFTs are classified by $\mathcal{N} = 4$ SYM theories with arbitrary gauge group, possibly with the addition of topological terms in the action. With a lower amount of supersymmetry such a complete classification is not available, although some progress has been made in the last two decades for SCFTs with $\mathcal{N} \geq 2$ SUSY [206, 207, 208, 209, 210, 211, 212, 213, 214, 215, 216, 217, 218, 219, 220, 221, 222, 223, 224, 225, 204, 226, 227, 203, 228, 229]. An important ingredient that renders a classification program feasible is the existence of a Coulomb branch (CB), an r -complex-dimensional space of vacua, with r the rank of the SCFT, where on general points the low energy dynamics is that of a $\mathcal{N} \geq 2$ $U(1)^r$ gauge theory where all the charged states are massive. On non-general singular points of the CB some charged states become massless and give rise to non-trivial dynamics in the IR.

The the analysis of the interesting physics of $\mathcal{N} \geq 2$ SCFTs boils down to what happens at singularities of the CB, as discussed for example in the seminal paper by Seiberg and Witten [230]. The theory arising on a codimension- n singularity is a theory with rank $n < r$, making it possible to study $\mathcal{N} \geq 2$ SCFTs “by induction” on the rank: the properties of a rank- r theory are related to the properties of the theories supported on its singularities, which have rank less than r . This procedure has been referred as CB stratification [204] and in the following we will borrow this terminology.

We will adapt the general ideas of the stratification to the charge lattice Γ of $\mathcal{N} \geq 2$ theories which is the lattice of electromagnetic charges under $U(1)^r$ of the massive states in a generic vacua of the CB, and the associated Dirac pairing J . In $\mathcal{N} = 2$ theories there is a close connection between the charge lattice Γ and the 1-form symmetry group $G^{(1)}$ [29, 231, 14, 232], which allow us to study the generalized symmetries of these theories directly from their charge lattices. Indeed the objects charged under 1-form symmetries, which are Wilson-’t Hooft lines [233] in a generic CB vacua, are constrained by the spectrum of charged local states through the Dirac quantization condition. For example, given a basis of the charge lattice, the Dirac pairing matrix J in this basis is related to the order of $G^{(1)}$ as follows [231]:

$$\left|G^{(1)}\right| = |\text{Pf}(J)| \quad (8.1)$$

It is possible to obtain more refined informations about the 1-form symmetries and the spectrum of line operators from the charge lattice. The electromagnetic charges of line operators can be obtained as a maximal set of charges that can be added to the charge lattice Γ without breaking the Dirac quantization condition. Generally there are multiple choices for this set of line operators which correspond to multiple *global structures* for the same local dynamics. A rough outline of the procedure is as follows. Given a charge lattice Γ then any line operator ℓ must have integer Dirac pairing with any charge in Γ :

$$\langle \ell, \gamma \rangle \in \mathbb{Z} \quad \forall \gamma \in \Gamma \quad (8.2)$$

in order for the line operator to be well defined with respect to the Aharonov-Bohm effect. For the same reason, any two line operators ℓ_i, ℓ_j must satisfy:

$$\langle \ell_i, \ell_j \rangle \in \mathbb{Z} \quad \forall i, j \quad (8.3)$$

The analysis of the solutions of (8.2) and (8.3) is simplified by the fact that the non-trivial information about the line spectrum is contained in the lines with charges inside the fundamental domain in Γ , therefore we can study line operators up to the equivalence relations:

$$\ell \sim \ell + \gamma \quad \forall \gamma \in \Gamma \quad (8.4)$$

In Chapter 9 we will determine the 1-form symmetries and global structures of a class of $\mathcal{N} = 3$ SCFTs called S-fold SCFTs by explicitly computing the charges of line operators, the results are summarized in Table 9.1.

2-form symmetries, on the other hand, are related to discrete gauging [28]. In 4d gauging a discrete 0-form symmetry generates a magnetic 2-form symmetry, whose topological operators are the Wilson lines of the discrete gauge group. On top of that, if the 0-form symmetry acts non-trivially on the CB, gauging it generates singularities on the CB in correspondence of the fixed points under the action of the symmetry. There are no massless states on these new singularities, therefore there are no BPS states whose central

charge vanishes there. This means that 2-form symmetries can be used as indicators of discrete gauging, and the same is true for CB singularities with no massless charged state. In Chapter 10 we study this phenomena in S-fold SCFTs as well as in exceptional S-fold SCFTs. We will recover the known results for S-fold SCFTs, obtained via M-theory considerations in [199], and we will show that some exceptional S-fold SCFTs are discrete gauging of free theories. Our results for exceptional S-fold SCFTs are summarized in Table 10.1.

All in all, in $\mathcal{N} \geq 2$ SCFTs the structure of higher form symmetries can give information about the local dynamics, namely on the charge lattice and BPS condition of charged states, and viceversa. In this thesis we only study SCFTs with $\mathcal{N} = 3$ supersymmetry, but the techniques described can be applied to the case of $\mathcal{N} = 2$ SCFTs as well.

8.1 S-fold SCFTs

Historically, S-folds represent the first examples of $\mathcal{N} = 3$ SCFTs in four spacetime dimensions, discovered by Garcia-Etxebarria and Regalado in [197]. A key role in the analysis of [197] is based on the existence, in the string theory setup, of non-perturbative extended objects that generalizes the notion of orientifolds, the *S*-folds (see [234, 235] for their original definition). From the field theory side, the projection implied by such *S*-folds on $\mathcal{N} = 4$ SYM has been associated to the combined action of an R-symmetry and an S-duality twist on the model at a fixed value of the holomorphic gauge coupling, where the global symmetry is enhanced by opportune discrete factors. Four possible \mathbb{Z}_k have been identified, corresponding to $k = 2, 3, 4$ and 6 . While the \mathbb{Z}_2 case corresponds to the original case of the orientifolds [163, 164, 165, 166, 167, 168], where actually the holomorphic gauge coupling does not require to be fixed, the other values of k correspond to new projections that can break supersymmetry down to $\mathcal{N} = 3$. The analysis has been further refined in [199], where the discrete torsion, in analogy with the case of orientifolds, has been added to this description. In this way, it has been possible to achieve a classification of such $\mathcal{N} = 3$ *S*-folds SCFT in terms of the Shephard–Todd complex reflection groups.

S-fold SCFTs can be engineered in Type IIB string theory as the low energy theory on the worldvolume of a stack of n D3-branes that probe a terminal singularity. This singularity is obtained by a \mathbb{Z}_k quotient of Type IIB which involves both a spacetime orbifold and an S-duality action, which becomes a symmetry for particular values of the axiodilaton. The spacetime orbifold is $\mathbb{R}^{3,1} \times (\mathbb{C}^3/\mathbb{Z}_k)$, where D3-branes are extended along $\mathbb{R}^{3,1}$, and the S-duality action is given by an element $\rho_k \in SL(2, \mathbb{Z})$ of the S-duality group of Type IIB. One can think about this non-geometric spacetime as follows: looping around a cycle in $\mathbb{C}^3/\mathbb{Z}_k$ every object in string theory is acted upon by the S-duality transformation ρ_k . This Type IIB non-geometric singularity can alternatively be described by a geometric singularity in F-theory, where the F-theory torus has a ρ_k monodromy around the $\mathbb{C}^3/\mathbb{Z}_k$ singularity. The F-theory picture will not be relevant in this paper, and we refer the reader to the original literature on this topic [197, 199].

The S-duality element ρ_k must generate a \mathbb{Z}_k subgroup of $SL(2, \mathbb{Z})$, which is only possible for $k = 1, 2, 3, 4, 6$. Furthermore, the axiodilaton τ must be fixed by ρ_k in order for the subgroup generated by ρ_k to be a symmetry of the theory. The S-duality elements ρ_k with the corresponding values of τ are listed in Table 9.2. In the absence of the S-fold the stack of D3 brane preserves sixteen supercharges in 4d: $Q_i, i = 1, 2, 3, 4^1$. The S-duality

¹Each Q is a four dimensional Dirac spinor with four components.

transformation ρ_k acts on the supercharges as [236]:

$$\rho_k : Q_i \rightarrow e^{\frac{\pi i}{k}} Q_i \quad i = 1, 2, 3, 4 \quad (8.5)$$

On the other hand the spacetime orbifold corresponds to an R-symmetry transformation $r_k \in SU(4)_R$ and can be chosen such that its action on the supercharges is:

$$r_k : \begin{cases} Q_i \rightarrow e^{-\frac{\pi i}{k}} Q_i & i = 1, 2, 3 \\ Q_4 \rightarrow e^{\frac{3\pi i}{k}} Q_4 \end{cases} \quad (8.6)$$

Under the combined action $\rho_k \cdot r_k$ the supercharges $Q_{1,2,3}$ are preserved while Q_4 transforms as:

$$\rho_k \cdot r_k : Q_4 \rightarrow e^{\frac{2\pi i}{k}} Q_4 \quad (8.7)$$

For $k = 1, 2$ this supercharge is preserved as well and the resulting 4d theory has $\mathcal{N} = 4$ supersymmetry. The case $k = 1$ corresponds to no projection at all, and engineers $\mathfrak{su}(N)$ $\mathcal{N} = 4$ SYM, while the case $k = 2$ corresponds to the orientifold plane $O3$ and engineers $\mathcal{N} = 4$ SYM with gauge algebra $\mathfrak{d}_n, \mathfrak{b}_n$ or \mathfrak{c}_n depending on the discrete torsion to be discussed briefly. The cases of interest in this paper are $k = 3, 4, 6$ where generally only twelve supercharges are preserved and the low energy theory on the stack of D3-branes is an $\mathcal{N} = 3$ SCFT.

It was shown in [199] that generally one has the possibility to introduce a discrete torsion in the S-fold background, that is a non-trivial flux for the Type IIB 2-form fields B_2 and C_2 around a non-contractible 2-cycle of the holographic background $AdS_5 \times (S^5/\mathbb{Z}_k)$. The 2-form fields transform in the two dimensional representation of the S-duality group $SL(2, \mathbb{Z})$, therefore their flux on this 2-cycle is classified by the second twisted cohomology groups $H_2(AdS_5 \times (S^5/\mathbb{Z}_k); (\mathbb{Z} \oplus \mathbb{Z})_{\rho_k}) = H_2(S^5/\mathbb{Z}_k; (\mathbb{Z} \oplus \mathbb{Z})_{\rho_k})$. These groups were computed in [199], see also [237] for a review. One finds:

$$H_2 \left(S^5/\mathbb{Z}_k; (\mathbb{Z} \oplus \mathbb{Z})_{\rho_k} \right) = \begin{cases} \mathbb{Z}_2 \times \mathbb{Z}_2, & k = 2 \\ \mathbb{Z}_3, & k = 3 \\ \mathbb{Z}_2, & k = 4 \\ \mathbb{1}, & k = 6 \end{cases} \quad (8.8)$$

where $\mathbb{1}$ is the trivial group. Therefore there are four choices of discrete torsion for the orientifold ($k = 2$) corresponding to the $O3^-$, $O3^+$, $\widetilde{O3}^-$ and $\widetilde{O3}^+$ orientifold planes respectively. For $k = 3$ there are three choices, one with trivial discrete torsion and two with non-trivial discrete torsion. The two choices with non-zero discrete torsion are related by charge conjugation so there are only two physically different choices: trivial or non-trivial discrete torsion. Finally for $k = 4$ one can have trivial or non-trivial discrete torsion and for $k = 6$ the only choice is to have trivial discrete torsion.

In summary the S-fold setup of [197], briefly reviewed above, gives rise to an infinite family of $\mathcal{N} = 3$ SCFTs parametrized by the number r of D3-branes, the order of the quotient k and, when allowed, the choice of discrete torsion. There are five variants of $\mathcal{N} = 3$ S-folds which we denote as $S_{k,\ell}$ following the notation of [199]. Here $\ell = 1$ corresponds to the absence of discrete torsion and $\ell = k$ corresponds to non-trivial discrete torsion. The five variants are therefore $S_{3,1}, S_{4,1}, S_{6,1}, S_{3,3}$ and $S_{4,4}$.

8.2 Exceptional S-folds

In [197] the authors presented an alternative M-theory construction of regular S-fold theories dual to the Type IIB setup described above. This allowed them to generalize the S-fold construction of [197] to a wider class of theories parametrize by an ADE algebra and the order of the S-fold projection $k = 3, 4, 6$. In this classification the regular S-folds are associated to the A_n algebras. Let us briefly review the results of [197] in preparation for Chapter 10, where we will analyze various properties of the S-folds associated to the E_r algebras.

The S-fold projection involves an element of the S-duality group as well as an element of the R-symmetry $SO(6)$ of $\mathcal{N} = 4$ $SU(N)$ SYM, which is a rotation transverse to the D3 branes in the Type IIB setup. By compactifying two directions T_E^2 transverse to the D3-brane stack we generally break the R-symmetry to $SO(4) \times \mathbb{Z}_2$, although for particular values of the complex structure of the torus the R-symmetry enhances to $SO(4) \times \mathbb{Z}_4$ for $\tau_E = i$ or $SO(4) \times \mathbb{Z}_6$ for $\tau_E = e^{2\pi i/3}$. These subgroups of the original $SO(6)$ R-symmetry are enough to perform the S-fold projection.

Now we may T-dualize along one compact transverse direction, giving a Type IIA setup, and then uplift to M-theory. By carefully tracking the action of the various symmetries along these manipulations, it was shown that the regular S-fold setup is dual to M-theory on $\mathbb{R}^{1,3} \times (S_M^1 \times S_T^1 \times S_E^1 \times \mathbb{C}^2)/\mathbb{Z}_k$, with a stack of N M5-branes along $\mathbb{R}^{1,3} \times S_M^1 \times S_T^1$. The radii of the various circles are related by:

$$R_M = R \quad R_T = \text{Im}(\tau)R \quad R_E = \frac{1}{\text{Im}(\tau)R^2} \tag{8.9}$$

And the \mathbb{Z}_k quotient act as a rotation on \mathbb{C}^2 and on the torus $S_M^1 \times S_T^1$, as well as a non-geometric quotient on $S_M^1 \times S_T^1 \times S_E^1$ fixing the ρ parameter of this torus to be order 1:

$$\rho = \int_{T^3} C + i\sqrt{\det G} \tag{8.10}$$

We now have an S-fold construction that involves a stack of N M5-branes. Famously, on flat spacetime, this stack engineers the $(2, 0)$ 6d theory of type A_N once the center of mass motion is decoupled. It is natural to ask whether it is possible to generalize this setup to the other $(2, 0)$ 6d theories, namely the type D and type E theories. In [197] it was shown that such a construction is possible and involves a non-geometric setup, meaning that there is no duality frame where the system is described by string theory in a geometric background. By contrast, the regular S-fold setup is dual to F-theory on a geometric terminal singularity.

In this thesis we will study exceptional S-fold theories as a particular projection of the corresponding $\mathcal{N} = 4$ SYM theories obtained by compactifying the $(2, 0)$ theory on a torus. Indeed both the R-symmetry and the S-duality involved in the S-fold quotient are present in the 4d theory, allowing us to understand some properties of the S-fold theories directly in 4d. There are some subtleties in this approach given by the fact that quantities of interest, for example the moduli space and the charge lattice, are only defined up to Weyl transformations of the gauge algebra, as explained in [5]. This approach is expanded upon in Chapter 8, while we refer the reader to the original literature [197, 238] for the M-theory construction of exceptional S-fold theories.

A recipe for genuine lines: 1-form symmetries in S -fold SCFTs

The goal of this Chapter consists in classifying one-form symmetries for regular S -fold SCFTs, constructing the lattices of line operators and identifying which models possess non-invertible symmetries. The main motivation behind this expectation is that for the rank-2 S -folds, in absence of discrete torsion, the SCFTs enhance to $\mathcal{N} = 4$ SYM [199] where these properties are present. The existence of non-trivial one-form symmetries in some exceptional $\mathcal{N} = 3$ theories has also been argued in [217].

Our strategy adapts the one presented in [29] to S -fold setups. There, the spectrum of lines is built from the knowledge of the electromagnetic charges of massive states in a generic point of the Coulomb branch. These charges are read from the BPS quiver, under the assumption that the BPS spectrum is a good representative of the whole spectrum of electromagnetic charges. In the case of S -folds however such a BPS quiver description has not been worked out and we extract the electromagnetic charges of dynamical particles from the knowledge of the (p, q) -strings configurations in the Type IIB setup [239, 240]. The main assumption behind the analysis is that such charges are a good representative of the electromagnetic spectrum.

We proceed as follows. First we choose an $\mathcal{N} = 3$ theory constructed via an S -fold projection of Type IIB. This consists in having N D3-branes, together with their images, on the background of an S -fold. At a generic point of the Coulomb branch, the corresponding low energy gauge dynamics corresponds to a $U(1)^N$ gauge theory where each $U(1)$ is associated to a D3. Then we list all (p, q) -strings that can be stretched between D3-branes and their images. They have electric and magnetic charges with respect to $U(1)^N$. Eventually we run the procedure of [29]. This consist in finding all the lines that are genuine, i.e. have integer Dirac pairing with the local particles, modulo screening by the dynamical particles. This gives the lattice of possible charges, then the different global structures correspond to maximal sub-lattices of mutually local lines.

Our results are summarized in Table 9.1. In the first column, one finds the type of S -fold projection that has been considered. Such projections are identified by the two integers k and ℓ in $S_{k,\ell}$. The integer k corresponds to the \mathbb{Z}_k projection while the second integer ℓ is associated to the discrete torsion. Then, when considering an $S_{k,\ell}$ S -fold on a stack of N D3-branes the complex reflection group associated to such a projection is $G(k, k/\ell, N)$. In the second column, we provide the one-form symmetry that we found in our analysis, and in the third, the number of inequivalent line lattices that we have obtained. The

S -fold	One-form symmetry	# of inequivalent lattices	Non-invertible symmetry
$S_{3,1}$	\mathbb{Z}_3	2	Yes
$S_{3,3}$	$\mathbb{1}$	1	No
$S_{4,1}$	\mathbb{Z}_2	2	Yes
$S_{4,4}$	$\mathbb{1}$	1	No
$S_{6,1}$	$\mathbb{1}$	1	No

Table 9.1 Summary of the results of Chapter 9. $\mathbb{1}$ represents a trivial group.

last column specifies whether there exist cases that admit non-invertible symmetries. Indeed, here we find that in some of the cases there exists a zero-form symmetry mapping some of the different line lattices, that are therefore equivalent. Furthermore in such cases we expect the existence of non-invertible symmetries obtained by combining the zero-form symmetry with a suitable gauging of the one-form symmetry.

A remarkable observation strengthening our results regards the fact that our analysis reproduces the limiting $G(k, k, 2)$ cases, where supersymmetry enhances to $\mathcal{N} = 4$ with $\mathfrak{su}(3)$, $\mathfrak{so}(5)$ and \mathfrak{g}_2 gauge groups for $k = 3, 4$ and 6 respectively. Another check of our result is that it matches with the cases $G(3, 1, 1)$ and $G(3, 3, 3)$, where an $\mathcal{N} = 1$ Lagrangian picture has been worked out in [241]. The 1-form symmetries of S -fold SCFTs were also computed in [237] from the Type IIB setup. Whenever our results can be compared with those of [237] we find a perfect agreement, providing a reliable and independent check for our results.

9.1 Generalities

9.1.1 Global structures from the IR

The strategy adopted here, as already discussed in the introduction, is inspired by the one of [29]. The main difference is that instead of using BPS quivers, not yet available for our S -folds, we take advantage of the type IIB geometric setups and probe the charge spectrum with (p, q) -strings – the bound state of p fundamental strings F1 and q Dirichlet strings D1.¹

Despite this difference, the rest of the procedure is the one of [29] which we now summarize. Denote as

$$\gamma^i = (e_1^{(i)}, m_1^{(i)}; \dots; e_r^{(i)}, m_r^{(i)}) \quad (9.1)$$

a basis vector of the electromagnetic lattice of dynamical state charges under the $U(1)_e^r \times U(1)_m^r$ gauge symmetry on the Coulomb branch. The spectrum of lines can be determined by considering a general line \mathcal{L} with charge

$$\ell = (e_1^{(l)}, m_1^{(l)}; \dots; e_r^{(l)}, m_r^{(l)}). \quad (9.2)$$

This is a genuine line operator if the Dirac pairings with all dynamical states Ψ are inte-

¹In order to provide the IR spectrum of line operators of the SCFTs from this UV perspective, we assume the absence of wall-crossing. While such an assumption is *a priori* motivated by the high degree of supersymmetry, *a posteriori* it is justified by the consistency of our results with the literature.

ger:

$$\langle \Psi, \mathcal{L} \rangle \in \mathbb{Z} \quad \forall \Psi. \tag{9.3}$$

This can be rephrased as the condition

$$\sum_{j=1}^r e_j^{(i)} m_j^{(l)} - m_j^{(i)} e_j^{(l)} \in \mathbb{Z} \quad \forall i. \tag{9.4}$$

Furthermore, inserting a local operator with charge γ_i on the worldline of a line with charge ℓ shifts its charge by γ_i . Therefore if a line with charge ℓ appears in the spectrum then a line with charges $\ell + \sum k_i \gamma_i$ with $k_i \in \mathbb{Z}$ must also appear. When classifying the spectrum of charges of the line operators of a QFT it is then useful to consider the charges ℓ modulo these insertions of local states. This gives rise to equivalence classes of charges with respect to the relation:

$$\ell \sim \ell + \gamma_i \quad \forall i. \tag{9.5}$$

Borrowing the nomenclature of [29], we will refer to such identification as screening and we will work with each equivalence class by picking one representative. The genuine lines after screening form a lattice. In general two such lines are not mutually local and a choice of global structure corresponds to a choice of a maximal sublattice of mutually local lines.

9.1.2 Charged states in $S_{k,l}$ -folds

We aim to determine the electromagnetic charges of the local states generated by (p, q) -strings stretched between (images of) D3-branes in presence of an S -fold. The S -fold background of Type IIB string theory consist of a spacetime $\mathbb{R}^4 \times (\mathbb{R}^6/\mathbb{Z}_k)$ where the \mathbb{Z}_k quotient involves an S-duality twist by an element $\rho_k \in SL(2, \mathbb{Z})$ of order k , where $k = 2, 3, 4, 6$. For $k > 2$ the value of the axio-dilaton vev is fixed by the requirement that it must be invariant under the modular transformation associated to ρ_k . The matrices ρ_k and the corresponding values² of τ are given in Table 9.2.

$SL(2, \mathbb{Z})$	$S^2 = -\mathbb{1}_2$	$(ST)^{-1}$	S	$(S^3T)^{-1}$
k	2	3	4	6
ρ_k	$\begin{pmatrix} -1 & 0 \\ 0 & -1 \end{pmatrix}$	$\begin{pmatrix} 0 & 1 \\ -1 & -1 \end{pmatrix}$	$\begin{pmatrix} 0 & -1 \\ 1 & 0 \end{pmatrix}$	$\begin{pmatrix} 0 & -1 \\ 1 & 1 \end{pmatrix}$
ρ_k^{-1}	$\begin{pmatrix} -1 & 0 \\ 0 & -1 \end{pmatrix}$	$\begin{pmatrix} -1 & -1 \\ 1 & 0 \end{pmatrix}$	$\begin{pmatrix} 0 & 1 \\ -1 & 0 \end{pmatrix}$	$\begin{pmatrix} 1 & 1 \\ -1 & 0 \end{pmatrix}$
τ	any τ	$e^{2i\pi/3}$	i	$e^{2i\pi/3}$

Table 9.2 Elements ρ_k of $SL(2, \mathbb{Z})$ of order k used in S -fold projections, and the corresponding fixed coupling τ .

A stack of N D3-branes probing the singular point of the S -fold background engineer an

²In our convention, an $SL(2, \mathbb{Z})$ transformation of the axio-dilaton $\tau \rightarrow (a\tau + b)/(c\tau + d)$ relates to a matrix $\rho_k = \begin{pmatrix} d & c \\ b & a \end{pmatrix}$. We also have $S = \begin{pmatrix} 0 & -1 \\ 1 & 0 \end{pmatrix}$ and $T = \begin{pmatrix} 1 & 0 \\ 0 & 1 \end{pmatrix}$.

$\mathcal{N} = 3$ field theory on the worldvolume of the stack of D3-branes. It is useful to consider the k -fold cover of spacetime, and visualize the N D3-branes together with their $(k-1)N$ images under the S_k -fold projection. We are going to label the m -th image of the i -th D3-brane with the index i_m , where $i = 1, \dots, N$ and $m = 1, \dots, k$.

Under the S -fold projection, the two-form gauge fields of the closed string sector B_2 and C_2 transform in the fundamental representation:

$$\begin{pmatrix} B_2 \\ C_2 \end{pmatrix} \rightarrow \rho_k \begin{pmatrix} B_2 \\ C_2 \end{pmatrix}. \quad (9.6)$$

Consistently, the (p, q) strings charged under these potentials are mapped to (p', q') where:

$$(p' q') = (p q) \cdot \rho_k^{-1}. \quad (9.7)$$

We denote a state associated to a (p, q) connecting the i_m -th D3-brane and the j_n D3-brane as:

$$|p, q\rangle_{i_m, j_n} = |-p, -q\rangle_{j_n, i_m}, \quad (9.8)$$

where we identify states with both opposite charges and orientation.

First, strings linking branes in the same copy of $\mathbb{R}^6/\mathbb{Z}_2$ transform as follows:

$$|p, q\rangle_{i_m, j_m} \rightarrow \zeta_k^{-1} |p', q'\rangle_{i_{m+1}, j_{m+1}}, \quad (9.9)$$

where (p', q') are related to (p, q) by (9.7) and ζ_k is the primitive k -th root of unity. These states always collectively give rise to a single state in the quotient theory, with charges:

$$D3_i D3_j : (0, 0; \dots; \overbrace{p, q}^{i\text{-th}}; \dots; \overbrace{-p, -q}^{j\text{-th}}; \dots; 0, 0). \quad (9.10)$$

An important ingredient we need to add to our picture is the discrete torsion for B_2 and C_2 [242, 199]. In presence of such a discrete torsion, a string going from the i_m -th brane to the j_{m+1} -th brane should pick up an extra phase which depends only on its (p, q) -charge and the couple $(\theta_{\text{NS}}, \theta_{\text{RR}})$. More precisely, one expects that the S -fold action can be written as follows [243]:³

$$|p, q\rangle_{i_m, j_{m+1}} \rightarrow \zeta_k^{-1} e^{2\pi i(p\theta_{\text{NS}} + q\theta_{\text{RR}})} |p', q'\rangle_{i_{m+1}, j_{m+2}}, \quad (9.11)$$

where again (p', q') are related to (p, q) by (9.7). For $i \neq j$, this always leads to the following state in the projected theory [244, 245]:⁴

$$D3_i D3_j^\rho : (0, 0; \dots; \overbrace{p, q}^{i\text{-th}}; \dots; \overbrace{-(p q) \cdot \rho_k}^{j\text{-th}}; \dots; 0, 0). \quad (9.12)$$

Note that this is the only case that might not lead to any state in the quotient theory when $i = j$, i.e. when a string links a brane and its image. When the quotient state exists, it has

³We thank Shani Meynet for pointing out [243] to us.

⁴The action on (p, q) involves ρ_k^{-1} , see (9.7). In writing (9.12) however, we measure the charge with respect to the brane in the chosen fundamental domain, hence the appearance of ρ_k instead of its inverse.

charges

$$D3_i D3_i^\rho : (0, 0; \dots; \overbrace{(p\ q) - (p\ q) \cdot \rho_k}^{i\text{-th}}; \dots; 0, 0) . \tag{9.13}$$

Analogously, strings twisting around the S-fold locus n -times pick up n -times the phase in (9.11).

A last remark is that discrete torsion allows some strings to attach to the S-fold if the latter has the appropriate NS and/or RR charge. If this is the case, the state is mapped as in (9.9):

$$|p, q\rangle_{S_k i_m} \rightarrow |p', q'\rangle_{S_k i_{m+1}} , \tag{9.14}$$

and provides the following charge in the projected theory:

$$S_k D3_i : (0, 0; \dots; \overbrace{p, q}^{i\text{-th}}; \dots; 0, 0) . \tag{9.15}$$

These rules are illustrated and details on discrete torsion are provided in the remaining of this section for orientifolds and S-folds separately.

The case with $k = 2$: orientifolds

In this subsection we apply the formalism described above for orientifolds and reproduce the spectrum of strings known in the literature.

The matrix ρ_2 is diagonal, therefore the two p and q factors can be considered independently. In this case the field theory obtained after the projection is Lagrangian and can be studied in perturbative string theory with unoriented strings. Discrete torsion takes value in $(\theta_{NS}, \theta_{RR}) \in \mathbb{Z}_2 \oplus \mathbb{Z}_2$, giving four different choices of O3-planes related by $SL(2, \mathbb{Z})$ actions [242], see Table 9.3.

O3-planes	$O3^-$	$O3^+$	$\widetilde{O3}^-$	$\widetilde{O3}^+$
$(\theta_{NS}, \theta_{RR})$	$(0, 0)$	$(1/2, 0)$	$(0, 1/2)$	$(1/2, 1/2)$

Table 9.3 Different discrete torsions on O3-planes.

The orientifold action is then recovered from (9.9) and (9.11) with $\zeta_2 = -1$. First, we have

$$|p, q\rangle_{i_1 j_1} \rightarrow -| -p, -q\rangle_{i_2 j_2} = -|p, q\rangle_{j_2 i_2} . \tag{9.16}$$

For the strings that stretch from one fundamental domain of $\mathbb{R}^6/\mathbb{Z}_2$ to the next, there are four cases depending on the values of θ_{NS} and θ_{RR} :

$$\begin{aligned} O3^- & : |p, q\rangle_{i_1 j_2} \rightarrow -|p, q\rangle_{j_1 i_2} , \\ O3^+ & : |p, q\rangle_{i_1 j_2} \rightarrow -e^{p\pi i} |p, q\rangle_{j_1 i_2} , \\ \widetilde{O3}^- & : |p, q\rangle_{i_1 j_2} \rightarrow -e^{q\pi i} |p, q\rangle_{j_1 i_2} , \\ \widetilde{O3}^+ & : |p, q\rangle_{i_1 j_2} \rightarrow -e^{(p+q)\pi i} |p, q\rangle_{j_1 i_2} . \end{aligned} \tag{9.17}$$

The cases with $k > 2$: S -folds

The construction discussed above can be applied to $S_{k>2}$ in order to obtain the string states in the quotient theory. For $k > 2$, the discrete torsion groups have been computed in [199], the result being $\theta_{\text{NS}} = \theta_{\text{RR}} \in \mathbb{Z}_3$ for the S_3 -case and $\theta_{\text{NS}} = \theta_{\text{RR}} \in \mathbb{Z}_2$ for the S_4 -case. The S_6 -fold does not admit non-trivial discrete torsion. It was also pointed out that, for the S_3 -case, the choices $\theta_{\text{NS}} = \theta_{\text{RR}} = 1/3$ and $\theta_{\text{NS}} = \theta_{\text{RR}} = 2/3$ are related by charge conjugation; therefore everything boils down to whether the discrete torsion is trivial or not. Following the notation of [199], we denote as $S_{k,1}$ the S -folds with trivial discrete torsion and as $S_{k,k}$ the S -folds with non-trivial discrete torsion.

As before, the only states that might not lead to any state in the quotient theory are the strings linking different covers of $\mathbb{R}^6/\mathbb{Z}_k$. These transform as follows:

$$\begin{aligned}
 S_{3,1} &: |p, q\rangle_{i_1 j_{m+1}} \rightarrow e^{-i2\pi/3} |q - p, -p\rangle_{i_2 j_{m+2}}, \\
 S_{3,3} &: |p, q\rangle_{i_1 j_{m+1}} \rightarrow e^{-i2\pi/3} e^{im(p+q)2\pi/3} |q - p, -p\rangle_{i_2 j_{m+2}}, \\
 S_{4,1} &: |p, q\rangle_{i_1 j_{m+1}} \rightarrow e^{-i\pi/2} | -q, p\rangle_{i_2 j_{m+2}}, \\
 S_{4,4} &: |p, q\rangle_{i_1 j_{m+1}} \rightarrow e^{-i\pi/2} e^{im(p+q)\pi} | -q, p\rangle_{i_2 j_{m+2}}, \\
 S_{6,1} &: |p, q\rangle_{i_1 j_{m+1}} \rightarrow e^{-i\pi/3} |p - q, p\rangle_{i_2 j_{m+2}}.
 \end{aligned} \tag{9.18}$$

This shows that no state is projected out for $S_{3,1}$ and $S_{3,3}$. Analogously to the orientifold cases, we project out some strings linking mirror branes: $|p, q\rangle_{i_n i_{n+2}}$ in $S_{4,1}$ and $S_{4,4}$, and $|p, q\rangle_{i_n i_{n+3}}$ in $S_{6,1}$ respectively.

Finally, we get extra strings linking the S -fold to D-branes for the cases with discrete torsion. Following the discussion in [245], we know that these S -folds admit all kinds of p and q numbers:

$$S_{3,3} : |p, q\rangle_{S_{3,3} i_n}, \quad S_{4,4} : |p, q\rangle_{S_{4,4} i_n}. \tag{9.19}$$

9.1.3 Dirac pairing from (p, q) -strings

Having determined the states associated to (p, q) -strings that survive the S -fold projection we now analyze the electromagnetic charges of these states. It is useful to consider the system of a stack of D3-branes and an $S_{k,\ell}$ -fold on a generic point of the Coulomb branch. This corresponds to moving away the D3-branes from the S -plane. On a generic point of the Coulomb branch, the low energy theory on the D3-branes is a $U(1)_i^N$ gauge symmetry, where each $U(1)_i$ factor is associated to the i -th D3-brane. The theory includes massive charged states generated by the (p, q) -strings studied in the previous section. A (p, q) -string stretched between the i -th and j -th D3-brane has electric charge p and magnetic charge q under $U(1)_i$ as well as electric charge $-p$ and magnetic charge $-q$ under $U(1)_j$, and is neutral with respect to other branes. We organize the charges under the various $U(1)$ s in a vector:

$$(e_1, m_1; e_2, m_2; \dots; e_N, m_N) \tag{9.20}$$

where e_i and m_i are the electric and magnetic charge under $U(1)_i$, respectively. In this notation the charge of a string stretched between the i -th and j -th D3-brane in the same cover of $\mathbb{R}^6/\mathbb{Z}_2$ has charge:

$$D3_i D3_j : (0, 0; \dots; \overbrace{p, q}^{i\text{-th}}; 0, 0; \dots; \overbrace{-p, -q}^{j\text{-th}}; \dots), \tag{9.21}$$

where the dots stand for null entries. We will keep using this notation in the rest of the Chapter. A (p, q) -string stretched between the i -th D3-brane and the l -th image of the j -th D3-brane imparts electromagnetic charges (p, q) under $U(1)_i$ and charges $-(p, q)\rho_k^l$ under $U(1)_j$. In formulas:

$$D3_i D3_j^l : (0, 0; \dots; \overbrace{p, q}^{i-th}; 0, 0; \dots; \overbrace{-(p, q) \cdot \rho_k^l}^{j-th}; \dots). \quad (9.22)$$

The last ingredient for our analysis is given by the Dirac pairing between two states. Consider a state Ψ with charges e_i, m_i under $U(1)_i$ and a state Ψ' with charges e'_i, m'_i under $U(1)_i$. The pairing between F1 and D1-strings in Type IIB dictates that the Dirac pairing between these states is given by:

$$\langle \Psi, \Psi' \rangle = \sum_{i=1}^N (e_i m'_i - m_i e'_i). \quad (9.23)$$

By using this construction we can reproduce the usual Dirac pairing of $\mathcal{N} = 4$ SYM with $ABCD$ gauge algebras. As an example we now reproduce the Dirac pairing of D_N , engineered as a stack of N D3-branes probing an $O3^-$ -plane. In this case the allowed (p, q) -strings have the following charges:

$$\begin{aligned} D3_i D3_j : (0, 0; \dots; \overbrace{p, q}^{i-th}; 0, 0; \dots; \overbrace{-p, -q}^{j-th}; \dots) \\ D3_i D3_j^o : (0, 0; \dots; \overbrace{p, q}^{i-th}; 0, 0; \dots; \overbrace{p, q}^{j-th}; \dots) \end{aligned} \quad (9.24)$$

The states associated to $(1, 0)$ -strings correspond to the \mathcal{W} bosons while the states associated to $(0, 1)$ -strings correspond to magnetic monopoles \mathcal{M} . For each root \mathcal{W}_i of D_N let \mathcal{M}_i be the corresponding coroot. More precisely if \mathcal{W}_i is associated to a $(1, 0)$ -string connecting two D3-branes, then the coroot \mathcal{M}_i corresponds to the string $(0, 1)$ stretched between the same pair of D3-branes. The only non-vanishing Dirac pairing is the one between a \mathcal{W}_i boson and an \mathcal{M}_j monopole. This pairing between the simple (co)roots \mathcal{W}_i and \mathcal{M}_j is given by the intersection between \mathcal{W}_i and \mathcal{W}_j , explicitly:

$$\langle \mathcal{W}_i, \mathcal{M}_j \rangle = (A_{D_N})_{i,j}, \quad (9.25)$$

where A_{D_N} is the Cartan matrix of the D_N algebra, corresponding to an $\mathfrak{so}(2N)$ gauge theory. Indeed the intersection between F1 strings in the background of an $O3^-$ reproduces the intersection of the roots of D_N . The Dirac pairing (9.25) reproduces the Dirac pairing of $\mathfrak{so}(2N)$ $\mathcal{N} = 4$ SYM. Similar constructions for $O3^+$, $\widetilde{O3}^-$, and $\widetilde{O3}^+$ lead to the B and C cases (while branes in absence of orientifold would give A). The corresponding gauge algebras are summarized in Table 9.4.

9.1.4 Lines in O3-planes

Before moving to new results, we illustrate our method with well understood O3-planes. Specifically, we consider placing $N = 2$ D3-branes in the background of an $O3^+$ -plane.

In this specific example, the F1-strings corresponding to elementary dynamical states in

O3-planes	F1-string	D1-string	F1-D1 bound state
$O3^-$	$\mathfrak{so}(2N)$	$\mathfrak{so}(2N)$	$\mathfrak{so}(2N)$
$O3^+$	$\mathfrak{usp}(2N)$	$\mathfrak{so}(2N+1)$	$\mathfrak{usp}(2N)$
$\widetilde{O3}^-$	$\mathfrak{so}(2N+1)$	$\mathfrak{usp}(2N)$	$\mathfrak{usp}(2N)$
$\widetilde{O3}^+$	$\mathfrak{usp}(2N)$	$\mathfrak{usp}(2N)$	$\mathfrak{so}(2N+1)$

Table 9.4 F1-string, D1-string, and the F1-D1 bound state providing respectively the electric, magnetic, and dyonic charges of the projected $\mathcal{N} = 4$ gauge theory.

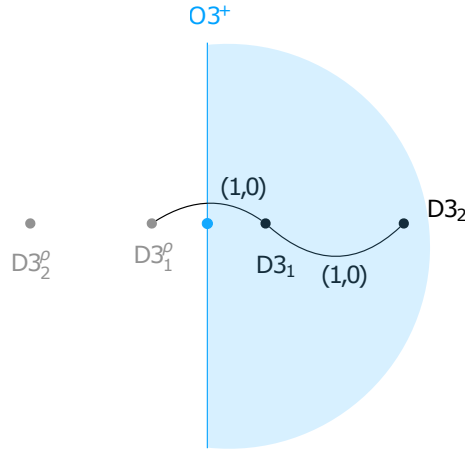


Figure 9.1 A pictorial representation of two D3-branes probing the $O3^+$ orientifold on a generic point of the Coulomb branch. The light blue shaded area is a possible choice of fundamental domain under the spacetime identification induced by the orientifold. Black (gray) dots represent (images of) D3-branes. Black lines correspond to (p, q) -strings stretched between D3-branes. In particular, we drew (p, q) -strings generating the \mathcal{W} -bosons corresponding to simple roots $\mathcal{N} = 4 \mathfrak{usp}(4)$ SYM.

the quotient theory can be chosen to be $|1, 0\rangle_{1_2 1_1}$ and $|1, 0\rangle_{1_1 2_1}$. The first links the $i = 1$ brane to its mirror ($D3_1^\rho D3_1$) and the second links the $i = 1$ to the $i = 2$ brane ($D3_1 D3_2$). A pictorial representation of this setup is shown in Figure 9.1. In the notation of the previous section, they lead to \mathcal{W}_i -bosons in the gauge theory with the following charge basis:

$$D3_1^\rho D3_1 : w_1 = (2, 0; 0, 0), \quad D3_1 D3_2 : w_2 = (-1, 0; 1, 0). \quad (9.26)$$

These generate the algebra $\mathfrak{usp}(4)$ of electric charges. The elementary magnetic monopoles \mathcal{M}_i come from the D1-strings $|0, 1\rangle_{O3^+ 1_1}$ and $|0, 1\rangle_{1_1 2_1}$, and provide the following charges:

$$O3^+ D3_1 : m_1 = (0, 1; 0, 0), \quad D3_1 D3_2 : m_2 = (0, -1; 0, 1). \quad (9.27)$$

This generates the algebra $\mathfrak{so}(5)$ of magnetic charges. Finally, the elementary $(1, 1)$ -strings leading to states in the quotient theory can be chosen to be $|1, 1\rangle_{1_2 1_1}$ and $|1, 1\rangle_{1_1 2_1}$,

i.e. $D3_1^{\ell}D3_1$ and $D3_1D3_2$ respectively. They provide dyons \mathcal{D}_i :

$$D3_1^{\ell}D3_1 : d_1 = (2, 2; 0, 0), \quad D3_1D3_2 : d_2 = (-1, -1; 1, 1), \quad (9.28)$$

which reproduces an $\mathfrak{usp}(4)$ algebra. We will limit ourselves to considering the \mathcal{W} -bosons and magnetic monopoles \mathcal{M} . Indeed, they generate the full lattice of electromagnetic charges admissible in the orientifold theory. See that

$$d_1 = w_1 + 2m_1 \quad d_2 = w_2 + m_2. \quad (9.29)$$

Clearly, all other allowed (p, q) -charges can be reconstructed in this way. The Dirac pairing between these elementary electromagnetic charges reads

$$\begin{aligned} \langle \mathcal{W}_1, \mathcal{W}_2 \rangle &= \langle \mathcal{M}_1, \mathcal{M}_2 \rangle = 0, \\ \langle \mathcal{M}_1, \mathcal{W}_2 \rangle &= 1, \\ \langle \mathcal{W}_1, \mathcal{M}_1 \rangle &= \langle \mathcal{M}_2, \mathcal{W}_1 \rangle = \langle \mathcal{W}_2, \mathcal{M}_2 \rangle = 2. \end{aligned} \quad (9.30)$$

Now, introduce a line operator \mathcal{L} with charge vector ℓ . It is convenient to express it in the basis of dynamical charges:

$$\ell = \alpha_1 w_1 + \alpha_2 w_2 + \beta_1 m_1 + \beta_2 m_2, \quad (9.31)$$

where α_i and β_i to be determined. Screening with respect to \mathcal{W}_1 and \mathcal{W}_2 imposes

$$\alpha_1 \sim \alpha_1 + 1, \quad \alpha_2 \sim \alpha_2 + 1, \quad (9.32)$$

respectively, while screening with respect to \mathcal{M}_1 and \mathcal{M}_2 imposes

$$\beta_1 \sim \beta_1 + 1, \quad \beta_2 \sim \beta_2 + 1. \quad (9.33)$$

Mutual locality with respect to the dynamical charges requires the quantities

$$\begin{aligned} \langle \mathcal{L}, \mathcal{W}_1 \rangle &= -2\beta_1 + 2\beta_2, & \langle \mathcal{L}, \mathcal{W}_2 \rangle &= \beta_1 - 2\beta_2, \\ \langle \mathcal{L}, \mathcal{M}_1 \rangle &= 2\alpha_1 - \alpha_2, & \langle \mathcal{L}, \mathcal{M}_2 \rangle &= -2\alpha_1 + 2\alpha_2, \end{aligned} \quad (9.34)$$

to be integers. All these constraints set

$$\alpha_1 = \frac{e}{2} \quad \alpha_2 = 0, \quad \beta_1 = 0, \quad \beta_2 = \frac{m}{2} \quad \text{mod } 1, \quad (9.35)$$

with $e, m = 0, 1$. Linearity of the Dirac pairing then guarantees mutual locality with respect to the full dynamical spectrum. Thus, the charge of the most general line (modulo screening) must read:

$$\ell_{e,m} = \frac{1}{2}(2e, -m; 0, m). \quad (9.36)$$

A choice of global structure consists in finding a set of mutually local lines. The mutual locality condition between two lines \mathcal{L} and \mathcal{L}' with charges $\ell_{e,m}$ and $\ell_{e',m'}$ is given by:

$$\langle \mathcal{L}, \mathcal{L}' \rangle = \frac{1}{2}(-em' + e'm) \in \mathbb{Z}. \quad (9.37)$$

Equivalently:

$$em' - me' = 0 \pmod{2}. \quad (9.38)$$

We find three such sets, each composed of a single line with non-trivial charge: $\ell_{1,0}$, $\ell_{0,1}$, or $\ell_{1,1}$. In agreement with [20], we find that the line with charge $\ell_{1,0}$ transforms as a vector of $\mathfrak{usp}(4)$ and the theory is $USp(4)$. The line with charge $\ell_{0,1}$ transforms as a spinor of $\mathfrak{so}(5)$ and corresponds to the global structure $(USp(4)/\mathbb{Z}_2)_0$. The line with charge $\ell_{1,1}$ transforms both as a vector and a spinor, and the gauge group is $(USp(4)/\mathbb{Z}_2)_1$. Motivated by the match between our results (obtained through the procedure described above) and the global structures of Lagrangian theories [20], in the next sections we use our method to analyze the line spectra of S -fold theories.

9.2 Lines in S -folds with $\mathcal{N} = 4$ enhancement

We now derive the spectrum of mutually local lines for the gauge theories obtained with $N = 2$ D3-branes in the background of an $S_{k,1}$ plane, in each case $k = 3, 4$ and 6 . More precisely, exploiting the strategy spelled out in Section 9.1, we first compute the electromagnetic charge lattice of local states generated by (p, q) -strings. From this we extract the possible spectra of lines and compare them with the ones obtained in an $\mathcal{N} = 4$ Lagrangian formalism [20], since these theories have been claimed to enhance to $\mathcal{N} = 4$ SYM [49]. Matching the spectra provides an explicit dictionary between the various lattices and corroborates the validity of our procedure. In section 9.3 we will then generalize the analysis to the pure $\mathcal{N} = 3$ $S_{k,\ell}$ projections for any rank, thus providing the full classification for the one-form symmetries in all such cases.

9.2.1 Lines in $\mathfrak{su}(3)$ from $S_{3,1}$

Dynamical states and their charges

Two D3-branes probing the singular point of the $S_{3,1}$ -fold are claimed to engineer $\mathfrak{su}(3)$ $\mathcal{N} = 4$ SYM. The charges of states generated by (p, q) -strings stretching between $D3_1$ and $D3_2$ or its first copy (see Figure 9.2) are

$$D3_1 D3_2 : (p, q; -p, -q), \quad D3_1 D3_2^\rho : (p, q; q, q-p), \quad D3_1 D3_2^{\rho^2} : (p, q; p-q, p). \quad (9.39)$$

One may also consider copies of the strings listed in Equation 9.39 such as:

$$D3_1^\rho D3_2^\rho : (-q, p-q; q, q-p), \quad (9.40)$$

as well as the strings going from one D3-brane to its own copies, for instance⁵

$$D3_1 D3_1^\rho : (2p-q, p+q; 0, 0). \quad (9.41)$$

The charges of a generic string $D3_1 D3_2^{\rho^2}$ in (9.39) can be expressed in terms of $D3_1 D3_2$

⁵In the absence of discrete torsion, these states have not been considered previously in the literature [246, 245], and we do here for the sake of consistency with the analysis of section 9.1. Note however that since their charge (which is the only feature that matters in order to derive line spectra) can be expressed as linear combinations of the charges of more conventional states, our results are independent of whether we consider them or not.

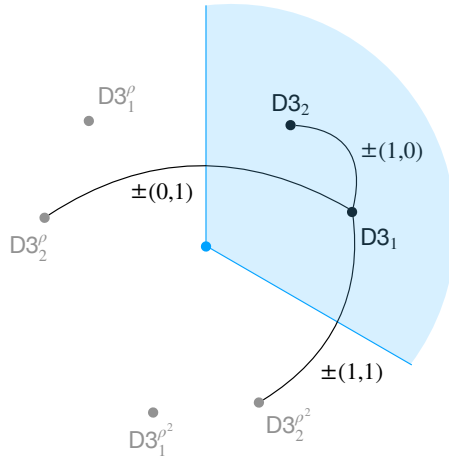


Figure 9.2 A pictorial representation of two D3-branes probing the $S_{3,1}$ -fold. The transverse directions to the S -fold are shown. The light blue dot represents the position of the $S_{3,1}$ -fold. The light blue shaded area is a possible choice of fundamental domain under the spacetime identification induced by the $S_{3,1}$ -fold. Black (gray) dots represent (images of) D3-branes. Black lines correspond to (p, q) -strings stretched between D3-branes. In particular, we drew (p, q) -strings corresponding to \mathcal{W} -bosons of $\mathcal{N} = 4 \mathfrak{su}(3)$ SYM.

and $D3_1 D3_2^\rho$ charges:

$$D3_1 D3_2^{\rho^2} : (p, q; p - q, p) = q(1, 0; -1, 0) + (q - p)(0, 1; 0, -1) + (p - q)(1, 0; 0, -1) + p(0, 1; 1, 1), \quad (9.42)$$

where the first two vectors on the RHS come from $D3_1 D3_2$ with $p = 1, q = 0$ and $p = 0, q = 1$ respectively, and the last two come from $D3_1 D3_2^\rho$ with $p = 1, q = 0$ and $p = 0, q = 1$ respectively. Acting with ρ_3 , one can express all $D3_1^\rho D3_2^\rho$ and $D3_1^{\rho^2} D3_2^{\rho^2}$ charges in terms of $D3_1 D3_2$ charges. The charges $D3_i D3_j^\rho$ can also be expressed as linear combinations of $D3_1 D3_2^\rho$ and $D3_2^\rho D3_1^\rho$ charges. All in all, we find that the charges of the strings $D3_1 D3_2$ and $D3_1 D3_2^\rho$ form a basis of the lattice of dynamical charges.

The states corresponding to the \mathcal{W} -bosons generate the $\mathfrak{su}(3)$ algebra. One can take the strings $D3_1 D3_2$ with $p = 1$ and $q = 0$ and $D3_1 D3_2^\rho$ with $p = 0$ and $q = 1$ as representing a choice of positive simple roots. Their electromagnetic charge w reads:

$$w_1 = (1, 0; -1, 0), \quad w_2 = (0, 1; 1, 1). \quad (9.43)$$

Furthermore, one can choose the strings $D3_1 D3_2$ with $p = 0$ and $q = 1$ and $D3_1 D3_2^\rho$ with $p = -1$ and $q = -1$ as generating the charge lattice of magnetic monopoles \mathcal{M} of $\mathcal{N} = 4$ SYM with gauge algebra $\mathfrak{su}(3)$:

$$m_1 = (0, 1; 0, -1), \quad m_2 = (-1, -1; -1, 0). \quad (9.44)$$

The qualification of electric charges \mathcal{W} and magnetic monopoles \mathcal{M} of the $\mathcal{N} = 4$ theory

makes sense since the Dirac pairing reads:

$$\begin{aligned}\langle \mathcal{W}_1, \mathcal{W}_2 \rangle &= \langle \mathcal{M}_1, \mathcal{M}_2 \rangle = 0, \\ \langle \mathcal{W}_1, \mathcal{M}_1 \rangle &= \langle \mathcal{W}_2, \mathcal{M}_2 \rangle = 2, \\ \langle \mathcal{W}_1, \mathcal{M}_2 \rangle &= \langle \mathcal{W}_2, \mathcal{M}_1 \rangle = -1.\end{aligned}\tag{9.45}$$

In [246, 245], it has been shown that these states correspond indeed to BPS states, and this is a strong check of the claim of the supersymmetry enhancement in this case.

Line lattices

Having identified the electromagnetic lattice of charges of (p, q) -strings we can now construct the spectrum of line operators and the corresponding one-form symmetries. It is useful to consider the charge $\ell = (e_1, m_1; e_2, m_2)$ of a general line \mathcal{L} to be parameterized as follows:

$$\begin{aligned}\ell &= \alpha_1 w_1 + \alpha_2 w_2 + \beta_1 m_1 + \beta_2 m_2 \\ &= (\alpha_1 - \beta_2, \alpha_2 + \beta_1 - \beta_2; -\alpha_1 + \alpha_2 - \beta_2, \alpha_2 - \beta_1).\end{aligned}\tag{9.46}$$

Screening with respect to w_i and m_i translates as the identifications:

$$\alpha_i \sim \alpha_i + 1, \quad \beta_i \sim \beta_i + 1.\tag{9.47}$$

The Dirac pairing between the generic line \mathcal{L} with charge ℓ given in (9.46) and the states \mathcal{W} and \mathcal{M} must be an integer, i.e.:

$$\begin{aligned}\langle \mathcal{L}, \mathcal{W}_1 \rangle &= 2\beta_1 - \beta_2, & \langle \mathcal{L}, \mathcal{W}_2 \rangle &= -\beta_1 + 2\beta_2, \\ \langle \mathcal{L}, \mathcal{M}_1 \rangle &= -2\alpha_1 + \alpha_2, & \langle \mathcal{L}, \mathcal{M}_2 \rangle &= \alpha_1 - 2\alpha_2\end{aligned} \in \mathbb{Z}.\tag{9.48}$$

Mutual locality with respect to the other states then follows by linearity as soon as (9.48) holds. Combining (9.47) and (9.48) we have

$$\alpha_1 = -\alpha_2 = \frac{e}{3}, \quad \text{and} \quad \beta_1 = -\beta_2 = \frac{m}{3},\tag{9.49}$$

for $e, m = 0, 1, 2$. Then, the charge of the most general line compatible with the spectrum of local operators modulo screening reads

$$\ell_{e,m} = \frac{1}{3}(2e - m, e + m; -e - m, e - 2m).\tag{9.50}$$

These charges form a finite 3×3 square lattice. The Dirac pairing between two lines \mathcal{L} and \mathcal{L}' with charges $\ell_{e,m}$ and $\ell_{e',m'}$ is

$$\langle \mathcal{L}, \mathcal{L}' \rangle = \frac{2}{3}(em' - e'm).\tag{9.51}$$

Two lines \mathcal{L} and \mathcal{L}' are mutually local if their Dirac pairing is properly quantized. In our conventions this corresponds to the requirement that $\langle \mathcal{L}, \mathcal{L}' \rangle$ is an integer:

$$e'm - em' = 0 \pmod{3}.\tag{9.52}$$

The lattice of lines together with the mutual locality condition obtained in (9.52) fully

specifies the global structure of the $S_{3,1}$ SCFT of rank-2.

Our result is equivalent to the one obtained in [20] from the Lagrangian description of $\mathfrak{su}(3)$ $\mathcal{N} = 4$ SYM theory. Let us first write the charges in (9.50) as:

$$\ell_{e,m} = e \frac{w_1 - w_2}{3} + m \frac{m_1 - m_2}{3}. \quad (9.53)$$

Note that $(w_1 - w_2)/3$ (respectively, $(m_1 - m_2)/3$) is a weight of the electric (respectively, magnetic) algebra $\mathfrak{su}(3)$ with charge 1 under the center \mathbb{Z}_3 of the simply-connected group $SU(3)$. Therefore, the line $\ell_{e,m}$ corresponds to a Wilson-'t Hooft line of charge (e, m) under $\mathbb{Z}_3 \times \mathbb{Z}_3$.

As shown in [20], there are four possible lattices of mutually local Wilson-'t Hooft lines specified by two integers $i = 0, 1, 2$ and $p = 1, 3$. The corresponding gauge theories are denoted $(SU(3)/\mathbb{Z}_p)_i$ and relate to the line spectra we have obtained as follows:

$$\begin{aligned} SU(3) &\leftrightarrow \{\ell_{0,0}, \ell_{1,0}, \ell_{2,0}\}, \\ (SU(3)/\mathbb{Z}_3)_0 &\leftrightarrow \{\ell_{0,0}, \ell_{0,1}, \ell_{0,2}\}, \\ (SU(3)/\mathbb{Z}_3)_1 &\leftrightarrow \{\ell_{0,0}, \ell_{1,1}, \ell_{2,2}\}, \\ (SU(3)/\mathbb{Z}_3)_2 &\leftrightarrow \{\ell_{0,0}, \ell_{2,1}, \ell_{1,2}\}. \end{aligned} \quad (9.54)$$

It follows from linearity and screening that each lattice in the S -fold picture is determined by a single non-trivial representative, that can itself be identified by two integers (e, m) . For example, a possible choice is

$$(e, m) = (1, 0), (0, 1), (1, 1), (2, 1). \quad (9.55)$$

9.2.2 Lines in $\mathfrak{so}(5)$ from $S_{4,1}$

Dynamical states and their charges

Two D3-branes probing the singular point of the $S_{4,1}$ -fold are claimed to engineer $\mathfrak{so}(5)$ $\mathcal{N} = 4$ SYM. Following a reasoning similar to one of the $S_{3,1}$ -fold case, we can write all string charges as linear combinations of two kinds of strings, say

$$D3_1 D3_2 : (p, q; -p, -q), \quad D3_1 D3_2^\ell : (p, q; -q, p). \quad (9.56)$$

States corresponding to the \mathcal{W} -bosons of $\mathcal{N} = 4$ SYM are generated by $D3_1 D3_2$ with $p = 1$ and $q = 0$, and $D3_1 D3_2^\ell$ with $p = -1$ and $q = -1$. Their charges are

$$w_1 = (1, 0; -1, 0), \quad w_2 = (-1, -1; 1, -1). \quad (9.57)$$

These states generate the algebra $\mathfrak{so}(5)$ with short and long positive simple roots w_1 and w_2 , respectively. A possible choice of states corresponding to elementary magnetic monopoles \mathcal{M} is $D3_1 D3_2$ with $p = -1$ and $q = 1$, and $D3_1 D3_2^\ell$ with $p = 1$ and $q = 0$. The charges of these strings are:

$$m_1 = (-1, 1; 1, -1), \quad m_2 = (1, 0; 0, 1), \quad (9.58)$$

with m_1 the long and m_2 the short positive simple roots of the Langland dual algebra $\mathfrak{usp}(4)$. The Dirac pairings between \mathcal{W} and \mathcal{M} are as expected:

$$\begin{aligned} \langle \mathcal{W}_1, \mathcal{W}_2 \rangle &= \langle \mathcal{M}_1, \mathcal{M}_2 \rangle = 0, \\ \langle \mathcal{W}_1, \mathcal{M}_1 \rangle &= \langle \mathcal{W}_2, \mathcal{M}_2 \rangle = \langle \mathcal{M}_1, \mathcal{W}_2 \rangle = 2, \\ \langle \mathcal{M}_2, \mathcal{W}_1 \rangle &= 1. \end{aligned} \quad (9.59)$$

Line lattices

We begin by parametrizing the charge ℓ of a general line \mathcal{L} as:

$$\begin{aligned} \ell &= \alpha_1 w_1 + \alpha_2 w_2 + \beta_1 m_1 + \beta_2 m_2 \\ &= (\alpha_1 - \alpha_2 - \beta_1 + \beta_2, \beta_1 - \alpha_2; -\alpha_1 + \alpha_2 + \beta_1, -\alpha_2 - \beta_1 + \beta_2). \end{aligned} \quad (9.60)$$

Screening with respect to the local states \mathcal{W} and \mathcal{M} translates as:

$$\alpha_i \sim \alpha_i + 1, \quad \beta_i \sim \beta_i + 1. \quad (9.61)$$

Mutual locality with respect to the dynamical states generated by (p, q) -strings reads:

$$\begin{aligned} \langle \mathcal{L}, \mathcal{W}_1 \rangle &= 2\beta_1 - \beta_2 \\ \langle \mathcal{L}, \mathcal{W}_2 \rangle &= -2\beta_1 + 2\beta_2 \\ \langle \mathcal{L}, \mathcal{M}_1 \rangle &= -2\alpha_1 + 2\alpha_2 \\ \langle \mathcal{L}, \mathcal{M}_2 \rangle &= \alpha_1 - 2\alpha_2 \end{aligned} \in \mathbb{Z}. \quad (9.62)$$

This imposes $\alpha_1 = \beta_2 = 0$ and $\alpha_2, \beta_1 \in \frac{1}{2}\mathbb{Z}$, and therefore the charge of the most general line compatible with the spectrum of local states can be written as:

$$\ell_{e,m} = \frac{e}{2} w_2 + \frac{m}{2} m_1 = \frac{1}{2}(-e - m, -e + m; e + m, -e - m). \quad (9.63)$$

The Dirac pairing between two lines \mathcal{L} and \mathcal{L}' with charges $\ell_{e,m}$ and $\ell_{e',m'}$ is:

$$\langle \mathcal{L}, \mathcal{L}' \rangle = \frac{1}{2}(e'm - em'). \quad (9.64)$$

Two such lines are mutually local if their Dirac pairing if $\langle \mathcal{L}, \mathcal{L}' \rangle$ is an integer, i.e.:

$$(e'm - em') = 0 \pmod{2}. \quad (9.65)$$

Therefore, the allowed lines form a finite 2×2 square lattice parametrized by $e, m = 0, 1$, where the mutual locality condition is given by (9.65). This reproduces the expected global structures of $\mathcal{N} = 4$ $\mathfrak{so}(5)$ SYM. There are three possible choices of maximal lattices of mutually local lines which correspond to the three possible global structures of $\mathfrak{so}(5)$. The explicit mapping can be obtained by comparing the electromagnetic charges of the lines with the charges of the \mathcal{W} bosons and monopoles \mathcal{M} , along the lines of the analysis of above in the $\mathfrak{su}(3)$ case. We obtain the following global structures:

$$\begin{aligned} Spin(5) &\leftrightarrow \{\ell_{0,0}, \ell_{1,0}\}, \\ SO(5)_0 &\leftrightarrow \{\ell_{0,0}, \ell_{0,1}\}, \\ SO(5)_1 &\leftrightarrow \{\ell_{0,0}, \ell_{1,1}\}. \end{aligned} \quad (9.66)$$

9.2.3 Trivial line in \mathfrak{g}_2 from $S_{6,1}$

Dynamical states and their charges

Two $D3$ -branes probing the singular point of the $S_{6,1}$ -fold are claimed to engineer \mathfrak{g}_2 $\mathcal{N} = 4$ SYM. The charges of states generated by (p, q) -strings are:

$$\begin{aligned}
D3_1 D3_2 & : (p, q; -p, -q), & D3_1 D3_2^\ell & : (p, q; -q, p - q), \\
D3_1 D3_2^{\ell^2} & : (p, q; p - q, p), & D3_1 D3_2^{\ell^3} & : (p, q; p, q), \\
D3_1 D3_2^{\ell^4} & : (p, q; q, -p + q), & D3_1 D3_2^{\ell^5} & : (p, q; -p + q, -p), \\
& \text{etc.}
\end{aligned} \tag{9.67}$$

As shown in [199] and as before, one can choose a set of strings representing dynamical particles and generating the algebra \mathfrak{g}_2 .

Line lattice

The analysis of the charge spectrum in the case of the $S_{6,1}$ -fold can be carried out along the lines of the previous sections. One can show that the only line that is mutually local with respect to the local states generated by (p, q) -strings modulo screening is the trivial line with charges $\ell = (0, 0; 0, 0)$. This is consistent with the enhancement to $\mathcal{N} = 4$ with gauge algebra \mathfrak{g}_2 because the center of the simply-connected G_2 is trivial, which implies the absence of non-trivial lines [20]. There is only one possible global structure, and the one-form symmetry is trivial.

9.3 Lines in $\mathcal{N} = 3$ S -folds

In this section, we generalize the procedure spelled out in the previous sections to S -folds theories of arbitrary rank, and later to the cases with non-trivial discrete torsion for the B_2 and C_2 fields. This allows us to classify the line spectrum for every $\mathcal{N} = 3$ S -fold theory, and identify the one-form symmetry group as well as the allowed global structures for a given theory.

The basic ingredients needed in the analysis are the lattice of electromagnetic charges of local states and the Dirac pairing, both of which can be inferred from the Type IIB setup along the lines of the rank-2 cases studied in Section 9.2. As already emphasized, we work under the assumption that the states generated by (p, q) -string form a good set of representatives of the electromagnetic charge lattice of the full spectrum.

Note that it does not strictly make sense to talk about (p, q) -strings on the $\mathbb{R}^4 \times \mathbb{R}^6 / \mathbb{Z}_k$ S -fold background because the S -fold projection involves an $SL(2, \mathbb{Z})$ action which mixes F1 and D1 strings. This is analogous to the fact that in the orientifold cases it only makes sense to consider unoriented strings, since the orientifold action reverses the worldsheet parity (equivalently, it involves the element $-\mathbb{1}_2 \in SL(2, \mathbb{Z})$). Nevertheless it makes sense to consider oriented strings (together with their images) on the double cover of the spacetime; this allows the computation of the electromagnetic charge lattice of local states and the Dirac pairing, as reviewed in Section 9.1. Similarly when dealing with S_k -folds we consider (p, q) -strings on the k -cover of the spacetime, and extract from this the charges of local states and the Dirac pairing. The spectrum of lines can then be obtained using the procedure of [29] reviewed in Section 9.1.

9.3.1 Lines in $S_{3,1}$ -fold

Let us first determine the lattice of electromagnetic charges of dynamical states. The charges generated by (p, q) -strings on the background of an $S_{3,1}$ fold are given by

$$D3_i D3_j^{\ell} : (0, 0; \dots; \overbrace{p, q}^{i\text{-th}}; \dots; -\overbrace{(p \ q)}^{j\text{-th}} \cdot \rho_3^{\ell}; \dots; 0, 0). \tag{9.68}$$

This expression is obtained from a (p, q) -string stretched between the i -th D3-brane and the ℓ -th image of the j -th D3-brane. Recall that ρ_3 generates a \mathbb{Z}_3 subgroup of $SL(2, \mathbb{Z})$. A possible basis for the lattice of charges generated by (p, q) -strings is given by:

$$\begin{aligned} w_1 &= (1, 0; -1, 0; \dots), \\ w_2 &= (0, 1; 1, 1; \dots), \\ m_1 &= (0, 1; 0, -1; \dots), \\ m_2 &= (-1, -1; -1, 0; \dots), \\ P_i &= (1, 0; 0, 0; \dots; \overbrace{-1, 0}^{i\text{-th}}; 0, 0; \dots), \\ Q_i &= (0, 1; 0, 0; \dots; \overbrace{0, -1}^{i\text{-th}}; 0, 0; \dots), \end{aligned} \tag{9.69}$$

where w_i and m_i are the charges of the corresponding states in the rank-2 case, with all other entries set to 0. Let \mathcal{P}_i and \mathcal{Q}_i be the states with charges P_i and Q_i respectively, for $i = 3, \dots, N$. Note that when the rank is $N > 2$, it does not make sense to talk about \mathcal{W} -bosons and magnetic monopoles \mathcal{M} since the pure $\mathcal{N} = 3$ theories are inherently strongly coupled and do not admit a Lagrangian description. Nevertheless, we will denote \mathcal{W}_i and \mathcal{M}_i the states with charges w_i and m_i respectively, by analogy with the above.

The charge ℓ of a general line \mathcal{L} can be written as the linear combination:

$$\ell = \alpha_1 w_1 + \alpha_2 w_2 + \beta_1 m_1 + \beta_2 m_2 + \sum_{i=3}^N (\delta_i P_i + \gamma_i Q_i). \tag{9.70}$$

Besides, screening translates into the identifications:

$$\alpha_i \sim \alpha_i + 1, \quad \beta_i \sim \beta_i + 1, \quad \delta_i \sim \delta_i + 1, \quad \gamma_i \sim \gamma_i + 1. \tag{9.71}$$

Let us now analyze the constraints imposed on this line given by mutual locality with respect to the dynamical states generated by (p, q) -strings. Our results are summarized in Table 9.5.

Consider the mutual locality conditions:

$$\langle \mathcal{L}, \mathcal{P}_i - \mathcal{P}_j \rangle = \delta_i - \delta_j \in \mathbb{Z} \quad \Rightarrow \quad \delta_i = \delta_j = \delta \quad i, j = 3, \dots, N, \tag{9.72}$$

and

$$\langle \mathcal{L}, \mathcal{Q}_i - \mathcal{Q}_j \rangle = \gamma_j - \gamma_i \in \mathbb{Z} \quad \Rightarrow \quad \gamma_j = \gamma_i = \gamma \quad i, j = 3, \dots, N. \tag{9.73}$$

Rank	Line charge
$3n$	$\ell_{r,s} = \frac{r}{3}w_1 + \frac{s}{3}w_2 - \frac{r}{3}m_1 - \frac{s}{3}m_2 + \frac{r+s}{3}(P-Q)$
$3n+1$	$\ell_{r,s} = \frac{r}{3}w_1 + \frac{r-s}{3}w_2 + \frac{s}{3}m_1 + \frac{r}{3}m_2 + \frac{r+s}{3}(P-Q)$
$3n+2$	$\ell_{r,s} = \frac{r}{3}w_1 - \frac{r}{3}w_2 + \frac{s}{3}m_1 - \frac{s}{3}m_2 - \frac{r+s}{3}(P-Q)$

Table 9.5 The charges of allowed lines in the $S_{3,1}$ -fold theories. The charges w_i, m_i, P and Q are given in (9.69), and $r, s = 0, 1, 2$. The mutual locality condition for two lines with charges $\ell_{r,s}$ and $\ell_{r',s'}$ is $rs' - sr' = 0 \pmod 3$.

Furthermore, there are dynamical states with charges:

$$\begin{aligned}
 (0, 0; \dots; \overbrace{1, -1}^{i-th}; \dots) &= (p, q; \dots; \overbrace{-p, -q}^{i-th}; \dots) \Big|_{\substack{p=0 \\ q=1}} + (p, q; \dots; \overbrace{p-q, p}^{i-th}; \dots) \Big|_{\substack{p=0 \\ q=-1}} , \\
 (0, 0; \dots; \overbrace{2, 1}^{i-th}; \dots) &= (p, q; \dots; \overbrace{-p, -q}^{i-th}; \dots) \Big|_{\substack{p=-1 \\ q=0}} + (p, q; \dots; \overbrace{p-q, p}^{i-th}; \dots) \Big|_{\substack{p=1 \\ q=0}} .
 \end{aligned}
 \tag{9.74}$$

Mutual locality with respect to these implies:

$$\gamma = -\delta, \quad \delta \in \frac{1}{3}\mathbb{Z} .
 \tag{9.75}$$

Therefore, the charge of a general line can be rewritten as:

$$\ell = \alpha_1 w_1 + \alpha_2 w_2 + \beta_1 m_1 + \beta_2 m_2 + \delta(P-Q) ,
 \tag{9.76}$$

where

$$\begin{aligned}
 P &= \sum_{i=3}^N p_i = (N-2, 0; 0, 0; -1, 0; -1, 0; \dots; -1, 0) , \\
 Q &= \sum_{i=3}^N q_i = (0, N-2; 0, 0; 0, -1; 0, -1; \dots; 0, -1) .
 \end{aligned}
 \tag{9.77}$$

In (9.77), we have modified our notation slightly since the dots \dots now represent a sequence of pairs $(-1, 0)$ and $(0, -1)$ for P and Q respectively. Mutual locality between the line \mathcal{L} and the generators of the charge lattice of dynamical states imposes the following

constraints:

$$\begin{aligned}
\langle \mathcal{L}, \mathcal{P}_i \rangle &= (N-1)\delta - \alpha_2 - \beta_1 + \beta_2, \\
\langle \mathcal{L}, \mathcal{Q}_i \rangle &= (N-1)\delta + \alpha_1 - \beta_2, \\
\langle \mathcal{L}, \mathcal{W}_1 \rangle &= (N-2)\delta - 2\beta_1 + \beta_2, \\
\langle \mathcal{L}, \mathcal{W}_2 \rangle &= (N-2)\delta - 2\beta_2 + \beta_1, \\
\langle \mathcal{L}, \mathcal{M}_1 \rangle &= (N-2)\delta + 2\alpha_1 - \alpha_2, \\
\langle \mathcal{L}, \mathcal{M}_2 \rangle &= -2(N-2)\delta - \alpha_1 + 2\alpha_2
\end{aligned} \in \mathbb{Z}. \quad (9.78)$$

One can compute the following:

$$\begin{aligned}
\langle \mathcal{L}, \mathcal{W}_1 + 2\mathcal{W}_2 \rangle &= 3(N-2)\delta - 3\beta_2 \in \mathbb{Z} \Rightarrow \beta_2 \in \frac{1}{3}\mathbb{Z}, \\
\langle \mathcal{L}, \mathcal{M}_1 + 2\mathcal{M}_2 \rangle &= -3\alpha_1 \in \mathbb{Z} \Rightarrow \alpha_1 \in \frac{1}{3}\mathbb{Z}, \\
\langle \mathcal{L}, \mathcal{W}_1 - \mathcal{W}_2 \rangle &= 3(\beta_2 - \beta_1) \in \mathbb{Z} \Rightarrow \beta_1 \in \frac{1}{3}\mathbb{Z}, \\
\langle \mathcal{L}, \mathcal{M}_1 - \mathcal{M}_2 \rangle &= 3(N-2)\delta + 3(\alpha_1 - \alpha_2) \in \mathbb{Z} \Rightarrow \alpha_2 \in \frac{1}{3}\mathbb{Z}.
\end{aligned} \quad (9.79)$$

In brief, we have found that $\alpha_i, \beta_i, \delta \in \frac{1}{3}\mathbb{Z}$. It is now useful to treat separately three cases, depending on the value of $N \bmod 3$. In all these cases we find that the lines modulo screening can be arranged in a finite 3×3 lattice, the one-form symmetry group is \mathbb{Z}_3 and there are four choices of global structure.

Case $N = 3n$

The mutual locality conditions in (9.78) can be written as:

$$\begin{aligned}
\langle \mathcal{L}, \mathcal{P}_i \rangle &= -\delta - \alpha_2 - \beta_1 + \beta_2, \\
\langle \mathcal{L}, \mathcal{Q}_i \rangle &= -\delta + \alpha_1 - \beta_2, \\
\langle \mathcal{L}, \mathcal{W}_1 \rangle &= \delta - 2\beta_1 + \beta_2, \\
\langle \mathcal{L}, \mathcal{W}_2 \rangle &= \delta - 2\beta_2 + \beta_1, \\
\langle \mathcal{L}, \mathcal{M}_1 \rangle &= \delta + 2\alpha_1 - \alpha_2, \\
\langle \mathcal{L}, \mathcal{M}_2 \rangle &= \delta - \alpha_1 + 2\alpha_2
\end{aligned} \in \mathbb{Z}. \quad (9.80)$$

One computes that:

$$\begin{aligned}
\langle \mathcal{L}, \mathcal{Q}_i + \mathcal{W}_1 \rangle &= \alpha_1 + \beta_1 \Rightarrow \beta_1 = -\alpha_1, \\
\langle \mathcal{L}, \mathcal{P}_i + \mathcal{W}_2 \rangle &= -\alpha_2 - \beta_2 \Rightarrow \beta_2 = -\alpha_2, \\
\langle \mathcal{L}, \mathcal{Q}_i \rangle &= -\delta + \alpha_1 + \alpha_2 \Rightarrow \delta = \alpha_1 + \alpha_2,
\end{aligned} \quad (9.81)$$

and this implies:

$$\alpha_1 = -\beta_1 = \frac{r}{3}, \quad \alpha_2 = -\beta_2 = \frac{s}{3}, \quad \delta = \frac{r+s}{3}, \quad r, s = 0, 1, 2. \quad (9.82)$$

Therefore the lines form a finite 3×3 lattice parametrized by r and s . Mutual locality between two general lines \mathcal{L} and \mathcal{L}' with charges $\ell_{r,s}$ and $\ell_{r',s'}$ reads:

$$\langle \mathcal{L}, \mathcal{L}' \rangle = \frac{2}{3}(sr' - rs') \in \mathbb{Z}, \quad (9.83)$$

or equivalently:

$$sr' - rs' = 0 \bmod 3. \quad (9.84)$$

There are four possible choices of maximal lattices of mutually local lines. As in the rank-2 case discussed in section 9.2, each lattice is uniquely identified by one of its element,

or equivalently by the pair (r, s) of one of its non-trivial elements:

$$(r, s) = \begin{cases} (1, 0) \leftrightarrow \{\ell_{0,0}, \ell_{1,0}, \ell_{2,0}\} \\ (0, 1) \leftrightarrow \{\ell_{0,0}, \ell_{0,1}, \ell_{0,2}\} \\ (1, 1) \leftrightarrow \{\ell_{0,0}, \ell_{1,1}, \ell_{2,2}\} \\ (1, 2) \leftrightarrow \{\ell_{0,0}, \ell_{1,2}, \ell_{2,1}\} \end{cases}. \quad (9.85)$$

Case $N = 3n + 1$

In this case the mutual locality constraints (9.78) are:

$$\begin{aligned} \langle \mathcal{L}, \mathcal{P}_i \rangle &= -\alpha_2 - \beta_1 + \beta_2 \\ \langle \mathcal{L}, \mathcal{Q}_i \rangle &= \alpha_1 - \beta_2 \\ \langle \mathcal{L}, \mathcal{W}_1 \rangle &= -\delta - 2\beta_1 + \beta_2 \\ \langle \mathcal{L}, \mathcal{W}_2 \rangle &= -\delta - 2\beta_2 + \beta_1 \\ \langle \mathcal{L}, \mathcal{M}_1 \rangle &= -\delta + 2\alpha_1 - \alpha_2 \\ \langle \mathcal{L}, \mathcal{M}_2 \rangle &= 2\delta - \alpha_1 + 2\alpha_2 \end{aligned} \in \mathbb{Z}. \quad (9.86)$$

One computes that:

$$\begin{aligned} \alpha_2 &= \alpha_1 - \beta_1, \\ \delta &= \alpha_1 + \beta_1, \\ \alpha_1 &= \beta_2. \end{aligned} \quad (9.87)$$

Therefore the most general α_i, β_i and δ satisfy:

$$\alpha_1 = \beta_2 = \frac{r}{3}, \quad \beta_1 = \frac{s}{3}, \quad \alpha_2 = \frac{r-s}{3}, \quad \delta = \frac{r+s}{3}, \quad r, s = 0, 1, 2. \quad (9.88)$$

The lines again form a finite 3×3 lattice parametrized by r and s . Mutual locality between two general lines \mathcal{L} and \mathcal{L}' with charges $\ell_{r,s}$ and $\ell_{r',s'}$ reads:

$$\langle \mathcal{L}, \mathcal{L}' \rangle = \frac{1}{3}(sr' - rs') \in \mathbb{Z}, \quad (9.89)$$

or equivalently:

$$sr' - rs' = 0 \pmod{3}. \quad (9.90)$$

Similarly to the case $N = 3n$ there are four possible choices of maximal lattices of mutually local lines that can be indexed by one of their element, or equivalently by $(r, s) = (1, 0), (0, 1), (1, 1), (1, 2)$.

Case $N = 3n + 2$

In this case, the mutual locality constraints (9.78) are

$$\begin{aligned} \langle \mathcal{L}, \mathcal{P}_i \rangle &= \delta - \alpha_2 - \beta_1 + \beta_2 \\ \langle \mathcal{L}, \mathcal{Q}_i \rangle &= \delta + \alpha_1 - \beta_2 \\ \langle \mathcal{L}, \mathcal{W}_1 \rangle &= -2\beta_1 + \beta_2 = \beta_1 + \beta_2 \\ \langle \mathcal{L}, \mathcal{W}_2 \rangle &= -2\beta_2 + \beta_1 \\ \langle \mathcal{L}, \mathcal{M}_1 \rangle &= 2\alpha_1 - \alpha_2 = -\alpha_1 - \alpha_2 \\ \langle \mathcal{L}, \mathcal{M}_2 \rangle &= -\alpha_1 + 2\alpha_2 \end{aligned} \in \mathbb{Z}. \quad (9.91)$$

One can compute that the solution is given by

$$\begin{aligned}\beta_2 &= -\beta_1, \\ \alpha_2 &= -\alpha_1, \\ \delta &= -\alpha_1 - \beta_1.\end{aligned}\tag{9.92}$$

Therefore the most general α_i, β_i and δ satisfy:

$$\alpha_1 = -\alpha_2 = \frac{r}{3}, \quad \beta_1 = -\beta_2 = \frac{s}{3}, \quad \delta = -\frac{r+s}{3}, \quad r, s = 0, 1, 2.\tag{9.93}$$

Dirac pairing between two general lines \mathcal{L} and \mathcal{L}' with charges $\ell_{r,s}$ and $\ell_{r',s'}$ reads:

$$\langle \mathcal{L}, \mathcal{L}' \rangle = \frac{2}{3}(sr' - rs') \in \mathbb{Z}.\tag{9.94}$$

Two such lines are mutually local if they satisfy the constraint:

$$sr' - rs' = 0 \pmod{3}.\tag{9.95}$$

As before, there are four possible choices of maximal lattices of mutually local lines that can be indexed by one of their element, or equivalently by

$$(r, s) = (1, 0), (0, 1), (1, 1), (1, 2).\tag{9.96}$$

9.3.2 Lines in $S_{4,1}$ -fold

We now study the spectrum of lines in theories engineered by a stack of D3-branes probing the $S_{4,1}$ -fold. The charges of states generated by a (p, q) -string on the background of an $S_{4,1}$ -fold read

$$D3_i D3_j^l : (0, 0; \dots; \overbrace{p, q}^{i-th}; \dots; \overbrace{-(p \ q) \cdot \rho_4^l}^{j-th}; \dots; 0, 0)\tag{9.97}$$

for a (p, q) -strings stretched between the i -th D3-brane and the l -th image of the j -th D3-brane. One possible basis for the lattice of charges generated by (p, q) -strings is:

$$\begin{aligned}w_1 &= (1, 0; -1, 0; 0, 0; \dots), \\ w_2 &= (-1, -1; 1, -1; 0, 0; \dots), \\ m_1 &= (-1, 1; 1, -1; 0, 0; \dots), \\ m_2 &= (1, 0; 0, 1; 0, 0; \dots), \\ P_i &= (1, 0; 0, 0; \dots; \overbrace{-1, 0}^{i-th}; 0, 0; \dots), \\ Q_i &= (0, 1; 0, 0; \dots; \overbrace{0, -1}^{i-th}; 0, 0; \dots),\end{aligned}\tag{9.98}$$

where w_i and m_i are the charges of the corresponding states in the rank-2 case, with all other entries set to 0. We denote $\mathcal{W}_i, \mathcal{M}_i, \mathcal{P}_i$ and \mathcal{Q}_i the states with charges w_i, m_i, P_i and Q_i , respectively.

The charge ℓ of a general line \mathcal{L} can be written as the linear combination:

$$\ell = \alpha_1 w_1 + \alpha_2 w_2 + \beta_1 m_1 + \beta_2 m_2 + \sum_{i=3}^N (\delta_i P_i + \gamma_i Q_i). \tag{9.99}$$

Screening translates into the identifications:

$$\alpha_i \sim \alpha_i + 1, \quad \beta_i \sim \beta_i + 1, \quad \delta_i \sim \delta_i + 1, \quad \gamma_i \sim \gamma_i + 1. \tag{9.100}$$

In the remainder of this section we compute the constraints imposed by mutual locality between the general line \mathcal{L} and dynamical states. Our results are summarized in Table 9.6.

Rank	Line charge
$2n$	$\ell_{r,s} = \frac{r}{2} w_2 + \frac{s}{2} m_1 + \frac{r+s}{2} (P - Q)$
$2n + 1$	$\ell_{r,s} = \frac{r}{2} w_1 + \frac{s}{2} w_2 + \frac{s}{2} m_1 + \frac{r}{2} m_2 + \frac{r}{2} (P - Q)$

Table 9.6 The charges of allowed lines in the $S_{4,1}$ -fold theories. The charges w_i, m_i, P and Q are given in (9.98), (9.77), and $r, s = 0, 1$. The mutual locality condition for two lines with charges $\ell_{r,s}$ and $\ell_{r',s'}$ is $rs' - sr' = 0 \pmod 2$.

Consider first the mutual locality conditions:

$$\langle \mathcal{L}, \mathcal{P}_i - \mathcal{P}_j \rangle = \delta_i - \delta_j \in \mathbb{Z} \quad \Rightarrow \quad \delta_i = \delta_j = \delta, \tag{9.101}$$

$$\langle \mathcal{L}, \mathcal{Q}_i - \mathcal{Q}_j \rangle = \gamma_j - \gamma_i \in \mathbb{Z} \quad \Rightarrow \quad \gamma_j = \gamma_i = \gamma. \tag{9.102}$$

Furthermore, there are dynamical states with charges:

$$\begin{aligned} (0, 0; \dots; \overbrace{1, -1}^{i\text{-th}}; \dots) &= (p, q; \dots; \overbrace{-p, -q}^{i\text{-th}}; \dots) \Big|_{\substack{p=0 \\ q=1}} + (p, q; \dots; \overbrace{-q, p}^{i\text{-th}}; \dots) \Big|_{\substack{p=0 \\ q=-1}}, \\ (0, 0; \dots; \overbrace{1, 1}^{i\text{-th}}; \dots) &= (p, q; \dots; \overbrace{-p, -q}^{i\text{-th}}; \dots) \Big|_{\substack{p=-1 \\ q=0}} + (p, q; \dots; \overbrace{-q, p}^{i\text{-th}}; \dots) \Big|_{\substack{p=1 \\ q=0}}. \end{aligned} \tag{9.103}$$

and mutual locality with respect to these states implies:

$$\gamma = -\delta, \quad \delta \in \frac{1}{2}\mathbb{Z}. \tag{9.104}$$

Therefore, the charge of a general line can be rewritten as:

$$\ell = \alpha_1 w_1 + \alpha_2 w_2 + \beta_1 m_1 + \beta_2 m_2 + \delta(P - Q), \tag{9.105}$$

where P and Q are defined in (9.77). Mutual locality between the line \mathcal{L} and the genera-

tors of the charge lattice of dynamical states implies:

$$\begin{aligned}
\langle \mathcal{L}, \mathcal{P}_i \rangle &= (N-1)\delta + \alpha_2 - \beta_1, \\
\langle \mathcal{L}, \mathcal{Q}_i \rangle &= (N-1)\delta + \alpha_1 - \alpha_2 - \beta_1 + \beta_2, \\
\langle \mathcal{L}, \mathcal{W}_1 \rangle &= (N-2)\delta - 2\beta_1 + \beta_2, \\
\langle \mathcal{L}, \mathcal{W}_2 \rangle &= 2(N-2)\delta - 2\beta_2 + 2\beta_1, \\
\langle \mathcal{L}, \mathcal{M}_1 \rangle &= 2\alpha_1 - 2\alpha_2 \\
\langle \mathcal{L}, \mathcal{M}_2 \rangle &= (N-2)\delta - \alpha_1 + 2\alpha_2
\end{aligned} \in \mathbb{Z}. \quad (9.106)$$

One computes the following:

$$\begin{aligned}
\langle \mathcal{L}, \mathcal{W}_1 + \mathcal{W}_2 - \mathcal{M}_1 - \mathcal{M}_2 \rangle &= -\beta_2 - \alpha_1 \in \mathbb{Z} \Rightarrow \beta_2 = -\alpha_1, \\
\langle \mathcal{L}, \mathcal{Q}_i + \mathcal{P}_i \rangle &= -2\beta_1 \in \mathbb{Z} \Rightarrow \beta_1 \in \frac{1}{2}\mathbb{Z}, \\
\langle \mathcal{L}, \mathcal{Q}_i - \mathcal{P}_i \rangle &= -2\alpha_2 \in \mathbb{Z} \Rightarrow \alpha_2 \in \frac{1}{2}\mathbb{Z}, \\
\langle \mathcal{L}, \mathcal{M}_1 \rangle &= 2\alpha_1 \in \mathbb{Z} \Rightarrow \alpha_1, \beta_2 \in \frac{1}{2}\mathbb{Z}.
\end{aligned} \quad (9.107)$$

We have thus shown that $\alpha_i, \beta_i, \delta \in \frac{1}{2}\mathbb{Z}$ and $\alpha_1 = -\beta_2$. It is now useful to treat separately the cases of odd and even N . In both cases we find that the lines form a 2×2 lattice, the one-form symmetry is \mathbb{Z}_2 and there are three choices of global structure.

Case $N = 2n$

Mutual locality conditions (9.106) read:

$$\begin{aligned}
\langle \mathcal{L}, \mathcal{P}_i \rangle &= -\delta - \beta_1 + \alpha_2 \\
\langle \mathcal{L}, \mathcal{Q}_i \rangle &= -\delta - \alpha_2 - \beta_1 \\
\langle \mathcal{L}, \mathcal{W}_1 \rangle &= \beta_2 \\
\langle \mathcal{L}, \mathcal{W}_2 \rangle &= 0 \\
\langle \mathcal{L}, \mathcal{M}_1 \rangle &= 0 \\
\langle \mathcal{L}, \mathcal{M}_2 \rangle &= -\alpha_1
\end{aligned} \in \mathbb{Z}, \quad (9.108)$$

and each solution can be written as:

$$\alpha_2 = \frac{r}{2}, \quad \beta_1 = \frac{s}{2}, \quad \alpha_1 = \beta_2 = 0, \quad \delta = \frac{r+s}{2}, \quad r, s = 0, 1. \quad (9.109)$$

Therefore the lines form a 2×2 lattice parametrized by r, s . Mutual locality between two lines \mathcal{L} and \mathcal{L}' with charges $\ell_{r,s}$ and $\ell_{r',s'}$ respectively translates into:

$$\langle \mathcal{L}, \mathcal{L}' \rangle = \frac{1}{2}(r's - rs') \in \mathbb{Z}, \quad (9.110)$$

or equivalently:

$$r's - rs' = 0 \pmod{2}. \quad (9.111)$$

The one-form symmetry group is thus \mathbb{Z}_2 and there are three different choices of maximal lattices of mutually local lines parametrized by $(r, s) = (1, 0), (0, 1), (1, 1)$.

Case $N = 2n + 1$

The Dirac pairings (9.106) read:

$$\begin{aligned}
 \langle \mathcal{L}, \mathcal{P}_i \rangle &= \alpha_2 - \beta_1, \\
 \langle \mathcal{L}, \mathcal{Q}_i \rangle &= -\alpha_2 - \beta_1, \\
 \langle \mathcal{L}, \mathcal{W}_1 \rangle &= \delta + \beta_2, \\
 \langle \mathcal{L}, \mathcal{W}_2 \rangle &= 0, \\
 \langle \mathcal{L}, \mathcal{M}_1 \rangle &= 0, \\
 \langle \mathcal{L}, \mathcal{M}_2 \rangle &= \delta - \alpha_1
 \end{aligned} \in \mathbb{Z}, \tag{9.112}$$

and the general solution can be written as:

$$\alpha_1 = \beta_2 = \delta = \frac{r}{2}, \quad \alpha_2 = \beta_1 = \frac{s}{2}, \quad r, s = 0, 1. \tag{9.113}$$

Mutual locality between two lines \mathcal{L} and \mathcal{L}' with charges $\ell_{r,s}$ and $\ell_{r',s'}$ respectively translates into:

$$\langle \mathcal{L}, \mathcal{L}' \rangle = \frac{1}{2}(r's - rs') \in \mathbb{Z}, \tag{9.114}$$

or equivalently:

$$r's - rs' = 0 \pmod{2}. \tag{9.115}$$

As in the previous case, the one-form symmetry group is therefore \mathbb{Z}_2 and there are three different choices of maximal lattices of mutually local lines that can be parametrized by:

$$(r, s) = (1, 0), (0, 1), (1, 1). \tag{9.116}$$

9.3.3 Trivial line in $S_{6,1}$ -fold

The analysis of the spectrum of lines in the case of the $S_{6,1}$ -fold can be carried out along the lines of the previous subsections. One finds that the integer lattice of charges associated to (p, q) -strings is fully occupied. To see this notice that there are two states with the following charges:

$$\begin{aligned}
 (1, 0; 0, 0; 0, 0; \dots) &= (p, q; p - q, p; 0, 0; \dots) \Big|_{\substack{p=0 \\ q=-1}} - (p, q; -q, p, 0, 0; \dots) \Big|_{\substack{p=1 \\ q=0}}, \\
 (0, 1; 0, 0; 0, 0; \dots) &= (1, 0; 0, 0; 0, 0; \dots) - (p, q; -p - q; 0, 0; \dots) \Big|_{\substack{p=0 \\ q=1}} \\
 &\quad - (p, q; -q, p; 0, 0; \dots) \Big|_{\substack{p=0 \\ q=-1}}.
 \end{aligned} \tag{9.117}$$

By combining these states with \mathcal{P}_i and \mathcal{Q}_i we can obtain states with electric or magnetic charge 1 with respect to the i -th brane, and all other charges set to zero. Let us now consider a general line \mathcal{L} with charge $\ell = (e_1, m_1; e_2, m_2, \dots)$. Mutual locality with respect to the local states we have just discussed implies:

$$e_i, m_i \in \mathbb{Z} \quad \forall i, \tag{9.118}$$

and the insertion of the same local states along the lines translates to the identification:

$$e_i \sim e_i + 1, \quad m_i \sim m_i + 1. \tag{9.119}$$

Therefore, the only allowed line modulo screening is the trivial line, with charge $\ell = (0, 0; 0, 0; \dots)$. This implies that the one form symmetry group is trivial, and accordingly there is only one possible choice of global form.

9.3.4 Trivial line in the discrete torsion cases

We generalize the analysis discussed in the previous sections to the cases with non-trivial discrete torsion in the $S_{3,3}$ -fold and $S_{4,4}$ -fold.

As we argued in Section 9.1 all the strings states that are present when the discrete torsion is trivial are also allowed when the discrete torsion is non-zero. Furthermore, there are strings ending on the S -fold itself, as discussed in Section 9.1. Thus, the lattice of charges of local states in the case of the $S_{3,3}$ -fold and $S_{4,4}$ -fold are generated by strings stretched between (images of) D3-branes – as in the cases with trivial discrete torsion – together with those additional strings. One can show that the integer lattice of electromagnetic charges of dynamical states is then fully occupied. Therefore, by a similar argument to the one used in the case of the $S_{6,1}$ -fold in Section 9.3.3, the only line that is allowed is the trivial one, and the one-form symmetry group is $\mathbb{1}$ for the $S_{3,3}$ -fold and $S_{4,4}$ -fold with non-zero discrete torsion.

9.4 Non-invertible symmetries

We now discuss the possible presence of non-invertible symmetries in S -fold theories. In the case of $\mathcal{N} = 4$ theories, the presence of S-duality orbits can imply the existence of non-invertible duality defects which are built by combining the action of some element of $SL(2, \mathbb{Z})$ and the gauging of a discrete one-form symmetry [247, 248, 249, 250, 251, 252, 253, 254, 255, 256, 257, 258].

Similar structures can be inferred from the S -fold construction. Consider moving one of the D3-brane along the non-contractible one-cycle of S^5/\mathbb{Z}_k until it reaches its original position. The brane configurations before and after this are identical, and therefore the S -fold theories are invariant under this action. Going around the non-contractible one-cycle of S^5/\mathbb{Z}_k in the case an $S_{k,l}$ -fold involves an $SL(2, \mathbb{Z})$ -transformation on the electric and magnetic charges e_i, m_i associated to the D3-brane that has been moved. Let Σ_k^i denote the process of moving the i -th D3-brane along the non-contractible cycle of an $S_{k,l}$ -fold. The action of Σ_k^i on the charges is:

$$\Sigma_k^i : \begin{pmatrix} e_j \\ m_j \end{pmatrix} \rightarrow \begin{cases} \rho_k \cdot \begin{pmatrix} e_j \\ m_j \end{pmatrix} & j = i \\ \begin{pmatrix} e_j \\ m_j \end{pmatrix} & j \neq i \end{cases} . \tag{9.120}$$

The charge lattice of dynamical states is invariant under Σ_k^i , while the set of line lattices can be shuffled. Consider for example the $S_{3,1}$ -case with rank $N = 2$. One can compute explicitly the following orbits:

$$(1, 0) \longleftrightarrow (0, 1) \longleftrightarrow (1, 1) \quad \begin{matrix} \curvearrowright \\ (1, 2) \end{matrix} , \tag{9.121}$$

where the pairs (e, m) parametrize the maximal sub-lattice of mutually local lines as dis-

cussed in section (9.2.1). Two line lattices connected by an arrow in (9.121) are mapped to each other under proper combinations of Σ_3^i .

This theory enhances to $\mathfrak{su}(3)$ $\mathcal{N} = 4$ SYM. Using the mapping (9.54) between the line lattices parametrized by (e, m) and the global structures of $\mathfrak{su}(3)$, the formula (9.121) reproduces the $\mathcal{N} = 4$ orbits under the element $ST \in SL(2, \mathbb{Z})$. As shown in the literature [247, 250, 251, 248], this transformation can be combined with a proper gauging of the one-form symmetry to construct the non-invertible self-duality defects of $\mathfrak{su}(3)$ at $\tau = e^{2\pi i/3}$. Therefore in our notation we expect the existence of non-invertible symmetries involving Σ_k^i for the lattices labeled by $(e, m) = (1, 0), (0, 1), (1, 1)$, and none in the $(e, m) = (1, 2)$ case.

Similarly, one can consider the orbits in the case of $S_{4,1}$ with $N = 2$, where the SCFT enhances to $\mathfrak{so}(5)$ $\mathcal{N} = 4$ SYM. By using the transformations Σ_4^i as above we find the following orbits

$$(0, 1) \longleftrightarrow (1, 0) \quad \begin{matrix} \curvearrowright \\ (1, 1) \end{matrix} , \tag{9.122}$$

where the pairs (e, m) parametrize the maximal sub-lattices of mutually local lines as discussed in section (9.2.2).

These reproduce the $\mathcal{N} = 4$ orbits under the element $S \in SL(2, \mathbb{Z})$. Again this transformation can be combined with a proper gauging of the one-form symmetry to construct the non-invertible self-duality defects of $\mathfrak{so}(5)$ at $\tau = i$.

Motivated by this match, one can expect that in the case of general rank, non-invertible symmetries will be present when multiple choices of maximal sub-lattices of mutually local lines are related by the transformations Σ_k^i , as above. The orbits are:

$$S_{3,1} : (1, 0) \longleftrightarrow (0, 1) \longleftrightarrow (1, 1) \quad (1, 2) \curvearrowright , \tag{9.123}$$

$$S_{4,1} : \begin{cases} (0, 1) \longleftrightarrow (1, 0) & (1, 1) \curvearrowright & N = 0 \pmod 2 \\ (1, 0) \longleftrightarrow (1, 1) & (0, 1) \curvearrowright & N = 1 \pmod 2 \end{cases} , \tag{9.124}$$

where the pairs (r, s) parametrize the maximal sub-lattices of mutually local lines as in section 9.3.

In the $S_{6,1}, S_{3,3}$ and $S_{4,4}$ -cases, there is only one possible global structure that is mapped to itself by the Σ_k^i transformations.

By analogy with the cases where there is $\mathcal{N} = 4$ enhancement, we expect the existence of non-invertible symmetries when the transformations Σ_k^i map different line lattices, built by combining this Σ_k^i -action with a suitable gauging of the one-form symmetry.

9.5 Conclusions

In this Chapter, we have exploited the recipe of [29] for arranging the charge lattice of genuine lines modulo screening by dynamical particles. We have adapted such strategy, originally designed for BPS quivers, to the case of (p, q) -strings, in order to access to the

electromagnetic charges of non-Lagrangian $\mathcal{N} = 3$ S -fold SCFTs. This procedure has allowed us to provide a full classification of the one-form symmetries of every S -fold SCFT. We singled out two cases with a non-trivial one-form symmetry, corresponding to the \mathbb{Z}_3 and the \mathbb{Z}_4 S -folds in absence of discrete torsion, denoted here as $S_{3,1}$ and $S_{4,1}$ respectively. Our results are consistent with the supersymmetry enhancement that takes place when two D3-branes are considered. Lastly, we discuss the possibility of non-invertible duality defects, by recovering the expected results for the cases with supersymmetry enhancement and proposing a generalization at any rank. A natural generalization of the analysis performed in this Chapter is to consider the exceptional $\mathcal{N} = 3$ theories [200, 5]. In Chapter 10 and 11 we will study exceptional S -folds of type E_r with an approach similar to the one discussed in this Chapter.

We left many open questions that deserve further investigations. It would for example be interesting to study in more details the projection of the states generated by the (p, q) -configurations in an S -fold background. In the present thesis, the only relevant information was the electromagnetic charges carried by these states, but a deeper analysis of the dynamics of these S -fold theories requires more work. This would in turn improve our understanding of their mass spectrum. For instance, a comparison of the BPS spectrum could be made exploiting the Lagrangian descriptions of [241]. This could also help finding the origin of the mapping between the multiple lattices found in the $S_{3,1}$ and $S_{4,1}$ -cases. Further investigations in this direction would deepen our geometric understanding of the non-invertible symmetries expected in this class of theories, along the lines of the brane analysis of [259, 260, 261].

It would also be of interest to generalize the analysis to the cases of S -folds with $\mathcal{N} = 2$ supersymmetry [262, 263] (see [264, 265] for similar analysis in class S theories). In the absence of BPS quivers, one needs to adapt the UV analysis of [29]. In general, one would like to find a stringy description that avoids wall crossing and allows reading the charge lattices and the one-form symmetries for such theories.

Exceptional S-folds and discrete gauging

In this Chapter, building upon the analysis and results of Chapter 9, we study a class of 4d SCFTs with $\mathcal{N} = 3$ SUSY called exceptional S-fold theories, first constructed in [200]. We analyze the structure of higher-form symmetries in conjunction with the charge lattice and the possibility of discrete gauging.

Not much is known about these theories aside from their geometric construction, a notable exception being the CB geometry computed in [5] by Kaidi, Gabi and Martone. Our analysis relies heavily on their approach as well as on the CB geometry itself. As discussed in Section 8.2, $\mathcal{N} = 3$ S-fold SCFTs are labelled by an integer $k = 3, 4, 6$, called the order of the S-fold, and a simply-laced Lie algebra \mathfrak{g} , and we will denote them as “S-folds of type \mathfrak{g} ” or more concisely as $\mathfrak{g}S_k$ -fold. The A_rS_k -folds, denoted here as “regular” S-folds, engineer the theories of [197], and are equivalent to non-geometric Type IIB setups. The D_rS_k -folds and E_rS_k -folds are called “exceptional” S-fold theories. In this thesis we only discuss the $\mathfrak{g} = E_r$ case, but our procedures can be straightforwardly applied to the D_rS_k -folds as well.

We thus consider a total of nine theories, the E_rS_k -folds, which are believed to be non-trivial interacting SCFTs with rank varying from 2 to 4. We show that all but one of these theories, the E_8S_4 -fold, are discrete gauging of free theories. This is essentially due to the fact that they do not admit a consistent charge lattice. Exceptional S-folds can be considered sporadic even when compared to the “regular” A_rS_k -folds, nevertheless the obstruction to having a consistent charge lattice that they exhibit generalizes nicely to arbitrary ranks, as we will discuss in Chapter 11.

For the sake of readability, let us outline the general strategy adopted in this Chapter and state the results. A summary of our results can be found in Table 10.1.

General strategy

Our approach to the study of charge lattices of S-fold theories reduces to two main ideas. The first idea is based on the results of [5], where it was shown that the moduli space of an S-fold SCFT of type \mathfrak{g} can be obtained as a slice of the moduli space of a “parent” $\mathcal{N} = 4$ SYM theory with gauge algebra \mathfrak{g} . In analogy with this result, we compute the charge lattice of an S-fold theory as a sublattice of the charge lattice of the parent $\mathcal{N} = 4$ SYM.

The second ingredient is the consistency of the structures of $\mathcal{N} = 2$ SCFTs along the Coulomb branch stratification. In our case this boils down to the fact that the charges that become massless at some codimension- n singularity on the Coulomb branch must generate the charge lattice of some rank- n theory supported on the singularity. If this is not the case, then the singularity can not support an interacting theory and must be empty. The singularity itself then supports a discrete gauging of a free theory, and the SCFT can be considered as a discrete gauging of a parent theory. In most exceptional S-fold theories we find that none of the codimension-1 singularity can support an interacting theory, signaling that the exceptional S-fold theory itself is a discrete gauging of a free $\mathcal{N} = 4$ theory.

This procedure is particularly powerful when considering the codimension-1 singularities of a maximally strongly coupled theory. If the singularity is non-empty then it must support a rank-1 $\mathcal{N} = 2$ SCFT. We have a full classification of these theories and their charge lattices are characterized by the absolute value of the Pfaffian of the Dirac pairing J :

$$|\text{Pf}(J)| = \begin{cases} 2 & \text{(discrete gauging of) } \mathcal{N} = 2^*SU(2)\text{SYM} \\ 1 & \text{otherwise} \end{cases} \quad (10.1)$$

For any other values of $|\text{Pf}(J)|$ on a codimension-1 singularity, the corresponding states can not be BPS and the singularity must be empty.

Given an exceptional S-fold theory our analysis roughly follows these steps:

- Determine the Coulomb branch geometry as was computed in [5]
- Compute the charge lattice and Dirac pairing from the parent $\mathcal{N} = 4$ theory.
- Compute the sublattice of charges that should become massless on all codimension-1 singularities
- If these lattices are compatible with one of the options in (10.1) there is a SCFT supported there, otherwise the singularity is empty.
- Also impose the constraints on the central charges, namely the formulae of [218].

At the end of these steps if there are some singularities which support an interacting SCFT we claim that the S-fold SCFT is non-trivial. Instead if all the singularities are empty we claim that the S-fold theory is a discrete gauging of a free theory.

Results

We find that all but one of the exceptional S-fold SCFTs of type E_r are discrete gauging of free theories, the exception being the S-fold of type E_8 with $k = 4$, also called the G_{31} theory. In particular, the S-fold theories of type E_6 and E_8 with $k = 3, 6$ do not have consistent charge lattices. In these theories, on any codimension-1 singularity the charges that should become massless span a rank-2 sublattice where the Dirac pairing is such that $|\text{Pf}(J^{(1)})| = 3$, and comparing with eq. (10.1) there is no rank-1 SCFT that can be supported there. Therefore all codimension-1 singularities are empty, and the S-fold theories themselves are discrete gauging of free theories. All S-fold theories of type E_7 and the S-fold theory of type E_6 with $k = 4$ admit a consistent charge lattice, but this lattice is incompatible with the constraints coming from the central charge formulae of [218].

$k \backslash \mathfrak{g}$	E_6	E_7	E_8
3	$\mathcal{C} = \mathbb{C}^3/G_{25}$ d.g. of $U(1)^3 \mathcal{N} = 4$	$\mathcal{C} = \mathbb{C}^3/G_{26}$ d.g. of $U(1)^3 \mathcal{N} = 4$	$\mathcal{C} = \mathbb{C}^4/G_{32}$ d.g. of $U(1)^4 \mathcal{N} = 4$
4	$\mathcal{C} = \mathbb{C}^2/G_8$ d.g. of $U(1)^2 \mathcal{N} = 4$	$\mathcal{C} = \mathbb{C}^2/G_8$ d.g. of $U(1)^2 \mathcal{N} = 4$	$\mathcal{C} = \mathbb{C}^4/G_{31}$ Interacting SCFT $G^{(1)} = \mathbb{1}, 12c = 372$
6	$\mathcal{C} = \mathbb{C}^2/G_5$ d.g. of $U(1)^2 \mathcal{N} = 4$	$\mathcal{C} = \mathbb{C}^3/G_{26}$ d.g. of $U(1)^3 \mathcal{N} = 4$	$\mathcal{C} = \mathbb{C}^4/G_{32}$ d.g. of $U(1)^4 \mathcal{N} = 4$

Table 10.1 Properties of exceptional S-folds of type $\mathfrak{g} = E_n$. For each theory the Coulomb branch \mathcal{C} is reproduced from [5] and we specify whether the theory is a discrete gauging (d.g) of a free theory. Red cells are theories whose Coulomb branch do not admit any consistent charge lattice, orange cells are theories where the charge lattice is incompatible with the constraints on the central charges. For the only interacting SCFT the 1-form symmetry group $G^{(1)}$ is written and the central charge is reproduced from [5].

The only S-fold theory of type E_n that has a well defined charge lattice compatible with the formulae of [218] is the G_{31} theory. We claim that this is an interacting SCFT. The theory has rank equal to 4 and the Coulomb branch and central charges are those computed in [5], see Table 10.1. Furthermore we find that the 1-form symmetry group of this theory is trivial.

10.1 Another look at S-folds SCFTs

In this Section we outline our procedure for analyzing various properties of $\mathcal{N} = 3$ S-fold theories. We do so by studying explicit examples of S-folds SCFTs engineered in Type IIB, which we denote as “regular” S-folds, providing various prescriptions that will apply to the general cases of exceptional S-folds [200] engineered in M-theory discussed in Section 10.2. All the results contained in this Section have already appeared in the literature and most of the techniques are well known, with the exception of the discussion given in Subsection 10.1.2. There we leverage the stratification of the Coulomb branch and the classification of $\mathcal{N} = 2$ rank 1 SCFTs to constrain the BPS spectrum and ultimately understand the 2-form symmetries of these theories. This argument, to the best of our knowledge, is original.

10.1.1 Moduli space

The S-fold theories have a moduli space of vacua parametrized by the motion of the N D3-branes on the transverse space $\mathbb{C}^3/\mathbb{Z}_k$ which is given by $(\mathbb{C}^3)^N/G(k, 1, N)$ [199], where $G(k, 1, N)$ is a crystallographic complex reflection group (CCRG). By choosing an $\mathcal{N} = 2$ subalgebra of the $\mathcal{N} = 3$ superalgebra the R-symmetry group is broken to $(SU(2) \times U(1))_R$ and the moduli space splits into a N -dimensional Coulomb branch, an $2N$ -dimensional Higgs branch and a mixed branch with respect to the choice of subalgebra. Of particular interest in this paper is the Coulomb branch, where the $U(1)$ R-symmetry is broken and the $SU(2)$ R-symmetry is preserved. In the brane picture the Coulomb branch can be identified with the space parametrized by the positions z_i of the N D3-branes on a 1-complex-dimensional slice \mathbb{C}/\mathbb{Z}_k of the transverse space. Here z_i is a complex number that parametrizes the position of the i -th D3-brane on this slice. The

Coulomb branch is then $\mathbb{C}^N/G(k, 1, N)$, where $G(k, 1, N)$ is generated by the transformations:

$$\begin{aligned} z_i &\rightarrow e^{\frac{2\pi i}{k}} z_i \\ z_i &\leftrightarrow z_j \end{aligned} \quad i, j = 1, \dots, N \quad (10.2)$$

The ring of polynomials in the z_i that are invariant under $G(k, 1, N)$ is freely generated, meaning that there are no non-trivial relations between the generators. There are N generators whose degrees are:

$$\Delta = (k, 2k, 3k, \dots, Nk) \quad (10.3)$$

The analysis of moduli space given so far has relied upon the brane picture for regular S-fold. Such a picture will not be available when we consider the generalization to exceptional S-fold, so an alternative approach is desirable. Kaidi, Martone and Zafrir presented a possible approach in [5], where they studied the moduli spaces of exceptional S-fold theories. Here we briefly review their results, more details can be found in the original paper. The idea is to start with a stack of Nk D3-branes in flat space. The low energy theory is then $\mathcal{N} = 4$ SYM with gauge algebra $\mathfrak{su}(Nk)$ and CB $(\mathbb{C})^{Nk}/\mathcal{W}(\mathfrak{su}(Nk))$ parametrized by the scalars Φ . Here $\mathcal{W}(\mathfrak{g})$ is the Weyl group of the Lie algebra \mathfrak{g} . Introducing an S_k -fold imposes the identification:

$$w \cdot \Phi = \mathcal{O}_k \Phi \quad (10.4)$$

Here \mathcal{O}_k is the action of the S-fold on the scalars, which is given by the R-symmetry transformation: $\mathcal{O}_k = e^{2\pi i/k}$. w is the Weyl element corresponding to the permutation of branes that maps each D3-brane to its first image under the S-fold and it is equal to the N -th power of the Coxeter element c :

$$\begin{aligned} w &= c^N \\ c &= s_1 \cdot s_2 \cdot \dots \cdot s_{Nk-1} \end{aligned} \quad (10.5)$$

where s_i is the reflection along the i -th simple root. Then (10.4) becomes:

$$c^N \cdot \Phi = e^{2\pi i/k} \Phi \quad (10.6)$$

Notice that (10.6) only requires to know the moduli space of the low energy field theory in the absence of the S-fold, which in this case is $\mathcal{N} = 4$ $SU(Nk)$ SYM, and does not rely on a brane picture. This allowed the authors of [5] to generalize this procedure to exceptional S-fold where the ‘‘parent’’ $\mathcal{N} = 4$ theory has gauge algebra \mathfrak{e}_n or \mathfrak{d}_n . This generalization requires a choice of an element w of the Weyl group, we will see that this choice is unique under a technical but reasonable assumption.

Mathematically Φ_C is a point in a space acted upon by a real reflection group (the Weyl group), and (10.6) identifies the eigenspace of the element w of the Weyl group (in this case c^N) with eigenvalue $e^{2\pi i/k}$. The action of the Weyl group on this eigenspace is called a reflection subquotient, and has been studied in generality in the mathematical literature, see [266] and reference therein for a comprehensive review of this topic. Here we report some results on reflection subquotient that are relevant for the study of moduli spaces of S-fold theories. Proofs and discussions regarding these mathematical results

can be found in [266], see **Theorem 11.24**, **Corollary 11.25**, **Theorem 11.28** and **Theorem 11.38** in that reference.

- The rank r of an S_k -fold $\mathcal{N} = 3$ theory is given by the number of degrees of CB invariants of the “parent” $\mathcal{N} = 4$ SYM that are divisible by k .
- The Coulomb branch of an S_k -fold $\mathcal{N} = 3$ theory is \mathbb{C}^r/\mathcal{C} with \mathcal{C} a complex crystallographic reflection group.
- The degrees of the generators of the S_k -fold Coulomb branch invariants are the degrees of \mathcal{C} , and are given by the degrees of invariants of the “parent” $\mathcal{N} = 4$ theory that are divisible by k .
- The codimension-1 singularities in the Coulomb branch of the S_k -fold $\mathcal{N} = 3$ theory are given by the intersection of the codimension-1 singularities of the “parent” $\mathcal{N} = 4$ theory with the $\mathcal{N} = 3$ Coulomb branch.

In the case of regular S-folds the “parent” theory is $SU(Nk)$ $\mathcal{N} = 4$ SYM, and the degrees of the generators of Coulomb branch invariants are:

$$2, 3, \dots, Nk \tag{10.7}$$

There are N degrees that are divisible by k :

$$k, 2k, \dots, Nk \tag{10.8}$$

that correspond to the degrees of the complex crystallographic reflection group $G(k, 1, N)$. This is consistent with the brane picture analysis, where the Coulomb branch was found to be $\mathbb{C}^N/G(k, 1, N)$.

When a brane picture is not available one needs to specify the element w of the Weyl of the “parent” $\mathcal{N} = 4$ theory that is involved in the S-fold projection (10.4). Modulo a technical assumption¹ such an element is unique up to conjugation and is characterized by having an r -dimensional eigenspace with eigenvalue $e^{2\pi i/k}$. Therefore the analysis of the Coulomb branch of exceptional S-fold theories boils down to finding an element w of the Weyl group that has an r -dimensional eigenspace with eigenvalue $e^{2\pi i/k}$.

Charge lattices of S-fold theories

In this Section we briefly recall the computation of the charge lattice of regular S-fold SCFTs performed in Chapter 9 and we give a field theoretic prescription to generalize the analysis to exceptional S-folds. Consider a stack of N D3-branes probing an S_k -fold without discrete torsion together with the $(k - 1)N$ image D3-branes. The local states of the SCFT are associated to finite length (p, q) -strings stretched between the D3-branes, plus their images under the S_k -fold. Denote as $|(p, q)\rangle_{i,j}$ a state associated to a (p, q) -string between the i -th and j -th D3-brane. The first image of this string is a (p', q') -string stretched between the $\pi(i)$ -th and $\pi(j)$ -th D3-brane. Here (p', q') are related to (p, q) by the S-duality transformation involved in the S-fold:

$$(p', q') = \rho_k \cdot (p, q) \tag{10.9}$$

¹Here, following [5], we assume that the rank of the $\mathcal{N} = 3$ theory is the highest possible.

And the $\pi(i)$ -th D3-brane is the first image of the i -th D3-brane. Let us number the D3-branes such that $\pi(i) = i + N$, and $i \sim i + kN$. The following states are invariant under the S-fold action:

$$\overline{|(p, q)\rangle}_{i,j} = \frac{1}{\sqrt{k}} \sum_{t=0}^{k-1} |(\rho_k)^t \cdot (p, q)\rangle_{\pi^t(i), \pi^t(j)} \quad (10.10)$$

The electromagnetic charges of the state $\overline{|(p, q)\rangle}_{i,j}$ can be written as a $2Nk$ -dimensional vector:

$$Q \left[\overline{|(p, q)\rangle}_{i,j} \right] = \frac{1}{\sqrt{k}} (e_1, \dots, e_{Nk}, m_1, \dots, m_{Nk}) \quad (10.11)$$

where e_i and m_i are the electric and magnetic charges under the i -th D3-brane, respectively. The Dirac pairing between two states ϕ and ψ with charges e_i, m_i and e'_i, m'_i is then:

$$\langle \phi, \psi \rangle = \frac{1}{k} \sum_{i=1}^{Nk} (e_i m'_i - e'_i m_i) \quad (10.12)$$

One can show that despite being represented by $2Nk$ -dimensional vectors the set of states invariant under the S-fold action (10.10) only span a $2N$ -dimensional lattice, which is the charge lattice of the rank- N S-fold SCFT.

In order to generalize this analysis to the exceptional S-fold case, let us express the various quantities of the S-fold theory (10.10), (10.11) and (10.12) in terms of field theoretical data of the “parent” $\mathcal{N} = 4$ $SU(kN)$ SYM theory, namely the roots $\alpha_{i,j}$ of $SU(kN)$ and the Cartan matrix $\mathcal{A}_{SU(Nk)}$. This can be done as follows. The string state $|(\rho_k)^t \cdot (p, q)\rangle_{i,j}$ correspond to a dyonic state with electric charge p and magnetic charge q with respect to a root $\alpha_{i,j}$ of $SU(kN)$:

$$|(\rho_k)^t \cdot (p, q)\rangle_{i,j} \rightarrow |\alpha_{i,j}, (\rho_k)^t \cdot (p, q)\rangle \quad (10.13)$$

The S-fold acts with a matrix ρ_k on the electric and magnetic charges (p, q) and acts as a permutation on the indices i, j . As discussed in the previous Section the permutation corresponds to the action of the Coxeter element c to the N -th power on the root $\alpha_{i,j}$. Suppressing the indices i, j the S-fold action can be written as:

$$S_k : |\alpha; (p, q)\rangle \rightarrow |c^N \cdot \alpha; \rho_k \cdot (p, q)\rangle \quad (10.14)$$

The states invariant under the S-fold (10.10) can be written in the following form in terms of the states of the “parent” $\mathcal{N} = 4$ theory:

$$\overline{|\alpha; (p, q)\rangle} = \frac{1}{\sqrt{k}} \sum_{t=0}^{k-1} |c^{tN} \cdot \alpha; (\rho_k)^t \cdot (p, q)\rangle \quad (10.15)$$

The charge lattice of the S-fold theory is spanned by these states for all choices of root $\alpha \in \Delta [SU(Nk)]$ and for any $p, q \in \mathbb{Z}$.

The electromagnetic charge of a state $\overline{|\alpha; (p, q)\rangle}$ is given by:

$$Q \left[\overline{|\alpha; (p, q)\rangle} \right] = \frac{1}{\sqrt{k}} \sum_{t=0}^{k-1} (w \otimes \rho_k)^t \cdot Q [|\alpha; (p, q)\rangle] \quad (10.16)$$

where $Q [|\alpha; (p, q)\rangle]$ is the electromagnetic charge of the corresponding state of $SU(Nk)$ $\mathcal{N} = 4$ SYM. Finally, the Dirac pairing defined on the charge lattice of the S-fold theory is obtained as a restriction of the Dirac pairing of $SU(Nk)$ $\mathcal{N} = 4$ SYM. Explicitly the Dirac pairing between two states of the S-fold theories with charges q_i and q_j is given by:

$$\langle q_i, q_j \rangle = q_i \cdot J_{SU(Nk)} \cdot q_j^T \tag{10.17}$$

where:

$$J_{SU(Nk)} = \begin{pmatrix} 0 & (\mathcal{A}_{SU(Nk)})^T \\ -\mathcal{A}_{SU(Nk)} & 0 \end{pmatrix} \tag{10.18}$$

is the Dirac pairing of the parent $SU(Nk)$ $\mathcal{N} = 4$ gauge theory [231]. Then the charge lattice $\Gamma_{N,k}$ of the S_k -fold theory is:

$$\Gamma_{N,k} = \left\{ Q [|\overline{(p, q)}\rangle_{i,j}] \mid p, q \in \mathbb{Z}, \quad i, j = 1, \dots, Nk \right\} \tag{10.19}$$

and the associated Dirac pairing is given by (10.17) and (10.18).

In this Chapter we are interested in the quantity $|\text{Pf}(J)|$. As already discussed in Chapter 9 the value of $|\text{Pf}(J)|$ is an invariant of any $\mathcal{N} = 2$ SCFT that equals the order of the 1-form symmetry group. One can intuitively think of this invariant as a measure of “how spread out” the charge lattice is. Indeed the number of electromagnetic charges that can be added to the charge lattice Γ without breaking the Dirac quantization condition is given by $|\text{Pf}(J)| - 1$. In this sense, the charge lattice Γ can not be arbitrarily dense, because $|\text{Pf}(J)|$ is at least 1. Crucially, in the rank-1 case there is also an upper bound for $|\text{Pf}(J)|$, given that we have a full classification of rank-1 $\mathcal{N} = 2$ SCFTs. The pfaffian of the Dirac pairing of a rank-1 SCFT is at most 2, therefore the 1-form symmetry group of a rank-1 SCFT is either \mathbb{Z}_2 or the trivial group.

Intuitively the upper bound for “how spread out” the charge lattice is in rank-1 SCFTs, together with the idea of stratification of the Coulomb branch, should impose an upper bound for higher rank theories as well. In Section 10.2 we will see that this is the case by studying explicit examples, namely exceptional S-fold SCFTs, while in Chapter 11 with discuss this idea in more generality.

Discrete torsion

Some S-fold backgrounds can admit a non-zero flux for the Type IIB 2-form fields around cycles of the transverse space. This is possible for $k = 2$, giving rise to the orientifold $O3^+$, $\widetilde{O3}^+$ and $\widetilde{O3}^-$, and for $k = 3, 4$ giving rise to fluxful S-folds denoted as $S_{3,3}$ and $S_{4,4}$. When the discrete torsion is non-zero the S-fold is magnetically charged under the corresponding 2-form field, and strings can end on the S-fold itself. Strings stretched between the S-fold and a D3-brane generate additional states in the SCFT with respect to the fluxless case, and the charge lattice is more dense. The states corresponding to strings stretched between the S-fold and a D3-brane can not be written in the form (10.15). In order to include them we are led to consider states of the general form:

$$|\overline{\alpha, (p, q)}\rangle_{\{p_{i,j}\}} = \frac{1}{\sqrt{k}} \sum_{i=0}^{k-1} \sum_{j=0}^1 p_{i,j} \left| c^{iN} \cdot \alpha; (\rho_k)^j \cdot (p, q) \right\rangle \tag{10.20}$$

where $p_{i,j}$ are integers such that the state (10.20) are invariant under the S-fold action (10.14). The sum over i runs from 0 to $k-1$ because c^N satisfies its characteristic equation, which is an order k polynomial equation, and similarly the sum over j runs from 0 to 1 because ρ_k satisfies an order 2 polynomial equation.

One can show that such states correctly reproduce the strings stretched between a D3-brane and the S-fold itself. We can therefore see that the presence of a non-trivial discrete torsion can be accounted for by considering the charge lattice spanned by the states (10.20) rather than (less general) states (10.15).

In the context of exceptional S-folds the states (10.20) will only play a minor role, therefore we will not discuss them further.

10.1.2 Discrete gauging and 2-form symmetries

The S-fold theories obtained from the Type IIB setup can sometimes have a non-trivial 2-form symmetry and can be seen as a discrete gauging of a “parent” theory [199]. Gauging a discrete 0-form symmetry of the parent theory gives rise to a magnetic 2-form symmetry, and viceversa. One can go from the parent theory to the daughter theory by gauging the relative discrete symmetry. This operation is therefore reversible, and one may choose to study either of the two theories without losing information. When this is the case it is convenient to study the parent theory itself, for example the Shapere-Tachikawa formula for the central charges is believed to hold only in the absence of 2-form symmetries.

In this Section we show how to detect 2-form symmetries that arise from the discrete gauging of a 0-form symmetry that acts on the Coulomb branch. We also give a consistency constraint for the BPS spectrum of $\mathcal{N} = 2$ SCFTs based on the classification of rank-1 theories. We elaborate this analysis in the cases of the $O3^-$ and the flux-less S_3 -fold. In Section 10.2 similar considerations will lead us to claim that some exceptional S-fold theories are discrete gaugings of free theories.

Strings across the flux-less orientifold

As a familiar example, consider the $O3^-$ plane, which corresponds to the S-fold with $k = 2$ and trivial discrete torsion. The low energy theory on a stack of N D3 branes on top of the $O3^-$ is $\mathcal{N} = 4$ SYM with gauge algebra $\mathfrak{so}(2N)$, and is believed to be a \mathbb{Z}_2 discrete gauging of the $\mathcal{N} = 4$ theory with gauge group $Spin(2N)$. Indeed the space parametrized by the transverse motion of the D3-branes is $\mathbb{C}^N / \left(\mathcal{W} [\mathfrak{so}(2N)] \rtimes \mathbb{Z}_2 \right)$, which is compatible with the moduli space of $\mathcal{N} = 4$ $Spin(2N)$ with an additional \mathbb{Z}_2 identification given by gauging charge conjugation. In this example the “parent” theory has trivial 2-form symmetry and has a \mathbb{Z}_2 0-form symmetry, namely charge conjugation. The theory on the stack of D3-branes is obtained by gauging this \mathbb{Z}_2 0-form symmetry, and therefore has a \mathbb{Z}_2 2-form symmetry.

The 2-form symmetry can be detected by looking at the moduli space $\mathbb{C}^N / \left(\mathcal{W} [\mathfrak{so}(2N)] \rtimes \mathbb{Z}_2 \right)$. In particular the singularities on moduli space given by the additional \mathbb{Z}_2 identifications correspond to configurations where one D3-brane is on top of the orientifold. There are no massless BPS charged states associated to this singularities because the ground state of strings connecting the D3-brane and its image, which have zero length, are projected out by the orientifold [267]. This is consistent with the fact that the \mathbb{Z}_2 identification on

moduli space is due to a discrete gauging of a \mathbb{Z}_2 0-form symmetry. In general a discrete gauging of a 0-form symmetry that acts non-trivially on the Coulomb branch produces singularities where no BPS state becomes massless. Suppose that an S-fold theory \mathcal{T} has a Coulomb branch:

$$\mathcal{C} = \mathbb{C}^N / (\mathcal{G} \rtimes \mathcal{G}') \quad (10.21)$$

and charge lattice Γ . Suppose that on the fixed loci of \mathcal{G} some state $\gamma \in \Gamma$ has zero central charge \mathcal{Z} , and therefore becomes massless, while on the fixed points of \mathcal{G}' all the states in the charge lattice are massive. Then \mathcal{T} has a non-trivial 2-form symmetry $G^{(2)} = \mathcal{G}'$ and can be regarded as a \mathcal{G}' discrete gauging of a “parent” theory \mathcal{T}' with Coulomb branch:

$$\mathcal{C}' = \mathbb{C}^N / (\mathcal{G}) \quad (10.22)$$

and with the same charge lattice Γ . The “parent” theory \mathcal{T}' has a 0-form symmetry which contains \mathcal{G}' as a discrete subgroup. Therefore we are able to detect the presence of a non-trivial discrete 2-form symmetry $G^{(2)}$ from the knowledge of the Coulomb branch and charge lattice if $G^{(2)}$ arises from a discrete gauging of a 0-form symmetry that acts non-trivially on the Coulomb branch.

In the example of the $O3^-$ given above the absence of charged massless states on the fixed points of the \mathbb{Z}_2 identification can be explained from string theoretical considerations, but one would like a field theoretical argument as well. Consider a point p in \mathbb{C}^N that is fixed under \mathbb{Z}_2 and is generic otherwise. The prescription given in Section 10.1 to compute the charge lattice Γ predicts massless states on this singularity corresponding to (p, q) -strings stretched between a D3-brane and its image. Denote as $\Gamma^{(1)}$ the sublattice of Γ spanned by these states. $\Gamma^{(1)}$ should be the charge lattice of a rank-1 QFT $\mathcal{T}^{(1)}$ whose Coulomb branch is given by the slice transverse to the singular locus in a neighborhood of p , namely \mathbb{C}/\mathbb{Z}_2 . A basis of $\Gamma^{(1)}$ is given by the states associated to an F1 and a D1 string which we denote as ψ and ϕ respectively. The Dirac pairing between these states is $\text{Pf}(J^{(1)}) = \langle \psi, \phi \rangle = 4$, therefore they are not mutually local and $\mathcal{T}^{(1)}$ must be an interacting CFT. We have denoted as $J^{(1)}$ the matrix representing the Dirac pairing of the rank-1 theory in this basis. Furthermore by the argument given in [29] (see Section 10.1) $\mathcal{T}^{(1)}$ should have a non-trivial 1-form symmetry group of order 4. A full classification of rank-1 $\mathcal{N} = 2$ SCFTs is available [207, 209, 206, 208], and a theory such as $\mathcal{T}^{(1)}$ does not exist. In particular the maximum order for the 1-form symmetry group of a rank-1 SCFT is 2 [231], saturated for example by $\mathcal{N} = 4$ $SU(2)$ SYM. We conclude that the states in $\Gamma^{(1)}$ can not be BPS, therefore on the fixed locus of the \mathbb{Z}_2 identification there are no massless states, consistently with the string theory prediction.

Strings across the flux-less S_3 -fold

We have shown that the analysis of the charges of states becoming massless on a singularity of the Coulomb branch imposes non-trivial constraints on the BPS spectrum of a theory. This is especially interesting to study in non-lagrangian theories, where discrete gaugings and 2-form symmetries are not readily apparent. As an example, we now show that in the flux-less S-folds with $k = 3$ the strings stretched between one D3-brane and its image are not BPS. Consequently, these theories are discrete gaugings of other $\mathcal{N} = 3$ “parent” theories, as originally discussed in [199]. A similar analysis in Section 10.2 will show that some exceptional S-fold theories, for example the G_5 theory discussed in Section 10.2.2, are discrete gaugings of free theories.

The Coulomb branch of the regular S_k -fold SCFT at rank r theories has two types of codimension 1 singularities on the Coulomb branch: singularities where two D3-branes coincide and singularities where one D3-brane is on top of the S-fold. When two D3-branes coincide the associated rank-1 theory is always $SU(2) \mathcal{N} = 4$ SYM, which is a consistent rank-1 SCFT, therefore we will focus on the other singularities. When one D3-brane is on top of the S-fold the corresponding rank-1 theory is the rank-1 version of the S-fold theory under consideration. In the case of flux-less S-folds the rank-1 theories are believed to be discrete gaugings of $U(1) \mathcal{N} = 4$, with no massless states charged under the $U(1)$. Let us show that this must indeed be the case for the $k = 3$ S-fold. In the absence of discrete torsion the charge sublattice $\Gamma^{(1)}$ is spanned by (p, q) -strings stretched between the D3-brane and its image. A possible basis for this lattice is given by the states associated to an F1 and a D1 string, let us denote them as $|f1\rangle$ and $|d1\rangle$ respectively. The Dirac pairing matrix in this basis is:

$$J^{(1)} = \begin{pmatrix} 0 & \langle f1, d1 \rangle \\ -\langle f1, d1 \rangle & 0 \end{pmatrix} \quad (10.23)$$

The order of the 1-form symmetry group is given by the Pfaffian of the Dirac pairing:

$$|G^{(1)}| = \left| \text{Pf} \left(J^{(1)} \right) \right| = \langle f1, d1 \rangle = \begin{cases} 3 & k = 3 \\ 2 & k = 4 \\ 1 & k = 6 \end{cases} \quad (10.24)$$

The Coulomb branch of these rank-1 theories is \mathbb{C}/\mathbb{Z}_k . For $k = 3$ the putative theory on this singularity is inconsistent because, as discussed above, the maximum order for the 1-form symmetry group of a rank-1 $\mathcal{N} = 2$ SCFT is 2. Therefore the states associated to strings stretched between a D3-brane and its images can not be BPS.

The Coulomb branch can thus be written as:

$$\mathcal{C} = \mathbb{C}^N / (G(3, 1, r)) = \mathbb{C}^N / (G(3, 3, r) \rtimes \mathbb{Z}_3) \quad (10.25)$$

where there are massless charged states on the fixed points of $G(3, 3, r)$ and there are no massless charged states on the fixed points of \mathbb{Z}_3 . This Coulomb branch is consistent with the Coulomb branch of a \mathbb{Z}_3 discrete gauging “parent” theory with Coulomb branch $\mathcal{C}' = \mathbb{C}^N / G(3, 3, r)$ and 2-form symmetry group \mathbb{Z}_3 , reproducing the M-theory results of [199]. Furthermore we have shown that in a flux-less S-fold background with $k = 3$ the states associated to strings stretched between a D3-brane and its image are not BPS, because otherwise the Coulomb branch stratification would be inconsistent. This further strengthens the analysis of the BPS spectrum of the rank-2 S-fold theories performed in [246, 245]. One could perform a similar analysis in the case of flux-full S-folds. The resulting rank-1 theories on the codimension-1 singularities are all consistent in this case, therefore the Coulomb branch of these theories is $\mathbb{C}^N / (G(k, 1, r))$ and there are massless charged states on all singularities.

Strings across the flux-less S_4 -fold

As a final example of our techniques before delving into the topic of exceptional S-folds we consider the fluxless S-fold with $k = 4$. Similarly to the case of the S_3 -fold we will show that the strings stretched between a D3-brane and its images do not produce BPS states. In addition to the analysis of the charge lattice we will also consider constraints on

the central charges of the theories supported on codimension-1 singularities. These two computations give incompatible results unless the strings across the S_4 -fold are not BPS and in return the S_4 -fold SCFTs must be discrete gaugings, reproducing the M-theory results of [199]. A similar phenomena happens in exceptional S-fold theories, for example the G_8 theory discussed in Section 10.2.3 turns out to be a discrete gauging of a free theory.

Consider the rank- r fluxless S_4 -fold SCFT. The Coulomb branch of the rank-1 SCFT on the singularity that arises when a D3-brane coincides with the S_4 -fold is parametrized by the motion of the D3-brane on a 1-complex-dimensional slice of the transverse space, and is therefore \mathbb{C}/\mathbb{Z}_4 . The order of the 1-form symmetry group of the rank-1 SCFT on this singularity was computed in (10.24):

$$|G^{(1)}| = \left| \text{Pf} \left(J^{(1)} \right) \right| = 2 \tag{10.26}$$

The only candidate for the rank-1 theory supported on this singularity is the $\mathcal{N} = 3$ preserving \mathbb{Z}_4 gauging of $SU(2) \mathcal{N} = 4$ SYM.

We may now consider the central charge of the S_4 -fold SCFTs. Assuming that the rank-1 theories on all the singularities are not empty and the S_4 -fold SCFTs are not discrete gaugings the central charges can be computed with the Shapere-Tachikawa formula [268]:

$$2(2a - c) = \sum_{j=1}^r \Delta_j - \frac{r}{2} = 2r^2 + \frac{3}{2}r \tag{10.27}$$

where $\{\Delta_i\} = \{4, 8, \dots, 4r\}$ are the degrees of invariants of $G(4, 1, r)$. The central charges may also be computed using the formulae of [218, 210] that relate data of the rank-1 theories supported on the codimension-1 singularities to the central charge of the rank- r theory:

$$12c = 2r + h_{\text{ECB}} + \sum_{i \in \mathcal{I}} \Delta_i^{\text{sing}} b_i \tag{10.28}$$

where b_i is a quantity associated with the rank-1 theory supported on the i -th codimension-1 singularity as follows:

$$b_i := \frac{12c_i - h_i - 2}{\Delta_i} \tag{10.29}$$

In our theory the extended Coulomb branch dimension is $h_{\text{ECB}} = r$ and the set \mathcal{I} consists of the two codimension-1 singularities. The scaling dimensions Δ_i^{sing} of these singularities can be found for example in [5], Appendix B. It turns out that the singularity associated to the collision of two D3-branes has scaling dimension $\Delta_1^{\text{sing}} = 4r(r - 1)$ and parameter $b_1 = b_{SU(2)} = 3$. The other singularity has scaling dimension $\Delta_2^{\text{sing}} = 4r$, therefore (10.28) reduces to:

$$12c = 3r + 12r(r - 1) + b_2 4r \tag{10.30}$$

Comparing with (10.27) with $a = c$ and solving for b_2 one finds:

$$b_2 = \frac{9}{2} \tag{10.31}$$

$$\begin{aligned}
\mathcal{A}_{E_6} &= \begin{pmatrix} 2 & -1 & 0 & 0 & 0 & 0 \\ -1 & 2 & -1 & 0 & 0 & 0 \\ 0 & -1 & 2 & -1 & 0 & -1 \\ 0 & 0 & -1 & 2 & -1 & 0 \\ 0 & 0 & 0 & -1 & 2 & 0 \\ 0 & 0 & -1 & 0 & 0 & 2 \end{pmatrix}, \\
\mathcal{A}_{E_7} &= \begin{pmatrix} 2 & -1 & 0 & 0 & 0 & 0 & 0 \\ -1 & 2 & -1 & 0 & 0 & 0 & 0 \\ 0 & -1 & 2 & -1 & 0 & 0 & 0 \\ 0 & 0 & -1 & 2 & -1 & 0 & -1 \\ 0 & 0 & 0 & -1 & 2 & -1 & 0 \\ 0 & 0 & 0 & 0 & -1 & 2 & 0 \\ 0 & 0 & 0 & -1 & 0 & 0 & 2 \end{pmatrix}, \\
\mathcal{A}_{E_8} &= \begin{pmatrix} 2 & -1 & 0 & 0 & 0 & 0 & 0 & 0 \\ -1 & 2 & -1 & 0 & 0 & 0 & 0 & 0 \\ 0 & -1 & 2 & -1 & 0 & 0 & 0 & 0 \\ 0 & 0 & -1 & 2 & -1 & 0 & 0 & 0 \\ 0 & 0 & 0 & -1 & 2 & -1 & 0 & -1 \\ 0 & 0 & 0 & 0 & -1 & 2 & -1 & 0 \\ 0 & 0 & 0 & 0 & 0 & -1 & 2 & 0 \\ 0 & 0 & 0 & 0 & -1 & 0 & 0 & 2 \end{pmatrix}
\end{aligned}$$

Figure 10.1 Cartan matrices of the exceptional algebras E_r , $r = 6, 7, 8$.

Which is compatible with having a rank-1 fluxfull S_4 -fold SCFT on the singularity corresponding to a D3-brane on top of the S_4 -fold. This is incompatible with the charge lattice computed above, indeed the only possible SCFT on this singularity compatible with the charge lattice is a discrete gauging of $\mathcal{N} = 4$ $SU(2)$ SYM, which would require $b_2 = 3$.

We conclude that the states associated to string stretched between a D3-brane and its images do not produce BPS states. Then the rank-1 theory arising when one D3-brane approaches the fluxless S_4 fold is not an interacting SCFT, but rather a discrete gauging of free $\mathcal{N} = 4$ Maxwell theory. The S_4 -fold SCFTs can then be thought as a \mathbb{Z}_4 discrete gauging of a parent theory with moduli space $\mathbb{C}^{3r}/G(4, 4, r)$, reproducing the results of [199].

10.2 Exceptional S-folds

In this Section we study exceptional S-fold $\mathcal{N} = 3$ SCFTs [200]. We apply the techniques spelled out in the previous Sections to compute the charge lattice of these theories, the order of the 1-form symmetry group and we determine when such SCFTs can be built as discrete gauging of a parent theory. The exceptional S-fold setup of [200], briefly reviewed below, engineers a set of SCFTs labelled by an algebra of type D_n or E_r , $r = 6, 7, 8$, and the order of the S-fold $k = 3, 4, 6$. The analysis can be generalized by including a suitable outer automorphism [5]. For simplicity in this paper we focus on the exceptional algebras $E_{6,7,8}$ with $k = 3, 4, 6$ and without outer automorphism twists. Extending our methods to the full set of exceptional S-fold SCFTs should not present any

major technical or conceptual difficulty, but we leave this task to future work. We are thus interested in 9 theories labelled by $k = 3, 4, 6$ and by the exceptional algebra E_r . We find compelling arguments that suggest that all but one of these theories do not admit a well defined charge lattice and are discrete gauging of free theories. In particular the only theory that, given our current understanding, is a proper interacting $\mathcal{N} = 3$ SCFTs is the G_{31} theory that can be engineered as the E_8S_4 -fold. Our results are summarized in Table 10.1.

10.2.1 S-folds from the $(2, 0) E_6$ theory

The six-dimensional $(2, 0)$ theory of type E_6 on torus $T^2 \times \mathbb{R}^4$ engineers $\mathcal{N} = 4$ SYM with gauge algebra E_6 in the 4d limit. When this compactification is complemented with the S-fold projection spelled out above one obtains the exceptional S-fold theories of interest. The strategy we adopt, introduced in full generality in Section 10.1, is to compute the effect of the S-fold projection directly on the four-dimensional charge lattice. This approach allows us to compute the charge lattice of the $\mathcal{N} = 3$ S-fold theories from the charge lattice of the $\mathcal{N} = 4$ SYM with gauge algebra E_6 . The analysis parallels the one in [5], where the moduli space of exceptional S-fold theories was computed as a subquotient of the moduli space of the $\mathcal{N} = 4$ SYM parent theory.

The charge lattice of $\mathcal{N} = 4 E_6$ SYM is spanned by the W-bosons, which are valued in the root lattice Δ of E_6 and by the magnetic monopoles, which are valued in coroot lattice Δ^\vee . Choose a basis for the root and coroot lattices given by a set of simple roots and the corresponding coroots respectively. In this basis the metric on the root lattice is given by the Cartan matrix \mathcal{A}_{E_6} of E_6 , see Figure 10.1, and the roots are represented by integer vectors with length $\sqrt{2}$. The simple roots are represented by vectors with one entry equals to 1 and the other entries equal to 0. A charge \tilde{Q} in the charge lattice $\Gamma = \Delta \otimes \Delta^\vee$ is represented by an integer twelve-dimensional vectors, where the first six entries are electric charges and the last six entries are magnetic charges:

$$\tilde{Q} = (e_1, e_2, \dots, e_6, m_1, m_2, \dots, m_6) \tag{10.32}$$

The Dirac pairing between two charge \tilde{Q} and \tilde{P} is given by $\tilde{Q} \cdot J_{E_6} \cdot \tilde{P}^T$ where the Dirac pairing J_{E_6} is given by [231]:

$$J_{E_6} = \begin{pmatrix} 0 & (\mathcal{A}_{E_6})^T \\ -\mathcal{A}_{E_6} & 0 \end{pmatrix} \tag{10.33}$$

In the following it will be more convenient to write the charges in a basis where we alternate electric charges and magnetic charge, namely:

$$Q = (e_1, m_1, e_2, m_2, \dots, e_6, m_6) \tag{10.34}$$

We will distinguish the charges in the two basis by using tildes for vectors in the first basis (10.32) and symbols without tildes in the second basis (10.34).

The Weyl group of E_6 is generated by the reflections along the simple roots, we denote the reflection along the i -th simple root as s_i . A useful element of the Weyl group is the Coxeter element c_{E_6} , defined as:

$$c_{E_6} = s_1 \cdot s_2 \cdot s_3 \cdot s_4 \cdot s_5 \cdot s_6 \tag{10.35}$$

\mathfrak{g}	degrees	codegrees
E_6	2,5,6,8,9,12	0,3,4,6,7,10
E_7	2,6,8,10,12,14,18	0,4,6,8,10,12,16
E_8	2,8,12,14,18,20,24,30	0,6,10,12,16,18,22,28

Table 10.2 Degrees and codegrees of the exceptional algebras E_r .

E_6				
k	w	r	ECCRG	Δ_i
3	$(c_{E_6})^4$	3	G_{25}	{6, 9, 12}
4	$(c_{E_6})^3$	2	G_8	{8, 12}
6	$(c_{E_6})^2$	2	G_5	{6, 12}

Table 10.3 Elements $w \in \mathcal{W}[E_6]$ that characterize the S-fold actions for the S-fold theories of type E_6 through (10.38) and (10.39). Here c_{E_6} is the Coxeter element of E_6 , r is the rank of the S-fold theory and in the fourth and fifth columns the exceptional complex crystallographic reflection group (ECCRG) associated to the S-fold theories and its degrees Δ_i are reproduced.

which has order equal to the Coxeter number $h_{E_6} = 12$:

$$(c_{E_6})^{12} = \text{Id} \tag{10.36}$$

The eigenvalues of the Coxeter element are $\lambda_i = e^{2\pi i/(m_i-1)}$ where $m_i, i = 1 \dots, 6$ are the degrees of the invariants of E_6 , tabulated in 10.2. In the basis given by the simple roots the Coxeter element is represented by the matrix:

$$c_{E_6} = \begin{pmatrix} 0 & 0 & 1 & 0 & -1 & -1 \\ 1 & 0 & 1 & 0 & -1 & -1 \\ 0 & 1 & 1 & 0 & -1 & -1 \\ 0 & 0 & 1 & 0 & -1 & 0 \\ 0 & 0 & 0 & 1 & -1 & 0 \\ 0 & 0 & 1 & 0 & 0 & -1 \end{pmatrix} \tag{10.37}$$

Consider now the exceptional S-fold setup that engineers an $\mathcal{N} = 3$ SCFT in four dimensions. In Section 10.1 we studied the S-fold projection along the lines of [5] and discussed how the rank, Coulomb branch, charge lattice and associated Dirac pairing can be computed directly from the $\mathcal{N} = 4$ parent theory, in this case $\mathcal{N} = 4$ E_6 SYM. Here we summarize the main results for ease of readability. The Coulomb branch of the $\mathcal{N} = 3$ S-fold theory is given by the solutions to:

$$w \cdot \phi_C = e^{2\pi i/k} \phi_C \tag{10.38}$$

where ϕ_C are elements of the Coulomb branch of E_6 $\mathcal{N} = 4$ SYM. The element $w \in \mathcal{W}[E_6]$ encodes the projection induced by the S-fold on the Coulomb branch and on the charge lattice of the E_6 $\mathcal{N} = 4$ theory. The rank r of the $\mathcal{N} = 3$ theory is given by the complex dimension of the eigenspace associated to the eigenvalue $e^{2\pi i/k}$ of w and we choose w such that the $\mathcal{N} = 3$ has maximum rank, following [5]. The degrees of basic Coulomb

branch invariants is then given by the degrees of invariants of E_6 that are divisible by k and the $\mathcal{N} = 3$ Coulomb branch itself is \mathbb{C}^r/G with G the complex reflection group with the correct degrees, see Table 10.3.

The charged states $\overline{|\alpha; (p, q)\rangle}$ of the $\mathcal{N} = 3$ theory are given by:

$$\overline{|\alpha; (p, q)\rangle} = \frac{1}{\sqrt{k}} \sum_{t=0}^{k-1} |w^t \cdot \alpha; (\rho_k)^t \cdot (p, q)\rangle \tag{10.39}$$

where $|\beta; (p, q)\rangle$ is a (p, q) -dyonic states of E_6 $\mathcal{N} = 4$ SYM associated to the root β of E_6 . The electromagnetic charge of a state $\overline{|\alpha; (p, q)\rangle}$ is given by;

$$Q \left[\overline{|\alpha; (p, q)\rangle} \right] = \frac{1}{\sqrt{k}} \sum_{t=0}^{k-1} (w \otimes \rho_k)^t \cdot Q [|\alpha; (p, q)\rangle] \tag{10.40}$$

where $Q [|\alpha; (p, q)\rangle]$ is the electromagnetic charge of the corresponding state of E_6 $\mathcal{N} = 4$ SYM, expressed as in (10.34). As an example the W-boson associated to the first root α_1 of E_6 has charge $Q [|\alpha_1; (1, 0)\rangle] = (1, 0; 0, 0; \dots)$ while the magnetic monopole associated to the first coroot has charge $Q [|\alpha_1; (0, 1)\rangle] = (0, 1; 0, 0; \dots)$.

One can consider more general states that are invariant under the S-fold action, see for example (10.20). In the case of regular S-folds some of these states appear in the presence of discrete torsion and correspond to strings stretched between the S-fold and a D3 brane. In the case of exceptional S-folds the states (10.20) can never be included consistently, therefore in the remainder of this paper we will only mention them briefly.

Finally, the Dirac pairing defined on the charge lattice of the $\mathcal{N} = 3$ theory is obtained as a restriction of the Dirac pairing of E_6 $\mathcal{N} = 4$ SYM (10.33). Explicitly the Dirac pairing between two states of the S-fold theories with charges q_i and q_j is given by:

$$\langle q_i, q_j \rangle = q_i \cdot J_{E_6} \cdot q_j^T \tag{10.41}$$

Notice that it is not guaranteed that $\langle q_i, q_j \rangle$ gives an integer result and one should check case by case that the Dirac pairing between any two charges of the S-fold theories is integer. In the following we do not consider any charge lattice where the Dirac pairing can take fractional values.

10.2.2 The $k = 6$ S-fold: G_5

The first exceptional S-fold theory that we consider is obtained as a \mathbb{Z}_6 S-fold compactification of the $(2, 0)$ six-dimensional E_6 theory to four dimension. The compactification preserves $\mathcal{N} = 3$ supersymmetry in four dimension and involves an S-duality transformation $\rho_6 \in SL(2, \mathbb{Z})$ and an R-symmetry twist. The Coulomb branch is given by the solutions to (10.38) with $k = 6$, namely:

$$w \cdot \phi_C = e^{\pi i/3} \phi_C \tag{10.42}$$

There are 2 invariants of E_6 whose degrees are divisible by 6, namely the invariants with degrees 6 and 12, and therefore we expect that the $\mathcal{N} = 3$ theory has rank $r = 2$. We choose an element $w \in \mathcal{W}[E_6]$ which has a two-dimensional eigenspace associated to

the eigenvalue $e^{\pi i/3}$:

$$w = (c_{E_6})^2 \tag{10.43}$$

which is the basis given by the simple roots is represented by the matrix:

$$w = \begin{pmatrix} 0 & 1 & 0 & -1 & 0 & 0 \\ 0 & 1 & 1 & -1 & -1 & -1 \\ 1 & 1 & 1 & -1 & -1 & -1 \\ 0 & 1 & 1 & -1 & 0 & -1 \\ 0 & 0 & 1 & -1 & 0 & 0 \\ 0 & 1 & 0 & 0 & -1 & 0 \end{pmatrix} \tag{10.44}$$

Then the Coulomb branch of the $\mathcal{N} = 3$ theory, given by the solutions to (10.42), is \mathbb{C}^2/G_5 where G_5 is the CCRG with degrees 6 and 12. Similarly the charge lattice of the $\mathcal{N} = 3$ theory can be obtained from the charge lattice of the $\mathcal{N} = 4 E_6$ SYM. Given a state of $\mathcal{N} = 4 E_6$ SYM associated to the root α with electric and magnetic charges (p, q) one can build a state $|\alpha, (p, q)\rangle$ that is invariant under the S-fold action:

$$\overline{|\alpha, (p, q)\rangle} = \frac{1}{\sqrt{6}} \sum_{t=0}^5 |w^t \cdot \alpha; (\rho_6)^t \cdot (p, q)\rangle \tag{10.45}$$

Consider the six states $\overline{|\alpha_i, (1, 0)\rangle}$ obtained with this projection from the W -bosons associated to the simple roots $\alpha_i, i = 1, \dots, 6$ of E_6 . The electromagnetic charges q_i of these states can be computed using (10.40):

$$\begin{aligned} q_1 &= \frac{1}{\sqrt{6}} (2, -1, 1, -2, 2, -4, 0, -3, 1, -2, 0, 0) \\ q_2 &= \frac{1}{\sqrt{6}} (1, -2, 3, -3, 2, -4, 1, -2, -1, -1, 2, -4) \\ q_3 &= \frac{1}{\sqrt{6}} (1, 1, 2, -1, 4, -2, 3, -3, 2, -1, 0, 0) \\ q_4 &= \frac{1}{\sqrt{6}} (-2, 1, -1, 2, -2, 4, 0, 3, -1, 2, 0, 0) \\ q_5 &= \frac{1}{\sqrt{6}} (-1, 2, -3, 3, -2, 4, -1, 2, 1, 1, -2, 4) \\ q_6 &= \frac{1}{\sqrt{6}} (0, 0, -2, 4, -2, 4, -2, 4, 0, 0, 2, 2) \end{aligned} \tag{10.46}$$

Notice that $q_1 = -q_4$ and $q_2 = -q_5$, therefore these charges span a four-dimensional lattice Γ :

$$\Gamma = \text{Span}_{\mathbb{Z}} \{q_1, q_2, q_3, q_6\} \tag{10.47}$$

The charges of states obtained from W -bosons associated to other roots of E_6 are included in Γ because the other roots are linear integer combinations of the simple roots and (10.40) is linear in the charges. One can also check that the charges of states $|\alpha_i, (0, 1)\rangle$ obtained from monopoles of E_6 are included in Γ as well, therefore by linearity Γ includes the charges of all the states (10.45). One may also consider the more general states (10.20). We checked explicitly that including some or all of these states either leaves Γ unchanged or produces fractional Dirac pairing between the states, which is inconsistent. Then (10.47) is the candidate for the charge lattice Γ of the $\mathcal{N} = 3 G_5$ exceptional S-fold theory. In the remainder of this section we will show that Γ is actually incom-

patible with a consistent Coulomb branch stratification, and we will argue that the low energy field theory is given by a discrete gauging of free $U(1)^2$ $\mathcal{N} = 4$ gauge theory.

Having computed a candidate Γ for the charge lattice of the G_5 theory we now study the Dirac pairing defined on this lattice and the sublattices of states that become massless on some Coulomb branch singularity. The Dirac pairing between two states with charges q_i and q_j is given by:

$$\langle q_i, q_j \rangle = q_i \cdot J_{E_6} \cdot q_j^T \quad (10.48)$$

where J_{E_6} is the Dirac pairing of the $\mathcal{N} = 4$ theory (10.33). In the basis of Γ given by q_1, q_2, q_3 and q_6 the Dirac pairing J_{G_5} of the $\mathcal{N} = 3$ theory is represented by the matrix:

$$J_{G_5} = \begin{pmatrix} 0 & -1 & 3 & -4 \\ 1 & 0 & -1 & 4 \\ -3 & 1 & 0 & -2 \\ 4 & -4 & 2 & 0 \end{pmatrix} \quad (10.49)$$

If Γ is the charge lattice of the G_5 theory then the order of the 1-form symmetry group is given by the absolute value of the Pfaffian of J_{G_5} :

$$\left| G_{G_5}^{(1)} \right| = |\text{Pf}(J_{G_5})| = 6 \quad (10.50)$$

Let us consider the states becoming massless on some codimension-1 singularity on the Coulomb branch. We can parametrize the Coulomb branch of the $\mathcal{N} = 4$ E_6 SYM with six complex scalars $\phi_i, i = 1, \dots, 6$, with identifications given by the Weyl group of E_6 . The Coulomb branch \mathcal{C}_{G_5} of the $\mathcal{N} = 3$ G_5 theory is given by the eigenspace of w with eigenvalue $e^{\pi i/3}$ and can be parametrized as follows as an embedding in \mathcal{C}_{E_6} :

$$\mathcal{C}_{G_5} = \left(\phi_3 - \phi_4, e^{i\pi/3}\phi_3 + e^{-i\pi/3}\phi_4, \phi_3, \phi_4, e^{2\pi i/3}(\phi_4 - \phi_3), \sqrt{3}e^{i\pi/6}\phi_3 + 2e^{4\pi i/3}\phi_4 \right) \quad (10.51)$$

The codimension-1 singularities of \mathcal{C}_{G_5} correspond to fixed points under the reflection of G_5 acting on this slice. As discussed in Section 10.1.1 can be obtained as the intersections of the codimension-1 singularities of the E_6 $\mathcal{N} = 4$ SYM with the slice (10.51). As an example consider the singularity $\mathcal{H}_{s_1}^{E_6}$ of \mathcal{C}_{E_6} corresponding to the fixed locus under s_1 , the reflection along the first simple root of E_6 , which is the 5-dimensional hyperplane:

$$\mathcal{H}_{s_1}^{E_6} = \{(\phi_1, 2\phi_1, \phi_3, \phi_4, \phi_5, \phi_6), \phi_i \in \mathbb{C}\} \quad (10.52)$$

The intersection of $\mathcal{H}_{s_1}^{E_6}$ with the slice \mathcal{C}_{G_5} gives a codimension-1 singularity $\mathcal{H}_{s_1}^{G_5}$ of the Coulomb branch of the G_5 theory:

$$\begin{aligned} \mathcal{H}_{s_1}^{G_5} &= \mathcal{H}_{s_1}^{E_6} \cap \mathcal{C}_{G_5} \\ &= \left(1, 2, \frac{1}{2}(5 - i\sqrt{3}), \frac{1}{2}(3 - i\sqrt{3}), -(-1)^{2/3}, \frac{1}{2}(3 - i\sqrt{3}) \right) \phi_3 \end{aligned} \quad (10.53)$$

The states that can become massless on $\mathcal{H}_{s_1}^{G_5}$ are those whose central charge Z vanish identically on $\mathcal{H}_{s_1}^{G_5}$. On a generic point ϕ of the Coulomb branch of E_6 $\mathcal{N} = 4$ SYM the

central charge Z of a state with charge q is given by:

$$Z[q] = \sum_{i,j=1}^6 \phi_i (A_{E_6})_{ij} (e_j + \tau m_j) \quad (10.54)$$

The central charges $Z[q_1]$ and $Z[q_3]$ of $|\overline{\alpha_1}, (1, 0)\rangle$ and $|\overline{\alpha_3}, (1, 0)\rangle$ identically vanish on the singularity $\mathcal{H}_{s_1}^{G_5}$, therefore the corresponding BPS states become massless on this singularity. One can also check that the sublattice $\Gamma^{\mathcal{H}_{s_1}^{G_5}}$ of charges of states that become massless on this singularity $\mathcal{H}_{s_1}^{G_5}$ is generated by q_1 and q_3 . The lattice $\Gamma^{\mathcal{H}_{s_1}^{G_5}}$ should correspond to the charge lattice of the rank-1 CFT supported on the singularity $\mathcal{H}_{s_1}^{G_5}$. The Dirac pairing restricted to the sublattice $\Gamma^{\mathcal{H}_{s_1}^{G_5}}$, which we denote as $J^{\mathcal{H}_{s_1}^{G_5}}$, has Pfaffin given by:

$$\left| \text{Pf} \left(J^{\mathcal{H}_{s_1}^{G_5}} \right) \right| = |\langle q_1, q_3 \rangle| = 3 \quad (10.55)$$

Which should be equal to the order of the 1-form symmetry group of the rank-1 theory supported on the singularity $\mathcal{H}_{s_1}^{G_5}$. Then the theory on this singularity would be a rank-1 $\mathcal{N} \geq 2$ SCFT with a 1-form symmetry group of order 3. All the rank-1 theories with $\mathcal{N} = 2$ or higher supersymmetry have been classified, and such a theory does not exist. In particular the maximum order of the 1-form symmetry group for a rank-1 $\mathcal{N} = 2$ SCFT is 2. We conclude that the theory living on this singularity of Coulomb branch is not a CFT, but rather a discrete gauging of free $U(1)$ $\mathcal{N} = 4$ Maxwell theory, which is the only other possibility². In particular this implies that there are no states becoming massless on the singularity, therefore the states with charges lying on the sublattice $\Gamma^{\mathcal{H}_{s_1}^{G_5}}$ are not BPS.

As another example, consider the singularity corresponding to the reflection s_6 along the sixth root of E_6 . The locus of the singularity $\mathcal{H}_{s_6}^{G_5}$ can be parametrized as:

$$\mathcal{H}_{s_6}^{G_5} = \left(1, \frac{1}{6} (9 - i\sqrt{3}), \left(2 - \frac{2i}{\sqrt{3}} \right), \left(1 - \frac{2i}{\sqrt{3}} \right), -(-1)^{2/3}, \left(1 - \frac{i}{\sqrt{3}} \right) \right) \phi_3 \quad (10.56)$$

and the sublattice of charges becoming massless on this singularity is spanned by q_6 and $(q_2 + q_3 - q_1)$. The Dirac pairing restricted to this sublattice has Pfaffian equal to:

$$\left| \text{Pf} \left(J^{\mathcal{H}_{s_6}^{G_5}} \right) \right| = |\langle q_6, q_2 + q_3 - q_1 \rangle| = 6 \quad (10.57)$$

Then the rank-1 CFT on this singularity should have a 1-form symmetry group of order 6. As was the case for the previous singularity, such a CFT does not exist, and the theory on this singularity must be a discrete gauging of free $U(1)$ $\mathcal{N} = 4$ Maxwell theory. We conclude that there are no states becoming massless on this singularity.

One can perform similar computations on all the singularities of the Coulomb branch of the G_5 $\mathcal{N} = 3$ theory. It turns out that all the codimension-1 singularities are equivalent, up to G_5 transformations, either to $\mathcal{H}_{s_1}^{G_5}$ or to $\mathcal{H}_{s_6}^{G_5}$. It follows that the rank-1 theories supported on every codimension-1 singularities of the Coulomb branch \mathcal{C}_{G_5} are discrete

²Remember that the exceptional S-fold theory are maximally strongly coupled, therefore the theories living on the singularities of the moduli space can not be IR-free theories.

gaugings of free $U(1) \mathcal{N} = 4$ Maxwell theory. Then there are no charged states becoming massless at any codimension-1 singularity, and the G_5 theory itself must be a discrete gauging of a free theory, namely free $U(1)^2 \mathcal{N} = 4$ gauge theory. Indeed, if any charged state with charge q become massless at the origin of the Coulomb branch, which is a codimension-2 singularity, then it satisfies the BPS bound and is massless whenever its central charge vanishes, namely on the codimension-1 hypersurface identified by $Z[q] = 0$. As we just discussed there are no charged states that become massless on any codimension-1 singularities, therefore there are no massless charged states on any point of the Coulomb branch, including the origin. In Chapter 11 we give additional evidence for this claim and show that it is in fact impossible to define a consistent charge lattice on a Coulomb branch with geometry \mathbb{C}^2/G_5 .

10.2.3 The $k = 4$ S-fold: G_8

In this Section we consider the exceptional S-fold SCFT obtained as a $k = 4$ S-fold of the $E_6(2,0)$ six-dimensional theory, called the G_8 SCFT. We find that the charge lattice is not consistent with the stratification proposed in [5]. In more detail, our analysis suggests that the theory supported on codimension-1 singularities in the Coulomb branch is the $\mathcal{N} = 3$ preserving \mathbb{Z}_4 gauging of $SU(2) \mathcal{N} = 4$ SYM, while the constraints from the central charge formulae are compatible with this theory being the rank-1 $S_{4,4}$ -fold SCFT. Therefore we claim that the G_8 theory is a discrete gauging of free $U(1)^2 \mathcal{N} = 4$ gauge theory.

The Coulomb branch of the G_8 theory is given by the solutions of (10.38) with w an element of the Weyl group of E_6 :

$$w = (c_{E_6})^3 \tag{10.58}$$

which satisfies $w^4 = \text{Id}$ and has a two-dimensional eigenspace with eigenvalue $e^{\pi i/2}$. The $\mathcal{N} = 3$ theory then has rank $r = 2$ and the degrees of invariants on the Coulomb branch are given by the degrees of E_6 that are divisible by 4, namely $\Delta_i = 8, 12$. The Coulomb branch is given by \mathbb{C}^2/G_8 where G_8 is the exceptional complex reflection group with the correct degrees of invariants.

The states that are invariant under the S-fold action can be computed using (10.39), (10.40). In particular the states obtained from the W-bosons corresponding to the simple roots of E_6 have charges:

$$\begin{aligned} q_1 &= \frac{1}{\sqrt{2}} (1, -1, 0, -2, 0, -2, -1, -1, 0, 0, 0, -2) \\ q_2 &= \frac{1}{\sqrt{2}} (0, 0, 1, -1, 0, -2, 0, -2, -1, -1, 0, 0) \\ q_3 &= \frac{1}{\sqrt{2}} (1, -1, 1, -1, 2, -2, 1, -1, 1, -1, 0, -2) \\ q_4 &= \frac{1}{\sqrt{2}} (-1, 1, 0, 2, 0, 2, 1, 1, 0, 0, 0, 2) \\ q_5 &= \frac{1}{\sqrt{2}} (0, 0, -1, 1, 0, 2, 0, 2, 1, 1, 0, 0) \\ q_6 &= \frac{1}{\sqrt{2}} (0, 2, 0, 2, 0, 4, 0, 2, 0, 2, 2, 2) \end{aligned} \tag{10.59}$$

Notice that $q_4 = -q_1$ and $q_5 = -q_2$, therefore these charges span a four-dimensional

lattice. By computing the charges of the states obtained from the magnetic monopoles of the E_6 $\mathcal{N} = 4$ theory and by linearity argument one shows that the candidate Γ for charge lattice Γ of the G_8 theory is:

$$\Gamma = \text{Span}_{\mathbb{Z}} \{q_1, q_2, q_3, q_6\} \quad (10.60)$$

The charge lattice in the basis $\{q_1, q_2, q_3, q_6\}$ is represented by the matrix J_{G_8} :

$$J_{G_8} = \begin{pmatrix} 0 & 1 & -1 & 2 \\ -1 & 0 & 1 & -2 \\ 1 & -1 & 0 & 2 \\ -2 & 2 & -2 & 0 \end{pmatrix} \quad (10.61)$$

And the order of the 1-form symmetry group is given by:

$$|G_{G_8}^{(1)}| = |\text{Pf}(J_{G_8})| = 2 \quad (10.62)$$

Next we can study the sublattices of charges of states becoming massless at codimension-1 singularities. All the codimension-1 singularities are related by G_8 transformations and the slices transverse to these singularities are locally \mathbb{C}/\mathbb{Z}_4 . Furthermore through similar computations to the ones spelled out in the previous section one finds that the charge lattice of the rank-1 theory supported on these singularities is generated by two charges Q_1 and Q_2 with $|\langle Q_1, Q_2 \rangle| = 2$. Then the rank-1 theory supported on the codimension-1 singularities is a $\mathcal{N} \geq 2$ SCFTs with Coulomb branch \mathbb{C}/\mathbb{Z}_4 and a non-trivial \mathbb{Z}_2 1-form symmetry. The only candidate is the $\mathcal{N} = 3$ preserving \mathbb{Z}_4 discrete gauging of $\mathcal{N} = 4$ $SU(2)$ SYM [269]. This is in contradiction with the analysis of the central charge of the G_8 theory performed in [217, 5], where the theory supported on the codimension-1 singularities was found to be the rank-1 $S_{4,4}$ -fold SCFT, denoted also as $S_{\emptyset,4}^{(1)}$. Let us briefly review this analysis.

Assuming that the G_8 theory is not a discrete gauging, the central charges $a = c$ can be computed with the Shapere-Tachikawa formula [268]:

$$2(2a - c) = \sum_{j=1}^r \Delta_j - \frac{r}{2} \quad (10.63)$$

where Δ_i are the degrees of the fundamental invariants on the Coulomb branch. In the case of the G_8 theory we have $\{\Delta_1, \Delta_2\} = \{8, 12\}$. On the other hand the formulae of [218, 210] allow us to relate the central charges of the G_8 theory with the data of the rank-1 theories supported on the codimension-1 singularities:

$$12c = 2r + h_{\text{ECB}} + \sum_{i \in \mathcal{I}} \Delta_i^{\text{sing}} b_i \quad (10.64)$$

where b_i is a quantity associated with the rank-1 theory supported on the codimension-1 singularities as follows:

$$b_i := \frac{12c_i - h_i - 2}{\Delta_i} \quad (10.65)$$

In our theory we have $h_{\text{ECB}} = r = 2$ and the set \mathcal{I} of strata consist of only one singularity with scaling dimension $\Delta^{\text{sing}} = \text{l.c.m.}(8, 12) = 24$ and parameter b . Then, remembering

that $a = c$ for any $\mathcal{N} = 3$ theory, one may solve for b and finds:

$$b = \frac{9}{2} \tag{10.66}$$

which is compatible with the rank-1 fluxfull S_4 -fold SCFT. In contrast, if the theory supported on the codimension-1 singularities was a discrete gauging of $SU(2)$ $\mathcal{N} = 4$ SYM, we would have $b_{SU(2)} = 3$.

We found that the charge lattice (10.60) is incompatible with analysis of the central charges performed via the stratification of the Coulomb branch³. Therefore we claim that charged states can not become massless on the singularities of the Coulomb branch. Similar to the case of the G_5 theory, studied in Section 10.2.2, we thus conclude that the G_8 theory is not an interacting SCFT but rather a discrete gauging of free $U(1)^2$ $\mathcal{N} = 4$ gauge theory. In Chapter 11 we will give additional evidence for this claim by showing that any well defined charge lattice on the Coulomb branch \mathbb{C}^2/G_8 is only compatible with having (a discrete gauging of) $SU(2)$ $\mathcal{N} = 4$ SYM supported on the codimension-1 singularities.

10.2.4 The $k = 3$ S-fold: G_{25}

In this section we study the theory obtained with a $k = 3$ exceptional S-fold from the $E_6(2, 0)$ six-dimensional theory, denoted as the G_{25} theory. By similar argument to the ones spelled out in the previous cases we find that this theory is a discrete gauging of $U(1)^3$ $\mathcal{N} = 4$ gauge theory. In particular the charge is incompatible with any choice of rank-1 SCFTs on the codimension-1 singularities of the Coulomb branch.

The Coulomb branch and charge lattice can be found respectively with (10.38) and (10.40) with:

$$w = (c_{E_6})^4 \tag{10.67}$$

which satisfies $w^3 = \text{Id}$ and has a three-dimensional eigenspace with eigenvalue $e^{2\pi i/3}$. The $\mathcal{N} = 3$ theory then has rank $r = 3$ and the degrees of invariants on the Coulomb branch are given by the degrees of E_6 that are divisible by 3, namely $\Delta_i = 6, 9, 12$. The Coulomb branch is given by \mathbb{C}^3/G_{25} where G_{25} is the exceptional complex reflection group with the correct degrees of invariants.

The lattice of electromagnetic charges associated to the rank-1 theory supported on the codimension-1 singularities can be computed with the techniques spelled out in the previous Sections. The result is that these lattices are generated by two charges Q_1 and Q_2 with $\langle Q_1, Q_2 \rangle = 3$, indicating that the rank-1 theory on these singularity should have a 1-form symmetry group of order 3. This is not possible and we conclude that the theory on the codimension-1 singularity is a discrete gauging of $\mathcal{N} = 4$ Maxwell theory. Therefore the G_{25} theory itself must be a discrete gauging of free $U(1)^3$ $\mathcal{N} = 4$ gauge theory, because charged states can not become massless anywhere on the Coulomb branch. In Chapter 11 we give additional evidence for this claim and show that it is impossible to define a consistent charge lattice on a Coulomb branch \mathbb{C}^3/G_{25} .

³Another possibility is that the Shapere-Tachikawa formula does not hold for the G_8 theory. In that case the G_8 theory could be an interacting SCFT with $12c = 78$. We do not consider this possibility further in this paper and trust the Shapere-Tachikawa formula for any theory that is not a discrete gauging.

E_7				
k	w	r	ECCRG	Δ_i
3	$(c_{E_7})^6$	3	G_{26}	{6, 12, 18}
4	$(c_{E_6})^3$	2	G_8	{8, 12}
6	$(c_{E_7})^3$	3	G_{26}	{6, 12, 18}

Table 10.4 Elements $w \in \mathcal{W}[E_7]$ that characterize the S-fold actions for the S-fold theories of type E_7 through (10.38) and (10.39). Here c_{E_7} and c_{E_6} are the Coxeter element of E_7 and the E_6 subalgebra, respectively, r is the rank of the S-fold theory and in the fourth and fifth columns the exceptional complex crystallographic reflection group (ECCRG) associated to the S-fold theories and its degrees Δ_i are reproduced.

10.2.5 S-folds from the $(2, 0)$ E_7 theory

In this section we consider the exceptional S-fold theories obtained from the $(2, 0)$ six dimensional theory of type E_7 . All the techniques that we use were spelled out in details in Section 10.1 and were applied to the E_6 case in Section 10.2.1. Therefore in this section we will only provide the informations that define the S-fold projection, namely the element $w \in \mathcal{W}[E_7]$, and the final results. The main result is that all the exceptional S-folds SCFTs obtained from the E_7 theories are discrete gauging of free $U(1)^r$ $\mathcal{N} = 4$ gauge theory, where r is the rank of the theory, see Table 10.4.

We work in a basis of the algebra E_7 given by simple roots α_i such that the Cartan matrix is the one in Figure 10.1. The reflections along the simple roots are denoted as s_i and the corresponding Coxeter element of E_7 is:

$$c_{E_7} = \prod_{i=1}^7 s_i = \begin{pmatrix} 0 & 0 & 0 & 1 & 0 & -1 & -1 \\ 1 & 0 & 0 & 1 & 0 & -1 & -1 \\ 0 & 1 & 0 & 1 & 0 & -1 & -1 \\ 0 & 0 & 1 & 1 & 0 & -1 & -1 \\ 0 & 0 & 0 & 1 & 0 & -1 & 0 \\ 0 & 0 & 0 & 0 & 1 & -1 & 0 \\ 0 & 0 & 0 & 1 & 0 & 0 & -1 \end{pmatrix} \tag{10.68}$$

which satisfies:

$$(c_{E_7})^{18} = \mathbb{1} \tag{10.69}$$

In defining the elements w involved in the S-fold projections we will also use the Coxeter element of the E_6 subalgebra:

$$c_{E_6} = \prod_{i=2}^7 s_i = \begin{pmatrix} 1 & 0 & 0 & 0 & 0 & 0 & 0 \\ 1 & 0 & 0 & 1 & 0 & -1 & -1 \\ 0 & 1 & 0 & 1 & 0 & -1 & -1 \\ 0 & 0 & 1 & 1 & 0 & -1 & -1 \\ 0 & 0 & 0 & 1 & 0 & -1 & 0 \\ 0 & 0 & 0 & 0 & 1 & -1 & 0 \\ 0 & 0 & 0 & 1 & 0 & 0 & -1 \end{pmatrix} \tag{10.70}$$

which satisfies:

$$(c_{E_6})^{12} = \mathbb{1} \tag{10.71}$$

The degrees and codegrees of E_7 are tabulated in Table 10.2. Let us now consider the exceptional S-fold theories parametrized with $k = 3, 4, 6$.

- **Case $k = 3, G_{26}$:** The Coulomb branch and charge lattice can be computed with (10.38) and (10.39) respectively with:

$$w = (c_{E_7})^6 \tag{10.72}$$

The theory is a rank 3 SCFT with Coulomb branch \mathbb{C}^3/G_{26} where G_{26} is the EC-CRG with degrees 6,12 and 18. There are two independent codimension-1 singularities that correspond to two rank-2 Coulomb branches with geometry \mathbb{C}^2/G_5 and $\mathbb{C}^2/G(3, 1, 2)$, respectively. The slice transverse to the G_5 singularity is \mathbb{C}/\mathbb{Z}_2 while the slice transverse to the $G(3, 1, 2)$ singularity is \mathbb{C}/\mathbb{Z}_3 . One can compute the order of the 1-form symmetry groups of the rank-1 theories supported on these singularities from the charge lattice, and we find:

$$\mathbb{Z}_2 \text{ singularity: } G^{(1)} = \mathbb{Z}_2 \qquad \mathbb{Z}_3 \text{ singularity: } G^{(1)} = \mathbb{Z}_3 \tag{10.73}$$

There is no rank-1 $\mathcal{N} = 2$ SCFT with a \mathbb{Z}_3 1-form symmetry, therefore we conclude that the \mathbb{Z}_3 singularity is empty and supports a discrete gauging of free $U(1) \mathcal{N} = 4$ Maxwell theory. Comparing with the analysis of the central charges performed in [5] the only option is that the \mathbb{Z}_2 singularity is empty as well and therefore the G_{26} theory is itself a discrete gauging of free $U(1)^3 \mathcal{N} = 4$ gauge theory.

- **Case $k = 4, G_8$:** The Coulomb branch and charge lattice can be computed with (10.38) and (10.39) respectively with:

$$w = (c_{E_6})^3 \tag{10.74}$$

The theory is a rank 2 SCFT with Coulomb branch \mathbb{C}^3/G_8 where G_8 is the EC-CRG with degrees 8 and 12. This theory is believed to be the same theory as the exceptional S-fold SCFT of type E_6 with $k = 4$ studied in Section 10.2.3. The rank-1 theory supported on the codimension-1 singularity has a \mathbb{Z}_2 1-form symmetry. Then following the same arguments as in Section 10.2.3 we find that this theory must be a discrete gauging of free $U(1)^2 \mathcal{N} = 4$ gauge theory.

- **Case $k = 6, G_{26}$:** The Coulomb branch and charge lattice can be computed with (10.38) and (10.39) respectively with:

$$w = (c_{E_7})^3 \tag{10.75}$$

The theory is a rank 3 SCFT with Coulomb branch \mathbb{C}^3/G_{26} where G_{26} is the ECCRG with degrees 6,12 and 18. Performing the same computations as in the $k = 3$ case we find that this theory must be a discrete gauging of free $U(1)^3 \mathcal{N} = 4$ gauge theory as well.

We argued that all the exceptional S-fold theories of type E_7 are not interacting SCFTs but rather discrete gauging of free theories. In Chapter 11 we will give additional evidence for this claim by showing that it is not possible to define a consistent charge lattice on the Coulomb branches of these theories.

E_8				
k	w	r	ECCRG	Δ_i
3	$(c_{E_8})^{10}$	4	G_{32}	{12, 18, 24, 30}
4	$(c_{E_8}(s_7s_8)^{-1}c_{E_8}c_{E_8}(s_7s_8)^{-1})^6$	4	G_{31}	{8, 12, 18, 24}
6	$(c_{E_8})^5$	4	G_{32}	{12, 18, 24, 30}

Table 10.5 Elements $w \in \mathcal{W}[E_8]$ that characterize the S-fold actions for the S-fold theories of type E_8 through (10.38) and (10.39). Here c_{E_8} is the Coxeter element of E_8 , s_i are the reflection along the i -th simple root, r is the rank of the S-fold theory and in the fourth and fifth columns the exceptional complex crystallographic reflection group (ECCRG) associated to the S-fold theories and its degrees Δ_i are reproduced.

10.2.6 S-folds from the $(2, 0) E_8$ theory

In this section we consider the exceptional S-fold theories obtained from the $(2, 0)$ six dimensional theory of type E_8 . Our main result is that the exceptional S-folds SCFTs obtained from the E_8 theories with $k = 3, 6$ are discrete gauging of free $U(1)^r \mathcal{N} = 4$ gauge theory, where r is the rank of the theory, see Table 10.5. On the other hand, the exceptional S-fold SCFT of type E_8 with $k = 4$, also known as the G_{31} theory, passes all consistency checks, therefore we expect it to be a non-trivial interacting $\mathcal{N} = 3$ SCFT. Considering also our results for the exceptional S-fold theories of type E_6 and E_7 the G_{31} theory is the only exceptional S-fold SCFT of type E which is a proper interacting theory. We also compute the 1-form symmetry group of the G_{31} theory and find it to be trivial.

We work in a basis of the algebra E_8 given by simple roots α_i such that the Cartan matrix is the one in Figure 10.1. The reflections along the simple roots are denoted as s_i and the corresponding Coxeter element of E_8 is:

$$c_{E_8} = \prod_{i=1}^8 s_i = \begin{pmatrix} 0 & 0 & 0 & 0 & 1 & 0 & -1 & -1 \\ 1 & 0 & 0 & 0 & 1 & 0 & -1 & -1 \\ 0 & 1 & 0 & 0 & 1 & 0 & -1 & -1 \\ 0 & 0 & 1 & 0 & 1 & 0 & -1 & -1 \\ 0 & 0 & 0 & 1 & 1 & 0 & -1 & -1 \\ 0 & 0 & 0 & 0 & 1 & 0 & -1 & 0 \\ 0 & 0 & 0 & 0 & 0 & 1 & -1 & 0 \\ 0 & 0 & 0 & 0 & 1 & 0 & 0 & -1 \end{pmatrix} \quad (10.76)$$

which satisfies:

$$(c_{E_8})^{30} = \mathbb{1} \quad (10.77)$$

- **Case $k = 3$ or 6 , G_{32} :** The exceptional S-folds of type E_8 with $k = 3$ and $k = 6$ give rise to the same field theory. The Coulomb branch and charge lattice can be computed with (10.38) and (10.39) respectively with:

$$w = \begin{cases} (c_{E_8})^{10}, & k = 3 \\ (c_{E_8})^5, & k = 6 \end{cases} \quad (10.78)$$

The Coulomb branch is \mathbb{C}^4/G_{32} with G_{32} the ECCRG with degrees 12,18,24 and 30.

There is only one codimension-1 singularity up to G_{32} transformation. The transverse slice to this singularity is \mathbb{C}/\mathbb{Z}_3 and the 1-form symmetry group of the theory supported on this singularity is \mathbb{Z}_3 . There is no rank-1 $\mathcal{N} = 2$ theory compatible with a \mathbb{C}/\mathbb{Z}_3 Coulomb branch and with a \mathbb{Z}_3 1-form symmetry group, therefore this singularity must be empty. Then the G_{32} theory itself must be a discrete gauging of free $U(1)^4 \mathcal{N} = 4$ gauge theory.

- **Case $k = 4, G_{31}$:** The Coulomb branch of the S-fold theory of type E_8 with $k = 4$ can be computed with (10.38) where:

$$w = \left(c_{E_8} (s_7 s_8)^{-1} c_{E_8} c_{E_8} (s_7 s_8)^{-1} \right)^6 \tag{10.79}$$

The Coulomb branch is \mathbb{C}^4/G_{31} where G_{31} is the ECCRG with degrees 8,12,20 and 24. Notice that in order for the S-fold theory to be rank 4, w must have a four eigenvalues i . w is real, therefore it must also have four eigenvalues $-i$, and thus $w^2 = -1$. Then one can consider the states:

$$\overline{|\alpha, (p, q)\rangle}_{\text{short}} = \frac{1}{\sqrt{2}} \sum_{t=0}^1 \left| w^t \cdot \alpha; (\rho_4)^t \cdot (p, q) \right\rangle \tag{10.80}$$

where α is a root of E_8 . The states (10.80) are invariant under the S-fold action for any α and (p, q) , therefore we consider the charge lattice Γ spanned by the charges of the states (10.80). A basis for this lattice is given by the charges q_i of the states $\overline{|\alpha_i, (1, 0)\rangle}_{\text{short}}$ obtained from the W-bosons associated with the simple roots α_i of E_8 with $i = 1, \dots, 8$:

$$\begin{aligned} q_1 &= \frac{1}{\sqrt{2}} (1, 0, 0, 0, 0, 0, 0, 0, 0, 0, 1, 0, 1, 0, 0, 0, 0) \\ q_2 &= \frac{1}{\sqrt{2}} (0, -1, 1, -2, 0, -3, 0, -4, 0, -5, 0, -4, 0, -2, 0, -2) \\ q_3 &= \frac{1}{\sqrt{2}} (0, 1, 0, 2, 1, 3, 0, 4, 0, 4, 0, 3, 0, 1, 0, 2) \\ q_4 &= \frac{1}{\sqrt{2}} (0, 0, 0, -1, 0, -2, 1, -2, 0, -2, 0, -1, 0, 0, 0, -1) \\ q_5 &= \frac{1}{\sqrt{2}} (0, -1, 0, -1, 0, -1, 0, -2, 1, -3, 0, -2, 0, -1, 0, -2) \\ q_6 &= \frac{1}{\sqrt{2}} (0, 0, 0, 1, 0, 1, 0, 2, 0, 3, 1, 2, 0, 1, 0, 2) \\ q_7 &= \frac{1}{\sqrt{2}} (0, 1, 0, 1, 0, 1, 0, 0, 0, 0, 0, 0, 1, 0, 0, 0) \\ q_8 &= \frac{1}{\sqrt{2}} (0, 1, 0, 1, 0, 2, 0, 3, 0, 4, 0, 2, 0, 1, 1, 2) \end{aligned} \tag{10.81}$$

The Dirac pairing $J_{G_{31}}$ in this basis can be computed with (10.41):

$$J_{G_{31}} = \begin{pmatrix} 0 & 0 & 0 & 1 & -1 & -1 & 1 & 1 \\ 0 & 0 & 0 & 0 & 0 & 1 & 0 & -1 \\ 0 & 0 & 0 & -1 & 1 & -1 & 1 & 0 \\ -1 & 0 & 1 & 0 & 0 & 0 & -1 & 0 \\ 1 & 0 & -1 & 0 & 0 & 0 & 0 & 1 \\ 1 & -1 & 1 & 0 & 0 & 0 & 0 & -1 \\ -1 & 0 & -1 & 1 & 0 & 0 & 0 & 0 \\ -1 & 1 & 0 & 0 & -1 & 1 & 0 & 0 \end{pmatrix} \quad (10.82)$$

The order of the 1-form symmetry group of the G_{31} is given by the absolute value of the Pfaffian of $J_{G_{31}}$:

$$\left|G^{(1)}\right| = |\text{Pf}(J_{G_{31}})| = 1 \quad (10.83)$$

Therefore the G_{31} theory has trivial 1-form symmetry.

Let us now consider the stratification of the Coulomb branch \mathbb{C}^4/G_{31} . There is one codimension-1 singularity up to G_{31} transformations and the sublattice of Γ corresponding to the states becoming massless on this singularity is compatible with $SU(2) \mathcal{N} = 4$ SYM. The transverse slice to this singularity is \mathbb{C}/\mathbb{Z}_2 which is compatible with the Coulomb branch of $SU(2) \mathcal{N} = 4$. This stratification is consistent with the central charge formulae of [218], as already checked in [5]. We briefly review the relevant computations here for ease of readability. The Shapere-Tachikawa formula with $a = c$ allow us to compute the central charges:

$$2c = \sum_{j=1}^r \Delta_j - \frac{r}{2} = 8 + 12 + 20 + 24 - 2 = 62 \quad (10.84)$$

While the formulae of [218] relate the central charges with data of the theory supported on the codimension-1 singularity. For the G_{31} theory this formula reads:

$$12c = 3r + \Delta^{\text{sing}}b = 12 + 120b \quad (10.85)$$

where $\Delta^{\text{sing}} = \text{lcm}(\Delta_i)$ is the scaling dimension of the codimension-1 singularity and b is associated to the data of the rank-1 theory supported on this singularity by (10.65). Solving for b we find:

$$b = 3 \quad (10.86)$$

which is consistent with having $SU(2) \mathcal{N} = 4$ SYM as the theory supported on the codimension-1 singularities.

To summarize, we have found that the exceptional S-fold theories of type E_8 with $k = 3, 6$ are discrete gauging of free theories. The exceptional S-fold theory of type E_8 with $k = 4$, denoted as the G_{31} theory, passes all the consistency checks that we have at our disposal. We are then lead to claim that the G_{31} theory is the only exceptional S-fold theory of type E that is a proper interacting SCFT. We have also found that the 1-form symmetry group of the G_{31} theory is trivial.

Charge lattices in $\mathcal{N} = 2$ SCFTs with $\varkappa \neq \{1, 2\}$

One of the main features of S-fold SCFTs is that they are maximally strongly coupled theories. This means that whenever a charged state becomes massless then another charged state which is mutually non-local with respect to the first one becomes massless as well. Then at any non-generic point of the Coulomb branch the low energy theory is strongly coupled and does not admit a conventional Lagrangian description. On the one hand this fact renders the study of S-fold SCFTs challenging, because the only vacua where perturbative techniques are viable are the most generic points of the Coulomb branch, where the low energy theory is simply $U(1)^r$ with no massless charged states. On the other hand, as was shown in [217], maximally strongly coupled theories have to satisfy a series of non-trivial constraints, and are quite restricted as a result. Motivated by the results of [217] in this Section we study the charge lattices of a large class of $\mathcal{N} = 2$ SCFTs that are maximally strongly coupled, namely $\mathcal{N} = 2$ SCFTs with characteristic dimension $\varkappa \neq \{1, 2\}$. All the regular and exceptional S-fold SCFTs belong to this class of theories except for the known cases where SUSY enhances to $\mathcal{N} = 4$ [199].

For the rest of this Chapter we only consider interacting rank- r SCFTs with $\varkappa \neq \{1, 2\}$. Our main results are:

Claim A: The order of the 1-form symmetry group $G^{(1)}$ of an $\mathcal{N} = 2$ rank-2 SCFT with $\varkappa \neq \{1, 2\}$ satisfies $1 \leq |G^{(1)}| \leq 4$. The upper bound can only be saturated by stacks of lower rank theories.

Claim B: An $\mathcal{N} = 2$ SCFT with $\varkappa \neq \{1, 2\}$ and rank $r \geq 2$ that is not a stack of lower rank theories must have at least one codimension-1 singularity that supports (a discrete gauging of) $\mathcal{N} = 2^*$ $SU(2)$ SYM.

We also apply the techniques that we develop to the exceptional S-fold theories, which provides an independent argument for claiming that most of these theories are not interacting SCFTs.

Let us review the definitions and results of [217] that will be useful in this Section. The characteristic dimension of an $\mathcal{N} = 2$ SCFT is defined as follows. Write the degrees of Coulomb branch invariants Δ_i as:

$$(\Delta_1, \dots, \Delta_N) = \lambda(d_1, \dots, d_2), \quad d_i \in \mathbb{Z}, \quad \text{gcd}(d_1, \dots, d_N) = 1 \quad (11.1)$$

Then the characteristic dimension is defined as:

$$\varkappa = \frac{1}{\{\lambda^{-1}\}} \quad (11.2)$$

where $\{x\}$ is defined as the unique real number such that $\{x\} = x \bmod 1$ and $0 < \{x\} \leq 1$. The characteristic dimension can only take eight values $\varkappa \in \{1, 6/5, 4/3, 3/2, 2, 3, 4, 6\}$. An SCFT with $\varkappa \neq \{1, 2\}$ is maximally strongly coupled and for any state with charge q , central charge $Z[q] \neq 0$ there is another state with charge p and central charge $Z[p] = \zeta Z[q]$ where:

$$\zeta = \begin{cases} e^{2\pi i/3} & \varkappa = 3, 3/2 \\ i & \varkappa = 4, 4/3 \\ e^{2\pi i/6} & \varkappa = 6, 6/5 \end{cases} \quad (11.3)$$

therefore the charge lattice Γ is mapped to a lattice $\mathbb{Z}[\zeta]^r$ by the central charge Z . The Dirac pairing between two charges p and q can be written as:

$$\langle q, p \rangle = \frac{1}{\zeta - \bar{\zeta}} (H(q, p) - H(p, q)) \quad (11.4)$$

here and in the remainder of this Section, with an abuse of notation, we denote with the same symbol the electromagnetic charges in Γ and the corresponding element in the lattice $\mathbb{Z}[\zeta]^r$. Here H is a positive definite Hermitian form:

$$H : \overline{\mathbb{Z}[\zeta]^r} \times \mathbb{Z}[\zeta]^r \rightarrow \mathbb{Z}[\zeta] \quad (11.5)$$

An important implication of having $\varkappa \neq \{1, 2\}$ is that when a state with charge q becomes massless then also a state with charge $p = \zeta q$ becomes massless. Then we can always choose a basis of the lattice of charges becoming massless at a codimension-1 singularity that is of the form $\{q, \zeta q\}$.

11.1 1-form symmetries of rank-2 $\mathcal{N} = 2$ SCFTs with $\varkappa \neq \{1, 2\}$

Consider a rank-2 $\mathcal{N} = 2$ SCFTs with $\varkappa \neq \{1, 2\}$. We choose a basis of the charge lattice Γ of the form $\{q_1, \zeta q_1, q_2, \zeta q_2\}$:

$$\Gamma = \text{Span}_{\mathbb{Z}}\{q_1, \zeta q_1, q_2, \zeta q_2\} \quad (11.6)$$

Were q_1 and ζq_1 become massless at some codimension-1 singularity \mathcal{H}_1 and q_2 and ζq_2 become massless at some other codimension-1 singularity \mathcal{H}_2 . q_1 and q_2 must be linearly independent for Γ to have dimension 4.

An interesting quantity to consider is the absolute value of the Pfaffian of the Dirac pairing J , which is an invariant of the charge lattice and intuitively tells us how sparse the charge lattice is. More precisely in [231] it was shown that this quantity is equal to the order of the 1-form symmetry group, which in turn is related to how much the charge lattice can be refined without breaking the Dirac quantization condition. The number of charges that can be added in the fundamental domain of the charge lattice while preserving the Dirac quantization condition is given by $|\text{Pf}(J)|$ minus 1.

Consider the rank-1 theory \mathcal{T}_i supported on the codimension-1 singularity \mathcal{H}_i . Its charge

lattice is spanned by $\{q_i, \zeta q_i\}$ and the Dirac pairing $J_{\mathcal{H}_i}$ is such that:

$$|\text{Pf}(J_{\mathcal{H}_i})| = \left| \text{Pf} \begin{pmatrix} 0 & \langle q_i, \zeta q_i \rangle \\ -\langle q_i, \zeta q_i \rangle & 0 \end{pmatrix} \right| = |\langle q_i, \zeta q_i \rangle| = H(q_i, q_i) \quad (11.7)$$

where in the last equality we used (11.3). \mathcal{T}_i is an $\mathcal{N} = 2$ rank-1 SCFT, therefore the 1-form symmetry is either \mathbb{Z}_2 , if this theory is (a discrete gauging of) $\mathcal{N} = 2^* SU(2)$ SYM, or trivial in any other case. Therefore we found:

$$H(q_i, q_i) = \begin{cases} 2 & \mathcal{T}_i \text{ is (a discrete gauging of) } \mathcal{N} = 2^* SU(2) \text{ SYM} \\ 1 & \text{otherwise} \end{cases} \quad (11.8)$$

Now let us compute the Pfaffian of the Dirac pairing $J^{(2)}$ of the rank-2 theory itself. We find:

$$\begin{aligned} |\text{Pf}(J^{(2)})| &= \left| \text{Pf} \begin{pmatrix} 0 & \langle q_1, \zeta q_1 \rangle & \langle q_1, q_2 \rangle & \langle q_1, \zeta q_2 \rangle \\ \langle \zeta q_1, q_1 \rangle & 0 & \langle \zeta q_1, q_2 \rangle & \langle \zeta q_1, \zeta q_2 \rangle \\ \dots & \dots & 0 & \langle q_2, \zeta q_2 \rangle \\ \dots & \dots & \langle \zeta q_2, q_2 \rangle & 0 \end{pmatrix} \right| \\ &= |\langle q_1, \zeta q_1 \rangle \langle q_2, \zeta q_2 \rangle - \langle q_1, q_2 \rangle \langle \zeta q_1, \zeta q_2 \rangle + \langle \zeta q_1, q_2 \rangle \langle q_1, \zeta q_2 \rangle| \\ &= H(q_1, q_1)H(q_2, q_2) - |H(q_1, q_2)|^2 \end{aligned} \quad (11.9)$$

where we dropped the absolute value in the last line because the Cauchy-Schwarz inequality ensures that the last expression is positive. We are now able to determine upper and lower bounds for this quantity:

$$1 \leq \left| \text{Pf}(J^{(2)}) \right| \leq H(q_1, q_1)H(q_2, q_2) \leq 4 \quad (11.10)$$

The first inequality holds because the Dirac pairing is integer and non-degenerate, while the last inequality follows from the analysis of the rank-1 theories supported on the codimension-1 singularities (11.8). The inequality:

$$\left| \text{Pf}(J^{(2)}) \right| \leq H(q_1, q_1)H(q_2, q_2) \quad (11.11)$$

is saturated only if $H(q_1, q_2)$ vanishes. Then in order to have a rank-2 SCFT with $\varkappa \neq \{1, 2\}$ with $|\text{Pf}(J^{(2)})| = 4$ it is necessary that for every choice of codimension-1 singularities $\mathcal{H}_1, \mathcal{H}_2$ the theories supported on the singularities is (a discrete gauging of) $\mathcal{N} = 2^*$ SYM and that $H(q_1, q_2) = 0$. This means that, for every choice of $\mathcal{H}_1, \mathcal{H}_2$, the charges becoming massless on \mathcal{H}_1 are mutually local with respect to the charges becoming massless on \mathcal{H}_2 . The rank-2 theory then must be a stack of the rank-1 theories supported on \mathcal{H}_i . We are not interested in theories that are stacks of lower rank theories, therefore we can drop the equal sign in (11.11), and (11.10) reduces to:

$$1 \leq \left| \text{Pf}(J^{(2)}) \right| \leq 3 \quad (11.12)$$

As already discussed the absolute value of the Pfaffian of the Dirac pairing is equal to the order of the 1-form symmetry group, therefore we find our first claim:

Claim A: The order of the 1-form symmetry group $G^{(1)}$ of an $\mathcal{N} = 2$ rank-2 SCFT with $\varkappa \neq \{1, 2\}$ satisfies $1 \leq |G^{(1)}| \leq 4$. The upper bound can only be saturated by stacks of lower rank theories.

Consider now a theory where $H(q_i, q_i) = 1$ for every choice of \mathcal{H}_i . As we just discussed equation (11.11) is only saturated for rank-2 theories that are stacks of rank-1 theories. Then for a $\mathcal{N} = 2$ rank-2 SCFT with $\varkappa \neq \{1, 2\}$ that is not a stack of lower rank theories we have:

$$1 \leq \left| \text{Pf} \left(J^{(2)} \right) \right| < 1 \quad (11.13)$$

This is a contradiction and signals that on such a Coulomb branch it is not possible to define a consistent charge lattice. We can then formulate our second claim in the case of rank-2:

Claim B': A rank-2 $\mathcal{N} = 2$ SCFT with $\varkappa \neq \{1, 2\}$ that is not a stack of lower rank theories must have at least one codimension-1 singularity that supports (a discrete gauging of) $\mathcal{N} = 2^* SU(2)$ SYM.

As we will see in the next Section this second claim generalizes to arbitrary rank.

In the context of $\mathcal{N} = 3$ exceptional S-fold SCFT the second claim already rules out some of the Coulomb branch geometries. The most straightforward to study are the G_5 theory that we studied in Section 10.2.2 as well as the G_4 theory that can be constructed from the $D_4(2, 0)$ six-dimensional theory with an S-fold procedure in the presence of an outer automorphism twist. Both these theories are maximally strongly coupled and only have codimension-1 singularities with a transverse slice \mathbb{C}/\mathbb{Z}_3 , which can not support a discrete gauging of $\mathcal{N} = 2^* SU(2)$ SYM.

The G_8 theory, studied in Section 10.2.3, is more subtle. There is one codimension-1 singularity with transverse slice \mathbb{C}/\mathbb{Z}_4 . Our second claim then imposes that the theory supported on this singularity is a \mathbb{Z}_4 gauging of $\mathcal{N} = 4 SU(2)$ SYM. On the other hand the analysis of the central charges with the formulae of [218] is not consistent with this choice, as already computed in [5] and as we discussed in Section 10.2.3. To summarize, we find that the exceptional S-fold theories G_4 , G_5 and G_8 can not be interacting SCFTs because it is not possible to define a consistent charge lattice on their Coulomb branches. Therefore these theories must be discrete gaugings of free $U(1)^r$ $\mathcal{N} = 4$ gauge theories, which is the only other possibility.

11.2 A constraint for the stratification of $\mathcal{N} = 2$ SCFTs

Consider a rank- r $\mathcal{N} = 2$ SCFT with $\varkappa \neq \{1, 2\}$ such that the rank-1 theories supported on all codimension-1 singularities are SCFTs with trivial 1-form symmetries. We can choose a basis of the charge lattice Γ such that:

$$\Gamma = \text{Span}_{\mathbb{Z}} \{q_1, \zeta q_1, \dots, q_r, \zeta q_r\} \quad (11.14)$$

where q_i and ζq_i become massless at some codimension-1 singularity \mathcal{H}_i and generate the charge lattice of the rank-1 theory supported there. Then we have:

$$H(q_i, q_i) = 1 \quad \forall i = 1, \dots, r \quad (11.15)$$

because $H(q_i, q_i)$ is equal to the order of the 1-form symmetry group of the theory supported on \mathcal{H}_i , which is trivial by hypothesis. The Cauchy-Schwarz inequality together with the fact that all the q_i are linearly independent imposes:

$$|H(q_i, q_j)|^2 < H(q_i, q_i)H(q_j, q_j) = 1 \quad \forall i \neq j \quad (11.16)$$

On the other hand $|H(q_i, q_j)|^2$ must be an integer because it can be written as an integer linear combination of Dirac pairings:

$$|H(q_i, q_j)|^2 = \langle q_i, q_j \rangle \langle \zeta q_i, \zeta q_j \rangle - \langle \zeta q_i, q_j \rangle \langle q_i, \zeta q_j \rangle \quad (11.17)$$

Then $|H(q_i, q_j)|^2$ must vanish and $H(q_i, q_j)$ vanishes as well as a consequence. The resulting Dirac pairing matrix is block diagonal with only 2×2 blocks:

$$J^{(r)} = \text{diag} \left\{ \begin{pmatrix} 0 & 1 \\ -1 & 0 \end{pmatrix}, \begin{pmatrix} 0 & 1 \\ -1 & 0 \end{pmatrix}, \dots, \begin{pmatrix} 0 & 1 \\ -1 & 0 \end{pmatrix} \right\} \quad (11.18)$$

This is the case for every choice of codimension-1 singularities \mathcal{H}_i , therefore the states becoming massless at any singularity \mathcal{H}_i are mutually local with respect to the states becoming massless at any other singularity. Then the rank- r theory must be a stack of r rank-1 theories. Therefore in order to have a rank- r SCFT that is not a stack of lower rank theories, one must allow for codimension-1 singularities \mathcal{H}_i that support either (a discrete gauging of) $\mathcal{N} = 2^* SU(2)$ SYM, which would imply that $H(q_i, q_i) = 2$, or an IR-free theory. This is our second claim:

Claim B: An $\mathcal{N} = 2$ SCFT with $\varkappa \neq \{1, 2\}$ and rank $r \geq 2$ that is not a stack of lower rank theories must have at least one codimension-1 singularity that supports (a discrete gauging of) $\mathcal{N} = 2^* SU(2)$ SYM.

The second claim provides additional evidence for the results that we obtained in Chapter 10, summarized in Table 10.1. There we showed that the charge lattice of most of the exceptional S-fold SCFTs of type E_r are not consistent, and therefore those theories must be discrete gaugings of free theories. Now we show that the same conclusions can be derived by applying **claim B** to the CB stratification of exceptional S-folds, computed in [5]. This argument will actually provide a stronger result regarding exceptional S-fold SCFTs: not only the charge lattices computed in Chapter 10 are inconsistent, but it is not possible to define any consistent charge lattice on the CB geometries of exceptional S-fold SCFTs of type E_r , with the exception of the G_{31} theory.

Claim B directly rules out the exceptional S-fold theories G_{25} and G_{32} as possible interacting SCFTs. Indeed in both cases all codimension-1 singularity have transverse slice \mathbb{C}/\mathbb{Z}_3 which can not support a discrete gauging of $\mathcal{N} = 2^* SU(2)$ SYM, and both theories are maximally strongly coupled and can not have IR-free theories supported on any singularity. In the case of the G_{26} theory, studied in Section 10.2.5, there is only one singularity with transverse slice \mathbb{C}/\mathbb{Z}_2 which could support $\mathcal{N} = 2^* SU(2)$ SYM, while the other singularity has transverse slice \mathbb{C}/\mathbb{Z}_3 . However, as computed in [5] and discussed

above, this choice is inconsistent with central charge formulae of [218]. To summarize, we find that the G_{25} , G_{26} and G_{32} theories can not be interacting SCFTs because it is not possible to define a consistent charge lattice on their Coulomb branches. Therefore these theories must be discrete gaugings of free theories, which is the only other possibility.

The only exceptional S-fold SCFT obtained from the $(2, 0)$ E_n six-dimensional theories that satisfies our constraint is the G_{31} theory. This is the SCFT obtained from the E_8 $(2, 0)$ theory with an exceptional S-fold of order $k = 4$. The Coulomb branch is \mathbb{C}^4/G_{31} and has one codimension-1 singularity with transverse slice \mathbb{C}/\mathbb{Z}_2 . Our constraint then imposes that the rank-1 theory supported on this singularity is $SU(2) \mathcal{N} = 4$ SYM, which is consistent with the analysis of the central charges performed in [5]. We claim that this theory is a proper interacting rank-4 SCFT, but it must be noted that the possibility of having a discrete gauging of $U(1)^4 \mathcal{N} = 4$ gauge theory is also consistent with all the constraints that are available. To solve this ambiguity it would be desirable to analyze the spectrum of charged operators directly from the M-theory setup of [200], but we leave this problem to future work.

11.2.1 Other exceptional S-folds

In this thesis we have analyzed the exceptional S-fold theories obtained from the $(2, 0)$ E_n six-dimensional theories, but it is also possible to define similar M-theory setups involving the $(2, 0)$ D_n theories, with or without outer automorphism twists, and generalizations to non-simply laced algebras have also been considered. We leave the detailed analysis of the charge lattices of the resulting theories to future work, but we can easily check if the Coulomb branches of such theories, computed in [5], satisfy our consistency conditions.

The Coulomb branches of the S-fold SCFTs obtained from the $(2, 0)$ D_n theories are $\mathbb{C}^r/G(k, m, r)$ for $k = 4, 6$ and m a divisor of k . In all these cases there is at least one codimension-1 singularity with transverse slice \mathbb{C}/\mathbb{Z}_2 which can support $SU(2) \mathcal{N} = 4$ SYM, therefore these theories satisfy our consistency condition.

The case of non-simply laced algebra generates one Coulomb branch geometry that does not appear in the exceptional S-fold theories of type E_n and D_n , namely \mathbb{C}^2/G_{12} . Here G_{12} is the exceptional complex reflection group with degrees 6 and 8. In this geometry there are codimension-1 singularity with transverse slice \mathbb{C}/\mathbb{Z}_2 that can support $SU(2) \mathcal{N} = 4$ SYM, therefore this theory satisfies our consistency checks.

As already discussed in [5] there are four possible geometries associated to ECCRGs that do not appear in any known construction but are consistent Coulomb branches for putative $\mathcal{N} = 3$ SCFTs. These geometries are \mathbb{C}^3/G_{24} , \mathbb{C}^4/G_{29} , \mathbb{C}^5/G_{33} and \mathbb{C}^6/G_{34} where G_i are ECCRGs. In all cases there are codimension-1 singularities that have transverse slice \mathbb{C}/\mathbb{Z}_2 and could support $SU(2) \mathcal{N} = 4$ SYM, therefore all these Coulomb branches satisfy our consistency condition.

11.3 Discussion and conclusions

In this and in the previous Chapters we studied the exceptional S-fold SCFTs discovered in [200] and their associated charge lattices. In Chapter 10 we analyzed explicitly all the exceptional S-folds of type E_r , computing their charge lattices by generalizing the techniques of [5]. Furthermore we considered the sublattices of charges that become massless at codimension-1 singularities of the Coulomb branch. By comparing these

charges with the charge lattices of rank-1 $\mathcal{N} = 2$ SCFTs we showed that some of the exceptional S-fold SCFTs can not be interacting theories because their charge lattice is not consistent. For exceptional S-folds of type E_r the only theory that admits a consistent charge lattice is the S-fold of type E_8 with $k = 4$, called the G_{31} theory. Thus we claimed that the G_{31} theory is an interacting SCFT, while all the other S-folds of type E_r are discrete gauging of free theories.

In this Chapter we provided additional evidence for this claim by studying the charge lattice of $\mathcal{N} = 2$ SCFTs with characteristic dimension $\varkappa \neq \{1, 2\}$. By exploiting the results and the formalism developed in [217] we computed an upper bound for the 1-form symmetries of rank-2 theories with $\mathcal{N} = 2$, denoted as **Claim A** throughout this Chapter, and we found a consistency constraint for the Coulomb branch stratification for such SCFTs at any rank, denoted as **Claim B** throughout this Chapter. When applied to the case of exceptional S-fold SCFTs this constraint, in combination with other constraints from [218], shows that all the S-folds of type E_r do not admit a consistent charge lattice except for the G_{31} theory.

There are multiple directions our work can be extended towards. As we already commented in main body of Chapter 10 the G_{31} theory passes all our consistency checks, but this does not guarantee that this theory is indeed an interacting SCFT and it may be a discrete gauging of a free theory. A possible way to determine whether this is the case would be to compute the 2-form symmetries of this theory directly from the M-theory construction along the lines of [237]. Indeed if the 2-form symmetry group is not trivial and can be gauged then the G_{31} theory should be a discrete gauging of some “parent” theory. A similar approach was adopted in [199] to understand the presence of discrete gauging in regular S-folds.

Our results on $\mathcal{N} = 2$ SCFTs with $\varkappa \neq \{1, 2\}$ could be expanded upon in different directions. It would be nice to generalize **Claim A** to arbitrary ranks, and understand whether a bound for the 1-form symmetry group exists also at higher ranks. Another interesting perspective would be to relax the condition on the characteristic dimension, and study theories with \varkappa equal to 1 or 2. This would require a different set of tools than the ones we used in this Chapter, for example considering the monodromies around Coulomb branch singularities along the lines of [209, 206, 223]. Recently a new relation between 1-form symmetries of $\mathcal{N} = 2$ SCFTs and Seiberg-Witten curves has been investigated [232], and it would be interesting to understand what are the connections (if any) with our results.

Future directions

In this Chapter we summarize and expand on the possible future directions the work presented in this thesis can be expanded towards. Some of the possible future directions suggested here are currently being explored by the author and collaborators.

3d dualities and integral identities: The analysis of 3d dualities spelled out in Chapters 3 and 4 can be generalized by considering different matter content, superpotential and gauge groups. Furthermore, there is a close relationship between the study of 3d $\mathcal{N} = 2$ QFTs and the integral identities between their partition functions on the squashed three-sphere. This allowed us to exploit the *duplication formula* to study and predict new IR dualities in Chapter 4. On the other hand, it would be nice to understand whether the *duplication formula* has a general physical interpretation. The *duplication formula* can be applied to obtain identities involving $SO(N)$ gauge groups starting from $USp(2N)$ gauge groups, and it would be interesting to understand whether this is only a mathematical trick or if it reflects some physical phenomena.

Webs of 3d dualities: IR dualities can often be related by RG flows and/or dimensional compactification, as we explored in details in Chapter 3 for a class of theories with D-type superpotential. Then a natural question is to understand which dualities are related in this way and which are independent. We can think of the independent dualities as fundamental dualities, while all the other dualities can be considered as a consequence of the fundamental ones. It is not established which dualities are independent, nor it is known whether all IR dualities can be related by RG flows. It would be useful to develop a more comprehensive view on this topic, as IR dualities are a powerful tool in the study of the strongly coupled regime of QFTs.

Conformal dualities and Calabi-Yaus: The phenomena of conformal duality between toric theories in the presence of orientifolds has been addressed in Chapters 5 through 7 from a field theoretical point of view. It is an open question to understand the notion of conformal duality for these theories from their Type IIB construction as stacks of D3-branes probing a toric CY cone on top of an orientifold. We were able to find a number of families of conformally dual theories, but a general mechanism underlying this phenomena is not understood, and a general prescription for generating new cases of conformally dual theories in this setup is not available. An

holographic analysis of this phenomenon from the Type IIB perspective could shed some light on these open questions and complement our field theoretical analysis.

Classification of SCFTs: A very ambitious goal in the study of QFTs is the classification of CFTs, which are fixed points of the RG flow. The classification with maximal supersymmetry in 4d is believed to be complete, composed of all $\mathcal{N} = 4$ SYM theories. With a lower amount of supersymmetry such a classification is not yet available, although promising results have been obtained for $\mathcal{N} = 2$ SCFTs at low rank. The analysis of consistency conditions for SCFTs, such as those developed in Chapter 11, provide a useful tool in the classification effort. Thus it would be nice to elaborate on the consistency condition called **Claim B** throughout this thesis, for example by refining it using informations on the Coulomb branch geometry. Another possible generalization would be to apply the ideas developed in Chapters 10 and 11 to $\mathcal{N} = 2$ SCFTs which are not maximally strongly coupled. This would probably require a more in-depth analysis of the charge lattice for those theories.

1-form symmetries in $\mathcal{N} = 2$ SCFTs: The upper bound for the 1-form symmetry group of rank-2 $\mathcal{N} = 2$ SCFTs with $\varkappa \neq \{1, 2\}$ that we analyzed in Chapter 11 does not have a generalization to higher ranks up to now. It would be nice to understand whether such a bound exists at arbitrary ranks, at least for theories with $\varkappa \neq \{1, 2\}$. SCFTs with $\varkappa \neq \{1, 2\}$ are maximally strongly coupled and do not admit a conventional lagrangian description, therefore understanding properties of their global symmetries would be a useful tool for studying such theories. Furthermore it would be interesting to study the implications of the existence of this bound on the dual gravity theory.

Appendices

Dualities with adjoint and without W_{monopole} on Z_{S^3}

Here we follow the sequential deconfinement procedure performed in Section 5.1, 5.2 and 5.3 of [2] on the partition function. These chains of confining/deconfining dualities allows to prove the dualities for symplectic (orthogonal) gauge group with two fundamentals (one vector), one adjoint without monopole superpotential. The identities needed are

$$\begin{aligned}
 Z_{SO(2n+1)}^{N_f=2n} &= \frac{\prod_{r=1}^{2n} \Gamma_h(\mu_r)}{\sqrt{-\omega_1 \omega_2}^n 2^n n!} \int_{C^n} \frac{\prod_{j=1}^n \prod_{r=0}^{2n} \Gamma_h(\mu_r \pm x_j)}{\prod_{1 \leq j < k \leq n} \Gamma_h(\pm x_j \pm x_k) \prod_{i=1}^n \Gamma_h(\pm x_i)} \prod_{j=1}^n dx_j \\
 &= \Gamma_h \left(\omega - \sum_{r=1}^{2n} \mu_r \right) \prod_{1 \leq r < s \leq 2n} \Gamma_h(\mu_r + \mu_s) \prod_{r=1}^{2n} \Gamma_h(\omega - \mu_r)
 \end{aligned} \tag{A.1}$$

$$\begin{aligned}
 Z_{USp(2n)}^{N_f=2n+2} &= \frac{1}{\sqrt{-\omega_1 \omega_2}^n 2^n n!} \int_{C^n} \frac{\prod_{a=1}^n \prod_{r=0}^{2n+2} \Gamma_h(\mu_r \pm y_a)}{\prod_{1 \leq a < b \leq n} \Gamma_h(\pm y_a \pm y_b) \prod_{a=1}^n \Gamma_h(\pm 2y_a)} \prod_{a=1}^n dy_a \\
 &= \Gamma_h \left(2\omega - \sum_{r=1}^{2n+2} \mu_r \right) \prod_{1 \leq r < s \leq 2n+2} \Gamma_h(\mu_r + \mu_s)
 \end{aligned} \tag{A.2}$$

$$\begin{aligned}
 Z_{SO(2n)}^{N_f=2n-1} &= \frac{1}{\sqrt{-\omega_1 \omega_2}^n 2^{n-1} n!} \int_{C^n} \frac{\prod_{j=1}^n \prod_{r=0}^{2n-1} \Gamma_h(\mu_r \pm x_j)}{\prod_{1 \leq j < k \leq n} \Gamma_h(\pm x_j \pm x_k)} \prod_{j=1}^n dx_j \\
 &= \Gamma_h \left(\omega - \sum_{r=1}^{2n-1} \mu_r \right) \prod_{1 \leq r < s \leq 2n-1} \Gamma_h(\mu_r + \mu_s) \prod_{r=1}^{2n-1} \Gamma_h(\omega - \mu_r)
 \end{aligned} \tag{A.3}$$

which correspond to limiting cases of Aharony duality.

Case I: $USp(2n)$

The partition function of theory \mathcal{T}_1 of [2] is:

$$Z_{\mathcal{T}_1} = \frac{\Gamma_h(\tau)^n}{(-\omega_1\omega_2)^{\frac{n}{2}} 2^n n!} \int \prod_{a=1}^n dy_a \frac{\Gamma_h(\pm y_a + m) \Gamma_h(\pm y_a + \omega - \frac{\tau}{2})}{\Gamma_h(\pm 2y_a)} \times \prod_{1 \leq a < b \leq n} \frac{\Gamma_h(\pm y_a \pm y_b + \tau)}{\Gamma_h(\pm y_a \pm y_b)} \quad (\text{A.4})$$

This is equivalent to a two-node quiver with gauge groups $SO(2n+1) \times USp(2n)$, denoted \mathcal{T}_1' with partition function:

$$Z_{\mathcal{T}_1'} = \frac{\Gamma_h(\tau)^n \Gamma_h(\omega + n\tau)}{(-\omega_1\omega_2)^n 2^{2n} n!^2} \int \prod_{a=1}^n dy_a \frac{\Gamma_h(\pm y_a + m) \Gamma_h(\pm y_a + \frac{\tau}{2})}{\Gamma_h(\pm 2y_a)} \prod_{i=1}^n dx_i \frac{\Gamma_h(\pm y_a \pm x_i + \frac{\tau}{2})}{\Gamma_h(\pm x_i)} \times \prod_{1 \leq a < b \leq n} \frac{1}{\Gamma_h(\pm y_a \pm y_b)} \prod_{1 \leq i < j \leq n} \frac{1}{\Gamma_h(\pm x_i \pm x_j)} \quad (\text{A.5})$$

These two expressions can be shown to coincide by using (A.1) to confine the orthogonal node. Then we dualize the symplectic node using (A.2):

$$Z_{\mathcal{T}_2} = \frac{\Gamma_h(\tau)^n \Gamma_h(\omega + n\tau) \Gamma_h(2\omega - m - \frac{\tau}{2} - n\tau)}{(-\omega_1\omega_2)^{\frac{n}{2}} 2^n n!} \int \prod_{i=1}^n dx_i \frac{\Gamma_h(\pm x_i + m + \frac{\tau}{2}) \Gamma_h(m + \frac{\tau}{2})}{\Gamma_h(\pm x_i)} \times \prod_{1 \leq i < j \leq n} \frac{\Gamma_h(\pm x_i \pm x_j + \tau) \Gamma_h(\pm x_i + \tau)}{\Gamma_h(\pm x_i \pm x_j)} \quad (\text{A.6})$$

The mass parameters for the symplectic gauge group satisfy

$$2\omega - (2n+1)\frac{\tau}{2} + \sum_{i=1}^n \left(\pm x_i + \frac{\tau}{2} \right) + \frac{\tau}{2} = 2\omega \quad (\text{A.7})$$

We then deconfine the adjoint using the confining duality with linear monopole superpotential (B.1):

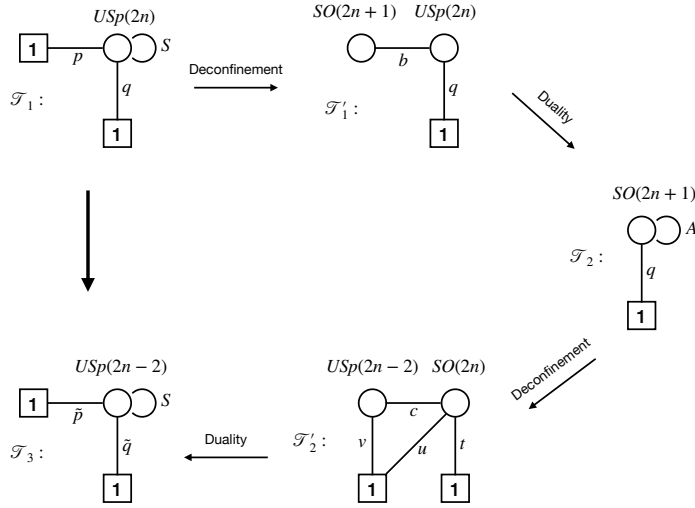


Figure A.1 Schematic representation of one step of the deconfinement procedure of [2] for the $USp(2n)$ model with adjoint. The partition functions of the model are:

	\mathcal{T}_1	\mathcal{T}'_1	\mathcal{T}_2	\mathcal{T}'_2	\mathcal{T}_3
Z_{S^3}	(A.4)	(A.5)	(A.6)	(A.8)	(A.9)

$$\begin{aligned}
 Z_{\mathcal{T}'_2} &= \frac{\Gamma_h(\tau)^n \Gamma_h(\omega + n\tau) \Gamma_h(2\omega - m - \frac{\tau}{2} - n\tau)}{(-\omega_1 \omega_2)^{\frac{n(n-1)}{2}} 2^{n(n-1)} n! (n-1)!} \int \prod_{i=1}^n dx_i \frac{\Gamma_h(\pm x_i + m + \frac{\tau}{2}) \Gamma_h(m + \frac{\tau}{2})}{\Gamma_h(\pm x_i)} \\
 &\times \prod_{1 \leq i < j \leq n} \frac{\Gamma_h(\pm x_i + n\tau) \Gamma_h(n\tau)}{\Gamma_h(\pm x_i \pm x_j)} \prod_{a=1}^{n-1} dy_a \frac{\Gamma_h(\pm y_a + 2\omega - (2n+1)\frac{\tau}{2})}{\Gamma_h(\pm 2y_a)} \\
 &\times \prod_{1 \leq a < b \leq n-1} \frac{1}{\Gamma_h(\pm y_a \pm y_b)} \prod_{a=1}^{n-1} \prod_{i=1}^n \Gamma_h\left(\pm x_i \pm y_a + \frac{\tau}{2}\right) \Gamma_h\left(\pm y_a + \frac{\tau}{2}\right)
 \end{aligned} \tag{A.8}$$

The last step consists in dualising the orthogonal node with (A.1):

$$\begin{aligned}
 Z_{\mathcal{T}_3} &= \frac{\Gamma_h(\tau)^n \Gamma_h(\omega - m - \frac{\tau}{2} - (2n-1)\tau) \Gamma_h(2m + \tau) \Gamma_h(2n\tau) \Gamma_h(\omega - m - \frac{\tau}{2})}{(-\omega_1 \omega_2)^{\frac{n-1}{2}} 2^{n-1} (n-1)!} \\
 &\times \int \prod_{a=1}^{n-1} dy_a \frac{\Gamma_h(\pm y_a + m + \tau) \Gamma_h(\pm y_a + \omega - \frac{\tau}{2})}{\Gamma_h(\pm 2y_a)} \prod_{1 \leq a < b \leq n} \frac{\Gamma_h(\pm y_a \pm y_b + \tau)}{\Gamma_h(\pm y_a \pm y_b)}
 \end{aligned} \tag{A.9}$$

This is equivalent to the theory \mathcal{T}_1 with a lower rank and additional singlets. The new mass for the fundamental q is $\tilde{m} = m + \tau$. The whole step is shown schematically in Figure A.1. By iterating these steps n times one gets to a confining theory with singlets described by (4.11).

Case II: $SO(2n)$

Now we consider a $SO(2n)$ theory with one fundamental and one adjoint with $W = 0$. The partition function is:

$$\frac{\Gamma_h(\tau)^n}{(-\omega_1\omega_2)^{\frac{n-1}{2}} 2^n n!} \int \prod_{i=1}^n dx_i \Gamma_h(\pm x_i + m) \prod_{1 \leq i < j \leq n} \frac{\Gamma_h(\pm x_i \pm x_j + \tau)}{\Gamma_h(\pm x_i \pm x_j)} \quad (\text{A.10})$$

we deconfine the adjoint with (A.2) and get to a quiver with gauge groups $USp(2n-2) \times SO(2n)$:

$$\begin{aligned} & \frac{\Gamma_h(\tau)^n \Gamma_h(n\tau)}{(-\omega_1\omega_2)^{n-1} 2^{n(n-1)} n! (n-1)!} \int \prod_{i=1}^n dx_i \Gamma_h(\pm x_i + m) \prod_{1 \leq i < j \leq n} \frac{1}{\Gamma_h(\pm x_i \pm x_j)} \\ & \times \prod_{a=1}^{n-1} dy_a \frac{\Gamma_h(\pm x_i \pm y_a + \frac{\tau}{2})}{\Gamma_h(\pm 2y_a)} \prod_{1 \leq a < b \leq n-1} \frac{1}{\Gamma_h(\pm y_a \pm y_b)} \end{aligned} \quad (\text{A.11})$$

Next we dualise the orthogonal node:

$$\begin{aligned} & \frac{\Gamma_h(\tau)^n \Gamma_h(n\tau) \Gamma_h(\omega - (n-1)\tau - m) \Gamma_h(2m) \Gamma_h(\omega - m)}{(-\omega_1\omega_2)^{\frac{n-1}{2}} 2^{n-1} (n-1)!} \\ & \times \int \prod_{a=1}^{n-1} dy_a \frac{\Gamma_h(\pm y_a + \omega - \frac{\tau}{2}) \Gamma_h(\pm y_a + m + \frac{\tau}{2})}{\Gamma_h(\pm 2y_a)} \prod_{1 \leq a < b \leq n-1} \frac{\Gamma_h(\pm y_a \pm y_b + \tau)}{\Gamma_h(\pm y_a \pm y_b)} \end{aligned} \quad (\text{A.12})$$

This is the USp theory with adjoint considered in the previous case with additional singlets. We use the result from the previous case to confine the gauge theory and recover (4.13).

Case III: $SO(2n+1)$

The case of orthogonal gauge group with odd rank is already covered in the computation for symplectic gauge group. This theory corresponds to the third step in the USp computation, namely (A.6), modulo the presence of some singlets. One can follow the confinement/deconfinement steps going from (A.6) to (A.9), then confine the USp gauge theory using the result from the previous case.

3d $SO(N)$ with $N + 1$ flavors and linear monopole superpotential

In this appendix we review the duality for $SO(N)$ gauge theories with $N + 1$ vectors Q_i and $\bar{W} = Y_+$ proposed by [2]. We further discuss the related identity between the partition functions. This is useful for the proofs of the dualities in the body of Chapter 4 because we use such dualities to deconfine the adjoint of symplectic gauge groups.

In this case the claim is that the model is dual to a WZ model, where the fields are the baryons $q = \epsilon_N(Q^N)$ and the symmetric meson S with superpotential $W = qSq + \det S$. In order to obtain the partition function for such a duality we start from $USp(2n)$ with linear monopole superpotential $W = Y_{USp}$ and $2n + 4$ fundamentals. The linear monopole imposes the constraint $\mu_1 + \dots + \mu_{2n+4} = 2\omega$ on the mass parameters μ_r of the fundamental fields in the partition function. The integral identity is [56]

$$\begin{aligned} & \frac{1}{(-\omega_1\omega_2)^{\frac{n}{2}} 2^n n!} \int_{C^n} \prod_{1 \leq j < k \leq n} \frac{1}{\Gamma_h(\pm x_j \pm x_k)} \prod_{j=1}^n \frac{\prod_{r=1}^{2n+4} \Gamma_h(\mu_r \pm x_j)}{\Gamma_h(\pm 2x_j)} dx_j \\ &= \prod_{1 \leq r < s \leq 2n+4} \Gamma_h(\mu_r + \mu_s) \end{aligned} \quad (\text{B.1})$$

If we then assign the mass parameters as $\mu_1 = \frac{\omega_1}{2}$ and $\mu_2 = \frac{\omega_1}{2}$, and we use the duplication formula on both sides of (B.1), we arrive at the identity

$$\begin{aligned} & \frac{\prod_{r=1}^{2n+2} \Gamma_h(\mu_r)}{(-\omega_1\omega_2)^{\frac{n}{2}} 2^n n!} \int_{C^n} \prod_{1 \leq j < k \leq n} \frac{1}{\Gamma_h(\pm x_j \pm x_k)} \prod_{j=1}^n \frac{\prod_{r=1}^{2n+2} \Gamma_h(\mu_r \pm x_j)}{\Gamma_h(\pm x_j)} dx_j \\ &= \prod_{1 \leq r \leq s \leq 2n+2} \Gamma_h(\mu_r + \mu_s) \prod_{r=1}^{2n+2} \Gamma_h(\omega - \mu_r) \end{aligned} \quad (\text{B.2})$$

with the constraint $\sum_{r=1}^{2n+2} \mu_r = \omega$. This corresponds to the case of $SO(2n+1)$ with $2n+2$ fundamentals. The arguments of the singlets on the dual side correspond to the mesons and to the baryons of the electric theory.

The even case is obtained by considering also $\mu_3 = 0$. In this case, by using the duplica-

tion formula on both sides of (B.1) we end up with

$$\begin{aligned} & \frac{1}{(-\omega_1\omega_2)^{\frac{n}{2}}2^{2n-1}n!} \int_{C^n} \prod_{1 \leq j < k \leq n} \frac{1}{\Gamma_h(\pm x_j \pm x_k)} \prod_{j=1}^n \prod_{r=1}^{2n+1} \Gamma_h(\mu_r \pm x_j) dx_j \\ &= \prod_{1 \leq r \leq s \leq 2n+1} \Gamma_h(\mu_r + \mu_s) \prod_{r=1}^{2n+1} \Gamma_h(\omega - \mu_r) \end{aligned} \tag{B.3}$$

with the constraint $\sum_{r=1}^{2n+1} \mu_r = \omega$. This corresponds to the case of $SO(2n)$ with $2n + 1$ fundamentals. The arguments of the singlets on the dual side correspond to the mesons and to the baryons of the electric theory.

As a consistency check we can perform a real mass flow by giving large masses of opposite sign to two vectors and retrieve the limiting case of Aharony duality. In (B.2) we fix:

$$\mu_{2n+1} = s + \nu, \quad \mu_{2n+2} = -s + \nu \tag{B.4}$$

and take the limit $s \rightarrow \infty$. The constraint reads $\omega - \sum_{r=1}^{2n} \mu_r = 2\nu$ and the divergent phases cancel between the RHS and the LHS. We obtain:

$$\begin{aligned} & \frac{\prod_{r=1}^{2n} \Gamma_h(\mu_r)}{(-\omega_1\omega_2)^{\frac{n}{2}}2^{2n}n!} \int_{C^n} \prod_{1 \leq j < k \leq n} \frac{1}{\Gamma_h(\pm x_j \pm x_k)} \prod_{j=1}^n \frac{\prod_{r=1}^{2n} \Gamma_h(\mu_r \pm x_j)}{\Gamma_h(\pm x_j)} dx_j \\ &= \Gamma_h \left(\omega - \sum_{r=1}^{2n} \mu_r \right) \prod_{1 \leq \mu_r \leq \mu_s \leq 2n} \Gamma_h(\mu_r + \mu_s) \prod_{r=1}^{2n} \Gamma_h(\omega - \mu_r) \end{aligned} \tag{B.5}$$

which corresponds to the limiting case of Aharony duality for $SO(N) = SO(2n + 1)$ and $2n$ vectors, with $W = 0$ [43].

Similarly in (B.3) we fix:

$$\mu_{2n} = s + \nu, \quad \mu_{2n+1} = -s + \nu \tag{B.6}$$

and obtain:

$$\begin{aligned} & \frac{1}{(-\omega_1\omega_2)^{\frac{n}{2}}2^{2n-1}n!} \int_{C^n} \prod_{1 \leq j < k \leq n} \frac{1}{\Gamma_h(\pm x_j \pm x_k)} \prod_{j=1}^n \prod_{r=1}^{2n-1} \Gamma_h(\mu_r \pm x_j) dx_j \\ &= \Gamma_h \left(\omega - \sum_{r=1}^{2n-1} \mu_r \right) \prod_{1 \leq \mu_r \leq \mu_s \leq 2n-1} \Gamma_h(\mu_r + \mu_s) \prod_{r=1}^{2n-1} \Gamma_h(\omega - \mu_r) \end{aligned} \tag{B.7}$$

which corresponds to the limiting case of Aharony duality for $SO(N) = SO(2n)$ and $2n - 1$ vectors, with $W = 0$ [43].

Further examples of multiplanarizable quivers

In this Appendix we give additional examples of multiplanarizable quivers studied in Chapter 7. In table C.1 is the list of cases that we have analyzed in detail. Two examples

$n_G \rightarrow n_G^\Omega$	(k_1, k_2, k_3)	Comments
$6 \rightarrow 4$	$(1, 1, 2) - (0, 2, 2)$	Original PdP _{3b/c} case, see [12]
$8 \rightarrow 5$	$(1, 1, 3) - (0, 2, 3)$	See App. C.0.1
$10 \rightarrow 6$	$(1, 1, 4) - (0, 2, 4)$	Two cases, see App. C.0.2
$12 \rightarrow 7$	$(1, 1, 5) - (0, 2, 5)$	See App. C.0.3
$12 \rightarrow 7$	$(2, 2, 4) - (0, 4, 4)$	Also $\Omega_{\text{f.p.}}$ for $(2,2,4)$, see App. C.0.4
$14 \rightarrow 8$	$(2, 2, 5) - (0, 4, 5)$	See Sec. 7.4.1
$16 \rightarrow 9$	$(2, 2, 6) - (0, 4, 6)$	Two cases, Sec. 7.4.2 and App. C.0.5
$18 \rightarrow 10$	$(3, 3, 6) - (2, 4, 6) - (0, 6, 6)$	Intermediate case, see App. C.0.6

Table C.1 List of cases (ordered by increasing number n_G^Ω of gauge groups after the projection) analyzed in detail in the Chapter 7.

have been studied in the core of Chapter 7. Here for completeness we briefly survey the other cases. We will give the brane tilings, the orientifold projections, specifying the choices of fixed lines or fixed points.

For each case we will also provide the choice of ranks (consistent with the general one discussed in Fig. 7.12) that allows to find the conformally dual models together with the projected superpotentials.

C.0.1 $(1, 1, 3) - (0, 2, 3)$

The dimers and the toric diagrams are given in Fig. C.1. The $(k_1, k_2, k_3) = (1, 1, 3)$ model is projected with fixed lines while the $(k_1, k_2, k_3) = (0, 2, 3)$ model is projected with fixed points. We assign the charges to the fixed points and lines as discussed in the body of Chapter 7. Again we do not distinguish between $\tau_1 = 1$ and $\tau_1 = -1$ and consider the two possibilities in a uniform language. The superpotential for the $(1, 1, 3)$ model after

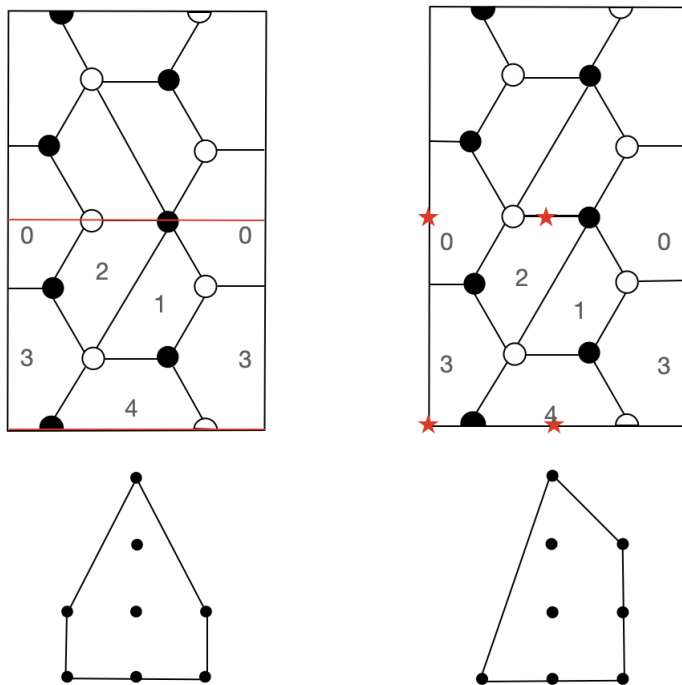


Figure C.1 Fixed-line and fixed-point projections for the (1, 1, 3) and the (0, 2, 3) models.

the fixed lines projection is

$$\begin{aligned} W_{(1,1,3)}^{\Omega_{fl.}} &= \frac{1}{2}T_{22}(X_{02}^2 - X_{01}^2 X_{12}^2) + X_{30}X_{01}X_{13} - X_{30}X_{02}X_{23} \\ &+ X_{41}X_{12}X_{23}Y_{34} - X_{41}X_{13}X_{34} + \frac{1}{2}\tilde{T}_{33} \left(X_{34}^2 - Y_{34}^2 \right) . \end{aligned} \quad (C.1)$$

The superpotential for the $(0, 2, 3)$ model after the fixed points projection is

$$\begin{aligned} W_{(0,2,3)}^{\Omega_{fp.}} &= T_{22}X_{01}X_{12}X_{02} + X_{30}X_{01}X_{13} - X_{30}X_{02}X_{23} \\ &+ X_{41}X_{12}X_{23}Y_{34} - X_{41}X_{13}X_{34} + \tilde{T}_{33}X_{34}Y_{34} , \end{aligned} \quad (C.2)$$

where, as in the body of Chapter 7, the gauge contractions are taken opportunely. The choice of gauge ranks that gives rise to the conformal duality is

$$N_0 = n, N_1 = N_2 = n - 2\tau, N_3 = n - 4\tau, N_4 = n - 6\tau . \quad (C.3)$$

The conformal duality can be associated to a pair of superpotentials with different signs by first applying Seiberg duality on node $SU(N_1)$. Then we can consider the combinations of the fields X_{34} with Y_{34} and X_{02} with M_{02} , where M_{02} in the dual phase is the meson $X_{01}X_{12}$, that is considered as elementary field after the duality on $SU(N_1)$. After these operations, the two superpotentials (C.1) and (C.2) become identical up to some signs. The conformal duality between the two models becomes then manifest and explicit, fitting with the discussion of Sec. 7.1.

C.0.2 $(1, 1, 4) - (0, 2, 4)$

The next case corresponds to the fixed line projection of $(k_1, k_2, k_3) = (1, 1, 4)$ and to the fixed point projection of $(k_1, k_2, k_3) = (0, 2, 4)$. In this case there are two possible projections for each models. These projections give different quivers and they are studied separately.

First case

The first possibility is represented in Fig. C.2. The superpotential for the $(1, 1, 4)$ model after the fixed-line projection is

$$\begin{aligned} W_{(1,1,4)}^{\Omega_{fl.}} &= \frac{1}{2}T_{22} \left(X_{02}^2 - X_{01}^2 X_{12}^2 \right) + X_{30}X_{01}X_{13} - X_{30}X_{02}X_{23} \\ &+ X_{41}X_{12}X_{23}Y_{34} - X_{41}X_{13}X_{34} + X_{63}X_{34}X_{46} - X_{63}Y_{34}Y_{46} \\ &+ \frac{1}{2}\tilde{T}_{44} \left(X_{46}^2 - Y_{46}^2 \right) . \end{aligned} \quad (C.4)$$

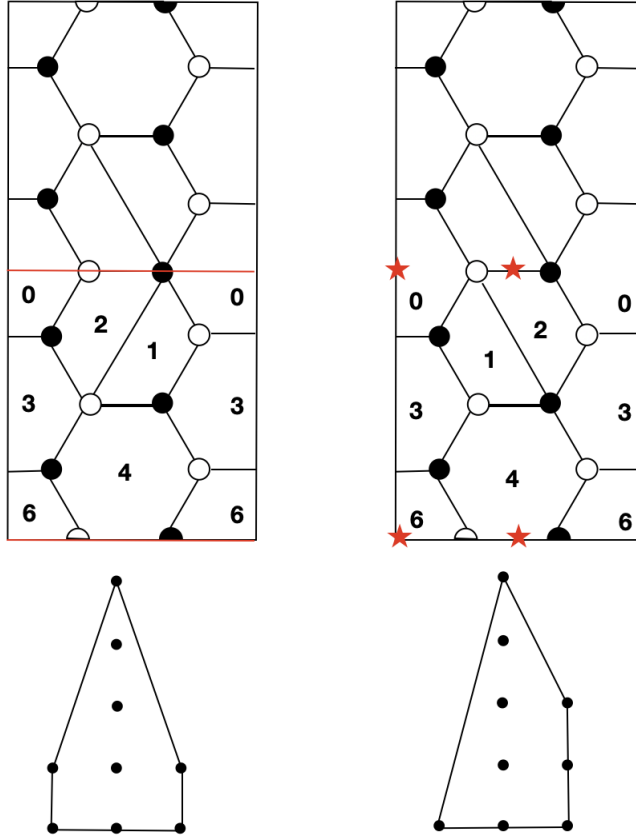


Figure C.2 Fixed lines and fixed points projections for $(1, 1, 4)$ and $(0, 2, 4)$. This is the first conformal duality obtained projecting these models.

The superpotential for the $(0, 2, 4)$ model after the fixed points projection is

$$\begin{aligned}
 W_{(0,2,4)}^{\Omega_{f.p.}} &= \frac{1}{2} T_{22} X_{01} X_{12} X_{02} + X_{30} X_{02} X_{23} - X_{30} X_{01} X_{13} \\
 &+ X_{41} X_{13} Y_{34} - X_{41} X_{12} X_{23} X_{34} + X_{63} X_{34} X_{46} - X_{63} Y_{34} Y_{46} \\
 &+ \frac{1}{2} \tilde{T}_{44} X_{46} Y_{46} .
 \end{aligned} \tag{C.5}$$

The choice of gauge ranks that gives rise to the conformal duality is

$$N_0 = n, N_1 = N_2 = n - 2\tau, N_3 = n - 4\tau, N_4 = n - 6\tau, N_6 = n - 8\tau . \tag{C.6}$$

We can use the usual tools, i.e. Seiberg duality on $SU(N_1)$ and suitable field redefinitions, such that (C.4) and (C.5) become identical up to some signs. The conformal duality between the two models becomes again explicit as in the general discussion of Sec. 7.1.

Second case

The first possibility is represented in Fig. C.3.

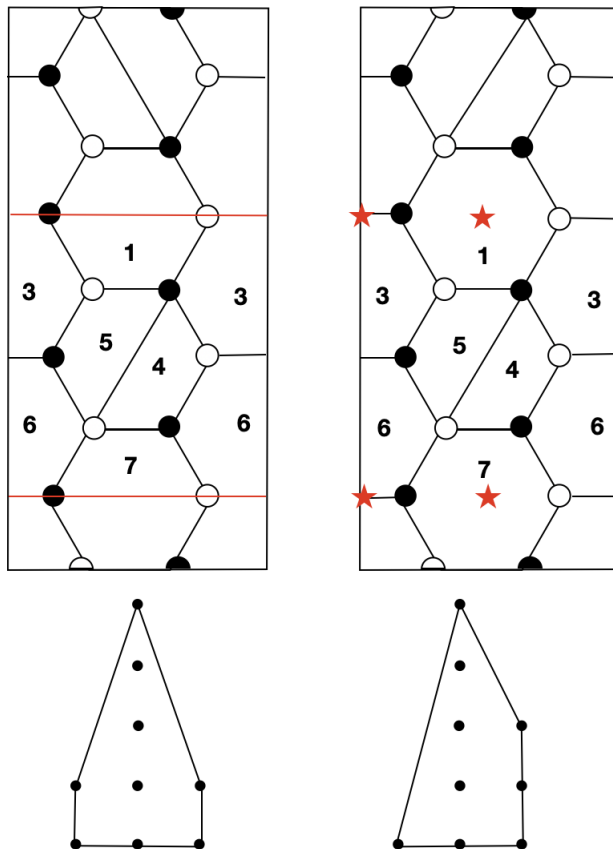


Figure C.3 Fixed-line and fixed-point projections for (1, 1, 4) and (0, 2, 4). This is the second conformal duality obtained projecting these models.

The superpotential for the (1, 1, 4) model after the fixed lines projection is

$$\begin{aligned}
 W_{(1,1,4)}^{\Omega_{\text{f.l.}}} &= \frac{1}{2}T_{33} \left(X_{13}^2 - Y_{13}^2 \right) + Y_{13}X_{35}X_{51} - X_{13}X_{34}X_{45}X_{51} \\
 &\quad + X_{34}X_{46}X_{63} - X_{35}X_{56}X_{63} + X_{56}Y_{67}X_{74}X_{45} - X_{46}X_{67}X_{74} \\
 &\quad + \frac{1}{2}T_{33} \left(X_{67}^2 - Y_{67}^2 \right) .
 \end{aligned}
 \tag{C.7}$$

The superpotential for the $(0, 2, 4)$ model after the fixed points projection is

$$\begin{aligned}
W_{(1,1,4)}^{\Omega_{fl.}} &= T_{33}X_{13}Y_{13} + Y_{13}X_{35}X_{51} - X_{13}X_{34}X_{45}X_{51} \\
&\quad + X_{34}X_{46}X_{63} - X_{35}X_{56}X_{63} + X_{56}Y_{67}X_{74}X_{45} - X_{46}X_{67}X_{74} \\
&\quad + T_{33}X_{67}Y_{67} .
\end{aligned} \tag{C.8}$$

The choice of gauge ranks that gives rise to the conformal duality is

$$N_1 = n, N_3 = n - 2\tau, N_4 = N_5 = n - 4\tau, N_6 = n - 6\tau, N_7 = n - 8\tau . \tag{C.9}$$

In this case, it can be shown that the two superpotentials in Eqs. (C.7)-(C.8) to be identical without any further duality. Indeed by substituting the combinations $X_{13} \pm Y_{13}$ and $X_{67} \pm Y_{67}$, the superpotentials (C.7) and (C.8) become identical up to some signs, making the conformal duality explicit.

C.0.3 $(1, 1, 5) - (0, 2, 5)$

The next case corresponds to the fixed line projection of $(k_1, k_2, k_3) = (1, 1, 5)$ and to the fixed-point projection of $(k_1, k_2, k_3) = (0, 2, 5)$. The dimers and the toric diagrams are given in Fig. C.4. There are also other models where the diagonal appears in the first hexagon on the tiling, but conformal duality works similarly and we show only these two dimers for simplicity. The superpotential for the $(1, 1, 5)$ model after the fixed-line projection is

$$\begin{aligned}
W_{(1,1,5)}^{\Omega_{fl.}} &= \frac{1}{2}T_{33} \left(X_{13}^2 - Y_{13}^2 \right) + Y_{13}Y_{34}X_{41} - X_{13}X_{34}X_{41} \\
&\quad + X_{34}X_{46}X_{63} - Y_{34}Y_{46}X_{63} + Y_{46}X_{68}X_{84} - X_{46}X_{67}X_{78}X_{84} \\
&\quad + X_{67}X_{79}X_{96} - X_{68}X_{89}X_{96} + \frac{1}{2}\tilde{T}_{77} \left(X_{78}^2 X_{89}^2 - X_{79}^2 \right) .
\end{aligned} \tag{C.10}$$

The superpotential for the $(0, 2, 5)$ model after the fixed points projection is

$$\begin{aligned}
W_{(0,2,5)}^{\Omega_{fl.}} &= T_{33}X_{13}Y_{13} + Y_{13}Y_{34}X_{41} - X_{13}X_{34}X_{41} \\
&\quad + X_{34}X_{46}X_{63} - Y_{34}Y_{46}X_{63} + Y_{46}X_{68}X_{84} - X_{46}X_{67}X_{78}X_{84} \\
&\quad + X_{67}X_{79}X_{96} - X_{68}X_{89}X_{96} + \tilde{T}_{77}X_{78}^2 X_{89}X_{79} .
\end{aligned} \tag{C.11}$$

The choice of gauge ranks that gives rise to the conformal duality is

$$\begin{aligned}
N_1 &= n, N_3 = n - 2\tau, N_4 = n - 4\tau, \\
N_6 &= n - 6\tau, N_7 = N_8 = n - 8\tau, N_9 = n - 10\tau .
\end{aligned} \tag{C.12}$$

The conformal duality between the two models becomes explicit as in Sec. 7.1, by applying a Seiberg duality on $SU(N_8)$, and considering the combinations $X_{13} \pm Y_{13}$ and $X_{79} \pm M_{79}$, where $M_{79} \equiv X_{78}X_{89}$.

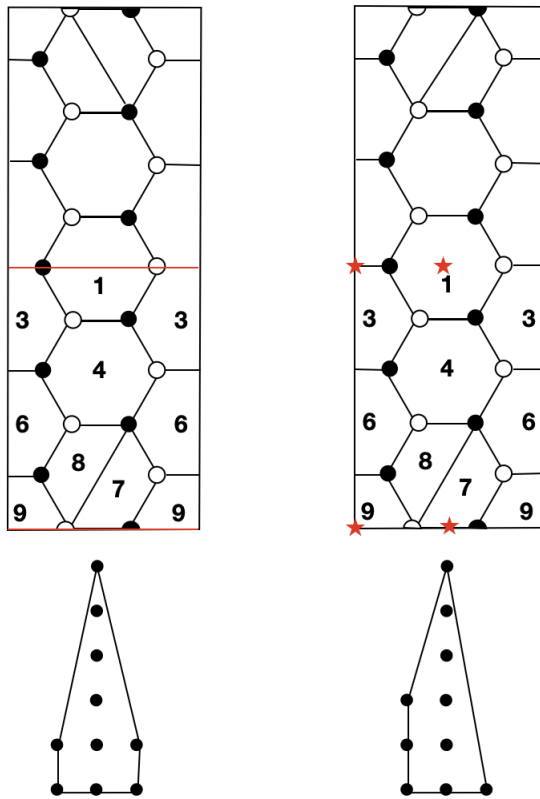


Figure C.4 Fixed lines and fixed points projections for $(1, 1, 5)$ and $(0, 2, 5)$.

C.0.4 $(2, 2, 4) - (0, 4, 4)$

Here we study two fixed line projections and one fixed point projection for $(k_1, k_2, k_3) = (2, 2, 4)$ and a fixed point projection of $(k_1, k_2, k_3) = (0, 4, 4)$. The projections are summarized in Fig. C.5. The superpotential for the $(2, 2, 4)$ model after the first fixed lines projection is

$$\begin{aligned}
 W_{(2,2,4)}^{\Omega_{f1}^1} &= \frac{1}{2} T_{00} \left(X_{02}^2 - X_{01}^2 X_{12}^2 \right) + X_{01} X_{13} X_{30} - X_{02} X_{23} X_{30} \\
 &\quad + X_{23} X_{35} X_{51} X_{12} - X_{13} X_{34} X_{45} X_{51} + X_{34} X_{46} X_{63} - X_{35} X_{56} X_{63} \\
 &\quad + \frac{1}{2} \tilde{T}_{44} \left(X_{45}^2 X_{56}^2 - X_{46}^2 \right) .
 \end{aligned} \tag{C.13}$$

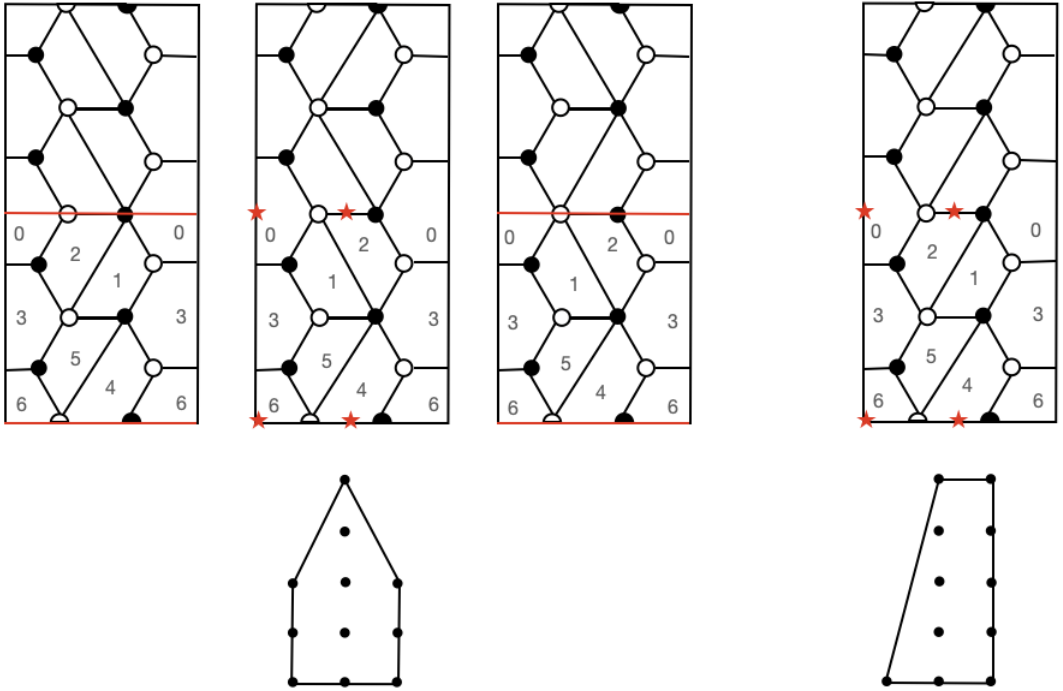


Figure C.5 Fixed lines and fixed-point projections for (2, 2, 4) and (0, 4, 4).

The superpotential for the (2, 2, 4) model after the fixed-point projection is

$$\begin{aligned}
 W_{(2,2,4)}^{\Omega_{\text{fp}}} &= T_{00} X_{02} X_{01} X_{12} + X_{02} X_{23} X_{30} - X_{01} X_{13} X_{30} \\
 &+ X_{13} X_{35} X_{51} - X_{23} X_{34} X_{45} X_{51} X_{12} + X_{34} X_{46} X_{63} - X_{35} X_{56} X_{63} \\
 &+ \tilde{T}_{44} X_{45} X_{56} X_{46} .
 \end{aligned} \tag{C.14}$$

The superpotential for the (2, 2, 4) model after the second fixed-line projection is

$$\begin{aligned}
 W_{(2,2,4)}^{\Omega_{\text{fl}}^2} &= \frac{1}{2} T_{00} \left(X_{01}^2 X_{12}^2 - X_{02}^2 \right) + X_{02} X_{23} X_{30} - X_{01} X_{13} X_{30} \\
 &+ X_{13} X_{35} X_{51} - X_{23} X_{34} X_{45} X_{51} X_{12} + X_{34} X_{46} X_{63} - X_{35} X_{56} X_{63} \\
 &+ \frac{1}{2} \tilde{T}_{44} \left(X_{45}^2 X_{56}^2 - X_{46}^2 \right) .
 \end{aligned} \tag{C.15}$$

The superpotential for the $(0, 4, 4)$ model after the fixed-point projection is

$$\begin{aligned}
 W_{(0,4,4)}^{\Omega_{\text{f.p.}}} &= T_{00}X_{02}X_{01}X_{12} + X_{01}X_{13}X_{30} - X_{02}X_{23}X_{30} \\
 &+ X_{23}X_{35}X_{51}X_{12} - X_{13}X_{34}X_{45}X_{51} + X_{34}X_{46}X_{63} - X_{35}X_{56}X_{63} \\
 &+ \tilde{T}_{44}X_{45}X_{56}X_{46} .
 \end{aligned} \tag{C.16}$$

The choice of gauge ranks that gives rise to the conformal duality is

$$N_0 = n, N_1 = N_2 = n - 2\tau, N_3 = n - 4\tau, N_4 = N_5 = n - 6\tau, N_6 = n - 8\tau \tag{C.17}$$

The situation here is similar to the one in sub-section 7.4.1. Indeed there are three cases that are Seiberg dual before the projections, and that become conformally dual after the projection. We can make the conformal dualities among the various model more explicit along the lines of the discussion in Sec. 7.1. By combining the dualities on node $SU(N_{1,2,3})$ and the suitable field redefinitions we can indeed prove that each pair of superpotentials become identical up to signs.

C.0.5 $(2, 2, 6) - (0, 4, 6)$: second case

Here we study another case involving the $(2, 2, 6)$ and $(0, 4, 6)$ models. Here we have two fixed line projections and one fixed point projection for $(k_1, k_2, k_3) = (2, 2, 4)$ and a fixed point projection of $(k_1, k_2, k_3) = (0, 4, 4)$. The projections are summarized in Fig. C.6. The superpotential for the $(2, 2, 6)$ model after the first fixed-line projection is

$$\begin{aligned}
 W_{(2,2,6)}^{\Omega_{\text{f.l.}}^1} &= \frac{1}{2}T_{33} \left(X_{13}^2 - Y_{13}^2 \right) + Y_{13}X_{34}X_{45}X_{51} - X_{13}X_{35}X_{51} \\
 &+ X_{35}X_{56}X_{63} - X_{34}X_{46}X_{63} + X_{46}X_{67}X_{78}X_{84} - X_{56}X_{68}X_{84}X_{45} \\
 &+ X_{68}X_{89}X_{96} - X_{67}X_{79}X_{96} + X_{79}Y_{90}X_{07} - X_{89}X_{90}X_{07}X_{78} \\
 &+ \frac{1}{2}\tilde{T}_{99}(X_{90}^2 - Y_{90}^2) .
 \end{aligned} \tag{C.18}$$

The superpotential for the $(2, 2, 6)$ model after the second fixed lines projection is

$$\begin{aligned}
 W_{(2,2,6)}^{\Omega_{\text{f.l.}}^2} &= \frac{1}{2}T_{33} \left(X_{13}^2 - Y_{13}^2 \right) + Y_{13}X_{34}X_{45}X_{51} - X_{13}X_{35}X_{51} \\
 &+ X_{35}X_{56}X_{63} - X_{34}X_{46}X_{63} + X_{46}X_{68}X_{84} - X_{56}X_{67}X_{78}X_{84}X_{45} \\
 &+ X_{67}X_{79}X_{96} - X_{68}X_{89}X_{96} + X_{89}Y_{90}X_{07}X_{78} - X_{79}X_{90}X_{07} \\
 &+ \frac{1}{2}\tilde{T}_{99} \left(X_{90}^2 - Y_{90}^2 \right) .
 \end{aligned} \tag{C.19}$$

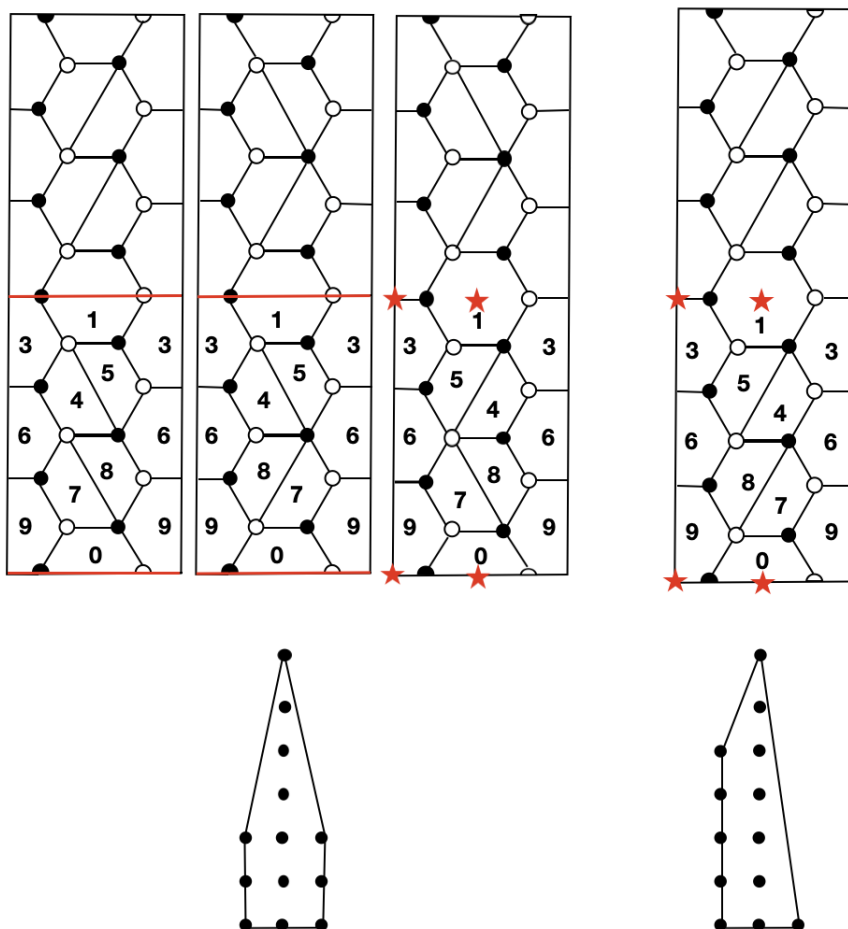


Figure C.6 Fixed-line and fixed-point projections for $(2, 2, 6)$ and $(0, 4, 6)$. This is the second conformal duality obtained projecting these models. The first one has been discussed in the body of Chapter 7 in Sec. 7.4.2.

The superpotential for the (2, 2, 6) model after the fixed points projection is

$$\begin{aligned}
 W_{(2,2,6)}^{\Omega_{\text{f.p.}}} &= T_{33}Y_{13}X_{13} + Y_{13}X_{35}X_{51} - X_{13}X_{34}X_{45}X_{51} \\
 &\quad + X_{34}X_{46}X_{63} - X_{35}X_{56}X_{63} + X_{56}X_{67}X_{78}X_{84}X_{45} - X_{46}X_{68}X_{84} \\
 &\quad + X_{68}X_{89}X_{96} - X_{67}X_{79}X_{96} + X_{79}Y_{90}X_{07} - X_{89}X_{90}X_{07}X_{78} \\
 &\quad + \tilde{T}_{99}Y_{90}X_{90} .
 \end{aligned} \tag{C.20}$$

The superpotential for the (0, 4, 6) model after the fixed points projection is

$$\begin{aligned}
 W_{(0,4,6)}^{\Omega_{\text{f.p.}}} &= T_{33}Y_{13}X_{13} + Y_{13}X_{35}X_{51} - X_{13}X_{34}X_{45}X_{51} \\
 &\quad + X_{34}X_{46}X_{63} - X_{35}X_{56}X_{63} + X_{56}X_{68}X_{84}X_{45} - X_{46}X_{67}X_{78}X_{84} \\
 &\quad + X_{67}X_{79}X_{96} - X_{68}X_{89}X_{96} + X_{89}Y_{90}X_{07}X_{78} - X_{79}X_{90}X_{07} \\
 &\quad + \tilde{T}_{99}Y_{90}X_{90} .
 \end{aligned} \tag{C.21}$$

The choice of gauge ranks that gives rise to the conformal duality is

$$\begin{aligned}
 N_1 &= n, \quad N_3 = n - 2\tau, \quad N_4 = N_5 = n - 4\tau, \\
 N_6 &= n - 6\tau, \quad N_7 = N_8 = n - 8\tau, \quad N_9 = n - 10\tau, \quad N_0 = n - 12\tau .
 \end{aligned} \tag{C.22}$$

The situation here is similar to the one in Sec. 7.4.2. The two cases with fixed lines are related by a field redefinition. Analogously the two cases with fixed points are related by a field redefinition. The cases with fixed lines are connected to the cases with fixed points by first considering Seiberg dualities on $SU(N_2)$ and $SU(N_5)$ and then by suitable field redefinitions.

C.0.6 (3, 3, 6) - (2, 4, 6) - (0, 6, 6)

The last case that we present in this appendix correspond to the fixed lines projection of (3, 3, 6) and to the fixed point projections of both (2, 4, 6) and (0, 6, 6).

This case is interesting because it is the first one where there are three different toric diagrams that give origin to conformal dualities after the projection. There are degenerate choices of (3, 3, 6) and (2, 4, 6) but here for simplicity we study only a single possibility. The other Seiberg dual case become conformally dual after the projection as in the cases discussed above. The toric diagrams, the dimers and the projections are represented in Fig. C.7. The fixed-line projection of the (3, 3, 6) model under investigation has superpotential

$$\begin{aligned}
 W_{(3,3,6)}^{\Omega_{\text{f.l.}}} &= \frac{1}{2}T_{22}(X_{02}^2 - X_{01}^2X_{12}^2) + X_{01}X_{13}X_{30} - X_{02}X_{23}X_{30} \\
 &\quad + X_{23}X_{34}X_{45}X_{51}X_{12} - X_{13}X_{35}X_{51} + X_{35}X_{56}X_{63} - X_{34}X_{46}X_{63} \\
 &\quad + X_{46}X_{68}X_{84} - X_{56}X_{67}X_{78}X_{84}X_{45} + X_{67}X_{79}X_{96} - X_{68}X_{89}X_{96} \\
 &\quad + \frac{1}{2}\tilde{T}_{77}(X_{78}^2X_{89}^2 - X_{79}^2) .
 \end{aligned} \tag{C.23}$$

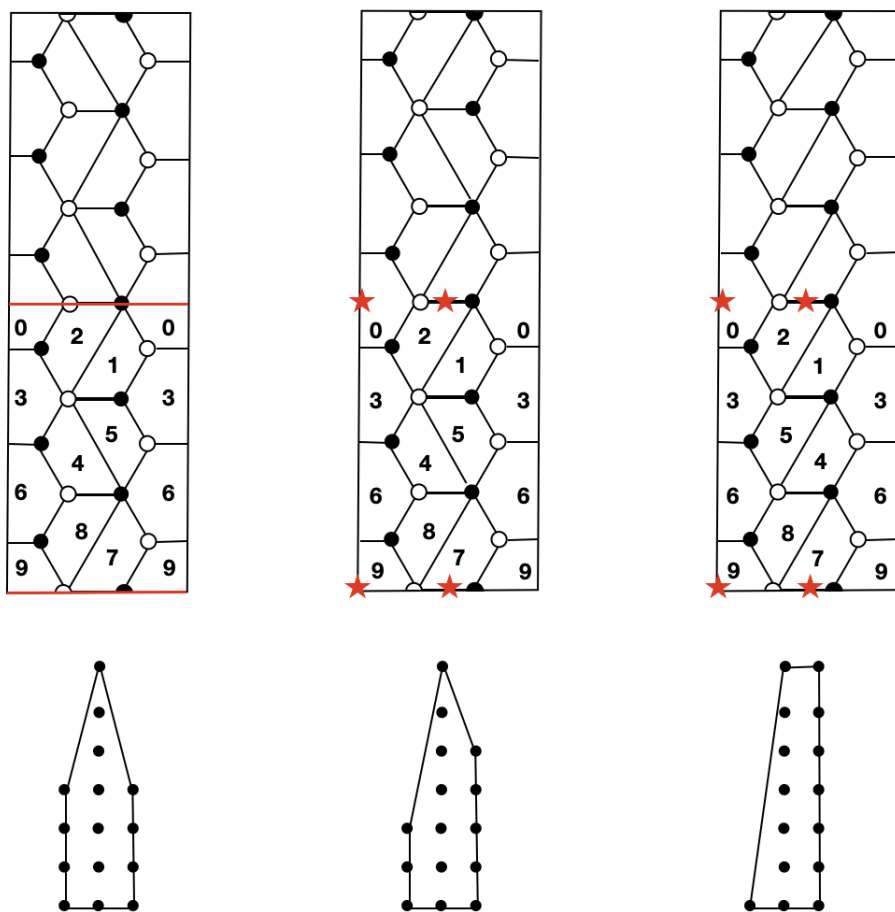


Figure C.7 Fixed-line projection of $(3, 3, 6)$ and fixed-point projections of $(2, 4, 6)$ and $(0, 6, 6)$.

The fixed point projection of the (2, 4, 6) model under investigation has superpotential

$$\begin{aligned}
W_{(2,4,6)}^{\Omega_{\text{f.p.}}} &= T_{22}X_{02}X_{01}X_{12} + X_{01}X_{13}X_{30} - X_{02}X_{23}X_{30} \\
&+ X_{23}X_{34}X_{45}X_{51}X_{12} - X_{13}X_{35}X_{51} + X_{35}X_{56}X_{63} - X_{34}X_{46}X_{63} \\
&+ X_{46}X_{68}X_{84} - X_{56}X_{67}X_{78}X_{84}X_{45} + X_{67}X_{79}X_{96} - X_{68}X_{89}X_{96} \\
&+ \tilde{T}_{77}X_{78}X_{89}X_{79} .
\end{aligned} \tag{C.24}$$

The fixed-point projection of the (0, 6, 6) model has superpotential

$$\begin{aligned}
W_{(0,6,6)}^{\Omega_{\text{f.p.}}} &= T_{22}X_{02}X_{01}X_{12} + X_{01}X_{13}X_{30} - X_{02}X_{23}X_{30} \\
&+ X_{23}X_{35}X_{51}X_{12} - X_{13}X_{34}X_{45}X_{51} + X_{34}X_{46}X_{63} - X_{35}X_{56}X_{63} \\
&+ X_{56}X_{68}X_{84}X_{45} - X_{46}X_{67}X_{78}X_{84} + X_{67}X_{79}X_{96} - X_{68}X_{89}X_{96} \\
&+ \tilde{T}_{77}X_{78}X_{89}X_{79} .
\end{aligned} \tag{C.25}$$

Finally, the ranks read

$$N_0 = n, \quad N_1 = N_2 = n - 2\tau, \quad N_3 = n - 4\tau, \quad N_4 = N_5 = n - 6\tau, \tag{C.26}$$

$$N_6 = n - 8\tau, \quad N_7 = N_8 = n - 10\tau, \quad N_9 = n - 12\tau . \tag{C.27}$$

The first two cases are related by Seiberg dualities on $SU(N_1)$ and $SU(N_8)$ and by suitable field redefinitions. The second and the third case are related by Seiberg duality on $SU(N_4)$ and field redefinitions. The first and the third cases are then related by Seiberg duality on $SU(N_{1,4,8})$ and field redefinitions.

This concludes the analysis showing that the superpotentials of the three cases become identical up to sign factors, fitting with the analysis of section 7.1.

Counting phases of multiplanarizable quivers

Given a general model (k_1, k_2, k_3) from Chapter 7 there could be various configurations with the same numbers, i.e. various choices to combine the squares and the hexagons in the reduced cell of the dimer after the orientifold projection. For simplicity, let us call the reduced cell C_Ω . A dual family of models can be denoted with two numbers (k, k_3) , where $k_1 + k_2 = k$; also, denote $k_3 = 2k + p$, so that we can distinguish between two cases: $p = 0$ and $p \neq 0$.

Let us focus first with $p = 0$, so the dual family is identified by $(k, 2k)$. There are only k pairs of squares in the central column of C_Ω , a certain number n_{WE} with a long edge oriented along the WE axis and another n_{EW} along EW , related to k_1 and k_2 as explained above. We ask the question: how many configurations are there with a certain number of n_{WE} and n_{EW} ? In other words, how many conformally dual models in a family (k, k_3) ? We need to count the combinations of these elements that fill k position. Since there are 2 choices per position, $n_{EW} = k - n_{WE}$ and in total there are 2^k configurations. These can be counted as

$$2^k = \sum_{n_{WE}=0}^k \binom{k}{n_{WE}}, \quad (\text{D.1})$$

where each summand $\binom{k}{n_{WE}}$ is the number of configurations of a model with k squares of which n_{WE} are WE oriented, the remaining $n_{EW} = k - n_{WE}$ are EW . However, some of them are equivalent, i.e. they give the same quiver and superpotential with some indices recast. First, we can exchange $n_{WE} \leftrightarrow n_{EW}$, which means the cell C_Ω is reflected along a vertical axis and the property of the binomial coefficient

$$\binom{k}{n_{WE}} = \binom{k}{k - n_{WE}} = \binom{k}{n_{EW}} \quad (\text{D.2})$$

account for this reflection. We need to count only the configurations until $n_{WE} = \lfloor \frac{k}{2} \rfloor$. Second, each set of configurations $\binom{k}{n_{WE}}$ has an equivalence class, for we can reflect along a horizontal axis and a configuration is mapped to another one. If k is odd, there is always one mapped to itself. The number of inequivalent configurations of a cell N_{C_Ω}

with k pairs of squares and no hexagons is then

$$N_{C_\Omega} = \binom{k}{0} + \sum_{n_{WE}=1}^{\lfloor \frac{k}{2} \rfloor} \frac{1}{2} \binom{k}{n_{WE}}, \quad k \text{ even},$$

$$N_{C_\Omega} = \binom{k}{0} + \sum_{n_{WE}=1}^{\lfloor \frac{k}{2} \rfloor} \frac{1}{2} \left[\binom{k}{n_{WE}} + 1 \right], \quad k \text{ odd}. \quad (\text{D.3})$$

It is crucial to note that the orientifold projection is not yet chosen, i.e. the \mathbb{Z}_2 involution is not specified. Each inequivalent arrangement of squares in $\binom{k}{n_{WE}}$ gives a cell C_Ω , and we choose a fixed point projection if the \mathbb{Z}_2 image cell $\overline{C}_\Omega = C_\Omega$. The copy has the same number of WE pairs of squares $\overline{n}_{WE} = n_{WE}$, so that $k_1 = 2n_{WE}$ and $k_2 = 2k - k_1 = 2n_{EW}$. Thus, a projection with fixed points must have k_1 and k_2 even. We can express Eq. D.3 in terms of k_1 and count the number of orientifold projections with fixed points as

$$N_{C_\Omega}^{\text{f.p.}} = \binom{k}{0} + \sum_{k_1=2}^{2\lfloor \frac{k}{2} \rfloor} \frac{1}{2} \binom{k}{\frac{k_1}{2}}, \quad k \text{ even},$$

$$N_{C_\Omega}^{\text{f.p.}} = \binom{k}{0} + \sum_{k_1=2}^{2\lfloor \frac{k}{2} \rfloor} \frac{1}{2} \left[\binom{k}{\frac{k_1}{2}} + 1 \right], \quad k \text{ odd}. \quad (\text{D.4})$$

Each summand in Eq. D.4 counts the number of inequivalent fixed point projections with the same $(k_1, 2k - k_1, 2k)$. We can depict Eq. D.4 as the sum of the possible fixed points projections of a toric diagram with $(k_1, 2k - k_1, 2k)$.

On the other hand, the fixed lines projection is given by $\overline{C}_\Omega = -C_\Omega$. This \mathbb{Z}_2 involution changes the direction of the squares, so it sends $n_{WE} \rightarrow \overline{n}_{EW}$ and $n_{EW} = k - n_{WE} \rightarrow \overline{n}_{WE} = k - \overline{n}_{EW}$. As a consequence, $k_1 = n_{WE} + \overline{n}_{WE} = k_2 = k$, with no restriction on k_1 being even or odd. The number of models projected with fixed lines is

$$N_{C_\Omega}^{\text{f.l.}} = \binom{k}{0} + \sum_{n_{WE}=1}^{\lfloor \frac{k}{2} \rfloor} \frac{1}{2} \binom{k}{n_{WE}}, \quad k \text{ even},$$

$$N_{C_\Omega}^{\text{f.l.}} = \binom{k}{0} + \sum_{n_{WE}=1}^{\lfloor \frac{k}{2} \rfloor} \frac{1}{2} \left[\binom{k}{n_{WE}} + 1 \right], \quad k \text{ odd}, \quad (\text{D.5})$$

all of them with $(k_1, k_2, k_3) = (k, k, 2k)$.

Let us show two examples. Consider $k = 1$, which gives the PdP family of models. The unique $\binom{k}{0}$ configuration gives the reduced cell C_Ω . Then we can perform the projection with fixed points, so that the \mathbb{Z}_2 copy $\overline{C}_\Omega = C_\Omega$ and we have $\text{PdP}_{3c}^\Omega(k_1, k_2, k_3) = (0, 2, 2)$. Or, we can perform the orientifold projection with fixed lines, so that $\overline{C}_\Omega = -C_\Omega$ and we have $\text{PdP}_{3b}^\Omega(k_1, k_2, k_3) = (1, 1, 2)$.

Consider now $k = 2$, studied in Sec. C.0.4. The first configuration is $\binom{2}{0}$, and we can decide for fixed-point projection $\overline{C}_\Omega = C_\Omega$ or fixed-line projection $\overline{C}_\Omega = -C_\Omega$, respectively the rightmost $(k_1, k_2, k_3) = (0, 4, 4)$ and the leftmost $(k_1, k_2, k_3) = (2, 2, 4)$ dimers in Fig. C.5. Then, we have $\binom{2}{1}$, whose reduced cell C_Ω is drawn in the central dimers of Fig. C.5, whose central left is given by a fixed-point orientifold $\overline{C}_\Omega = C_\Omega$ and central right by fixed-line orientifold $\overline{C}_\Omega = -C_\Omega$, both $(k_1, k_2, k_3) = (2, 2, 4)$.

When $p \neq 0$, we need to distinguish between two orientifold projections, Ω_A and Ω_B . The former consist in the projection where projected gauge factors come from the side of the cell C_Ω , whereas the latter in the projection where at least one projected gauge factor comes from the central line in C_Ω . When we add hexagons to the central lines of the cell C_Ω , i.e. $p \neq 0$, both types of the projection are allowed. If p is odd the number of complete hexagons $n_h = (p-1)/2$, as half hexagon is added at one of the boundary of the reduced cell C_Ω , in this case the projection is always Ω_B . If p is even we have two choices, projection Ω_A and $n_h = p/2$ complete hexagons in C_Ω , or projection Ω_B and $n_h = p/2 - 1$ complete hexagons in C_Ω and one half hexagons on each boundary of the reduced cell. Once we have defined the number n_h , we have $k+n_h = n_{WE} + n_{EW} + n_h$ slots to be filled with squares of the two types and hexagons. The three numbers (n_{WE}, n_{EW}, n_h) defines a model, since they are related to k_1, k_2 and k_3 . The number of possible configurations is the number of ways we can fill the slots, i.e. the number of permutations of 3 elements

$$\begin{aligned}
 P_{\binom{k+n_h}{k+n_h}}^{n_{WE}, (k-n_{WE}), n_h} &= \frac{(k+n_h)!}{n_{WE}!(k-n_{EW})!n_h!}, \\
 N_{C_\Omega} &= P_{\binom{k+n_h}{k+n_h}}^{0, k, n_h} + \sum_{n_{WE}=1}^{\lfloor \frac{k}{2} \rfloor} \frac{1}{2} P_{\binom{k+n_h}{k+n_h}}^{n_{WE}, (k-n_{WE}), n_h}, \quad (k+n_h) \text{ even}, \\
 N_{C_\Omega} &= P_{\binom{k+n_h}{k+n_h}}^{0, k, n_h} + \sum_{n_{WE}=1}^{\lfloor \frac{k}{2} \rfloor} \frac{1}{2} \left[P_{\binom{k+n_h}{k+n_h}}^{n_{WE}, (k-n_{WE}), n_h} + 1 \right], \quad (k+n_h) \text{ odd}, \quad (D.6)
 \end{aligned}$$

where we have already accounted for the exchange $n_{WE} \leftrightarrow n_{EW}$ and the reflection of C_Ω around an horizontal axis. Note that for $p = 0$, i.e. $n_h = 0$, Eq. D.3 reduces to Eq. D.6.

Now, we need to choose the orientifold projection, either with fixed points $\overline{C}_\Omega = C_\Omega$ or with fixed lines $\overline{C}_\Omega = -C_\Omega$. As before, for fixed points orientifolds $k_1 = 2n_{WE}$, $k_2 = 2k - k_1 = n_{EW}$ and by definition $p = k_3 - 2k$. Again, we can express Eq. D.6 as a sum over k_1 even

$$\begin{aligned}
 N_{C_\Omega}^{\text{f.p.}} &= P_{\binom{k+n_h}{k+n_h}}^{0, k, n_h} + \sum_{k_1=2}^{2\lfloor \frac{k}{2} \rfloor} \frac{1}{2} P_{\binom{k+n_h}{k+n_h}}^{(k_1/2), (k-k_1/2), n_h}, \quad (k+n_h) \text{ even}, \\
 N_{C_\Omega}^{\text{f.p.}} &= P_{\binom{k+n_h}{k+n_h}}^{0, k, n_h} + \sum_{k_1=2}^{2\lfloor \frac{k}{2} \rfloor} \frac{1}{2} \left[P_{\binom{k+n_h}{k+n_h}}^{k_1/2, (k-k_1/2), n_h} + 1 \right], \quad (k+n_h) \text{ odd}, \quad (D.7)
 \end{aligned}$$

where each summand with the same value of k_1 gives the number of conformally dual

models with $(k_1, 2k - k_1, 2k + p)$. For fixed lines orientifolds, $k_1 = k_2 = k$ and

$$\begin{aligned}
 N_{C_\Omega}^{\text{f.l.}} &= P_{(k+n_h)}^{0,k,n_h} + \sum_{n_{WE}=1}^{\lfloor \frac{k}{2} \rfloor} \frac{1}{2} P_{(k+n_h)}^{n_{WE},(k-n_{WE}),n_h}, \quad (k+n_h) \text{ even}, \\
 N_{C_\Omega}^{\text{f.l.}} &= P_{(k+n_h)}^{0,k,n_h} + \sum_{n_{WE}=1}^{\lfloor \frac{k}{2} \rfloor} \frac{1}{2} \left[P_{(k+n_h)}^{n_{WE},(k-n_{WE}),n_h} + 1 \right], \quad (k+n_h) \text{ odd}, \quad (\text{D.8})
 \end{aligned}$$

and all are conformally dual models with $(k, k, 2k + p)$.

List of Publications

As of November 2023

Refereed publications

1. A. Amariti, D. Morgante, A. Pasternak, S. Rota and V. Tatitscheff, *One-form symmetries in $\mathcal{N} = 3$ S-folds*, SciPost 15 (2023) 4, 132 [2303.07299].
2. A. Amariti, M. Bianchi, M. Fazzi, S. Mancani, F. Riccioni and S. Rota, *Multi-planarizable quivers, orientifolds, and conformal dualities*, JHEP 09 (2023) 094 [2212.03913].
3. A. Amariti and S. Rota, *Symplectic gauge group on the Lens space*, JHEP 08 (2023) 137 [2210.12240].
4. A. Amariti, M. Bianchi, M. Fazzi, S. Mancani, F. Riccioni and S. Rota, *$\mathcal{N} = 1$ conformal dualities from unoriented chiral quivers*, JHEP 09 (2022) 235 [2207.10100].
5. A. Amariti and S. Rota, *Webs of 3d $\mathcal{N} = 2$ dualities with D-type superpotentials*, JHEP 01 (2023) 124 [2204.06961].
6. A. Amariti and S. Rota, *3d $N=2$ SO/USp adjoint SQCD: s-confinement and exact identities*, Nucl. Phys. B 987 (2023) 116068 [2202.06885].
7. A. Amariti, M. Fazzi, S. Rota and A. Segati, *Conformal S-dualities from O-planes*, JHEP 01 (2022) 116 [2108.05397].
8. A. Amariti and S. Rota, *3d $N=2$ dualities for $SU(Nc) \times U(1)$ Chern-Simons gauge theories*, Nucl. Phys. B 976 (2022) 115710 [2106.13762].
9. S. Forte, G. Ridolfi and S. Rota, *Threshold resummation of transverse momentum distributions beyond next-to-leading log*, JHEP 08 (2021) 110 [2106.11321].

Publications under review

1. A. Amariti and S. Rota, *An intertwining between conformal dualities and ordinary dualities*, arXiv:2211.12800.

Publications in preparation

1. A. Amariti and S. Rota, *Exceptional S-fold SCFTs are almost trivial*.

Acknowledgments

Ringrazio Antonio per avermi guidato in questi tre anni, per le pause sigaretta, le pause caffè e per aver dato corda a discorsi di fisica durati tutto il pomeriggio in cui funzionava tutto, e poi la mattina dopo non funzionava niente.

Ringrazio i miei genitori, mio fratello e mia sorella per avermi sostenuto in questi tre anni, come d'altra parte hanno fatto per i 25 anni precedenti.

Bibliography

- [1] M. Bianchi, G. Inverso, J. F. Morales and D. Ricci Pacifici, *Unoriented Quivers with Flavour*, *JHEP* **01** (2014) 128 [1307.0466].
- [2] S. Benvenuti and G. Lo Monaco, *A toolkit for ortho-symplectic dualities*, 2112.12154.
- [3] A. M. Uranga, *Towards mass deformed $N=4$ $SO(n)$ and $Sp(k)$ gauge theories from brane configurations*, *Nucl. Phys. B* **526** (1998) 241 [hep-th/9803054].
- [4] J. Park, R. Rabadan and A. M. Uranga, *$N=1$ type IIA brane configurations, chirality and T duality*, *Nucl. Phys. B* **570** (2000) 3 [hep-th/9907074].
- [5] J. Kaidi, M. Martone and G. Zafrir, *Exceptional moduli spaces for exceptional $\mathcal{N} = 3$ theories*, *JHEP* **08** (2022) 264 [2203.04972].
- [6] N. Seiberg and E. Witten, *Monopoles, duality and chiral symmetry breaking in $N=2$ supersymmetric QCD*, *Nucl. Phys. B* **431** (1994) 484 [hep-th/9408099].
- [7] A. Amariti and S. Rota, *Webs of 3d $\mathcal{N} = 2$ dualities with D-type superpotentials*, *JHEP* **01** (2023) 124 [2204.06961].
- [8] A. Amariti and S. Rota, *3d $N=2$ SO/USp adjoint SQCD: s-confinement and exact identities*, *Nucl. Phys. B* **987** (2023) 116068 [2202.06885].
- [9] A. Antinucci, M. Bianchi, S. Mancani and F. Riccioni, *Suspended fixed points*, *Nucl. Phys. B* **976** (2022) 115695 [2105.06195].
- [10] A. Amariti, M. Fazzi, S. Rota and A. Segati, *Conformal S-dualities from O-planes*, *JHEP* **01** (2022) 116 [2108.05397].
- [11] A. Amariti, M. Bianchi, M. Fazzi, S. Mancani, F. Riccioni and S. Rota, *$\mathcal{N} = 1$ conformal dualities from unoriented chiral quivers*, *JHEP* **09** (2022) 235 [2207.10100].
- [12] A. Antinucci, S. Mancani and F. Riccioni, *Infrared duality in unoriented Pseudo del Pezzo*, *Phys. Lett. B* **811** (2020) 135902 [2007.14749].

- [13] A. Amariti, M. Bianchi, M. Fazzi, S. Mancani, F. Riccioni and S. Rota, *Multi-planarizable quivers, orientifolds, and conformal dualities*, *JHEP* **09** (2023) 094 [2212.03913].
- [14] A. Amariti, D. Morgante, A. Pasternak, S. Rota and V. Tatitscheff, *One-form symmetries in $\mathcal{N} = 3$ S-folds*, *SciPost Phys.* **15** (2023) 132 [2303.07299].
- [15] N. Seiberg, *Electric - magnetic duality in supersymmetric nonAbelian gauge theories*, *Nucl. Phys. B* **435** (1995) 129 [hep-th/9411149].
- [16] D. Green, Z. Komargodski, N. Seiberg, Y. Tachikawa and B. Wecht, *Exactly Marginal Deformations and Global Symmetries*, *JHEP* **06** (2010) 106 [1005.3546].
- [17] K. A. Intriligator and P. Pouliot, *Exact superpotentials, quantum vacua and duality in supersymmetric $SP(N(c))$ gauge theories*, *Phys. Lett. B* **353** (1995) 471 [hep-th/9505006].
- [18] K. A. Intriligator and N. Seiberg, *Duality, monopoles, dyons, confinement and oblique confinement in supersymmetric $SO(N(c))$ gauge theories*, *Nucl. Phys. B* **444** (1995) 125 [hep-th/9503179].
- [19] I. Affleck, M. Dine and N. Seiberg, *Dynamical Supersymmetry Breaking in Supersymmetric QCD*, *Nucl. Phys. B* **241** (1984) 493.
- [20] O. Aharony, N. Seiberg and Y. Tachikawa, *Reading between the lines of four-dimensional gauge theories*, *JHEP* **08** (2013) 115 [1305.0318].
- [21] K. A. Intriligator and N. Seiberg, *Lectures on supersymmetric gauge theories and electric-magnetic duality*, *Nucl. Phys. B Proc. Suppl.* **45BC** (1996) 1 [hep-th/9509066].
- [22] M. J. Strassler, *An Unorthodox introduction to supersymmetric gauge theory*, in *Strings, Branes and Extra Dimensions: TASI 2001: Proceedings*, pp. 561–638, 2003, DOI [hep-th/0309149].
- [23] A. Bilal, *Introduction to supersymmetry*, hep-th/0101055.
- [24] S. S. Razamat and G. Zafrir, *$N = 1$ conformal dualities*, *JHEP* **09** (2019) 046 [1906.05088].
- [25] S. S. Razamat and G. Zafrir, *$\mathcal{N} = 1$ conformal duals of gauged E_n MN models*, *JHEP* **06** (2020) 176 [2003.01843].
- [26] S. S. Razamat, E. Sabag and G. Zafrir, *Weakly coupled conformal manifolds in 4d*, *JHEP* **06** (2020) 179 [2004.07097].
- [27] D. Gaiotto, G. W. Moore and A. Neitzke, *Framed BPS States*, *Adv. Theor. Math. Phys.* **17** (2013) 241 [1006.0146].
- [28] D. Gaiotto, A. Kapustin, N. Seiberg and B. Willett, *Generalized Global Symmetries*, *JHEP* **02** (2015) 172 [1412.5148].
- [29] M. Del Zotto and I. García Etxebarria, *Global Structures from the Infrared*, 2204.06495.
- [30] O. Aharony, *IR duality in $d = 3$ $N=2$ supersymmetric $USp(2N(c))$ and $U(N(c))$ gauge theories*, *Phys. Lett. B* **404** (1997) 71 [hep-th/9703215].

- [31] T. Dimofte and D. Gaiotto, *An E7 Surprise*, *JHEP* **10** (2012) 129 [1209.1404].
- [32] A. Giveon and D. Kutasov, *Seiberg Duality in Chern-Simons Theory*, *Nucl. Phys. B* **812** (2009) 1 [0808.0360].
- [33] K. Nii, *Duality and Confinement in 3d $\mathcal{N} = 2$ "chiral" $SU(N)$ gauge theories*, *Nucl. Phys. B* **939** (2019) 507 [1809.10757].
- [34] C. Hwang, K.-J. Park and J. Park, *Evidence for Aharony duality for orthogonal gauge groups*, *JHEP* **11** (2011) 011 [1109.2828].
- [35] B. Willett and I. Yaakov, *$\mathcal{N} = 2$ dualities and Z-extremization in three dimensions*, *JHEP* **10** (2020) 136 [1104.0487].
- [36] A. Kapustin, *Seiberg-like duality in three dimensions for orthogonal gauge groups*, 1104.0466.
- [37] C. Hwang, H. Kim and J. Park, *On 3d Seiberg-Like Dualities with Two Adjoints*, *Fortsch. Phys.* **66** (2018) 1800064 [1807.06198].
- [38] K. Nii, *3d duality with adjoint matter from 4d duality*, *JHEP* **02** (2015) 024 [1409.3230].
- [39] C. Hwang, S. Kim and J. Park, *Monopole deformations of 3d Seiberg-like dualities with adjoint matters*, 2202.09000.
- [40] D. Kutasov, A. Schwimmer and N. Seiberg, *Chiral rings, singularity theory and electric - magnetic duality*, *Nucl. Phys. B* **459** (1996) 455 [hep-th/9510222].
- [41] R. G. Leigh and M. J. Strassler, *Duality of $Sp(2N(c))$ and $S0(N(c))$ supersymmetric gauge theories with adjoint matter*, *Phys. Lett. B* **356** (1995) 492 [hep-th/9505088].
- [42] K. A. Intriligator, R. G. Leigh and M. J. Strassler, *New examples of duality in chiral and nonchiral supersymmetric gauge theories*, *Nucl. Phys. B* **456** (1995) 567 [hep-th/9506148].
- [43] F. Benini, C. Closset and S. Cremonesi, *Comments on 3d Seiberg-like dualities*, *JHEP* **10** (2011) 075 [1108.5373].
- [44] K. Intriligator and N. Seiberg, *Aspects of 3d $N=2$ Chern-Simons-Matter Theories*, *JHEP* **07** (2013) 079 [1305.1633].
- [45] J. H. Brodie, *Duality in supersymmetric $SU(N(c))$ gauge theory with two adjoint chiral superfields*, *Nucl. Phys. B* **478** (1996) 123 [hep-th/9605232].
- [46] J. H. Brodie and M. J. Strassler, *Patterns of duality in $N=1$ SUSY gauge theories, or: Seating preferences of theater going nonAbelian dualities*, *Nucl. Phys. B* **524** (1998) 224 [hep-th/9611197].
- [47] C. Csaki, M. Schmaltz and W. Skiba, *A Systematic approach to confinement in $N=1$ supersymmetric gauge theories*, *Phys. Rev. Lett.* **78** (1997) 799 [hep-th/9610139].
- [48] C. Csaki, M. Schmaltz and W. Skiba, *Confinement in $N=1$ SUSY gauge theories and model building tools*, *Phys. Rev. D* **55** (1997) 7840 [hep-th/9612207].
- [49] O. Aharony, S. S. Razamat, N. Seiberg and B. Willett, *3d dualities from 4d dualities*, *JHEP* **07** (2013) 149 [1305.3924].

- [50] M. Berkooz, *The Dual of supersymmetric SU(2k) with an antisymmetric tensor and composite dualities*, *Nucl. Phys. B* **452** (1995) 513 [hep-th/9505067].
- [51] S. Bajecot and S. Benvenuti, *S-confinements from deconfinements*, *JHEP* **11** (2022) 071 [2201.11049].
- [52] A. Kapustin, B. Willett and I. Yaakov, *Exact Results for Wilson Loops in Superconformal Chern-Simons Theories with Matter*, *JHEP* **03** (2010) 089 [0909.4559].
- [53] D. L. Jafferis, *The Exact Superconformal R-Symmetry Extremizes Z*, *JHEP* **05** (2012) 159 [1012.3210].
- [54] N. Hama, K. Hosomichi and S. Lee, *Notes on SUSY Gauge Theories on Three-Sphere*, *JHEP* **03** (2011) 127 [1012.3512].
- [55] N. Hama, K. Hosomichi and S. Lee, *SUSY Gauge Theories on Squashed Three-Spheres*, *JHEP* **05** (2011) 014 [1102.4716].
- [56] F. van de Bult, *Hyperbolic Hypergeometric Functions*, <http://www.its.caltech.edu/vdbult/Thesis.pdf>, Thesis (2008) .
- [57] F. A. H. Dolan, V. P. Spiridonov and G. S. Vartanov, *From 4d superconformal indices to 3d partition functions*, *Phys. Lett. B* **704** (2011) 234 [1104.1787].
- [58] V. Niarchos, *Seiberg dualities and the 3d/4d connection*, *JHEP* **07** (2012) 075 [1205.2086].
- [59] O. Aharony, S. S. Razamat, N. Seiberg and B. Willett, *3d dualities from 4d dualities for orthogonal groups*, *JHEP* **08** (2013) 099 [1307.0511].
- [60] C. Csáki, M. Martone, Y. Shirman, P. Tanedo and J. Terning, *Dynamics of 3D SUSY Gauge Theories with Antisymmetric Matter*, *JHEP* **08** (2014) 141 [1406.6684].
- [61] A. Amariti and C. Klare, *A journey to 3d: exact relations for adjoint SQCD from dimensional reduction*, *JHEP* **05** (2015) 148 [1409.8623].
- [62] A. Amariti, D. Forcella, C. Klare, D. Orlando and S. Reffert, *The braneology of 3D dualities*, *J. Phys. A* **48** (2015) 265401 [1501.06571].
- [63] A. Amariti, D. Forcella, C. Klare, D. Orlando and S. Reffert, *4D/3D reduction of dualities: mirrors on the circle*, *JHEP* **10** (2015) 048 [1504.02783].
- [64] A. Amariti, C. Csáki, M. Martone and N. R.-L. Lorier, *From 4D to 3D chiral theories: Dressing the monopoles*, *Phys. Rev. D* **93** (2016) 105027 [1506.01017].
- [65] C. Csaki, Y. Shirman, J. Terning and M. Waterbury, *Kaluza-Klein Monopoles and their Zero Modes*, *Phys. Rev. Lett.* **120** (2018) 071603 [1708.03330].
- [66] S. Benvenuti and S. Giacomelli, *Abelianization and sequential confinement in 2 + 1 dimensions*, *JHEP* **10** (2017) 173 [1706.04949].
- [67] F. Benini, S. Benvenuti and S. Pasquetti, *SUSY monopole potentials in 2+1 dimensions*, *JHEP* **08** (2017) 086 [1703.08460].
- [68] S. Benvenuti and S. Giacomelli, *Lagrangians for generalized Argyres-Douglas theories*, *JHEP* **10** (2017) 106 [1707.05113].

- [69] F. Nieri, Y. Pan and M. Zabzine, *3d Mirror Symmetry from S-duality*, *Phys. Rev. D* **98** (2018) 126002 [1809.00736].
- [70] A. Amariti and L. Cassia, *USp(2N_c) SQCD₃ with antisymmetric: dualities and symmetry enhancements*, *JHEP* **02** (2019) 013 [1809.03796].
- [71] S. Benvenuti, *A tale of exceptional 3d dualities*, *JHEP* **03** (2019) 125 [1809.03925].
- [72] A. Hanany and E. Witten, *Type IIB superstrings, BPS monopoles, and three-dimensional gauge dynamics*, *Nucl. Phys. B* **492** (1997) 152 [hep-th/9611230].
- [73] S. Kim, *The Complete superconformal index for N=6 Chern-Simons theory*, *Nucl. Phys. B* **821** (2009) 241 [0903.4172].
- [74] J. Kinney, J. M. Maldacena, S. Minwalla and S. Raju, *An Index for 4 dimensional super conformal theories*, *Commun. Math. Phys.* **275** (2007) 209 [hep-th/0510251].
- [75] D. Kutasov and J. Lin, *N=1 Duality and the Superconformal Index*, 1402.5411.
- [76] A. Kapustin, H. Kim and J. Park, *Dualities for 3d Theories with Tensor Matter*, *JHEP* **12** (2011) 087 [1110.2547].
- [77] V. P. Spiridonov and G. S. Vartanov, *Elliptic Hypergeometry of Supersymmetric Dualities*, *Commun. Math. Phys.* **304** (2011) 797 [0910.5944].
- [78] F. A. Dolan and H. Osborn, *Applications of the Superconformal Index for Protected Operators and q-Hypergeometric Identities to N=1 Dual Theories*, *Nucl. Phys. B* **818** (2009) 137 [0801.4947].
- [79] S. Golkar, *Conformal windows of SP(2N) and SO(N) gauge theories from topological excitations on R**3 x S**1*, *JHEP* **11** (2009) 076 [0909.2838].
- [80] M. Klein, *More confining N=1 SUSY gauge theories from nonAbelian duality*, *Nucl. Phys. B* **553** (1999) 155 [hep-th/9812155].
- [81] N. Aghaei, A. Amariti and Y. Sekiguchi, *Notes on Integral Identities for 3d Supersymmetric Dualities*, *JHEP* **04** (2018) 022 [1709.08653].
- [82] V. Niarchos, *R-charges, Chiral Rings and RG Flows in Supersymmetric Chern-Simons-Matter Theories*, *JHEP* **05** (2009) 054 [0903.0435].
- [83] O. Aharony and D. Fleischer, *IR Dualities in General 3d Supersymmetric SU(N) QCD Theories*, *JHEP* **02** (2015) 162 [1411.5475].
- [84] C. Hwang and J. Park, *Factorization of the 3d superconformal index with an adjoint matter*, *JHEP* **11** (2015) 028 [1506.03951].
- [85] A. Amariti and M. Fazzi, *Dualities for three-dimensional $\mathcal{N} = 2$ SU(N_c) chiral adjoint SQCD*, *JHEP* **11** (2020) 030 [2007.01323].
- [86] L. Mazzucato, *Remarks on the analytic structure of supersymmetric effective actions*, *JHEP* **12** (2005) 026 [hep-th/0508234].
- [87] K. Intriligator and E. Nardoni, *Deformations of W_{A,D,E} SCFTs*, *JHEP* **09** (2016) 043 [1604.04294].
- [88] B. Bajc, *Kutasov-Seiberg dualities and cyclotomic polynomials*, *JHEP* **06** (2019) 083 [1901.02846].

- [89] A. Amariti, *4d/3d reduction of s-confining theories: the role of the “exotic” D instantons*, *JHEP* **02** (2016) 139 [1507.05623].
- [90] K. Nii and Y. Sekiguchi, *Low-energy dynamics of 3d $\mathcal{N} = 2$ G_2 supersymmetric gauge theory*, *JHEP* **02** (2018) 158 [1712.02774].
- [91] K. Nii, *3d s-confinement for three-index matters*, *JHEP* **11** (2018) 099 [1805.06369].
- [92] K. Nii, *Exact results in 3d $\mathcal{N} = 2$ Spin(7) gauge theories with vector and spinor matters*, *JHEP* **05** (2018) 017 [1802.08716].
- [93] K. Nii, *Confinement in 3d $\mathcal{N} = 2$ Spin(N) gauge theories with vector and spinor matters*, *JHEP* **03** (2019) 113 [1810.06618].
- [94] K. Nii, *Confinement in 3d $\mathcal{N} = 2$ exceptional gauge theories*, 1906.10161.
- [95] K. Nii, *On s-confinement in 3d $\mathcal{N} = 2$ gauge theories with anti-symmetric tensors*, 1906.03908.
- [96] M. A. Luty, M. Schmaltz and J. Terning, *A Sequence of duals for Sp(2N) supersymmetric gauge theories with adjoint matter*, *Phys. Rev. D* **54** (1996) 7815 [hep-th/9603034].
- [97] L. E. Bottini, C. Hwang, S. Pasquetti and M. Sacchi, *Dualities from dualities: the sequential deconfinement technique*, 2201.11090.
- [98] A. Amariti, D. Orlando and S. Reffert, *Monopole Quivers and new 3D $\mathcal{N}=2$ dualities*, *Nucl. Phys. B* **924** (2017) 153 [1705.09297].
- [99] S. Giacomelli and N. Mekareeya, *Mirror theories of 3d $\mathcal{N} = 2$ SQCD*, *JHEP* **03** (2018) 126 [1711.11525].
- [100] A. Amariti, I. Garozzo and N. Mekareeya, *New 3d $\mathcal{N} = 2$ dualities from quadratic monopoles*, *JHEP* **11** (2018) 135 [1806.01356].
- [101] F. Aprile, S. Pasquetti and Y. Zenkevich, *Flipping the head of $T[SU(N)]$: mirror symmetry, spectral duality and monopoles*, *JHEP* **04** (2019) 138 [1812.08142].
- [102] S. Pasquetti and M. Sacchi, *From 3d dualities to 2d free field correlators and back*, *JHEP* **11** (2019) 081 [1903.10817].
- [103] S. Pasquetti and M. Sacchi, *3d dualities from 2d free field correlators: recombination and rank stabilization*, *JHEP* **01** (2020) 061 [1905.05807].
- [104] A. Arabi Ardehali, L. Cassia and Y. Lü, *From Exact Results to Gauge Dynamics on $\mathbb{R}^3 \times S^1$* , *JHEP* **08** (2020) 053 [1912.02732].
- [105] S. Benvenuti, I. Garozzo and G. Lo Monaco, *Sequential deconfinement in 3d $\mathcal{N} = 2$ gauge theories*, 2012.09773.
- [106] S. Benvenuti and P. Spezzati, *Mildly Flavoring domain walls in SU(N) SQCD: baryons and monopole superpotentials*, 2109.08087.
- [107] V. P. Spiridonov and G. S. Vartanov, *Superconformal indices of $\mathcal{N} = 4$ SYM field theories*, *Lett. Math. Phys.* **100** (2012) 97 [1005.4196].
- [108] V. P. Spiridonov and G. S. Vartanov, *Elliptic hypergeometry of supersymmetric dualities II. Orthogonal groups, knots, and vortices*, *Commun. Math. Phys.* **325** (2014) 421 [1107.5788].

- [109] S. N. M. Ruijsenaars, *First order analytic difference equations and integrable quantum systems*, *Journal of Mathematical Physics* **38** (1997) 1069 [<https://doi.org/10.1063/1.531809>].
- [110] S. N. M. Ruijsenaars, *A relativistic hypergeometric function*, *J. Comput. Appl. Math.* **178** (2005) 393–417.
- [111] N. Kurokawa and S. Koyama, *Multiple sine functions*, *Forum Mathematicum* **15** (2003) 839.
- [112] A. Amariti, *Integral identities for 3d dualities with $SP(2N)$ gauge groups*, 1509.02199.
- [113] S. Franco, A. Hanany, D. Krefl, J. Park, A. M. Uranga and D. Vegh, *Dimers and orientifolds*, *JHEP* **09** (2007) 075 [[0707.0298](https://arxiv.org/abs/0707.0298)].
- [114] O. Chacaltana, J. Distler and Y. Tachikawa, *Nilpotent orbits and codimension-two defects of 6d $N=(2,0)$ theories*, *Int. J. Mod. Phys. A* **28** (2013) 1340006 [[1203.2930](https://arxiv.org/abs/1203.2930)].
- [115] O. Chacaltana, J. Distler and A. Trimm, *A Family of 4D $\mathcal{N} = 2$ Interacting SCFTs from the Twisted A_{2N} Series*, 1412.8129.
- [116] S. Benvenuti and M. Kruczenski, *From Sasaki-Einstein spaces to quivers via BPS geodesics: $L^{**p,q|r}$* , *JHEP* **04** (2006) 033 [[hep-th/0505206](https://arxiv.org/abs/hep-th/0505206)].
- [117] A. Butti, D. Forcella and A. Zaffaroni, *The Dual superconformal theory for L^{**pqr} manifolds*, *JHEP* **09** (2005) 018 [[hep-th/0505220](https://arxiv.org/abs/hep-th/0505220)].
- [118] S. Franco, A. Hanany, D. Martelli, J. Sparks, D. Vegh and B. Wecht, *Gauge theories from toric geometry and brane tilings*, *JHEP* **01** (2006) 128 [[hep-th/0505211](https://arxiv.org/abs/hep-th/0505211)].
- [119] E. Witten, *Solutions of four-dimensional field theories via M theory*, *Nucl. Phys. B* **500** (1997) 3 [[hep-th/9703166](https://arxiv.org/abs/hep-th/9703166)].
- [120] A. M. Uranga, *Brane configurations for branes at conifolds*, *JHEP* **01** (1999) 022 [[hep-th/9811004](https://arxiv.org/abs/hep-th/9811004)].
- [121] M. Bianchi, D. Bufalini, S. Mancani and F. Riccioni, *Mass deformations of unoriented quiver theories*, *JHEP* **07** (2020) [[2003.09620](https://arxiv.org/abs/2003.09620)].
- [122] R. G. Leigh and M. J. Strassler, *Exactly marginal operators and duality in four-dimensional $N=1$ supersymmetric gauge theory*, *Nucl. Phys. B* **447** (1995) 95 [[hep-th/9503121](https://arxiv.org/abs/hep-th/9503121)].
- [123] M. J. Strassler, *Manifolds of fixed points and duality in supersymmetric gauge theories*, *Prog. Theor. Phys. Suppl.* **123** (1996) 373 [[hep-th/9602021](https://arxiv.org/abs/hep-th/9602021)].
- [124] M. J. Strassler, *The Duality cascade*, in *Theoretical Advanced Study Institute in Elementary Particle Physics (TASI 2003): Recent Trends in String Theory*, pp. 419–510, 5, 2005, DOI [[hep-th/0505153](https://arxiv.org/abs/hep-th/0505153)].
- [125] M. Bianchi, S. Cremonesi, A. Hanany, J. F. Morales, D. Ricci Pacifici and R. Seong, *Mass-deformed Brane Tilings*, *JHEP* **10** (2014) 027 [[1408.1957](https://arxiv.org/abs/1408.1957)].
- [126] P. C. Argyres, K. A. Intriligator, R. G. Leigh and M. J. Strassler, *On inherited duality in $N=1$ $d = 4$ supersymmetric gauge theories*, *JHEP* **04** (2000) 029 [[hep-th/9910250](https://arxiv.org/abs/hep-th/9910250)].

- [127] N. Halmagyi, C. Romelsberger and N. P. Warner, *Inherited duality and quiver gauge theory*, *Adv. Theor. Math. Phys.* **10** (2006) 159 [hep-th/0406143].
- [128] M. R. Douglas and G. W. Moore, *D-branes, quivers, and ALE instantons*, hep-th/9603167.
- [129] E. García-Valdecasas, S. Meynet, A. Pasternak and V. Tatitscheff, *Dimers in a Bottle*, *JHEP* **04** (2021) 274 [2101.02670].
- [130] I. R. Klebanov and E. Witten, *Superconformal field theory on three-branes at a Calabi-Yau singularity*, *Nucl. Phys.* **B536** (1998) 199 [hep-th/9807080].
- [131] V. Bouchard, *Lectures on complex geometry, Calabi-Yau manifolds and toric geometry*, hep-th/0702063.
- [132] N. C. Leung and C. Vafa, *Branes and toric geometry*, *Adv. Theor. Math. Phys.* **2** (1998) 91 [hep-th/9711013].
- [133] C. Closset, *Toric geometry and local Calabi-Yau varieties: An Introduction to toric geometry (for physicists)*, 0901.3695.
- [134] D. A. Cox, J. B. Little and H. Schenk, *Toric Varieties*. Graduate Studies in Mathematics, 2011.
- [135] A. Hanany and K. D. Kennaway, *Dimer models and toric diagrams*, hep-th/0503149.
- [136] S. Franco, A. Hanany, K. D. Kennaway, D. Vegh and B. Wecht, *Brane dimers and quiver gauge theories*, *JHEP* **01** (2006) 096 [hep-th/0504110].
- [137] B. Feng, A. Hanany, Y.-H. He and A. M. Uranga, *Toric duality as Seiberg duality and brane diamonds*, *JHEP* **12** (2001) 035 [hep-th/0109063].
- [138] S. Franco, A. Hanany, F. Saad and A. M. Uranga, *Fractional branes and dynamical supersymmetry breaking*, *JHEP* **01** (2006) 011 [hep-th/0505040].
- [139] A. Hanany and D. Vegh, *Quivers, tilings, branes and rhombi*, *JHEP* **10** (2007) 029 [hep-th/0511063].
- [140] A. Hanany, C. P. Herzog and D. Vegh, *Brane tilings and exceptional collections*, *JHEP* **07** (2006) 001 [hep-th/0602041].
- [141] K. D. Kennaway, *Brane Tilings*, *Int. J. Mod. Phys. A* **22** (2007) 2977 [0706.1660].
- [142] M. Yamazaki, *Brane tilings and their applications*, *Fortschritte der Physik* **56** (2008) 555 [0803.4474].
- [143] S. G. Naculich, H. J. Schnitzer and N. Wyllard, *1/N corrections to anomalies and the AdS / CFT correspondence for orientifolded N=2 orbifold and N=1 conifold models*, *Int. J. Mod. Phys. A* **17** (2002) 2567 [hep-th/0106020].
- [144] C.-h. Ahn, S. Nam and S.-J. Sin, *Orientifold in conifold and quantum deformation*, *Phys. Lett. B* **517** (2001) 397 [hep-th/0106093].
- [145] S. Imai and T. Yokono, *Comments on orientifold projection in the conifold and SO x USp duality cascade*, *Phys. Rev. D* **65** (2002) 066007 [hep-th/0110209].

- [146] Y. Tachikawa and B. Wecht, *Explanation of the Central Charge Ratio 27/32 in Four-Dimensional Renormalization Group Flows between Superconformal Theories*, *Phys. Rev. Lett.* **103** (2009) 061601 [0906.0965].
- [147] A. Hanany and R. Seong, *Brane tilings and reflexive polygons*, *Fortsch. Phys.* **60** (2012) 695 [1201.2614].
- [148] I. García-Etxebarria and B. Heidenreich, *Strongly coupled phases of $\mathcal{N} = 1$ S-duality*, *JHEP* **09** (2015) 032 [1506.03090].
- [149] S. Giacomelli, M. Moleti and R. Savelli, *Probing 7-branes on Orbifolds*, 2205.08578.
- [150] D. Forcella and A. Zaffaroni, *$N=1$ Chern-Simons theories, orientifolds and Spin(7) cones*, *JHEP* **05** (2010) 045 [0911.2595].
- [151] S. Franco, A. Mininno, A. M. Uranga and X. Yu, *2d $\mathcal{N} = (0, 1)$ gauge theories and Spin(7) orientifolds*, *JHEP* **03** (2022) 150 [2110.03696].
- [152] T. C. Collins and G. Székelyhidi, *K-Semistability for irregular Sasakian manifolds*, *J. Diff. Geom.* **109** (2018) 81 [1204.2230].
- [153] T. C. Collins and G. Székelyhidi, *Sasaki-Einstein metrics and K-stability*, *Geom. Topol.* **23** (2019) 1339 [1512.07213].
- [154] T. C. Collins, D. Xie and S.-T. Yau, *K stability and stability of chiral ring*, 1606.09260.
- [155] S. Benvenuti and S. Giacomelli, *Supersymmetric gauge theories with decoupled operators and chiral ring stability*, *Phys. Rev. Lett.* **119** (2017) 251601 [1706.02225].
- [156] A. Amariti, M. Fazzi, N. Mekareeya and A. Nedelin, *New 3d $\mathcal{N} = 2$ SCFT's with $\mathcal{N}^{3/2}$ scaling*, *JHEP* **12** (2019) 111 [1903.02586].
- [157] M. Fazzi and A. Tomasiello, *Holography, Matrix Factorizations and K-stability*, *JHEP* **05** (2020) 119 [1906.08272].
- [158] F. Alday et al., *The Pollica perspective on the (super)-conformal world*, *J. Phys. A* **54** (2021) 303001.
- [159] J. Bao, Y.-H. He and Y. Xiao, *Chiral rings, Futaki invariants, plethystics, and Gröbner bases*, *JHEP* **21** (2020) 203 [2009.02450].
- [160] T. C. Collins, D. Jafferis, C. Vafa, K. Xu and S.-T. Yau, *On Upper Bounds in Dimension Gaps of CFT's*, 2201.03660.
- [161] E. Barnes, K. A. Intriligator, B. Wecht and J. Wright, *Evidence for the strongest version of the 4d a-theorem, via a-maximization along RG flows*, *Nucl. Phys. B* **702** (2004) 131 [hep-th/0408156].
- [162] P. Pouliot, *Duality in SUSY SU(N) with an antisymmetric tensor*, *Phys. Lett. B* **367** (1996) 151 [hep-th/9510148].
- [163] A. Sagnotti, *Open Strings and their Symmetry Groups*, in *NATO Advanced Summer Institute on Nonperturbative Quantum Field Theory (Cargese Summer Institute)*, 9, 1987, hep-th/0208020.
- [164] G. Pradisi and A. Sagnotti, *Open String Orbifolds*, *Phys. Lett. B* **216** (1989) 59.

- [165] M. Bianchi and A. Sagnotti, *On the systematics of open string theories*, *Phys. Lett. B* **247** (1990) 517.
- [166] M. Bianchi and A. Sagnotti, *Twist symmetry and open string Wilson lines*, *Nucl. Phys. B* **361** (1991) 519.
- [167] J. Polchinski, *Dirichlet Branes and Ramond-Ramond charges*, *Phys. Rev. Lett.* **75** (1995) 4724 [hep-th/9510017].
- [168] C. Angelantonj and A. Sagnotti, *Open strings*, *Phys. Rept.* **371** (2002) 1 [hep-th/0204089].
- [169] Y. Imamura, K. Kimura and M. Yamazaki, *Comments on orientifold of brane tilings*, *Int. J. Mod. Phys. A* **23** (2008) 2299.
- [170] R. Argurio, M. Bertolini, S. Franco, E. García-Valdecasas, S. Meynet, A. Pasternak et al., *Dimers, Orientifolds and Anomalies*, *JHEP* **02** (2021) 153 [2009.11291].
- [171] I. G. Etxebarria, B. Heidenreich, M. Lotito and A. K. Sorout, *Deconfining $\mathcal{N} = 2$ SCFTs or the art of brane bending*, *JHEP* **03** (2022) 140 [2111.08022].
- [172] I. García-Etxebarria and B. Heidenreich, *S-duality in $\mathcal{N} = 1$ orientifold SCFTs*, *Fortsch. Phys.* **65** (2017) 1700013 [1612.00853].
- [173] I. Garcia-Etxebarria, B. Heidenreich and T. Wrase, *New $N=1$ dualities from orientifold transitions. Part I. Field Theory*, *JHEP* **10** (2013) 007 [1210.7799].
- [174] I. García-Etxebarria, B. Heidenreich and T. Wrase, *New $N=1$ dualities from orientifold transitions - Part II: String Theory*, *JHEP* **10** (2013) 006 [1307.1701].
- [175] R. Argurio, M. Bertolini, S. Meynet and A. Pasternak, *On supersymmetry breaking vacua from D-branes at orientifold singularities*, *JHEP* **12** (2019) 145 [1909.04682].
- [176] R. Argurio, M. Bertolini, S. Franco, E. García-Valdecasas, S. Meynet, A. Pasternak et al., *The Octagon and the Non-Supersymmetric String Landscape*, *Phys. Lett. B* **815** (2021) 136153 [2005.09671].
- [177] R. Argurio, M. Bertolini, S. Franco, E. García-Valdecasas, S. Meynet, A. Pasternak et al., *Dimers, Orientifolds and Stability of Supersymmetry Breaking Vacua*, *JHEP* **01** (2021) 061 [2007.13762].
- [178] R. Argurio, M. Bertolini, S. Franco, E. García-Valdecasas, S. Meynet, A. Pasternak et al., *The Octagon at large M* , 2207.00525.
- [179] L. E. Ibanez, F. Marchesano and R. Rabadan, *Getting just the standard model at intersecting branes*, *JHEP* **11** (2001) 002 [hep-th/0105155].
- [180] M. Wijnholt, *Geometry of Particle Physics*, *Adv. Theor. Math. Phys.* **13** (2009) 947 [hep-th/0703047].
- [181] M. Cicoli, I. n. G. Etxebarria, F. Quevedo, A. Schachner, P. Shukla and R. Valandro, *The Standard Model quiver in de Sitter string compactifications*, *JHEP* **08** (2021) 109 [2106.11964].
- [182] A. Addazi and M. Bianchi, *Neutron Majorana mass from exotic instantons*, *JHEP* **12** (2014) 089 [1407.2897].

- [183] A. Addazi and M. Bianchi, *Un-oriented Quiver Theories for Majorana Neutrons*, *JHEP* **07** (2015) 144 [1502.01531].
- [184] A. Addazi and M. Bianchi, *Neutron Majorana mass from Exotic Instantons in a Pati-Salam model*, *JHEP* **06** (2015) 012 [1502.08041].
- [185] A. Addazi, M. Bianchi and G. Ricciardi, *Exotic see-saw mechanism for neutrinos and leptogenesis in a Pati-Salam model*, *JHEP* **02** (2016) 035 [1510.00243].
- [186] S. Benvenuti and A. Hanany, *Conformal manifolds for the conifold and other toric field theories*, *JHEP* **08** (2005) 024 [hep-th/0502043].
- [187] Y. Imamura, H. Isono, K. Kimura and M. Yamazaki, *Exactly marginal deformations of quiver gauge theories as seen from brane tilings*, *Prog. Theor. Phys.* **117** (2007) 923 [hep-th/0702049].
- [188] A. Hanany, V. Jejjala, S. Ramgoolam and R.-K. Seong, *Consistency and Derangements in Brane Tilings*, *J. Phys. A* **49** (2016) 355401 [1512.09013].
- [189] F. Manzoni, *Algebro-geometrical orientifolds and IR dualities*, 2211.10113.
- [190] D. Berenstein and R. G. Leigh, *Discrete torsion, AdS / CFT and duality*, *JHEP* **01** (2000) 038 [hep-th/0001055].
- [191] D. Berenstein, V. Jejjala and R. G. Leigh, *Marginal and relevant deformations of N=4 field theories and noncommutative moduli spaces of vacua*, *Nucl. Phys. B* **589** (2000) 196 [hep-th/0005087].
- [192] G. C. Rossi, E. Sokatchev and Y. S. Stanev, *New results in the deformed N=4 SYM theory*, *Nucl. Phys. B* **729** (2005) 581 [hep-th/0507113].
- [193] G. C. Rossi, E. Sokatchev and Y. S. Stanev, *On the all-order perturbative finiteness of the deformed N=4 SYM theory*, *Nucl. Phys. B* **754** (2006) 329 [hep-th/0606284].
- [194] O. Lunin and J. M. Maldacena, *Deforming field theories with U(1) x U(1) global symmetry and their gravity duals*, *JHEP* **05** (2005) 033 [hep-th/0502086].
- [195] A. Ashmore, M. Petrini, E. L. Tasker and D. Waldram, *Exactly Marginal Deformations and Their Supergravity Duals*, *Phys. Rev. Lett.* **128** (2022) 191601 [2112.08375].
- [196] E. L. Tasker, *From β to η : a new cohomology for deformed Sasaki-Einstein manifolds*, *JHEP* **04** (2022) 075 [2112.09167].
- [197] I. García-Etxebarria and D. Regalado, *$\mathcal{N} = 3$ four dimensional field theories*, *JHEP* **03** (2016) 083 [1512.06434].
- [198] O. Aharony and M. Evtikhiev, *On four dimensional $N = 3$ superconformal theories*, *JHEP* **04** (2016) 040 [1512.03524].
- [199] O. Aharony and Y. Tachikawa, *S-folds and 4d $N=3$ superconformal field theories*, *JHEP* **06** (2016) 044 [1602.08638].
- [200] I. García-Etxebarria and D. Regalado, *Exceptional $\mathcal{N} = 3$ theories*, *JHEP* **12** (2017) 042 [1611.05769].
- [201] M. Lemos, P. Liendo, C. Meneghelli and V. Mitev, *Bootstrapping $\mathcal{N} = 3$ superconformal theories*, *JHEP* **04** (2017) 032 [1612.01536].

- [202] T. Bourton, A. Pini and E. Pomoni, *4d $\mathcal{N} = 3$ indices via discrete gauging*, *JHEP* **10** (2018) 131 [1804.05396].
- [203] P. C. Argyres, A. Bourget and M. Martone, *Classification of all $\mathcal{N} \geq 3$ moduli space orbifold geometries at rank 2*, *SciPost Phys.* **9** (2020) 083 [1904.10969].
- [204] P. C. Argyres, A. Bourget and M. Martone, *On the moduli spaces of 4d $\mathcal{N} = 3$ SCFTs I: triple special Kähler structure*, 1912.04926.
- [205] A. Amariti and G. Formigoni, *A note on 4d $\mathcal{N} = 3$ from little string theory*, *Nucl. Phys. B* **958** (2020) 115108 [2003.05983].
- [206] P. C. Argyres, M. Lotito, Y. Lü and M. Martone, *Geometric constraints on the space of $\mathcal{N} = 2$ SCFTs. Part II: construction of special Kähler geometries and RG flows*, *JHEP* **02** (2018) 002 [1601.00011].
- [207] P. Argyres, M. Lotito, Y. Lü and M. Martone, *Geometric constraints on the space of $\mathcal{N} = 2$ SCFTs. Part III: enhanced Coulomb branches and central charges*, *JHEP* **02** (2018) 003 [1609.04404].
- [208] P. C. Argyres, M. Lotito, Y. Lü and M. Martone, *Expanding the landscape of $\mathcal{N} = 2$ rank 1 SCFTs*, *JHEP* **05** (2016) 088 [1602.02764].
- [209] P. Argyres, M. Lotito, Y. Lü and M. Martone, *Geometric constraints on the space of $\mathcal{N} = 2$ SCFTs. Part I: physical constraints on relevant deformations*, *JHEP* **02** (2018) 001 [1505.04814].
- [210] M. Martone, *Testing our understanding of SCFTs: a catalogue of rank-2 $\mathcal{N} = 2$ theories in four dimensions*, *JHEP* **07** (2022) 123 [2102.02443].
- [211] J. Kaidi and M. Martone, *New rank-2 Argyres-Douglas theory*, *Phys. Rev. D* **104** (2021) 085004 [2104.13929].
- [212] D. Xie and S.-T. Yau, *4d $\mathcal{N}=2$ SCFT and singularity theory Part I: Classification*, 1510.01324.
- [213] B. Chen, D. Xie, S.-T. Yau, S. S. T. Yau and H. Zuo, *4D $\mathcal{N} = 2$ SCFT and singularity theory. Part II: complete intersection*, *Adv. Theor. Math. Phys.* **21** (2017) 121 [1604.07843].
- [214] Y. Wang, D. Xie, S. S. T. Yau and S.-T. Yau, *4d $\mathcal{N} = 2$ SCFT from complete intersection singularity*, *Adv. Theor. Math. Phys.* **21** (2017) 801 [1606.06306].
- [215] B. Chen, D. Xie, S. S. T. Yau, S.-T. Yau and H. Zuo, *4d $\mathcal{N} = 2$ SCFT and singularity theory Part III: Rigid singularity*, *Adv. Theor. Math. Phys.* **22** (2018) 1885 [1712.00464].
- [216] D. Xie and D. Zhang, *Mixed Hodge structure and $\mathcal{N} = 2$ Coulomb branch solution*, 2107.11180.
- [217] S. Cecotti, M. Del Zotto, M. Martone and R. Moscrop, *The Characteristic Dimension of Four-Dimensional $\mathcal{N} = 2$ SCFTs*, *Commun. Math. Phys.* **400** (2023) 519 [2108.10884].
- [218] M. Martone, *Towards the classification of rank- r $\mathcal{N} = 2$ SCFTs. Part I. Twisted partition function and central charge formulae*, *JHEP* **12** (2020) 021 [2006.16255].

- [219] P. C. Argyres and M. Martone, *Towards a classification of rank $r\mathcal{N} = 2$ SCFTs. Part II. Special Kahler stratification of the Coulomb branch*, *JHEP* **12** (2020) 022 [2007.00012].
- [220] M. Martone and G. Zafrir, *On the compactification of 5d theories to 4d*, *JHEP* **08** (2021) 017 [2106.00686].
- [221] P. Argyres and M. Martone, *Construction and classification of Coulomb branch geometries*, 2003.04954.
- [222] M. Caorsi and S. Cecotti, *Geometric classification of 4d $\mathcal{N} = 2$ SCFTs*, *JHEP* **07** (2018) 138 [1801.04542].
- [223] P. C. Argyres, C. Long and M. Martone, *The Singularity Structure of Scale-Invariant Rank-2 Coulomb Branches*, *JHEP* **05** (2018) 086 [1801.01122].
- [224] M. Caorsi and S. Cecotti, *Special Arithmetic of Flavor*, *JHEP* **08** (2018) 057 [1803.00531].
- [225] M. Caorsi and S. Cecotti, *Homological classification of 4d $\mathcal{N} = 2$ QFT. Rank-1 revisited*, *JHEP* **10** (2019) 013 [1906.03912].
- [226] P. C. Argyres and M. Martone, *Coulomb branches with complex singularities*, *JHEP* **06** (2018) 045 [1804.03152].
- [227] A. Bourget, A. Pini and D. Rodríguez-Gómez, *Gauge theories from principally extended disconnected gauge groups*, *Nucl. Phys. B* **940** (2019) 351 [1804.01108].
- [228] P. C. Argyres, Y. Lü and M. Martone, *Seiberg-Witten geometries for Coulomb branch chiral rings which are not freely generated*, *JHEP* **06** (2017) 144 [1704.05110].
- [229] T. Nishinaka and Y. Tachikawa, *On 4d rank-one $\mathcal{N} = 3$ superconformal field theories*, *JHEP* **09** (2016) 116 [1602.01503].
- [230] N. Seiberg and E. Witten, *Electric - magnetic duality, monopole condensation, and confinement in $N=2$ supersymmetric Yang-Mills theory*, *Nucl. Phys. B* **426** (1994) 19 [hep-th/9407087].
- [231] P. C. Argyres, M. Martone and M. Ray, *Dirac pairings, one-form symmetries and Seiberg-Witten geometries*, *JHEP* **09** (2022) 020 [2204.09682].
- [232] C. Closset and H. Magureanu, *Reading between the rational sections: Global structures of 4d $\mathcal{N} = 2$ KK theories*, 2308.10225.
- [233] A. Kapustin, *Wilson-'t Hooft operators in four-dimensional gauge theories and S-duality*, *Phys. Rev. D* **74** (2006) 025005 [hep-th/0501015].
- [234] A. Dabholkar and C. Hull, *Duality twists, orbifolds, and fluxes*, *JHEP* **09** (2003) 054 [hep-th/0210209].
- [235] C. M. Hull, *A Geometry for non-geometric string backgrounds*, *JHEP* **10** (2005) 065 [hep-th/0406102].
- [236] A. Kapustin and E. Witten, *Electric-Magnetic Duality And The Geometric Langlands Program*, *Commun. Num. Theor. Phys.* **1** (2007) 1 [hep-th/0604151].
- [237] M. Etheredge, I. Garcia Etxebarria, B. Heidenreich and S. Rauch, *Branes and symmetries for $\mathcal{N} = 3$ S-folds*, 2302.14068.

- [238] A. Kumar and C. Vafa, *U manifolds*, *Phys. Lett. B* **396** (1997) 85 [hep-th/9611007].
- [239] J. H. Schwarz, *An $SL(2, Z)$ multiplet of type IIB superstrings*, *Phys. Lett. B* **360** (1995) 13 [hep-th/9508143].
- [240] E. Witten, *Bound states of strings and p-branes*, *Nucl. Phys. B* **460** (1996) 335 [hep-th/9510135].
- [241] G. Zafrir, *An $\mathcal{N} = 1$ Lagrangian for an $\mathcal{N} = 3$ SCFT*, *JHEP* **01** (2021) 062 [2007.14955].
- [242] E. Witten, *Baryons and branes in anti-de Sitter space*, *JHEP* **07** (1998) 006 [hep-th/9805112].
- [243] J. J. Heckman, C. Lawrie, T. B. Rochais, H. Y. Zhang and G. Zoccarato, *S-folds, string junctions, and $\mathcal{N} = 2$ SCFTs*, *Phys. Rev. D* **103** (2021) 086013 [2009.10090].
- [244] A. Hanany and J. Troost, *Orientifold planes, affine algebras and magnetic monopoles*, *JHEP* **08** (2001) 021 [hep-th/0107153].
- [245] Y. Imamura, H. Kato and D. Yokoyama, *Supersymmetry Enhancement and Junctions in S-folds*, *JHEP* **10** (2016) 150 [1606.07186].
- [246] P. Agarwal and A. Amariti, *Notes on S-folds and $\mathcal{N} = 3$ theories*, *JHEP* **09** (2016) 032 [1607.00313].
- [247] Y. Choi, C. Cordova, P.-S. Hsin, H. T. Lam and S.-H. Shao, *Noninvertible duality defects in 3+1 dimensions*, *Phys. Rev. D* **105** (2022) 125016 [2111.01139].
- [248] J. Kaidi, K. Ohmori and Y. Zheng, *Kramers-Wannier-like Duality Defects in (3+1)D Gauge Theories*, *Phys. Rev. Lett.* **128** (2022) 111601 [2111.01141].
- [249] L. Bhardwaj, L. E. Bottini, S. Schafer-Nameki and A. Tiwari, *Non-Invertible Higher-Categorical Symmetries*, *SciPost Phys.* **14** (2023) 007 [2204.06564].
- [250] Y. Choi, C. Cordova, P.-S. Hsin, H. T. Lam and S.-H. Shao, *Non-invertible Condensation, Duality, and Triality Defects in 3+1 Dimensions*, 2204.09025.
- [251] J. Kaidi, G. Zafrir and Y. Zheng, *Non-invertible symmetries of $\mathcal{N} = 4$ SYM and twisted compactification*, *JHEP* **08** (2022) 053 [2205.01104].
- [252] L. Bhardwaj, S. Schafer-Nameki and J. Wu, *Universal Non-Invertible Symmetries*, *Fortsch. Phys.* **70** (2022) 2200143 [2208.05973].
- [253] T. Bartsch, M. Bullimore, A. E. V. Ferrari and J. Pearson, *Non-invertible Symmetries and Higher Representation Theory I*, 2208.05993.
- [254] A. Antinucci, F. Benini, C. Copetti, G. Galati and G. Rizi, *The holography of non-invertible self-duality symmetries*, 2210.09146.
- [255] L. Bhardwaj, S. Schafer-Nameki and A. Tiwari, *Unifying Constructions of Non-Invertible Symmetries*, 2212.06159.
- [256] T. Bartsch, M. Bullimore, A. E. V. Ferrari and J. Pearson, *Non-invertible Symmetries and Higher Representation Theory II*, 2212.07393.
- [257] L. Bhardwaj, L. E. Bottini, S. Schafer-Nameki and A. Tiwari, *Non-Invertible Symmetry Webs*, 2212.06842.

- [258] J. J. Heckman, M. Hubner, E. Torres, X. Yu and H. Y. Zhang, *Top Down Approach to Topological Duality Defects*, 2212.09743.
- [259] F. Apruzzi, I. Bah, F. Bonetti and S. Schafer-Nameki, *Non-Invertible Symmetries from Holography and Branes*, 2208.07373.
- [260] I. García Etxebarria, *Branes and Non-Invertible Symmetries*, *Fortsch. Phys.* **70** (2022) 2200154 [2208.07508].
- [261] J. J. Heckman, M. Hübner, E. Torres and H. Y. Zhang, *The Branes Behind Generalized Symmetry Operators*, *Fortsch. Phys.* **71** (2023) 2200180 [2209.03343].
- [262] F. Apruzzi, S. Giacomelli and S. Schäfer-Nameki, *4d $\mathcal{N} = 2$ S-folds*, *Phys. Rev. D* **101** (2020) 106008 [2001.00533].
- [263] S. Giacomelli, M. Martone, Y. Tachikawa and G. Zafrir, *More on $\mathcal{N} = 2$ S-folds*, *JHEP* **01** (2021) 054 [2010.03943].
- [264] V. Bashmakov, M. Del Zotto, A. Hasan and J. Kaidi, *Non-invertible Symmetries of Class \mathcal{S} Theories*, 2211.05138.
- [265] A. Antinucci, C. Copetti, G. Galati and G. Rizi, *"Zoology" of non-invertible duality defects: the view from class \mathcal{S}* , 2212.09549.
- [266] G. I. Lehrer and D. E. E. Taylor, *Unitary reflection groups*, vol. 20. Cambridge University Press, 2009.
- [267] A. Sen, *Strong coupling dynamics of branes from M theory*, *JHEP* **10** (1997) 002 [hep-th/9708002].
- [268] A. D. Shapere and Y. Tachikawa, *Central charges of $\mathcal{N}=2$ superconformal field theories in four dimensions*, *JHEP* **09** (2008) 109 [0804.1957].
- [269] P. C. Argyres and M. Martone, *4d $\mathcal{N} = 2$ theories with disconnected gauge groups*, *JHEP* **03** (2017) 145 [1611.08602].